



STRATIGRAPHIC ASSESSMENT OF THE DELMARVA INNER CONTINENTAL SHELF

Technical Report for Cooperative Agreement M16AC00001

Kelvin W. Ramsey, C. Robin Mattheus, John F. Wehmiller, Jaime L. Tomlinson, Trevor Metz
Delaware Geological Survey
University of Delaware

March 17, 2020 (Revised October 22, 2020)

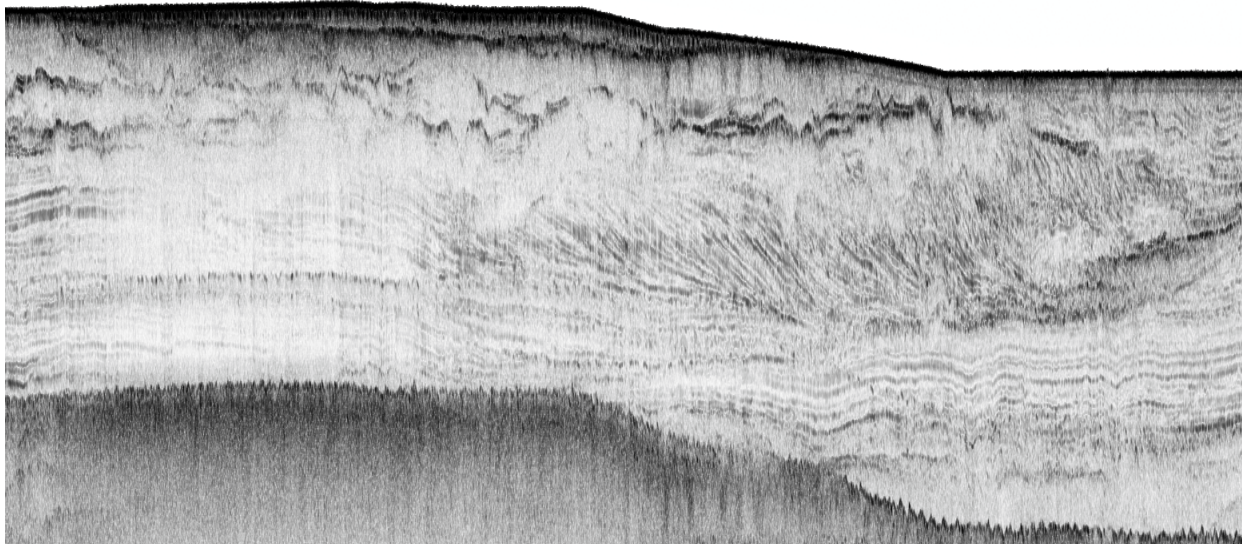


TABLE OF CONTENTS

ABSTRACT	1
INTRODUCTION	2
STUDY AREA AND BACKGROUND	3
DATASET AND ANALYTICAL APPROACH	6
Central Delmarva	6
Northern Delmarva	7
Seismic Processing and Analysis	7
Radiocarbon Dates	8
RESULTS AND DISCUSSION	17
Shallow seismic framework	17
Offshore age dates	24
Amino acid racemization	25
Paleovalleys	26
Delaware systems	26
Central Delmarva systems	27
Late Pleistocene drainage of the Delmarva inner continental shelf	33
REFERENCES	36
APPENDIX A – BOEM Vibracore Logs	36
APPENDIX B – DGS Texture Data	44
APPENDIX C – AECOM Texture Data	52
APPENDIX D- Amino Acid Racemization results	115

LIST OF FIGURES

FIGURE 1 – Map of the central-northern Delmarva Peninsula study area	4
FIGURE 2 – Data distribution map	9
FIGURE 3 – BOEM data distribution map	12
FIGURE 4 – Schematic of the general offshore stratigraphic framework	19
FIGURE 5 – Geologic cross sections	20
FIGURE 6 – Map of M1 stratigraphic pick distribution	21
FIGURE 7 – Surface map of M1 stratigraphic picks	22
FIGURE 8 – Isopach map of Quaternary sediment thickness	23
FIGURE 9 – Holocene radiocarbon dates plotted against depth	24
FIGURE 10 – Pleistocene radiocarbon dates plotted against depth	25
FIGURE 11 – Map of stratigraphic picks of valley bottoms	29
FIGURE 12 – Seismic examples showing incised valleys	30
FIGURE 13 – Map of interpreted paleovalleys	32
FIGURE 14 – Late Pleistocene drainage map	35

LIST OF TABLES

TABLE 1 – Information on previously-mapped paleovalleys	5
TABLE 2 – BOEM core locations	10
TABLE 3 – DGS texture sample inventory	13
TABLE 4 – AECOM texture sample inventory	14
TABLE 5 – Radiocarbon data from valley fills	31
TABLE 6 – Radiocarbon data from valley fills	31

ABSTRACT

This report documents an effort to map the shallow stratigraphy of the inner continental shelves off Delaware and Maryland utilizing offshore core and seismic reflection data collected for the BOEM Atlantic Sand Assessment Project from 2015 to 2017. Integrated with existing subsurface information in Delaware Geological Survey core databases and other geophysical datasets obtained from the United States Geological Survey and the Delaware Department of Natural Resources and Environmental Conservation, these data have offered the means of refining prior offshore stratigraphic models. Tight age constraint was possible through inclusion of dozens of radiocarbon ages, age estimates based on amino-acid racemization, and correlation to established onshore chronologic frameworks.

A structure map of the Tertiary-Quaternary boundary was created from stratigraphic picks of the top of the Beaverdam Formation, a thick and extensive fluvio-deltaic deposit mapped across the coastal plain and inner shelf. Overlying Quaternary sediments are thin to absent across portions of the Delaware inner shelf while the inner Maryland shelf is continuously covered by Pleistocene lagoonal and shallow marine deposits of several meters in thickness. Late Pleistocene valleys in Delaware are incised into the Beaverdam Formation while those in Maryland are not. Multiple generations of paleovalley are recognized from cross-cutting relationships and age dates of organics and shell materials found within the predominantly muddy valley fills.

Drainage patterns appear to have changed from the mid-Pleistocene to the late Pleistocene. In Maryland, this change is manifested in a shift in valley orientation. Mid-Pleistocene drainage is southward and coast-parallel, while late Pleistocene valleys are coast-perpendicular. The latter connect to modern estuaries. In Delaware, both mid-Pleistocene and late Pleistocene drainage is offshore towards the ancestral Delaware. A mid-Pleistocene paleovalley extending beneath the Bethany Beach Headland was not re-incised. This is likely because any topographic expression of the valley had been removed by transgressive ravinement. The next episode of incision favored the more erosive sands of the Beaverdam Formation over the stiff, estuarine valley fills. Evidence from the Coastal Plain suggests this occurred during Marine Isotope Stage (MIS) 6. While there is evidence surrounding the modern estuaries of Indian River and Rehoboth Bay that incision during MIS 2 reoccupied the MIS 6 location, there is no evidence on the shelf of this. This absence likely relates to the proximal location of the ancestral Delaware River at that time and influences on knickpoints up the tributaries. Exceptionally deep incision of the tributary drainage network, facilitated by glacial meltwater deepening the Delaware River, would have removed any evidence of the MIS 6 event.

INTRODUCTION

Stratigraphic framework models of continental shelves are foundational to offshore infrastructure design (e.g., windfarm siting and cable placement; Le Bot et al., 2005; Metz, 2015; Dix et al., 2016; Ponte, 2016) and sand-resource assessment (Field, 1979; Twitchell, 2011; Williams, 2012). Our conceptual understanding of Holocene coastal evolution also rests upon the tight constraint of late Pleistocene paleotopography (Shideler et al., 1984; Kraft and Belknap, 1986; Barnhardt et al., 1997; Rodriguez et al., 2004; Schimanski and Stattegger, 2005). Improving upon interpretations of the offshore stratigraphic framework (with improved data quality and spatial constraints) therefore has direct implications for parameterizing models of future coastal change (e.g., inundation models), taking into account predictions of sea-level rise and increased storm activity (Domingues et al. 2008; DeConto and Pollard 2016; Webster et al. 2005; Bender et al. 2010). Despite the importance of detailed knowledge of the shallow shelf stratigraphy, many subsurface models in use have not been updated in decades, spurring on efforts (such as this one) to refine them. Advanced (digital) methods of subsurface analysis, better geophysical imaging and processing powers, and larger datasets are facilitating these endeavors. The power of GIS-based imaging of subsurface structures is showcased by Childers and others (2019), for example, who remapped paleovalleys beneath Delaware Bay and adjacent shelf areas. The use of digital subsurface reflection records and a GIS-based imaging approach improved upon prior maps (Knebel and Circé, 1988; Kranz et al., 1993; and McGahey et al., 1991).

Recent data-collection and analysis efforts, promoted by the BOEM Atlantic Sand Assessment Project (ASAP), have facilitated renewed stratigraphic mapping of the central-northern Delmarva inner continental shelf. Particular emphasis was placed on delineating late Pleistocene drainage systems and establishing their relationships to the larger valleys of ancestral Delaware and Chesapeake systems. The main aim was to develop a better understanding of late Pleistocene paleotopography and its implications for coastal inundation during Holocene sea-level rise, a major driver of modern surface sediment distributions across the shelf (Mattheus et al., 2020). Few studies have addressed subsurface architecture here in detail. Most offshore stratigraphic work along the Delmarva Peninsula and adjoining regions has focused on the large paleovalleys (>5 km in width) near the Delaware and Chesapeake Bay mouths, which are associated with the ancestral Delaware and Susquehanna Rivers, respectively (Colman et al., 1990; Colman and Mixon, 1988; Foyle and Oertel, 1992; Oertel and Foyle, 1995; Twitchell et al., 1977; Childers et al., 2019). These valleys connect to large watersheds (>30,000 km²) that extend into the Piedmont. Smaller valleys (with widths <2 km) have been identified and partially mapped along the central to northern Delmarva by prior work (e.g., Toscano et al., 1989); however, connectivity between mapped valley segments and their chronology are uncertain and different studies have provided contrasting interpretations of the nature of late Pleistocene paleodrainage (Belknap and Kraft, 1985 versus Williams, 1999). Many of these valleys are tributaries to the larger ones and have small drainage basins (<1,000 km²) that are confined to the lower Coastal Plain.

STUDY AREA AND BACKGROUND

Many foundational studies of coastal geology have made use of past interpretations of the Delmarva offshore stratigraphy. In particular, controls of antecedent terrain configuration on Holocene inundation patterns and sediment-facies distributions have been discussed in detail from these data (Belknap and Kraft, 1981 and 1985; Demarest and Leatherman, 1985; Kraft and Belknap, 1986; Belknap et al., 1994). This work has shown how Pleistocene paleotopography dictated patterns of sediment accommodation during Holocene inundation, influencing sediment preservation and seafloor sediment-facies distributions. While offering a strong conceptual platform for understanding coastal development under sea-level rise conditions, refinement of the stratigraphic models has yet to be undertaken. Accurately siting paleovalleys is particularly important as they commonly contain the most complete record of Holocene transgression (Bratton et al. 2003; Heap and Nichol 1997; Rodriguez et al., 2008). Knowing where paleovalleys are located is also important for a number of practical reasons: A) As valley fills often contrast surrounding materials (in terms of texture), they often influence groundwater flow patterns across the coastal zone and commonly provide pathways for submarine groundwater discharge (Krantz et al. 2004; Manheim et al. 2004; Russoniello et al., 2013); B) Sandy valley fills have also been shown to source modern coastal systems (e.g. barrier islands; Timmons et al. 2010); and C) Irregular paleotopography can influence modern seafloor morphodynamics and sediment thicknesses (Edwards et al. 2003; Locker et al. 2003; Finkl et al. 2006).

Our current understanding of central Delmarva shelf paleodrainage (seaward of Assateague Island) is based on 1985-1987 seismic reflection data (Toscano et al., 1989), while the most recent assessment of the Delaware offshore was undertaken in the late 1990s by Williams (1999). These studies relied on analog seismic reflection records and relatively few cores from the inner shelf (compared to more recent offshore assessments; Mattheus et al., 2020). The former study delineated several late Pleistocene valley networks, associated with the modern Assawoman and Chincoteague Bays, while the latter generated an interpretation of the inner Delaware shelf in disagreement with prior models (Kraft, 1971; Belknap and Kraft, 1981 and 1985; Figure 1). Williams (1999) interprets multiple valley generations on the Delaware inner shelf, based on stratigraphic relationships, age estimates based on amino-acid racemization (AAR), and radiocarbon ages. However, how this relates to the nearby Delaware River paleovalleys is not clear. At least three valley generations of the ancestral Delaware and Susquehanna Rivers are documented by numerous stratigraphic assessments, respectively (Colman et al., 1990; McGahey et al., 1991; Krantz et al., 1993; Oertel and Foyle, 1995; Murphy, 1996; Childers, 2014; Childers et al., 2019). The role of smaller systems in-between is not conclusive.

Not only does scale make recognizing smaller incised valleys more challenging, but it also makes linking imaged valley sections more difficult. Large paleovalleys are more easily mapped beneath the shallow Chesapeake and Delaware Bay environments and from borehole data along the peninsula (Twitchell et al., 1977; Shideler et al., 1984; Colman and Mixon, 1988; Knebel and Circé, 1988; Genau et al., 1994), which informs their offshore trajectories. The smaller paleovalleys of the central to northern Delmarva originate at or near the last interglacial

shoreline and do not extent far landward. In many cases, they represent the headwater regions of drainage networks that developed on the shelf. Work by Mattheus and Rodriguez (2014) touches on the morphologic complexities of small systems originating near interglacial shorelines; in particular, they show how their development can be highly influenced by downstream processes (e.g., discharge regimes of confluent valleys and associated tributary knickpoint migration). Relationships between watershed size, a proxy for paleodischarge, and valley dimension (e.g. depth of incision and width) appear less predictable for smaller systems.

This study made use of a large aggregate dataset to map the central to northern Delmarva inner continental shelves in an effort to improve existing stratigraphic models and delineate paleovalleys. The primary goals of this mapping effort were to: A) Improve stratigraphic control with additional core information and an expanded geo-chronologic framework for the central-northern Delmarva offshore; B) Reconcile existing disagreements on the nature of Delaware's inner continental shelf stratigraphy and paleodrainage (i.e., Belknap and Kraft, 1985, versus Williams, 1999); and C) Assess late Pleistocene Delmarva shelf paleodrainage.

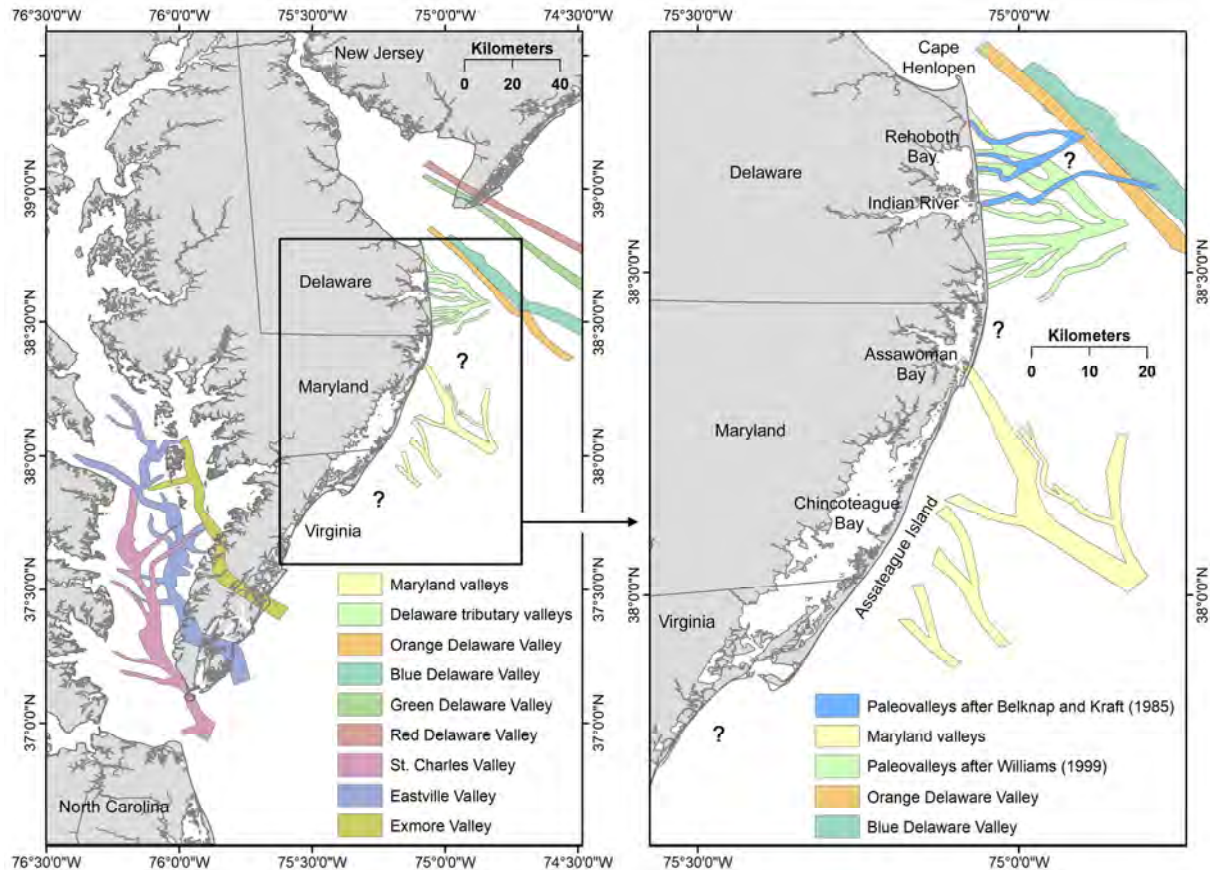


Figure 1) Map of the central-northern Delmarva Peninsula study area in context of the entire coastal margin, showing color-coded locations of previously mapped paleovalleys (references and age information in Table 1). The difference between Belknap and Kraft (1985) and Williams (1999) models of paleodrainage are shown in the inset map. Valley names are either adapted from the literature or assigned by location.

Table 1) Information on previously-mapped Delmarva offshore paleovalleys (shown in Figure 1). IDs for major incised valleys of the Delaware River are adapted from Childers (2014).

ID	Age	Reference(s)
‘Red Valley’	pre-MIS 6	McGeary et al. (1991); Krantz et al. (1993); Murphy (1996); Childers et al. (2019)
‘Green Valley’	MIS 6 (~150 ka)	McGeary et al. (1991); Krantz et al. (1993); Murphy (1996); Childers et al. (2019)
‘Orange Valley’	MIS 4 or 3 (30-70 ka)	McGeary et al. (1991); Krantz et al. (1993); Murphy (1996); Childers et al. (2019)
‘Blue Valley’	MIS 2 (~18 ka)	Twitchell et al., (1977); McGeary et al. (1991); Krantz et al. (1993); Murphy (1996); Childers et al. (2019)
Delaware shelf	MIS 2 (~18 ka)	Kraft (1971); Sheridan et al. (1974); Kraft (1977); Belknap & Kraft (1985)
Delaware shelf	MIS 2 (~18 ka) & older	Williams (1999)
Maryland shelf	MIS 2 (~18 ka) & older	Toscano et al. (1989)
Exmore Valley	pre-MIS 6	Colman & Mixon (1988); Colman et al. (1990); Foyle & Oertel (1992); Oertel & Foyle (1995)
Eastville Valley	MIS 6 (~150 ka)	Colman & Mixon (1988); Colman et al. (1990); Foyle & Oertel (1992); Oertel & Foyle (1995)
St. Charles Valley	MIS 2 (~18 ka)	Colman & Mixon (1988); Colman et al. (1990); Foyle & Oertel (1992); Oertel & Foyle (1995)

DATASET AND ANALYTICAL APPROACH

The BOEM-ASAP provided 60 offshore vibracores and 100s of trackline kilometers of high-resolution geophysical data, collected in 2015-2017 from Federal waters off the Delaware, Maryland, and Virginia coasts (Table 2). Cores, whose descriptive logs are provided in Appendix A, were subsampled for particle-size analysis. BOEM cores collected in 2016 were processed in-house (at the DGS; Table 3 and Appendix B) and BOEM cores collected in 2017 were processed by AECOM (Table 4). The Standard Sieve Method was used in both instances, yielding the following texture information: 1) Percent mud (silt and clay-sized particles), 2) Percent sand (particles between 63 µm and 2 mm), and Percent gravel (particles exceeding 2 mm in size). If samples were predominantly sandy (sand content >50%), relative proportions of very fine, fine, medium, coarse, and very coarse sand (as defined by the Wentworth size classification) were established. Statistical measures of median, mean, sorting, skewness, and kurtosis (as defined by Folk, 1974) were established by AECOM (Appendix C).

Newly-acquired data were integrated with existing core information (e.g. geologic logs) and seismic reflection datasets (from multiple origins). Much of the lithologic information was derived from United States Army Corps of Engineer (USACE) cores and State and Federal government reports. All data are housed in Delaware Geological Survey (DGS) data archives. Core information provided lithologic and, occasionally, chronologic mapping constraints. Interpretations of offshore geology benefited from stratigraphic templates of the Coastal Plain, where the landward extents of pre-Holocene geologic units are more accessible and abundantly documented (Ramsey, 1992, 1999, 2010, and 2011; Ramsey and Tomlinson, 2011 and 2012). Advances in geophysical imaging and processing capabilities (i.e., increased data resolution and positioning accuracies) have greatly improved our ability to map offshore stratigraphy; while some older datasets were revisited (e.g. Williams, 1999), they were not incorporated into this study given limitations of data quality and format (e.g., analog seismic reflection).

The analytical approach varied between the central Delmarva and Delaware offshore areas, primarily due to different data coverages (type and density; Figure 2). Mapping off the Maryland and Virginia portions of the shelf (i.e. the central Delmarva) had to rely more heavily on seismic reflection interpretations than that off Delaware's shores (i.e. the northern Delmarva), where stratigraphic assessment hinged on core picks because core data density averaged $\sim 1/\text{km}^2$. AAR-based age estimates of shells and radiocarbon dates from organics retrieved from core (peat, wood fragments, and shell material) refined chronostratigraphic interpretations (Wehmiller and Pellerito, 2015). The following subsections describe data coverages for the central and northern Delmarva regions separately, offering insight into dataset-specific management procedures.

Central Delmarva

A total of 1671.5 trackline kilometers of high-resolution ‘chirper’ seismic reflection data from the inner continental shelf between the Maryland-Delaware state line to offshore Exmore, Virginia, were obtained for stratigraphic mapping along the central Delmarva (Figure 2). The dataset, collected by the USGS in June to July of 2014 (as part of field activity 2014-002-FA),

utilized a 512i Edgetech subbottom profiler with a frequency range of 500 Hz to 12 kHz. Tracklines are coast-parallel and coast-perpendicular, the latter extending from around the toe of the shoreface to around 30 km offshore, where water depths are on the order of 25 m. Information on ~ 230 offshore vibracores from within the area of seismic coverage were compiled from Maryland Geological Survey reports (Toscano et al., 1989; Wells, 1994; Conkwright and Williams, 1996; Conkwright et al., 2000). Unfortunately, cores offered few stratigraphic insights as most had been collected across shoal fields (for sand assessment), limiting utility for characterizing deeper seismic reflections (e.g., the pre-Holocene). The lithologic information conveyed by Toscano and others (1989) and analysis of BOEM-ASAP cores (n=35; Table 2; Figure 3) was more useful in this regard.

Northern Delmarva

Stratigraphic mapping off the Delaware coast was based on information on over 450 offshore vibracores, including photographs, descriptions, texture data, and stratigraphic picks housed in DGS databases. This included 15 cores that were collected as part of the BOEM-ASAP (Figure 3). Core logs and texture information derived from these are provided in Appendix A; associated spatial data are shown in Table 2. The lithologic dataset was supplemented with 505 km of high-resolution ‘chirper’ seismic reflection data, collected in State waters off Delaware (within 3 miles from shore) by DNREC in 2013 and Federal waters by CB&I in 2015. The latter survey was conducted as part of the BOEM-ASAP, generating 203 trackline kilometers of ‘chirper’ data using an EdgeTech 3200 sub-bottom profiler with a 512i towfish and sweep frequency pulse of 0.7-12 kHz. Both datasets contain shore-perpendicular and shore-parallel tracklines and cover the area between toe of the shoreface and 15 km offshore, where water depths are on the order of 20 m.

Seismic Processing and Analysis

Sonar files were imported into Chesapeake Software’s SonarWiz 6 for processing and interpretation. While navigational offsets (i.e. forward/aft and port/starboard fish towpoint offsets) were accounted for during the original survey of offshore Delaware and included in the raw sub-bottom files (within a positioning accuracy of 10-15 cm), raw data had not been projected to any geoid/vertical datum. Seismic files (.jsf format) were subsequently batch-imported and bottom-tracked individually. Bottom tracking is the delineation of the seafloor position, which is generally the highest amplitude and first seismic reflection surface. A datum align function using the bottom track files and a 2015 USGS bathymetric DEM were applied for vertical correction, thereby factoring out tidal and wave effects. Depth conversions were based on two-way signal travel times and a 1,500 m/s sound velocity, the standard used for seawater and soft sediments (Chen et al., 1995; Colman et al., 1990; Knebel and Circé, 1988; Knebel et al., 1988; Shideler et al., 1984; Twitchell et al., 1977). Seafloor depths were checked against core information. Automatic gain control (AGC) and Time-varying Gain (TVG) functions enhanced the visibility of sub-surface reflections, proportionately amplifying weakened ones at depth.

All subsurface interpretations were based on basic stratigraphic principles (e.g. superposition and cross-cutting relationships) and the delineation of discordant stratal

relationships (e.g. erosional truncation and depositional onlap). Stratigraphic picks were made in SonarWiz 7, with the aid of imported core picks (where available), and exported as x, y, z files for subsequent mapping using ESRI's ArcGIS 10.5 software package. They were gridded into surfaces using the Natural Neighbor method of point interpolation. Picks on paleovalley bottoms (between opposite interfluves) were exported and used for delineation purposes, which took elevations and spatial trends (e.g. bearing) into account while connecting valley segments.

Radiocarbon Dates

The DGS Radiocarbon Date Database (DGSRDD) consists approximately 650 Holocene to Late Pleistocene dates primarily from the Delaware portion of the Peninsula but includes dates from Maryland and Virginia. The data were compiled from published dates, unpublished dates from various sources, and unpublished dates collected by the Delaware Geological Survey in support of surficial geologic mapping funded by STATEMAP, offshore geologic mapping, and sand resource studies funded by BOEM.

Dates were incorporated into the database only if there were supporting geographic locations (UTM northing and easting), sample elevation, and radiocarbon laboratory identifiers. In some cases, northing and easting were generated using GIS georeferenced site location maps and elevations determined by DEMs or topographic maps. Sample elevations were determined by recorded sample depths relative to land surface elevation. The elevations are in feet rather than meters as the land surface and sample elevations (or depths) were initially reported in feet and are recorded as such in the DGSRDD. Land surface elevations are highly variable in accuracy. Many onshore elevations were determined prior to the advent of LIDAR and extrapolated from topographic maps with five-foot contour intervals. Some offshore vibracore elevation tops also have issues with lack of documentation of tidal corrections and method of water depth determination (Mattheus and Ramsey, 2020).

Detailed surficial geologic mapping in Delaware provides the context for the Holocene deposits. Integrating landscape imagery (DEM's) and mapping of surficial deposits illuminates the distribution of Holocene age sediments and their surficial expression. Surficial mapping is conducted using a combination of hand auger borings, split spoon cores, and drillers and geologists logs from wells and geotechnical borings. Point data density is on the order of hundreds of points per 1:24,000 quadrangle. Mapping of coastal deposits (swamp, marsh, barrier) uses the same techniques with the addition of vibracores in the marsh environments. Mapping offshore relies upon vibracore data collected primarily for sand resource assessment for beach nourishment sands integrated with subbottom geophysical data and bathymetric DEM's. Density of point data is not as extensive as onshore but the supplemental geophysical data ground-truthed by cores offers a reliable map base and geologic context of the radiocarbon dates.

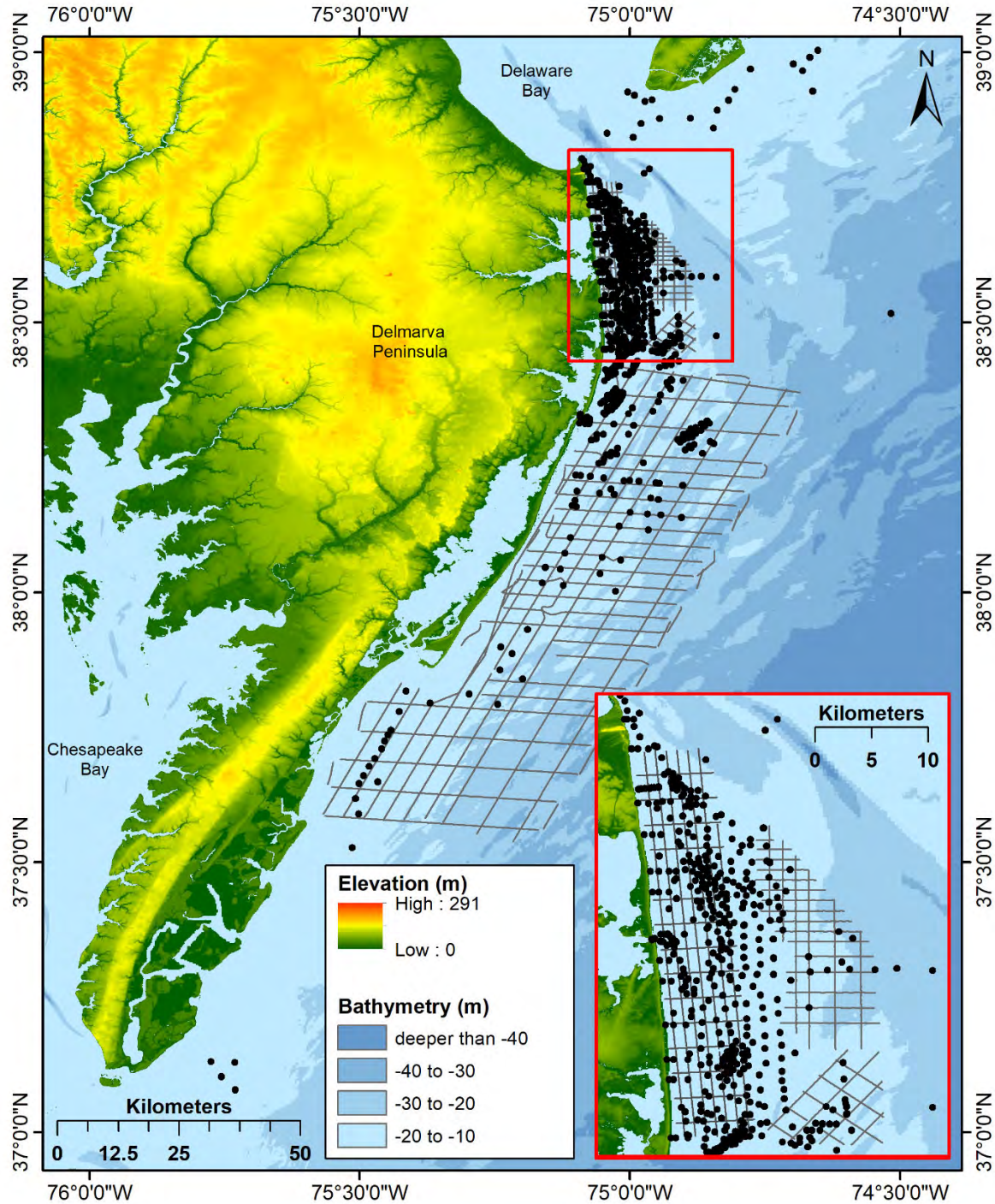


Figure 2) Data distribution map showing geophysical tracklines (gray) and sediment core locations (black) against FEMA-derived, color-coded elevation/bathymetry raster files. An inset (red outline) is shown of the offshore DE area, where core-data density is high (~1 core per km^2). Cores collected and studied specifically for the BOEM-ASAP are shown in Figure 3 and listed in Table 2.

Table 2) BOEM-ASAP core locations (UTM Zone 18N). Locations are plotted in Figure 3.

DGSID	Local ID	Northing (m)	Easting (m)	Elevation (ft.)	Length (ft.)
Zz82-63	VA-2015-01	4051062	428082	-48.5	17
Zz82-64	VA-2015-04	4056733	432677	-55.6	15.9
Zz82-65	VA-2015-04a	4056733	432677	-55.7	8.1
Zz82-66	VA-2015-05	4060652	433086	-48.6	13.5
Zz82-67	VA-2015-05a	4060652	433086	-48.8	10
Xh54-01	VA-2015-06	4198160	483322	-61.9	13.3
Xh54-02	VA-2015-06a	4198160	483322	-62	13.5
Zh31-01	VA-2015-08	4182877	478447	-67.8	16.5
Zg23-01	VA-2015-09	4184957	473834	-55.6	13.3
Zg23-02	VA-2015-09a	4184957	473834	-55.5	7.7
Uk12-01	MD-2015-01	4232411	502209.8	-62.5	19.3
Uj35-02	MD-2015-03	4228736	499020	-69.3	14.2
Uj35-03	MD-2015-03a	4228736	499020	-69	9.9
Uj43-01	MD-2015-04	4227044	496899	-52.2	17.5
Vj34-01	MD-2015-05	4219404	498220	-56.2	19.3
Wj22-01	MD-2015-07	4213018	495485	-45.4	18.3
Rk25-03	DE-2015-01	4258535	506592	-39.4	16.9
Ok52-05	DE-2015-03	4280133	502630	-51	12.7
Ok52-06	DE-2015-03a	4280133	502630	-51	4.9
Qk24-01	DE-2015-05	4267282	505356	-60.5	20
Pk54-01	DE-2015-07	4271818	505327	-62.4	13.7
Pl41-02	DE-2015-08	4274005	507417	-64.9	12.6
Pk13-01	DE-2016-01	4278034	503111	-57.4	17.3
Pk23-02	DE-2016-02	4277025	503188	-60	16.6
Pk23-03	DE-2016-03	4276196	503269	-59.4	18.5
Pk33-01	DE-2016-04	4275040	503338	-58.2	16.2
Zz82-68	VA-2016-01	4177555	461001	-47.6	17.9
Zz82-69	VA-2016-02	4176636	460564	-49.2	17.7
Zz82-70	VA-2016-03	4175402	459980	-51.5	16.8
Zz82-71	VA-2016-04	4170098	457439	-51.5	17.9

Zz82-72	VA-2016-05	4168248	456548	-45.2	17.7
Zz82-73	VA-2016-06	4166696	455813	-40.2	18.6
Pk13-02	DE-2017-01	4279480.5	504033.5	-54.1	19.8
Pk33-02	DE-2017-02	4275639.7	503556	-63.7	16.7
Pk43-01	DE-2017-03	4274146.1	503557	-58.8	19.5
Sk44-01	MD-2017-01	4245025.7	504585.7	-45.7	19.7
Sk53-01	MD-2017-02	4243001.7	503712.8	-42.7	18.5
Tj54-01	MD-2017-03	4234131.6	497841	-41.8	19.6
Tj35-01	MD-2017-04	4238291.7	499802.1	-43	19.2
Tk21-01	MD-2017-05	4240116.9	500606.9	-53.5	19.8
Vi14-01	MD-2017-06	4223687.1	490615.4	-43.2	19.8
Ui54-01	MD-2017-07	4224661.8	491081.5	-53.5	19.1
Tj15-01	MD-2017-08	4242445.8	499790.1	-39.4	19.4
Yh21-01	VA-2017-01	4194634.2	478985.5	-57.2	20
Yh41-01	VA-2017-02	4189866.3	478798.1	-57.5	19.3
Yh54-01	VA-2017-03	4187971.5	482490.3	-68.4	19.5
Yh22-01	VA-2017-04	4193300.2	480831.1	-49.8	19.7
Zz82-83	VA-2017-05	4103885.4	435114.4	-49.1	19.1
Zz82-84	VA-2017-06	4106565.8	432824.1	-40.4	20
Zz82-85	VA-2017-07	4109686	431161.8	-37.2	19.6
Zz82-86	VA-2017-08	4109434.2	435066.6	-42.9	19.3
Zz82-87	VA-2017-09	4153460.6	454583.8	-29.9	17
Zz82-88	VA-2017-10	4163500.9	455186.4	-36.4	19.1
Zz82-89	VA-2017-11	4183159.5	467466.4	-33	20
Zz82-90	VA-2017-12	4185607.9	463544.6	-29	19.9
Zz82-91	VA-2017-13	4171756.9	458373.3	-44.1	19.3
Zz82-92	VA-2017-14	4173791.9	459536.5	-43.1	19.3
Zz82-93	VA-2017-15	4181354.4	462387.8	-35.8	20
Zz82-94	VA-2017-16	4160434.3	455687.6	-31.5	18.5
Zz82-95	VA-2017-17	4167002.6	458823.6	-36.5	19.2

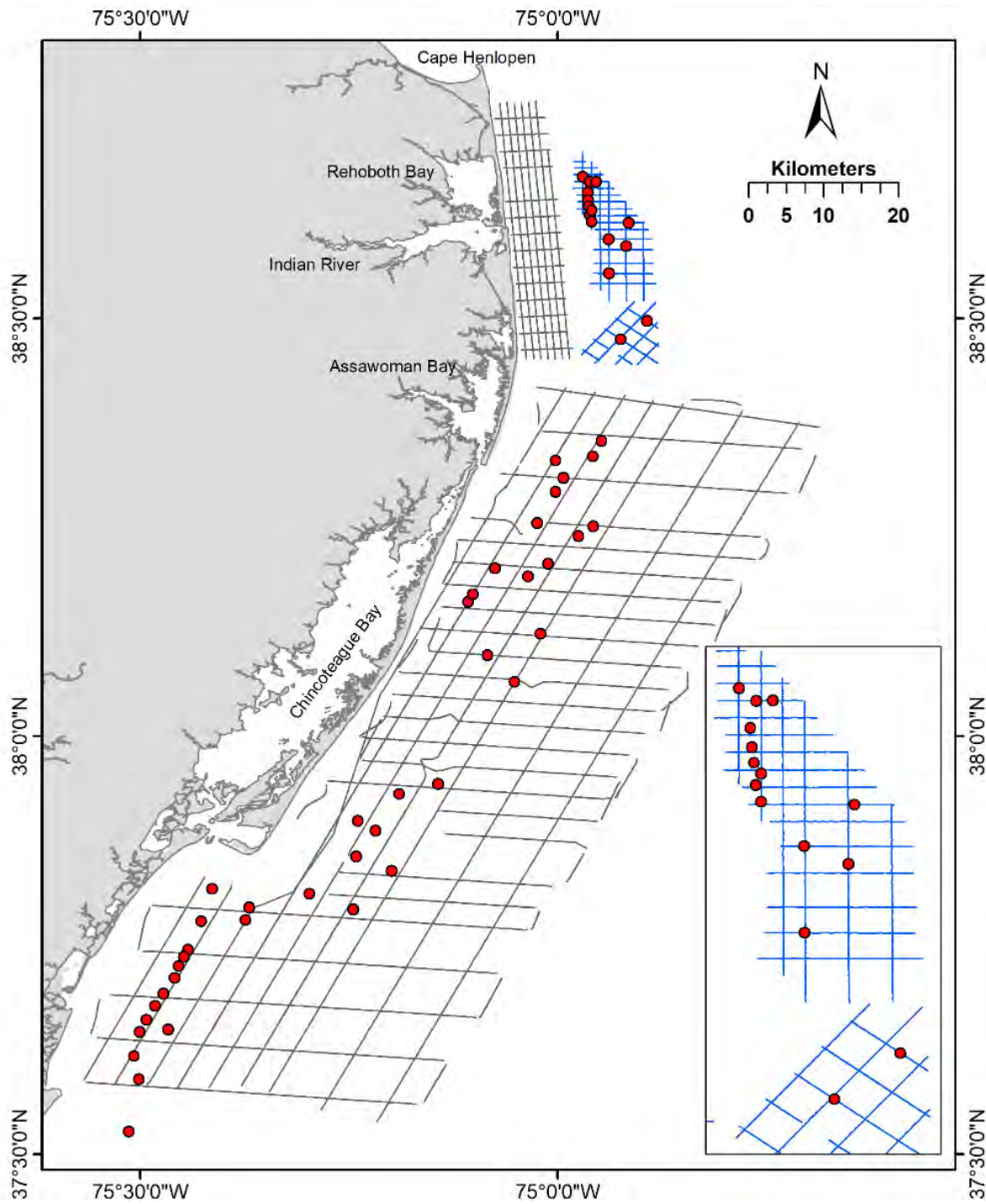


Figure 3) Map showing the distribution of cores collected as part of the BOEM-ASAP (red) against high-resolution 'chirper' seismic data coverage. Geophysical tracklines are shown in blue (for offshore Delaware).

Table 3) Inventory of texture samples that were collected for the BOEM project in 2016 and processed by the DGS in 2017. Start and stop depths are in feet.

Core	ID	Start	Stop	Core	ID	Start	Stop	Core	ID	Start	Stop
Pk13-01	115274.1	0.4	0.55	PK23-03	115283.2	6.4	6.55	Zz82-69	115296.2	16.7	16.85
Pk13-01	115274.2	1.5	1.65	PK23-03	115283.3	7.45	7.6	Zz82-69	115296.3	17.4	17.55
Pk13-01	115274.3	2.5	2.65	PK23-03	115283.4	8.5	8.65	Zz82-70	115297.1	0.25	0.4
Pk13-01	115274.4	3.5	3.65	PK23-03	115283.5	9.65	9.8	Zz82-70	115297.2	1.2	1.35
Pk13-01	115274.5	4.5	4.65	PK23-03	115284.1	10.5	10.65	Zz82-71	115301.1	0.6	0.75
Pk13-01	115275.1	5.5	5.65	PK23-03	115284.2	11.5	11.65	Zz82-71	115301.2	1.5	1.65
Pk13-01	115275.2	6.5	6.65	PK23-03	115284.3	12.65	12.8	Zz82-71	115301.3	2.5	2.65
Pk13-01	115275.3	7.5	7.65	PK23-03	115284.4	13.5	13.65	Zz82-71	115301.4	3.5	3.65
Pk13-01	115275.4	8.4	8.55	PK23-03	115284.5	14.5	14.65	Zz82-71	115301.5	4.3	4.45
Pk13-01	115275.5	9.5	9.65	PK23-03	115284.6	15.5	15.65	Zz82-71	115302.1	5.5	5.65
Pk13-01	115276.1	10.5	10.65	PK23-03	115284.7	16.3	16.45	Zz82-71	115302.2	6.5	6.65
Pk13-01	115276.2	11.5	11.65	PK33-01	115285.1	0.5	0.65	Zz82-71	115302.3	7.5	7.65
Pk13-01	115276.3	12.4	12.55	Zz82-68	115289.1	0.7	0.85	Zz82-71	115302.4	8.5	8.65
Pk13-01	115276.4	13.5	13.65	Zz82-68	115289.2	1.7	1.85	Zz82-71	115302.5	9.5	9.65
Pk13-01	115276.5	14.5	14.65	Zz82-68	115289.3	2.6	2.75	Zz82-71	115303.1	10.5	10.65
Pk13-01	115277.1	15.4	15.55	Zz82-68	115289.4	3.4	3.55	Zz82-71	115303.2	11.5	11.65
Pk13-01	115277.2	16.5	16.65	Zz82-68	115289.5	4.6	4.75	Zz82-71	115303.3	12.5	12.65
Pk13-01	115277.3	17.5	17.65	Zz82-68	115290.1	5.75	5.9	Zz82-71	115303.4	13.4	13.55
Pk13-01	115277.4	18.5	18.65	Zz82-68	115290.2	6.4	6.55	Zz82-71	115303.5	14.5	14.65
Pk13-01	115277.5	19.5	19.65	Zz82-68	115290.3	7.55	7.7	Zz82-71	115304.1	15.3	15.45
PK23-02	115278.1	3.5	3.65	Zz82-68	115290.4	8.7	8.85	Zz82-71	115304.2	16.5	16.65
PK23-02	115278.2	4.6	4.75	Zz82-68	115290.5	9.5	9.65	Zz82-71	115304.3	17.7	17.85
PK23-02	115279.1	5.5	5.65	Zz82-68	115291.1	10.5	10.65	Zz82-71	115304.4	18.4	18.55
PK23-02	115279.2	6.45	6.6	Zz82-68	115291.2	11.55	11.7	Zz82-71	115304.5	19	19.15
PK23-02	115279.3	7.5	7.65	Zz82-68	115291.3	12.55	12.7	Zz82-73	115309.1	1.6	1.75
PK23-02	115279.4	8.5	8.65	Zz82-68	115291.4	13.5	13.65	Zz82-73	115309.2	2.4	2.55
PK23-02	115279.5	9.5	9.65	Zz82-68	115291.5	14.85	15	Zz82-73	115309.3	3.6	3.75
PK23-02	115280.1	10.5	10.65	Zz82-68	115292.1	15.6	15.75	Zz82-73	115309.4	4.7	4.85
PK23-02	115280.2	11.5	11.65	Zz82-68	115292.2	16.5	16.65	Zz82-73	115310.1	5.4	5.55
PK23-02	115280.3	12.5	12.65	Zz82-69	115293.1	0.4	0.55	Zz82-73	115310.2	6.2	6.35
PK23-02	115280.4	13.5	13.65	Zz82-69	115293.2	1.5	1.65	Zz82-73	115310.3	7.8	7.95
PK23-02	115280.5	14.5	14.65	Zz82-69	115293.3	2.65	2.8	Zz82-73	115310.4	8.75	8.9
PK23-02	115281.1	15.5	15.65	Zz82-69	115293.4	3.4	3.55	Zz82-73	115310.5	9.35	9.5
PK23-02	115281.2	16.5	16.65	Zz82-69	115293.5	4.3	4.45	Zz82-73	115311.1	10.5	10.65
PK23-02	115281.3	17.4	17.55	Zz82-69	115294.1	5.5	5.65	Zz82-73	115311.2	11.5	11.65
PK23-02	115281.4	18.5	18.65	Zz82-69	115294.2	6.4	6.55	Zz82-73	115311.3	12.35	12.5
PK23-02	115281.5	19.1	19.25	Zz82-69	115294.3	7.25	7.4	Zz82-73	115311.4	13.4	13.55
PK23-03	115282.1	0.7	0.85	Zz82-69	115294.4	8.5	8.65	Zz82-73	115311.5	14.5	14.65
PK23-03	115282.2	1.4	1.55	Zz82-69	115295.1	10.5	10.65	Zz82-73	115312.1	15.5	15.65
PK23-03	115282.3	2.5	2.65	Zz82-69	115295.2	11.5	11.65	Zz82-73	115312.2	16.5	16.65
PK23-03	115282.4	3.5	3.65	Zz82-69	115295.3	12.05	12.2	Zz82-73	115312.3	17.5	17.65
PK23-03	115282.5	4.5	4.65	Zz82-69	115295.4	13.8	13.95	Zz82-73	115312.4	18.5	18.65
PK23-03	115283.1	5.5	5.65	Zz82-69	115296.1	15.6	15.75	Zz82-73	115312.5	19	19.15

Table 4) Inventory of texture samples that were collected for the BOEM project in 2017 and processed by AECOM in 2018. Start and stop depths are in feet.

Core	ID	Start	Stop	Core	ID	Start	Stop	Core	ID	Start	Stop
PK13-02	117227.2	1	1.2	Tj15-01	117266.3	7	7.2	Zz82-87	117303.4	17	17.2
PK13-02	117227.3	2	2.2	Tj15-01	117266.4	8	8.2	Zz82-87	117303.5	18	18.2
PK13-02	117227.4	3	3.2	Tj15-01	117266.5	9	9.2	Zz82-88	117304.1	0	0.2
PK13-02	117227.5	4	4.2	Tj15-01	117267.1	10	10.2	Zz82-88	117304.2	1	1.2
PK13-02	117228.1	8	8.2	Tj15-01	117267.2	11	11.2	Zz82-88	117304.3	2	2.2
PK13-02	117228.2	9	9.2	Tj15-01	117267.3	12	12.2	Zz82-88	117304.4	3	3.2
PK13-02	117229.1	10	10.2	Tj15-01	117267.4	13	13.2	Zz82-88	117304.5	4	4.2
PK13-02	117229.2	11	11.2	Tj15-01	117267.5	14	14.2	Zz82-88	117305.1	5	5.2
PK13-02	117229.3	12	12.2	Yh41-01	117273.1	0	0.2	Zz82-88	117305.2	6	6.2
PK13-02	117229.4	13	13.2	Yh41-01	117273.2	1	1.2	Zz82-88	117305.3	7	7.2
PK13-02	117229.5	14	14.2	Yh41-01	117273.3	2	2.2	Zz82-88	117305.4	8	8.2
PK13-02	117229.6	15	15.2	Yh41-01	117273.4	3	3.2	Zz82-88	117305.5	9	9.2
PK13-02	117229.7	16	16.2	Yh41-01	117273.5	4	4.2	Zz82-88	117306.1	10	10.2
PK43-01	117234.1	0	0.2	Yh41-01	117274.1	5	5.2	Zz82-88	117306.2	11	11.2
PK43-01	117234.2	1	1.2	Yh41-01	117274.2	6	6.2	Zz82-88	117306.3	12	12.2
PK43-01	117234.3	2	2.2	Yh41-01	117274.3	7	7.2	Zz82-88	117306.4	13	13.2
PK43-01	117234.4	3	3.2	Yh41-01	117274.4	8	8.2	Zz82-88	117306.5	14	14.2
PK43-01	117234.5	4	4.2	Yh41-01	117274.5	9	9.2	Zz82-88	117307.1	15	15.2
PK43-01	117235.1	5	5.2	Yh41-01	117275.1	10	10.2	Zz82-88	117307.2	16	16.2
PK43-01	117235.2	6	6.2	Yh41-01	117275.2	11	11.2	Zz82-88	117307.3	17	17.2
PK43-01	117235.3	7	7.2	Yh41-01	117275.3	12	12.2	Zz82-88	117307.4	18	18.2
PK43-01	117235.4	8	8.2	Yh41-01	117275.4	13	13.2	Zz82-88	117307.5	19	19.2
PK43-01	117235.5	9	9.2	Yh41-01	117275.5	14	14.2	Zz82-89	117308.1	0	0.2
PK43-01	117236.1	10	10.2	Yh41-01	117276.1	15	15.2	Zz82-89	117308.2	1	1.2
PK43-01	117236.2	11	11.2	Yh41-01	117276.2	16	16.2	Zz82-89	117308.3	2	2.2
PK43-01	117236.3	12	12.2	Yh41-01	117276.3	17	17.2	Zz82-89	117308.4	3	3.2
PK43-01	117236.4	13	13.2	Yh54-01	117277.1	0	0.2	Zz82-89	117308.5	4	4.2
PK43-01	117236.5	14	14.2	Yh54-01	117277.2	1	1.2	Zz82-89	117309.1	5	5.2
PK43-01	117237.1	15	15.2	Yh54-01	117277.3	2	2.2	Zz82-89	117309.2	6	6.2
PK43-01	117237.2	16	16.2	Yh54-01	117277.4	3	3.2	Zz82-89	117309.3	7	7.2
PK43-01	117237.3	17	17.2	Yh54-01	117277.5	4	4.2	Zz82-89	117309.4	8	8.2
PK43-01	117237.4	18	18.2	Yh54-01	117278.1	5	5.2	Zz82-89	117309.5	9	9.2
PK43-01	117237.5	19	19.2	Yh54-01	117278.2	6	6.2	Zz82-89	117310.1	10	10.2
Sk44-01	117238.1	0	0.2	Yh54-01	117278.3	7	7.2	Zz82-89	117310.2	11	11.2
Sk44-01	117238.2	1	1.2	Yh54-01	117278.4	8	8.2	Zz82-89	117310.3	12	12.2
Sk44-01	117238.3	2	2.2	Yh54-01	117278.5	9	9.2	Zz82-89	117311.1	15.3	15.5
Sk44-01	117238.4	3	3.2	Yh54-01	117279.1	10	10.2	Zz82-89	117311.2	16	16.2

Sk44-01	117238.5	4	4.2	Yh54-01	117279.2	11	11.2	Zz82-90	117312.1	0	0.2
Sk44-01	117239.1	5	5.2	Yh54-01	117279.3	12	12.2	Zz82-90	117312.2	1	1.2
Sk44-01	117239.2	6	6.2	Yh54-01	117279.5	14	14.2	Zz82-90	117312.3	2	2.2
Sk44-01	117239.3	7	7.2	Yh54-01	117280.1	15	15.2	Zz82-90	117312.4	3	3.2
Sk44-01	117239.4	8	8.2	Yh54-01	117280.2	16	16.2	Zz82-90	117312.5	4	4.2
Sk44-01	117239.5	9	9.2	Yh54-01	117280.3	17	17.2	Zz82-90	117313.1	5	5.2
Sk44-01	117240.1	10	10.2	Yh54-01	117280.4	18	18.2	Zz82-90	117313.2	6	6.2
Sk44-01	117240.2	11	11.2	Yh54-01	117280.5	19	19.2	Zz82-90	117313.3	7	7.2
Sk44-01	117240.3	12	12.2	Yh22-01	117281.1	0	0.2	Zz82-90	117313.4	8	8.2
Sk44-01	117240.4	13	13.2	Yh22-01	117281.2	1	1.2	Zz82-90	117313.5	9	9.2
Sk44-01	117240.5	14	14.2	Yh22-01	117281.3	2	2.2	Zz82-91	117318.2	12	12.2
Sk44-01	117241.1	15	15.2	Yh22-01	117282.1	8	8.2	Zz82-91	117318.3	13	13.2
Sk44-01	117241.2	16	16.2	Yh22-01	117282.2	9.5	9.7	Zz82-91	117318.4	14	14.2
Sk44-01	117241.3	17	17.2	Yh22-01	117283.1	10	10.2	Zz82-91	117319.1	15	15.2
Sk44-01	117241.4	18	18.2	Yh22-01	117283.2	11	11.2	Zz82-91	117319.2	16	16.2
Sk44-01	117241.5	19	19.2	Yh22-01	117283.3	12	12.2	Zz82-91	117319.3	17	17.2
SK53-01	117242.2	0	0.2	Zz82-83	117285.2	0	0.2	Zz82-91	117319.4	18	18.2
SK53-01	117242.3	1	1.2	Zz82-83	117285.3	1	1.2	Zz82-91	117319.5	19	19.2
SK53-01	117242.4	2	2.2	Zz82-83	117285.4	2	2.2	Zz82-92	117320.1	0	0.2
SK53-01	117242.5	3	3.2	Zz82-83	117285.5	3	3.2	Zz82-92	117320.2	1	1.2
SK53-01	117242.6	4	4.2	Zz82-83	117285.6	4	4.2	Zz82-92	117320.3	2	2.2
SK53-01	117243.1	5	5.2	Zz82-83	117286.1	5	5.2	Zz82-92	117320.4	3	3.2
SK53-01	117243.2	6	6.2	Zz82083	117286.2	6	6.2	Zz82-92	117320.5	4	4.2
SK53-01	117243.3	7	7.2	Zz82-83	117286.3	7	7.2	Zz82-92	117321.1	5	5.2
SK53-01	117243.4	8	8.2	Zz82-83	117286.4	8	8.2	Zz82-92	117321.2	6	6.2
SK53-01	117243.5	9	9.2	Zz82-83	117286.5	9	9.2	Zz82-92	117321.3	7	7.2
SK53-01	117244.1	10	10.2	Zz82-83	117287.1	12	12.2	Zz82-92	117321.4	8	8.2
SK53-01	117244.2	11	11.2	Zz82-83	117287.2	13	13.2	Zz82-92	117321.5	9	9.2
SK53-01	117244.3	12	12.2	Zz82-83	117288.1	15	15.2	Zz82-92	117322.5	13	13.2
SK53-01	117244.4	13	13.2	Zz82-83	117288.2	16	16.2	Zz82-92	117322.6	14	14.2
SK53-01	117244.5	14	14.2	Zz82-83	117288.3	17	17.2	Zz82-92	117323.1	15	15.2
SK53-01	117244.6	15	15.2	Zz82-83	117288.4	18	18.2	Zz82-92	117323.2	16	16.2
SK53-01	117244.7	16	16.2	Zz82-84	117289.3	0	0.2	Zz82-92	117323.3	17	17.2
Tj54-01	117245.2	0	0.2	Zz82-84	117289.4	1	1.2	Zz82-94	117328.1	0	0.2
Tj54-01	117245.3	1	1.2	Zz82-84	117289.5	2	2.2	Zz82-94	117328.2	1	1.2
Tj54-01	117245.4	2	2.2	Zz82-84	117289.6	3	3.2	Zz82-94	117328.3	2	2.2
Tj54-01	117245.5	3	3.2	Zz82-84	117289.7	4	4.2	Zz82-94	117328.4	3	3.2
Tj54-01	117245.6	4	4.2	Zz82-84	117290.2	5	5.2	Zz82-94	117328.5	4	4.2
Tj54-01	117246.2	5	5.2	Zz82-84	117290.3	6	6.2	Zz82-94	117329.2	5	5.2
Tj54-01	117246.3	6	6.2	Zz82-84	117290.4	7	7.2	Zz82-94	117329.3	6	6.2
Tj54-01	117246.4	7	7.2	Zz82-84	117290.5	8	8.2	Zz82-94	117329.4	7	7.2
Tj54-01	117246.5	8	8.2	Zz82-84	117290.6	9	9.2	Zz82-94	117329.5	8	8.2

Tj54-01	117246.6	9	9.2	Zz82-84	117291.1	10	10.2	Zz82-94	117329.6	9	9.2
Tj54-01	117247.2	10	10.2	Zz82-84	117291.2	11	11.2	Zz82-84	117330.1	10	10.2
Tj54-01	117247.3	11	11.2	Zz82-84	117291.3	12	12.2	Zz82-94	117330.2	11	11.2
Tj54-01	117247.4	12	12.2	Zz82-84	117291.4	14	14.2	Zz82-94	117330.3	12	12.2
Tj54-01	117247.5	13	13.2	Zz82-84	117291.5	13	13.2	Zz82-94	117330.4	13	13.2
Tj54-01	117247.6	14	14.2	Zz82-85	117292.1	0	0.2	Zz82-94	117330.5	14	14.2
Tj54-01	117248.1	15	15.2	Zz82-85	117292.2	1	1.2	Zz82-94	117330.6	15	15.2
Tj54-01	117248.2	16	16.2	Zz82-85	117292.3	2	2.2	Zz82-95	117331.1	0	0.2
Tj54-01	117248.3	17	17.2	Zz82-85	117292.4	3	3.2	Zz82-95	117331.2	1	1.2
Tj35-01	117249.2	0	0.2	Zz82-85	117292.5	4	4.2	Zz82-95	117331.3	2	2.2
Tj35-01	117249.3	1	1.2	Zz82-85	117293.1	5	5.2	Zz82-95	117331.4	3	3.2
Tj35-01	117249.4	2	2.2	Zz82-85	117293.2	6	6.2	Zz82-95	117331.5	4	4.2
Tj35-01	117249.5	3	3.2	Zz82-85	117293.3	7	7.2	Zz82-95	117332.1	5	5.2
Tj35-01	117249.6	4	4.2	Zz82-85	117293.4	8	8.2	Zz82-95	117332.2	6	6.2
Tj35-01	117250.2	5	5.2	Zz82-85	117293.5	9	9.2	Zz82-95	117332.3	7	7.2
Tj35-01	117250.3	6	6.2	Zz82-85	117294.1	10	10.2	Zz82-95	117332.4	8	8.2
Tj35-01	117250.4	7	7.2	Zz82-85	117294.2	11	11.2	Zz82-95	117333.1	10.1	10.3
Tj35-01	117250.5	8	8.2	Zz82-85	117294.3	12	12.2	Zz82-95	117333.2	11	11.2
Tj35-01	117250.6	9	9.2	Zz82-85	117294.4	13	13.2	Zz82-95	117333.3	12	12.2
Tj35-01	117251.1	10	10.2	Zz82-85	117294.5	14	14.2	Zz82-95	117333.4	13	13.2
Tj35-01	117251.2	11	11.2	Zz82-85	117295.1	16	16.2	Zz82-95	117333.5	14	14.2
Tj35-01	117251.3	12	12.2	Zz82-85	117295.2	18	18.2	Zz82-95	117334.1	15	15.2
Tj35-01	117251.4	13	13.2	Zz82-85	117295.3	19	19.2	Zz82-95	117334.2	16	16.2
Tj35-01	117251.5	14	14.2	Zz82-86	117296.2	0	0.2	Zz82-95	117334.3	17	17.2
Tj35-01	117252.1	15	15.2	Zz82-86	117296.3	1	1.2	Zz82-95	117334.4	18	18.2
Tj35-01	117252.2	16	16.2	Zz82-86	117296.4	2	2.2	Zz82-95	117334.5	19	19.2
Tj35-01	117252.3	17	17.2	Zz82-86	117296.5	4	4.2	Oj12-02	104498.2	12	12.2
Tj35-01	117252.4	18	18.2	Zz82-86	117297.1	5	5.2	Oj12-02	104496.1	2	2.2
Tj35-01	117252.5	19	19.2	Zz82-86	117297.2	6	6.2	Oj12-02	104496.2	4	4.2
TK21-01	117253.1	4	4.2	Zz82-86	117297.3	9	9.2	Oj12-02	104497.1	6	6.2
TK21-01	117254.1	5	5.2	Zz82-86	117298.1	10	10.2	Oj12-02	104497.2	8	8.2
TK21-01	117254.2	6	6.2	Zz82-86	117298.2	11	11.2	Oj12-02	104498.1	10	10.2
TK21-01	117254.3	7	7.2	Zz82-86	117298.3	12	12.2	Oj33-02	104476.3	6	6.2
TK21-01	117254.4	8	8.2	Zz82-86	117298.4	13	13.2	Oj33-02	104475.1	2	2.2
TK21-01	117254.5	9	9.2	Zz82-86	117298.5	14	14.2	Oj33-02	104475.2	4	4.2
TK21-01	117255.1	10	10.2	Zz82-86	117299.1	15	15.2	Oj34-06	104501.4	0	0.2
TK21-01	117255.2	11	11.2	Zz82-86	117299.2	16	16.2	Oj34-06	104504.1	16	16.2
TK21-01	117255.3	12	12.2	Zz82-86	117299.3	17	17.2	Oj34-06	104503.2	14	14.2
TK21-01	117255.4	13	13.2	Zz82-86	117299.4	18	18.2	Oj34-06	104503.1	12	12.2
TK21-01	117255.5	14	14.2	Zz82-86	117299.5	19	19.2	Oj34-06	104502.3	10	10.2
TK21-01	117256.1	15	15.2	Zz82-87	117300.1	0	0.2	Oj34-06	104502.2	8	8.2
TK21-01	117256.2	16	16.2	Zz82-87	117300.2	1	1.2	Oj34-06	104502.1	6	6.2

TK21-01	117256.3	17	17.2	Zz82-87	117300.3	2	2.2	Oj34-06	104501.6	4	4.2
TK21-01	117256.4	18	18.2	Zz82-87	117300.4	3	3.2	Oj34-06	104501.5	2	2.2
Vi14-01	117258.1	8	8.2	Zz82-87	117300.5	4	4.2	Oj44-01	104509.3	0	0.2
Vi14-01	117258.2	9	9.2	Zz82-87	117301.1	5	5.2	Oj44-01	104509.4	2	2.2
Vi14-01	117259.1	10	10.2	Zz82-87	117301.2	6	6.2	Oj44-02	104511.2	12	12.2
Vi14-01	117259.2	11	11.2	Zz82-87	117301.3	7	7.2	Oj44-02	104510.1	4	4.2
Vi14-01	117259.3	12	12.2	Zz82-87	117301.4	8	8.2	Oj44-02	104510.2	6	6.1
Vi14-01	117259.4	13	13.2	Zz82-87	117301.5	9	9.2	Oj44-02	104510.3	8	8.2
Tj15-01	117265.1	0	0.2	Zz82-87	117302.1	10	10.2	Oj44-02	104511.1	10	10.2
Tj15-01	117265.2	1	1.2	Zz82-87	117302.2	11	11.2	Oj34-04	104479.3	4	4.2
Tj15-01	117265.3	2	2.2	Zz82-87	117302.3	12	12.2	Oj34-04	104479.2	2	2.2
Tj15-01	117265.4	3	3.2	Zz82-87	117302.4	13	13.2	Oj34-04	104479.1	0	0.2
Tj15-01	117265.5	4	4.2	Zz82-87	117302.5	14	14.2	Oj34-04	104480.2	8	8.2
Tj15-01	117266.1	5	5.2	Zz82-87	117303.2	15	15.2	Oj34-04	104480.3	10	10.2
Tj15-01	117266.2	6	6.2	Zz82-87	117303.3	16	16.2	Oj34-04	104480.4	6	6.2

RESULTS AND DISCUSSION

Shallow seismic framework

Seismic reflection ('chirper') images of the inner continental shelf capture the stratigraphy of the upper 10-20 m of the subsurface; depth penetration and seismic image quality appear to vary as a function of water depth and geology (i.e., muddy versus sandy seafloor compositions).

Subsurface resolution was observed to be poorest across shoaling areas and close to shore, where strong acoustic echoes are caused by highly-reflective sandy bottoms, obscuring deeper reflections; shallow water depths also lessen the imaging window before arrival of the bottom multiple, prompting stronger reliance on core records. Only one stratigraphic horizon is continuously traced across the shallow subsurface from the datasets studied here. This high-amplitude reflection surface was previously mapped across the Maryland inner continental shelf by Toscano and others (1989; Figure 4). It is therefore also referred to as the 'M1' reflector. It represents a time-transgressive contact separating Tertiary and Quaternary strata, which are either Pleistocene or Holocene above the contact, depending on location. Offshore data and stratigraphic insights from work along the Coastal Plain and barriers document the regional character of this surface (Ramsey, 1999 and 2010). M1 is gently seaward-dipping (~0.5 m/km) and maps the upper bounding surface of the late Tertiary Beaverdam Formation. This unit, whose base is not resolved in seismic reflection data (Figures 3 and 4), is around 30 m thick across the lower Coastal Plain and consists of silty, fluviodeltaic sands and gravels (Ramsey, 2010). Across Delaware's inner shelf, it is occasionally found cropping out on the seafloor amidst thin and discontinuous shoal sands (Mattheus et al., 2020; Figure 5). The Beaverdam Formation's internal seismic reflection character, which contains hummocky patterns and signs of lateral accretion, distinguish it from overlying estuarine units (e.g. Sinepuxent Formation;

Figure 3) and valley fills (Figure 4), defined by horizontal to slightly inclined or wavy parallel reflections indicative of accretionary processes. The Sinepuxent, a late Pleistocene lagoonal complex mapped close to shore and within the lower Coastal Plain along the length of the study area (Ramsey, 1999 and 2010; Ramsey and Tomlinson, 2012) is distinctly characterized by horizontal, parallel beds (Figure 4). It is capped by surface M2, above which sediments are Holocene in age (if present).

While the M1 reflector is mapped across the entire area of data coverage (Figure 6), obscured only beneath thick shoal bodies and shallow-water areas, there is a fundamental difference between its manifestations off the Delaware coast and that off the central Delmarva. The M1 reflector off Delaware represents mostly an amalgam of surfaces across paleovalley interfluves (Figure 5). In particular, this is where the base of the Quaternary and the base of the Holocene are coincidental. A model representing the interpolated M1 surface shows little topographic variance across most of the central Delmarva. Offshore of Chincoteague Bay, for example, few indicators of incision into the surface are imaged (Figure 7). Paleovalleys here are not deeply enough incised for the M1 structure map to reveal their locations. Many of these valleys incised to the depth of the M1 surface and no deeper (Figure 4). Paleovalley incision into the Beaverdam Formation off the Delaware coast contrasts this trend. The extremely shallow nature of the M1 surface here, which is <15 m across much of the inner shelf, is deeply incised by shelf valleys (with depths >40 m in some cases; Figures 5 and 7). Across interfluves, the M1 reflector is occasionally coincidental with the modern seafloor, signaling the absence of Quaternary sediment at these locations (and an overall thin cover across much of the Delaware shelf). Figure 5 shows seismic interpretations constrained by core data off the Delaware coast. Cores penetrating the valley interfluves (DGS97-47 and BOEM_DE2015-07) sampled only Beaverdam Formation and its reworked surface deposits (a transgressive gravel lag), while core BOEM-DE2015-05 penetrated a compound valley fill, sampling estuarine materials of both Pleistocene and Holocene age. The M1 surface across the interfluvium thus represents an amalgam of these two unconformities. Stratigraphic examples shown here typify the northern Delmarva framework, where the M1 reflector is topographically varied (due to the presence of paleovalleys), unlike elsewhere along the Delmarva.

While 25 cores off Delaware sampled the Beaverdam Formation at the seafloor and many more encountered it at shallow depths (Mattheus et al., 2020), none from offshore Maryland or Virginia did. This is partly due to the fact that most coring endeavors off Maryland have predominantly targeted large shoal bodies for texture/resource analysis, failing to penetrate deeply enough to establish this stratigraphic pick (Wells, 1994; Conkwright and Williams, 1996; Conkwright et al., 2000). The Beaverdam Formation here is inferred to exist beneath thicker Quaternary sediment packages based on seismic correlation alone. An isopach map, created from the interpolated M1 surface and a dataset of modern bathymetry (FEMA-derived) captures variances in Quaternary sediment thickness (Figure 8). High values (up to around 28 m) are encountered close to the barrier shoreline, particularly off the central Delmarva, where major offshore shoal bodies are situated and where deeply incised paleovalleys are found. Low values (and zero values) occur where cores have sampled the Beaverdam at the seafloor or just beneath

thin sheet sands or gravel lag deposits. Contrary to this, the shelf area off Chincoteague Island (most of the central study area) shows Quaternary sediment thickness to vary as a function of shoal thickness, given that valleys here did not incise deeper than the M1 surface (Figure 4). The Delaware offshore and the southernmost portion of the study area (south of Chincoteague), where modern sediment cover is thin (and in the former case, discontinuous), shows Quaternary sediment thickness to vary mainly as a function of valley location (Figure 8). Thickness maxima here are on the order of those further south.

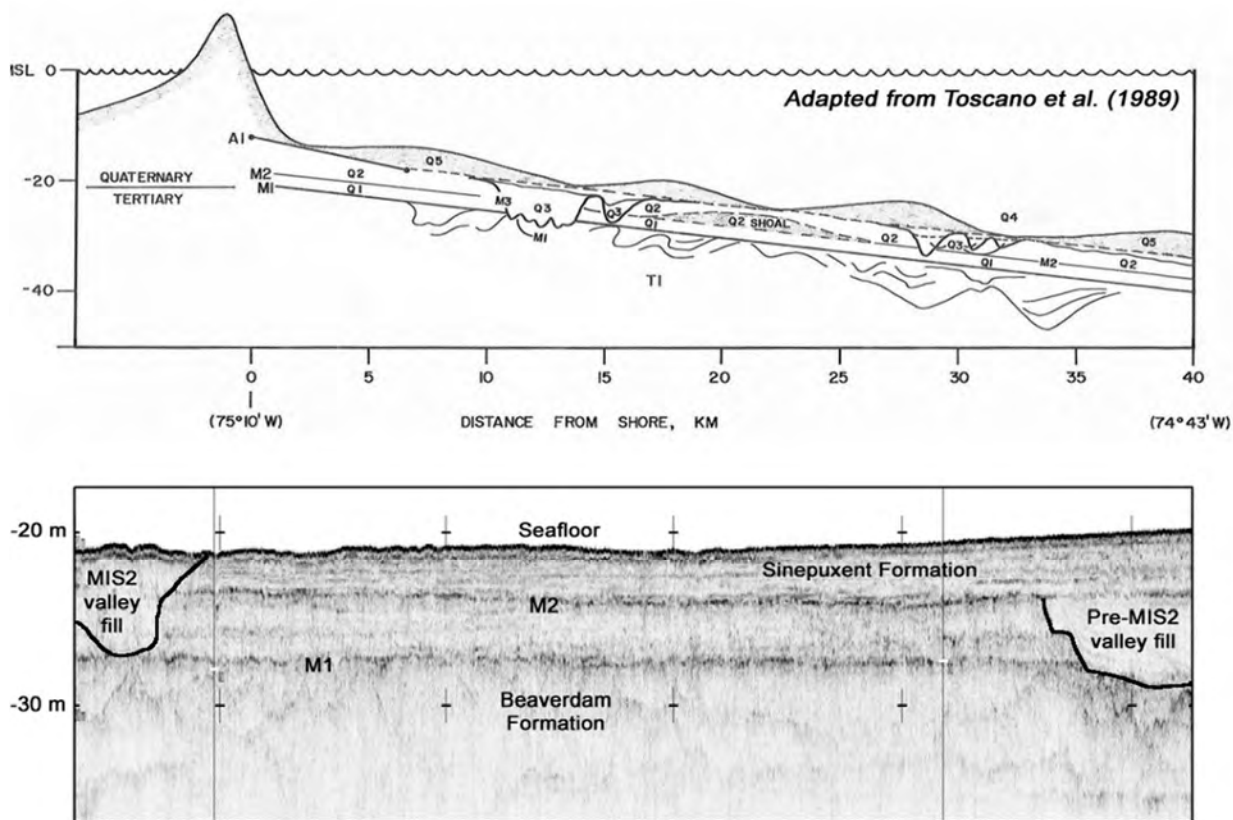


Figure 4) Schematic adapted from Toscano and others (1989), showing the interpreted shallow stratigraphic framework in dip orientation off Maryland (landward is to the left), along with an example seismic section in strike orientation (USGS 2014 dataset; corresponds to Figure 12b, whose location is shown in Figure 11) with surfaces M1 and M2 labeled. Shown are also two valley fills that, based on their stratigraphic association, represent two different episodes of incision. This sort of juxtaposition is not distinctly addressed in the model by Toscano and others. Cores sample the Sinepuxent Formation, a late Pleistocene estuarine unit (Ramsey, 2010), above M2.

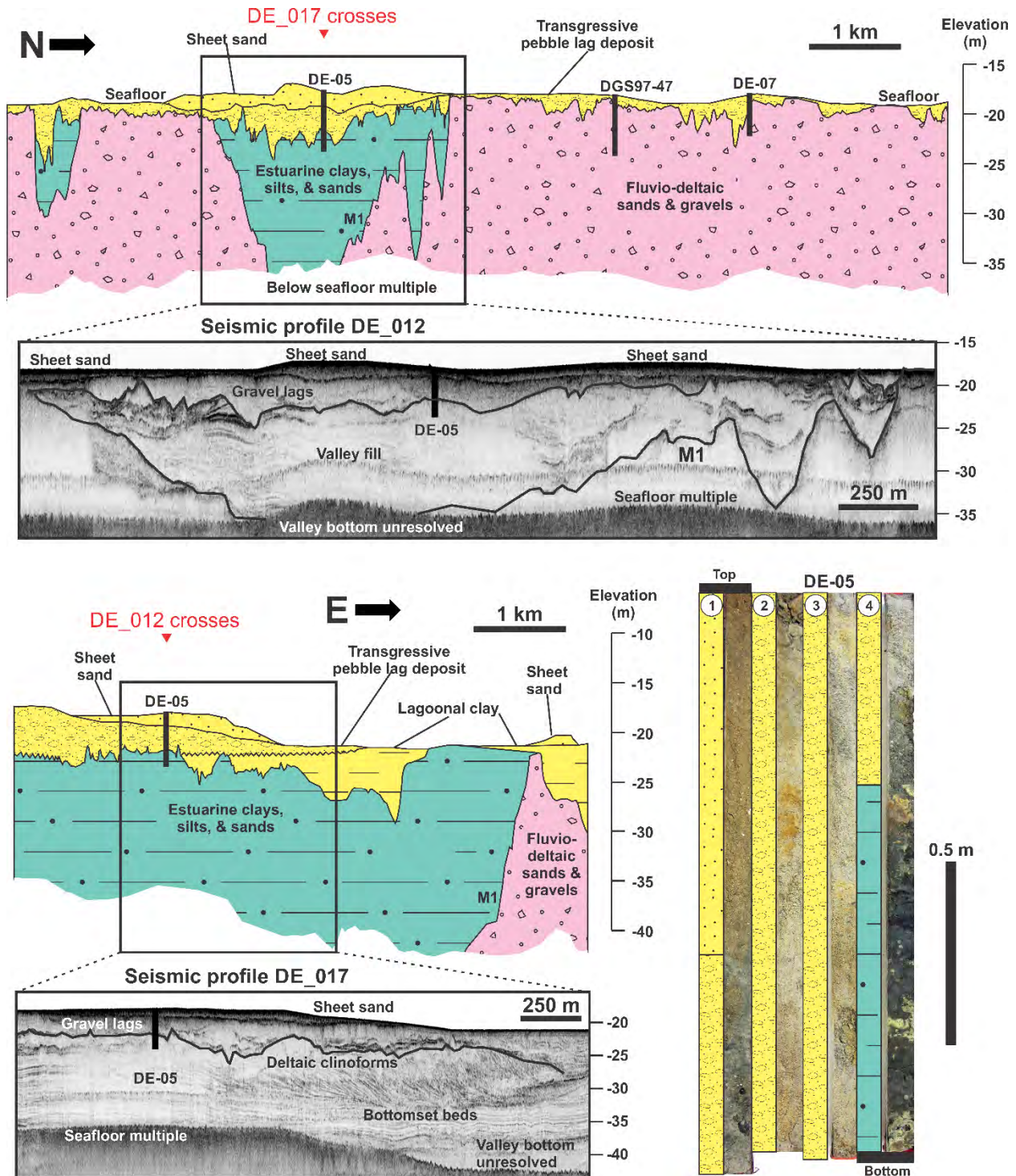


Figure 5). Geologic cross sections based on core and reflection data. Locations are shown in Figure 6. They intersect a paleovalley in strike (a) and dip (b) orientation. Core photos are also shown of BOEM DE_2015-05 (DGSID = Qk24-01), collected from the center of the paleovalley (in aerial view), as part of the Atlantic Sand Assessment Project.

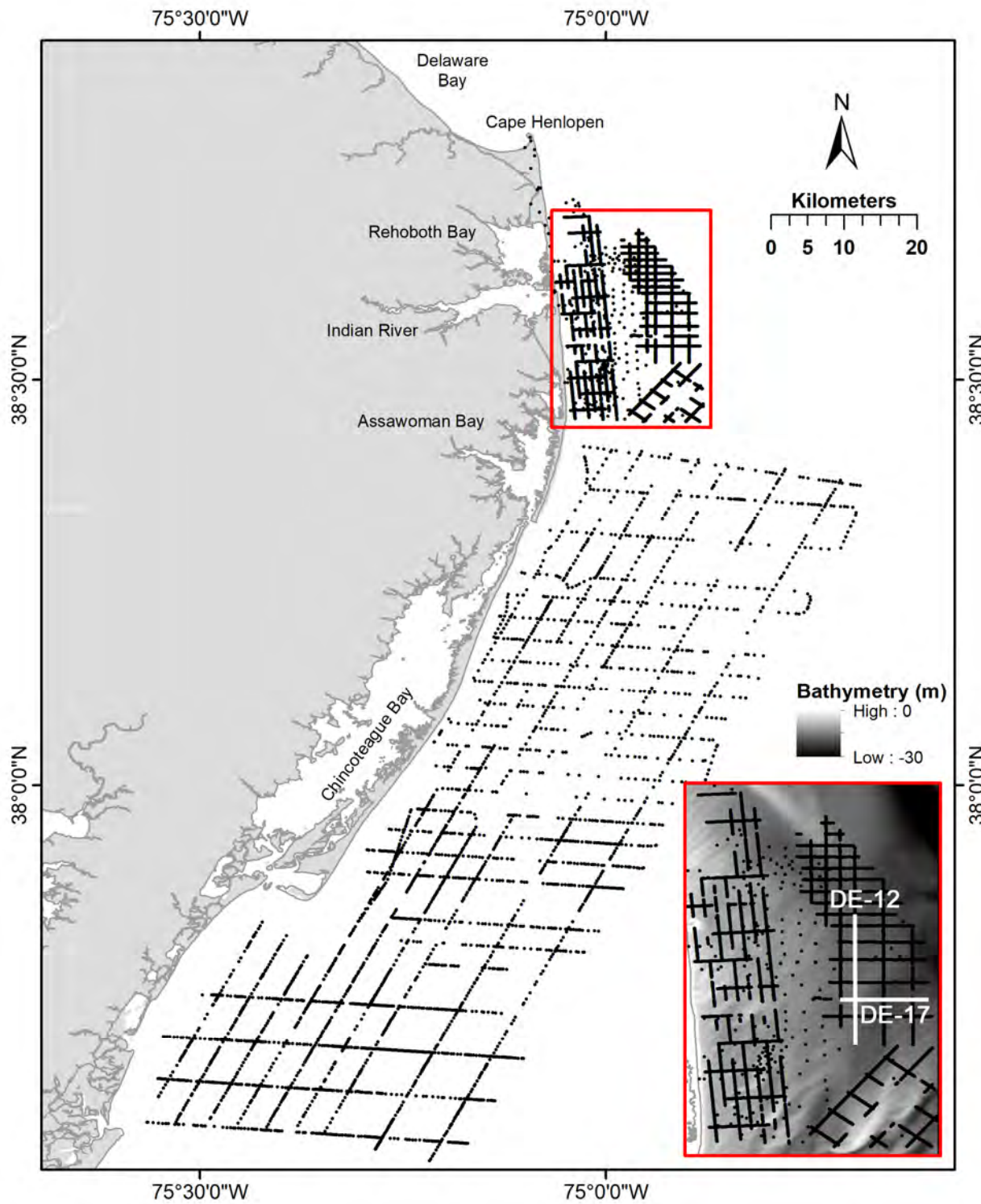


Figure 6) Map showing the distribution of M1 stratigraphic picks from seismic reflection and core data. An inset map (red outline) zooms in on offshore Delaware and shows pick distribution in context of seafloor elevation. Notable is the absence of M1 picks across major shoaling areas (i.e. sand ridges and close to shore), where the high-reflectance seafloor multiple obscures stratigraphic analysis.

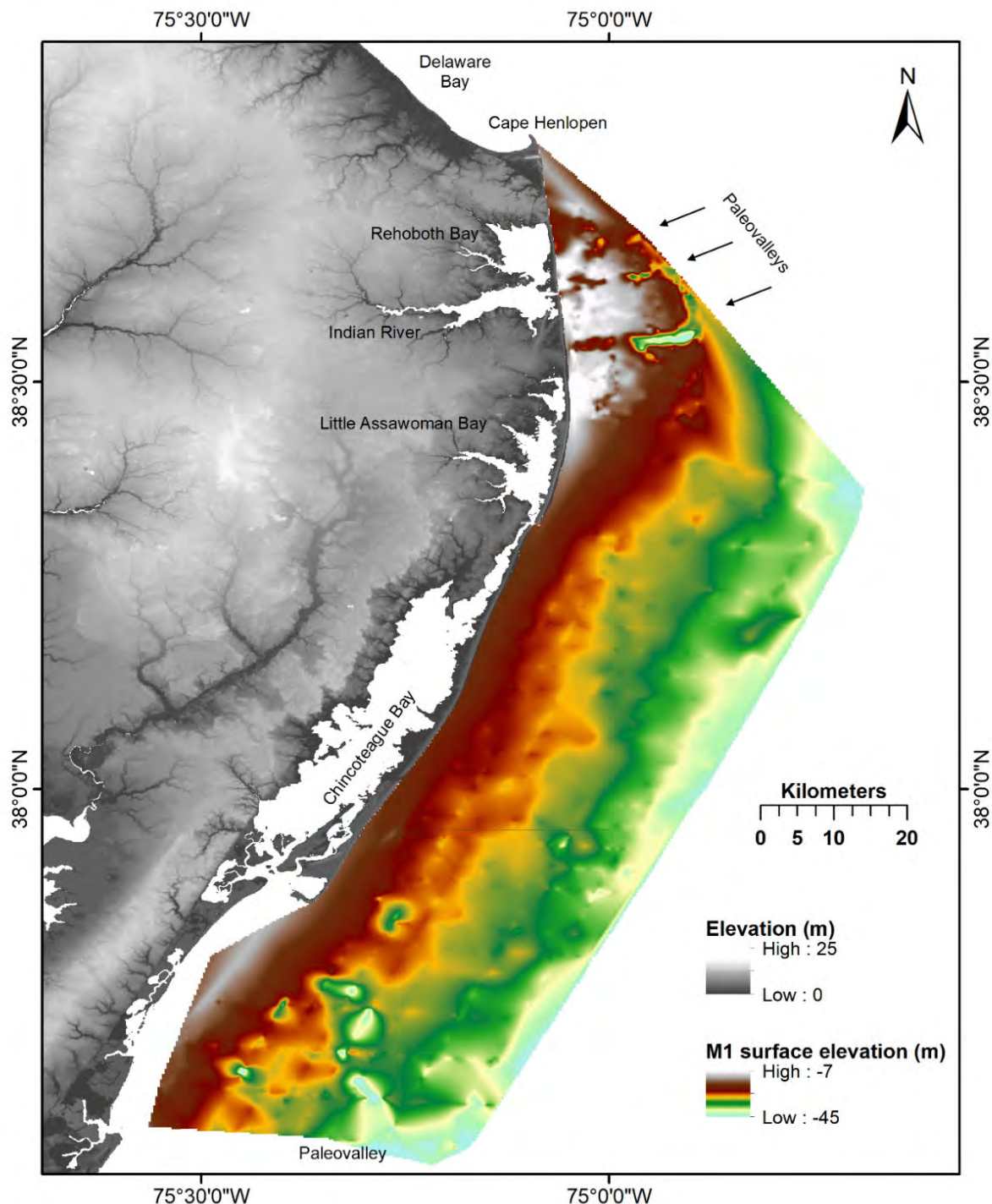


Figure 7) Surface map of gridded M1 stratigraphic picks (shown in Figure 4) using the Natural Neighbor method of interpolation. This surface represents the unconformity separating the late Tertiary Beaverdam Formation from overlying Pleistocene and Holocene sediments.

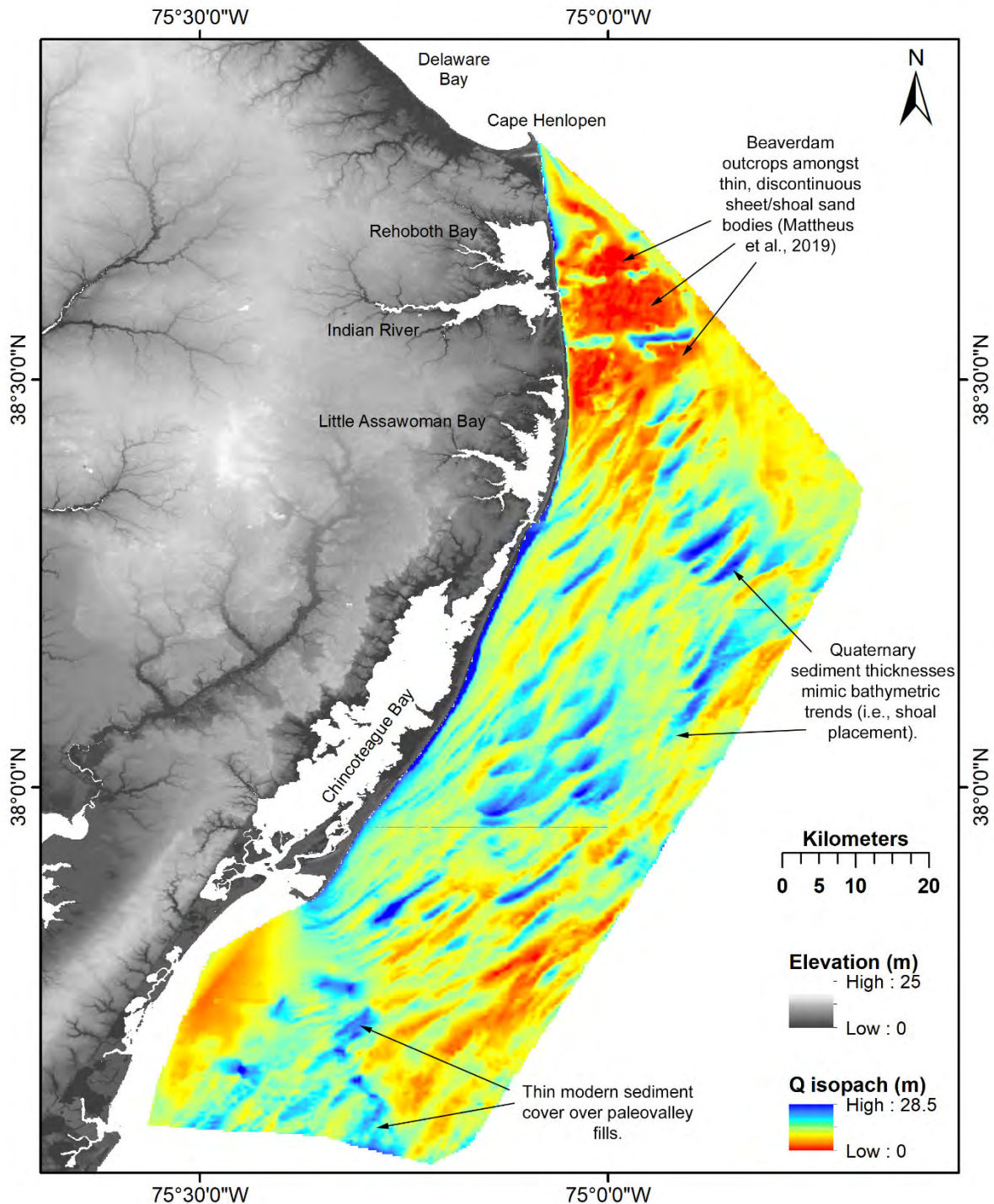


Figure 8) Isopach map of Quaternary sediment thickness generated from the M1 surface model (Figure 6) and modern seafloor topography (FEMA). Notable is the absence of Quaternary sediments across much of the DE inner continental shelf. Thick Pleistocene and/or Holocene sediment packages here are generally affiliated with paleovalley fills and isolated sand ridges. The outcropping of the Beaverdam Formation at the seafloor is captured in 25 sediment cores (Mattheus et al., 2020).

Offshore age dates

Radiocarbon dates of Quaternary offshore deposits generated by the ASAP consist of three types: Organic samples from marsh and lagoon deposits, wood debris in marine deposits, and mollusk shells. Organic samples, mainly plant debris, were used to verify that muddy marsh and lagoon deposits were of Holocene age and provided date data regarding the Holocene rise of sea level (Figure 11). Dates from wood debris in marine deposits indicate that the deposits were of Holocene age or that they contained woody debris reworked from older deposits. Dates from shell material were used to verify data from AAR analyses that the shells were of Holocene or Pleistocene age. Two experiments were run at the NOSAMS laboratory at Woods Hole on shells that yielded Pleistocene ages. The experiments were sequential dissolution and dating of shell layers to determine if the shells were contaminated by young carbon and if so, different layers would yield different dates. The experiments were positive that dates from shells yielding late Pleistocene ages (30,000 to 50,000 BP yr) are suspect and may be much older. Some shells collected from beaches in Virginia barrier islands were also analyzed to determine the degree of reworking of sediment from older material versus from Holocene transgressive deposits. The data indicate that there is a mix of ages verified by AAR data (J.F. Wehmiller personal communication). These dates are helpful where offshore cores are scarce but seismic data may be available in determining the age of seismic units being reworked offshore.

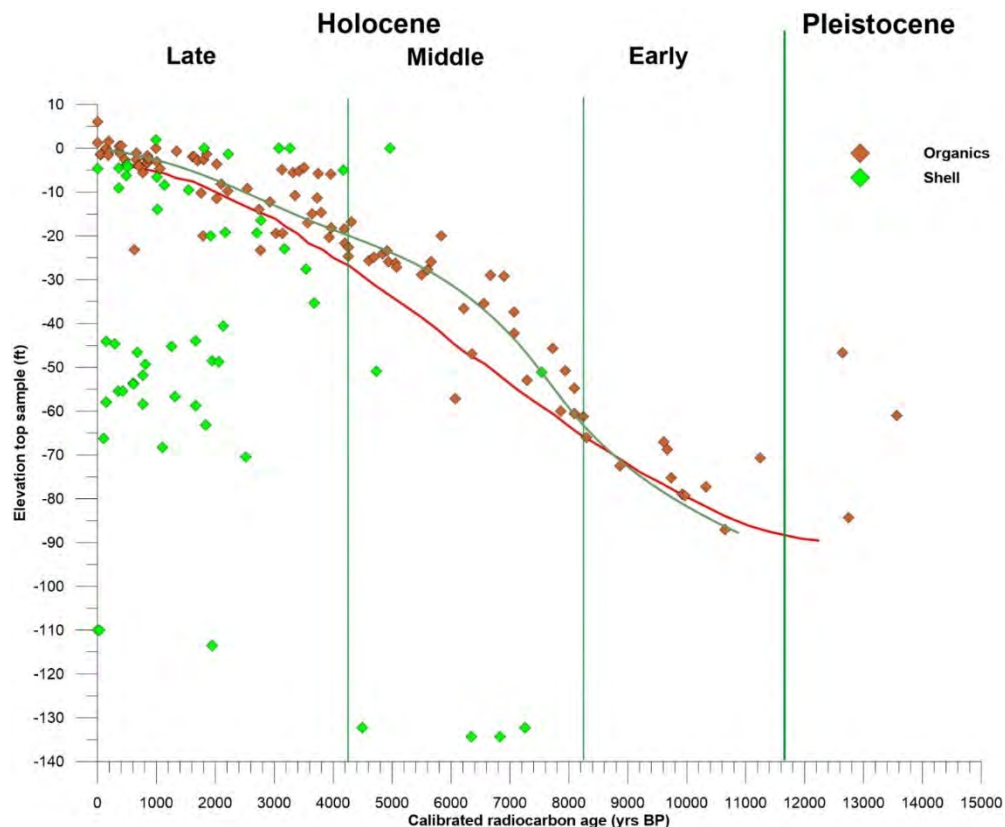


Figure 9)
Holocene
radiocarbon dates
from coastal and
offshore Atlantic
Delmarva
Peninsula. Red
curve is Delaware
sea-level rise curve
from Nikitina and
others. Green
curve is
approximate
Holocene sea-level
rise curve from
ages of marsh and
lagoon organic
deposits from the
Atlantic Delmarva
Peninsula. Data
are in Data File A.

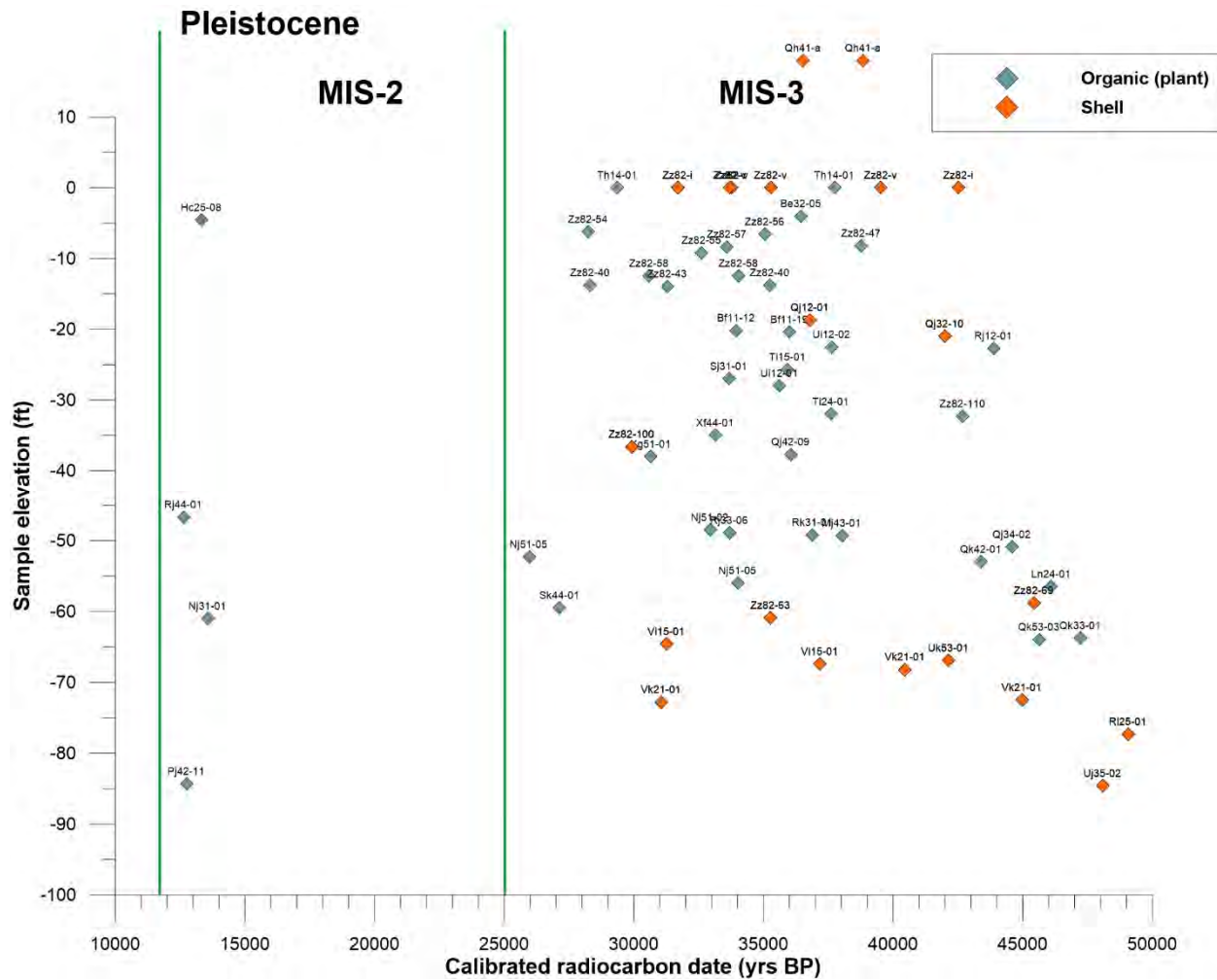


Figure 10) Pleistocene radiocarbon dates from the Delmarva Atlantic Coast and Offshore. Identifiers are DGS site identifiers. Data are in Data File B.

Amino acid racemization results

79 BOEM vibracores were sampled for mollusk shells for amino acid racemization (AAR). These were compared with similar analyses from onshore sites (>20) to develop a regional chronologic framework for near-surface offshore stratigraphic units. Results for 994 amino acid racemization analyses are included as an excel spreadsheet in the supplemental data. The primary function of the analyses was to determine if the deposits are Holocene, late Pleistocene, or older. For Holocene and latest Pleistocene (<50 ka), some analyses were paired with radiocarbon dates as a method of calibration. A fuller explanation of the AAR results, documentation, and publications related to the project are given in the Appendix at the end of this document

Paleovalleys

In seismic reflection images, paleovalleys were recognized as high-amplitude, high-relief surfaces truncating underlying surfaces and strata. Stratigraphic picks on valley bottoms and flanks were exported separately from the 2014 USGS seismic dataset (apart from M1). This was done because valley locations here could not be delineated from the T-Q boundary model, as was the case for offshore Delaware (Figure 6). Valley picks, shown in Figure 11, were color-coded by inferred genetic association, which was assessed from the following parameters: 1) Valley cross-sectional information, particularly widths and depths; 2) Valley-fill characteristics (from available core data) and seismic reflection character; and 3) Spatial trends (i.e. valley orientations). This analysis relied on the assumption is that valley widths and depths increase in the offshore direction with increasing drainage contribution (Mattheus et al., 2007; 2011); measured valley depths tend to increase offshore, albeit for few variances (on the order of few meters), which can be attributed to the effects of localized scouring at tributary junctions or within valley bends. Uncertainties in valley depth were also a function of limited imaging due to gas wipeout or strong seafloor multiples; this is also why paleovalleys imaged off the Delaware coast appear disjointed in Figure 7. Valley-width relationships off the central Delmarva also did not always follow the anticipated trend of general widening in the downstream direction. A reason for this could be differential valley-width modification during transgressive ravinement. Steep valley flanks are imaged meeting the seafloor (Figure 12), attesting to this process. As there is no insight into how much of the valley tops has been lost, a common datum for comparing valley widths along dip is elusive. Transgressive wave ravinement is likely to have impacted different parts of the shelf to varying degrees as a function of both time and shelf morphology. The most useful guides to connecting valley segments were thus the character of the internal reflection configurations (e.g., uniformity in pattern) and spatial associations (i.e. valley orientations and superposition). Knowledge of whether valleys were imaged obliquely, in dip-orientation, or perpendicular to gradient was particularly useful. Valley-fill characteristics facilitated distinction between Holocene and older valley fills in corroboration with geochronological data, helping ensure that age-equivalent drainage networks were properly delineated. Stratification within Pleistocene valley fills was often more distinctly resolved than in Holocene fills, likely due to increased compaction and degassing. Organic-rich fills within late Pleistocene valleys often generate zones of gas wipeout of seismic signals.

Delaware systems

Three paleovalleys were mapped across the Delaware inner continental shelf, incised into the shallow inner shelf platform (which is <15 m of water depth; Figure 7). The northernmost valleys trend to the east/northeast, whereupon they connect to the ancestral, late Pleistocene (MIS2) Delaware River (Figure 1), based on prior work by Kraft (1971), Twitchell and others (1977), Belknap and Kraft (1981 and 1985), and Childers and others (2019). These interpretations are corroborated by Holocene radiocarbon ages derived from organic materials found within cores penetrating the valley fills (Table 5; Figure 13). Both valleys are around 1 km in width and slightly sinuous. Tributary junctions are resolved; however, transgressive ravinement has truncated most of the tributaries and they cannot be traced very far up-dip. The

late Pleistocene trunk valleys off Delaware shelf run landward beneath the modern barrier shoreline (e.g., at the modern Indian River inlet location) and modern estuaries (e.g. Rehoboth Bay). Chrzatowski (1986) characterized the Holocene valley fill sediments here in great detail. The third paleovalley off Delaware, which is situated to the south of the aforementioned, does not connect to a modern estuary; it instead runs beneath the town of Bethany Beach, approximately 6.5 km south of the Indian River inlet. It is close to twice as wide as the others (~2 km) and is also affiliated with the remnants of smaller tributaries on the shelf, truncated at or near the modern seafloor. Prior geophysical mapping of the shelf by Williams (1999) has suggested that this valley predates the last glacio-eustatic cycle; its landward extent has also been mapped across the adjacent Coastal Plain subsurface by Ramsey (1999 and 2010). The corresponding valley fill deposits belong to the mid-Pleistocene Omar Formation; radiocarbon ages from dated fill materials (of organic origin) are either radiocarbon dead or close to it (>33.5 ka; Table 5; Figure 13), reflecting likely contamination with younger radiocarbon. This is supported by the stratigraphy as the Sinepuxent Formation, a shore-parallel lagoon body formed during the last interglacial (MIS5e) is cut into the Omar Formation within 2 km of shore (Mattheus et al., 2020) and along the lowermost Coastal Plain (Ramsey, 2010). Minor re-incision (<5 m) into this paleovalley fill occurred during the last glacio-eustatic cycle along the outer portions of the study area (>5 km from shore), as showcased by seismic profiles DE12 and DE17, collected in strike and dip orientations across/along the valley, respectively (Figure 5). Unlike across the Maryland and Virginia portions of the Delmarva shelf, valley bottoms were rarely imaged off Delaware. A more detailed assessment of valley morphology and longitudinal gradients was therefore not possible.

Central Delmarva systems

Two paleovalley generations are preserved off the coast of Maryland. Three late Pleistocene valleys are clearly delineated and shown to extend in parallel to the southeast (Figures 11-13). The southernmost of these likely extends beneath Assawoman Bay and is associated with the paleo-St. Martin River, mapped beneath the modern estuary by Wells and others (1994). A Holocene AAR age estimate (Core UK53-01; Table 6; Figure 13) constrains this particular valley fill temporally, while similarities in valley width, gradient, orientation, stratigraphic position, and acoustic characteristics suggest the other parallel valleys are late Pleistocene as well. These three paleovalleys are underlain by an obliquely-trending valley network of mid-Pleistocene or older age, based on stratigraphic association and an AAR age estimate (core VK21-01; Table 6; Figure 13). Figures 4 and 10b capture the stratigraphic framework of this region and the spatial relationships between valley generations. The late Pleistocene (Sangamon) Sinepuxent Formation occurs overlying surface M2 in this region of the shelf. Its lower bounding surface truncates the fill deposits of the older valley system while it is incised by the younger valley networks. This infers a late Pleistocene age (MIS2) for the stratigraphically younger valleys and a mid-Pleistocene age (probably MIS6, but possibly older) for the valley truncated by M2. The younger valley in the example shown (delineated from ‘light blue’ stratigraphic picks; Figure 11) is one of three in parallel MIS2 valleys that incised into the Sinepuxent. The widths of the late Pleistocene valleys are on the order of 1 km (Figure 11), making them

comparable to the time-equivalents off the Delaware coast (Figure 7); the similarities extend to fill character as well. The older paleovalley is wider (comparable to Delaware's 'Omar' valley) and characterized by more gradual longitudinal gradients. However, exact age equivalency is not established (beyond the understanding that both valley fills are Pleistocene). The pre-Sangamon valley off Maryland trends to the south, a stark deviation from the trend set by the late Pleistocene systems along this portion of the coastal margin. It eventually turns to the east for a more shore-perpendicular trajectory, making it difficult to ascertain from the available data coverage whether it contributed drainage to the ancestral Susquehanna River (Figure 1) or comprised the headwater region of an independent shelf drainage system bound for the shelf break.

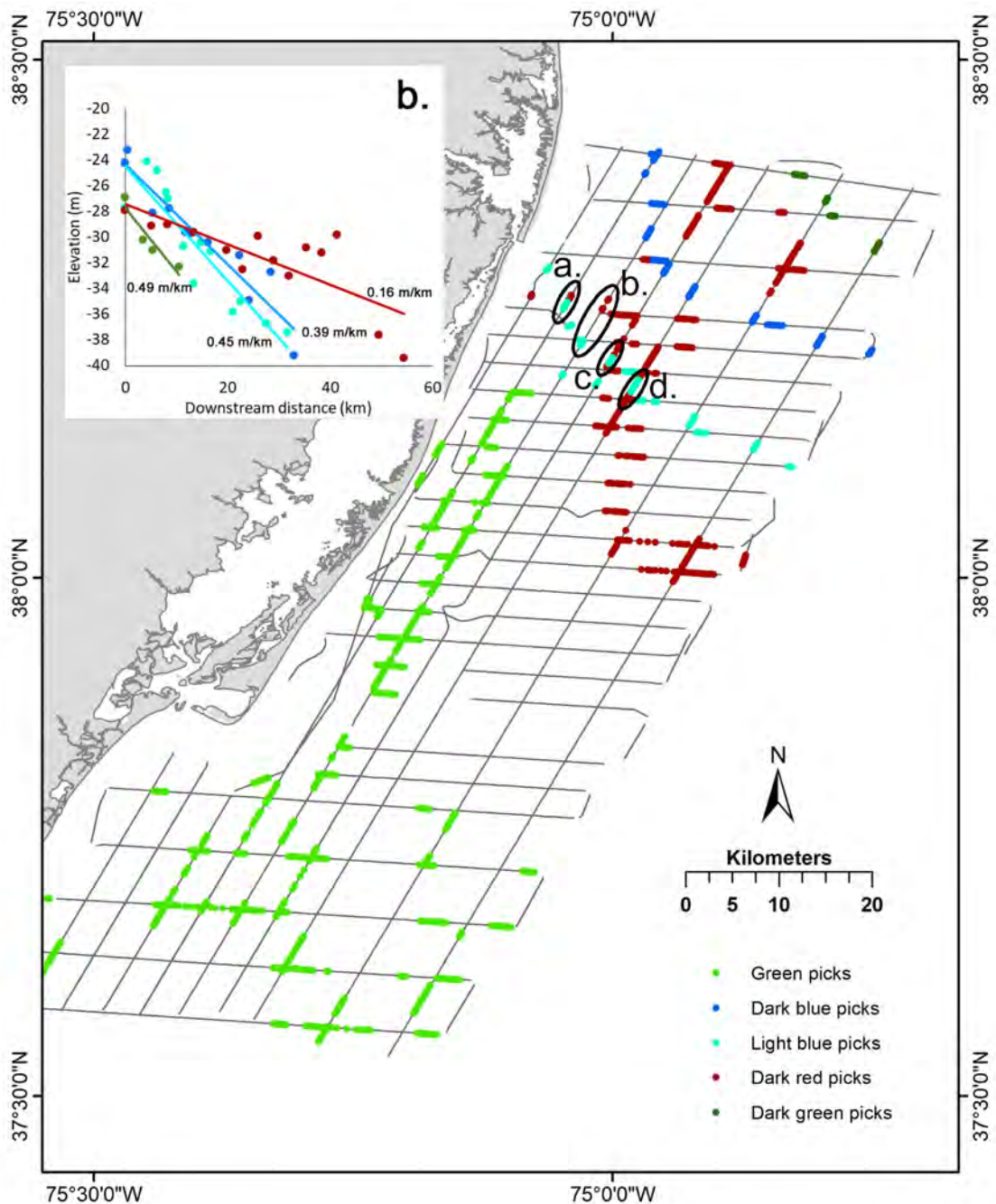


Figure 11) Map of offshore Maryland and Virginia showing portions of the 2014 USGS ‘chirper’ seismic grid contain channel/valley forms (a) and accompanying slopes, calculated from maximum depths of incision at each valley cross section (b). Stratigraphic picks of valley flanks and bottoms, which are above or coincidental with the M1 reflector (unlike across the inner Delaware shelf), are color-coded by valley, as determined from dimensions, internal reflection configurations, slopes, and stratigraphic superposition (and thus age). The locations of seismic examples shown in Figure 12 (parts a through d) are labeled.

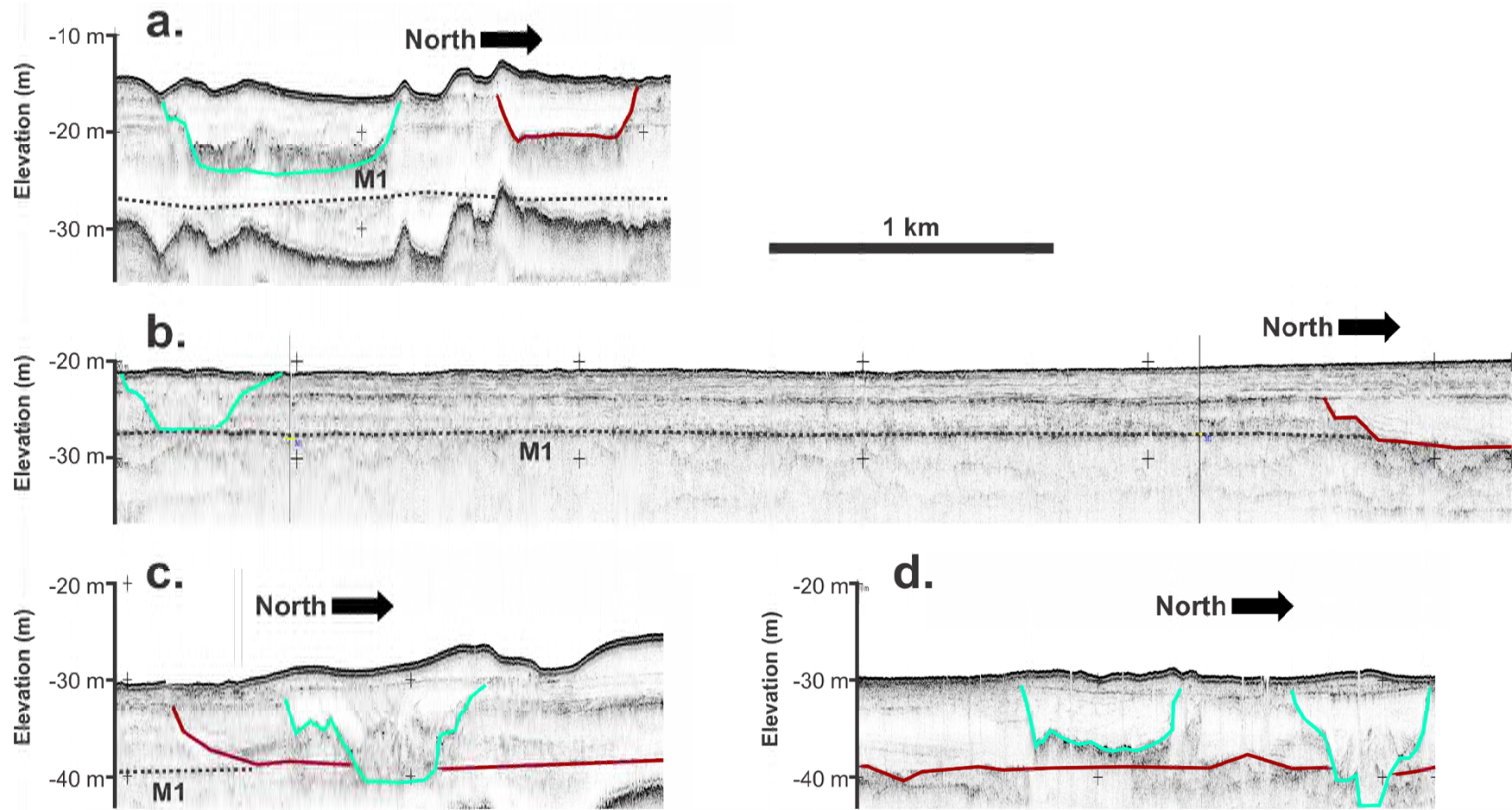


Figure 12) Select seismic images showing the stratigraphic relationship between light blue and dark red picks (and valleys), which are mapped across the Maryland inner continental shelf (Figure 11). Delineated valley bottoms are generally shallower than the M1 reflector here. Stratigraphic superposition concludes that the light blue valley, which is of the same generation as the dark blue and green valleys (based on geomorphic characteristics, valley trends and modern coastal associations, and fill characteristics), is younger than the dark red, most likely representing incision into the shelf associated with MIS2.

Table 5) Radiocarbon data on sampled paleovalley or estuarine fills (compiled from DGS database). Refer to Mattheus and others (2020) for Geologic unit descriptions.

DGSID	LOCALID	Northing	Easting	Ground elevation (ft.)	Sample elevation (ft.)	Sample material	Geologic unit	Conventional C-14 age
Pj42-11	R4115	4273390.5	494614.9	6.66	-84.3	basal peat	Qm	10800
Pj12-04	JCK-E3-81	4279338.5	495682.4	-30	-37.4	wood	Ql	6220
Oj55-01	KHV-142	4279816.6	498804.2	-54.1	-70.7	organics	Ql	9840
Pj14-01	KHV-95	4278228	498437.6	-49.6	-60.6	basal peat	Ql	7280
Qk43-01	DGS92-10	4263279.5	504392.2	-56	-66.5	peat	Qo	46000
Qk43-01	DGS92-10	4263279.5	504392.2	-56	-66.8	peat	Qo	42200
Qj33-02	JCK-I3-81	4265745	496837.3	-29	-38.4	wood	Qsi	33510
Qj33-02	JCK-I3-81	4265745	496837.3	-29	-36.4	peat	Qsi	35140
Qk33-01	DGS97-58	4265098	503349.8	-52.25	-75.73	peat	Qo	43700
Qk42-01	DGS04-07	4264807	502298	-50.7	-53	wood	Qo	39130

Table 6) AAR age estimates on sampled paleovalley or estuarine fills (compiled from DGS database). Refer to Mattheus and others (2020) for Geologic unit descriptions.

DGSID	LOCALID	Northing	Easting	Ground elevation (ft.)	Sample elevation (ft.)	Genera	Number of analyses	Geologic unit	Age estimate
Uk53-01	MGS-18-1142	4225140	503406	-61.99	9.5	Spisula, Ensis, Mercenaria, Crassostrea Mulinia,	6	Ql	Holocene
Vk21-01	MGS-20-1430	4222242	500073	-61.99	9.5	Astarte, Ensis, Spisula	10	Ql	L. Pleistocene

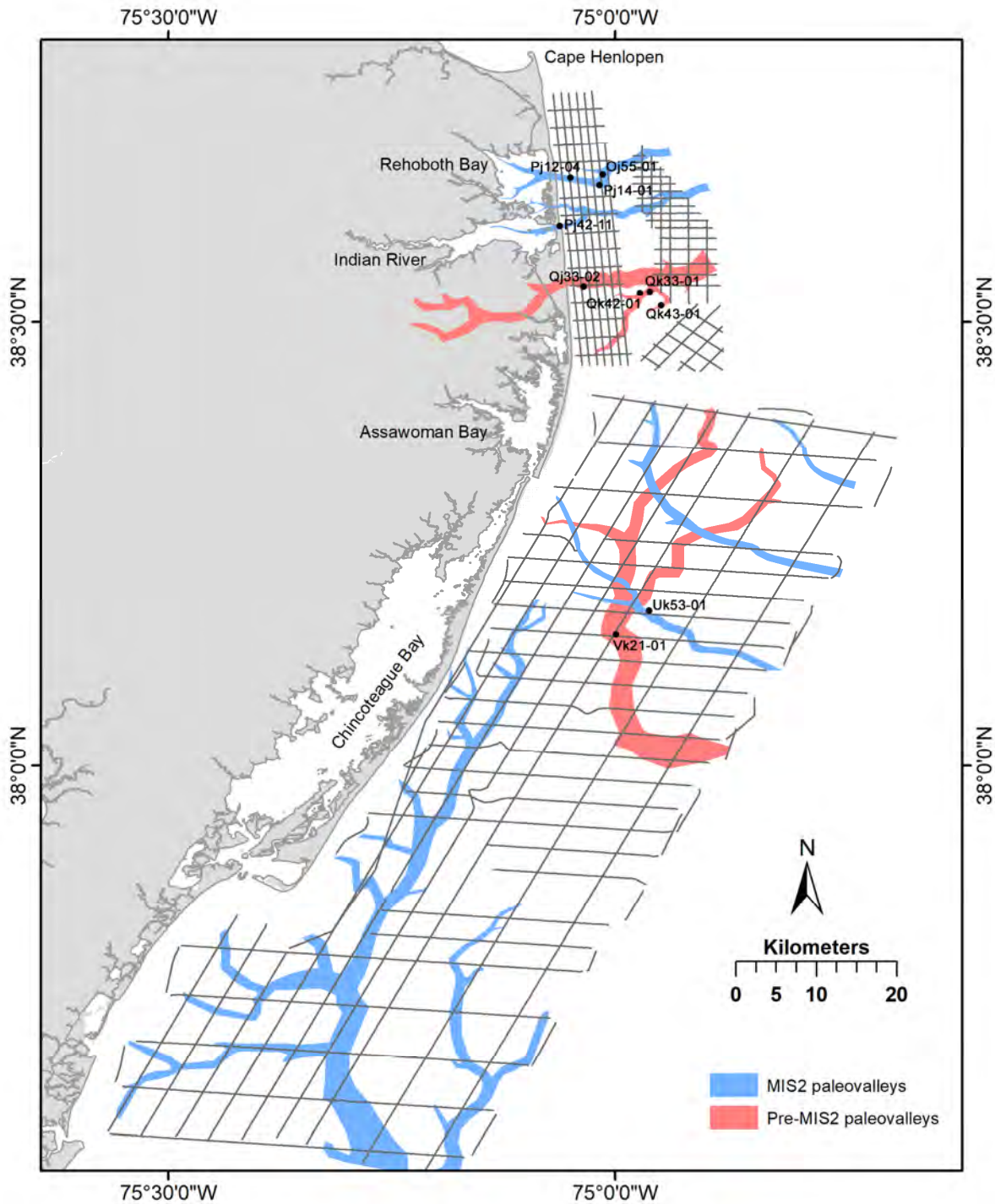


Figure 13) Map showing delineated MIS2 (blue) and older (red) paleovalleys, based on recognition in seismic reflection imagery. Age relationships for Delaware paleovalleys are based on C-14 ages and association with modern estuaries and geologic mapping of the Coastal Plain (Ramsey, 1999 and 2010) while age relationships for offshore Maryland and Virginia are based on stratigraphic association (e.g. to the MIS5e Sinepuxent Formation).

Late Pleistocene drainage of the Delmarva inner continental shelf

A map of late Pleistocene drainage across the Delmarva shelf was constructed from results of this investigation along with insights provided by other studies (Figure 14). The location of the late Pleistocene (i.e. MIS2) Delaware paleovalley is based on work by Twitchell and others (1977), which has since been corroborated by additional, high-resolution seismic reflection data and a GIS-based mapping approach (Childers; 2019). The ancestral Delaware's tributary system within Delaware Bay had originally been mapped by Knebel and Circé (1988), while drainage contributions from the adjacent Delaware inner continental shelf are based on our re-assessment. Delaware paleovalleys were mapped into modern estuaries by Chrzatowski (1986), who sampled the Pleistocene surface beneath Rehoboth and Indian River estuaries in core. Valley locations on the shelf, now constrained from high-resolution digital sub-bottom reflection imagery and abundant core data (Figure 2), differ from prior models, offering reconciliatory insight into past disagreements. The Belknap and Kraft (1985) model more closely resembles our interpretations of the subsurface (Figures 1 and 12); Williams (1999), on the contrary, interprets valleys to extend to the southeast (paralleling the trend of the ancestral Delaware valley) before merging with a system located where we map the pre-MIS2 'Omar' paleovalley (Figure 14). Modern subsurface constraints, promoted by over 450 offshore sediment cores and ~500 km of high-resolution 'chirper' data, confirm that the valleys originating from the Rehoboth and Indian River estuaries trend to the east/northeast, eventually connecting to the ancestral Delaware, mapped by Twitchell and others (1977) and reaffirmed by Childers and others (2019).

There are many tributaries mapped by Williams (1999) that are not accounted for in our study. Some of these could be part of the middle-Pleistocene Omar Formation, which is extensively mapped across the lower Coastal Plain (Ramsey, 2010). In particular, the E-W trending trunk valley mapped by Williams (and this study), which is unaffiliated with a modern estuary, may connect to additional tributaries. One prominent confluence is resolved by our study, trending to the northeast and merging with the pre-MIS2 trunk valley around 10 km from shore (Figure 14). While the general trend of paleodischarge from the area to the south conforms to the model proposed by Williams (1999), far fewer tributaries are imaged. Given discrepancies (between studies) regarding paleodrainage pattern across the shelf area fronting the modern Delaware coastal estuaries, it is necessary to entertain the possibility that differences in data resolution may be biasing subsurface interpretations. The shallow nature of the Beaverdam Formation across valley interfluves (Figures 7 and 8) offer a possible explanation. Its internal architecture, characteristic of fluvial processes, includes features such as large crossbeds (i.e., lateral accretion) and cut-and-fill structures associated with a dynamic alluvial environment. These sedimentary structures could easily be mistaken for paleovalleys, particularly in lower-resolution (and largely unprocessed) analog datasets and in absence of comparable core constraints. Our high-resolution 'chirper' dataset and strong lithologic data control provided by >450 offshore cores (25 of which place the Beaverdam Formation at the modern seafloor; Mattheus et al., 2020) reveal how spatially limited these sedimentary structures are, unlike valleys. Improved digital imaging capabilities have also allowed associations to the M1 reflector to be more distinctly established (Figure 4). It is likely that, in absence of this type of data

control, linkages were made between true valley segments and adjacent depositional features within the Beaverdam Formation.

Late Pleistocene drainage across the central Delmarva shelf is either to the southeast, as is the case with the three paleovalleys of similar size, gradient, and orientation, or to the south, as applies to a coast-parallel trunk valley fed by approximately a dozen coast-perpendicular tributaries reaching towards the barrier (Figure 14). This interpretation differs from that of Toscano and others (1989) in many ways. It appears that the older interpretation imaged pre-MIS2 valley segments (where our ‘dark red’ valley picks overlap their interpreted valley locations), but incorporated these into an interpretation of late Pleistocene paleodrainage. This is best illustrated by comparing interpretations in Figure 14c. The southernmost of the three upper Maryland valleys coincides with valley locations proposed by Toscano and others (1989); however, this is not mapped as a continuous valley, but connected to a portion of the pre-MIS2 valley, constrained well by our high-resolution ‘chirper’ dataset (Figures 10 and 11). It would have been difficult to recognize the cross-cutting relationship in absence of high data quality, particularly given that depths of incision are comparable. Once more, this likely reflects the shortcomings of the analog data previously used for subsurface mapping. The differences between the valley networks mapped from the 2014 USGS ‘chirper’ dataset and the 1980s vintage interpretations are stark and tell very different stories about the nature of late Pleistocene paleodrainage. Unfortunately, additional data are necessary to determine whether this drainage contributed to the ancestral Delaware, proximally situated to the north (Figure 1) or made up part of a separate drainage basin connecting the central shelf to the shelf break. Our assessment also fails to determine whether the southward-bound late Pleistocene flow (towards the Virginia shelf) eventually connected to the St. Charles paleovalley, which is mapped across the southern tip of the Delmarva Peninsula and into the Chesapeake (Colman et al., 1990; Colman & Mixon, 1988; Foyle & Oertel, 1992; Oertel & Foyle, 1995). Observations of terrestrial drainage patterns towards the Chesapeake Bay, which trend to the southeast across the Delmarva interior (Figure 1), argue that this scenario, favored by the former valleys orientation, would conform to established trends. Renewed data-collection and mapping efforts around the southern tip of the Delmarva, where past studies have resolved a high degree of stratigraphic complexity related to the presence of many large valley generations, would help bridge this gap.

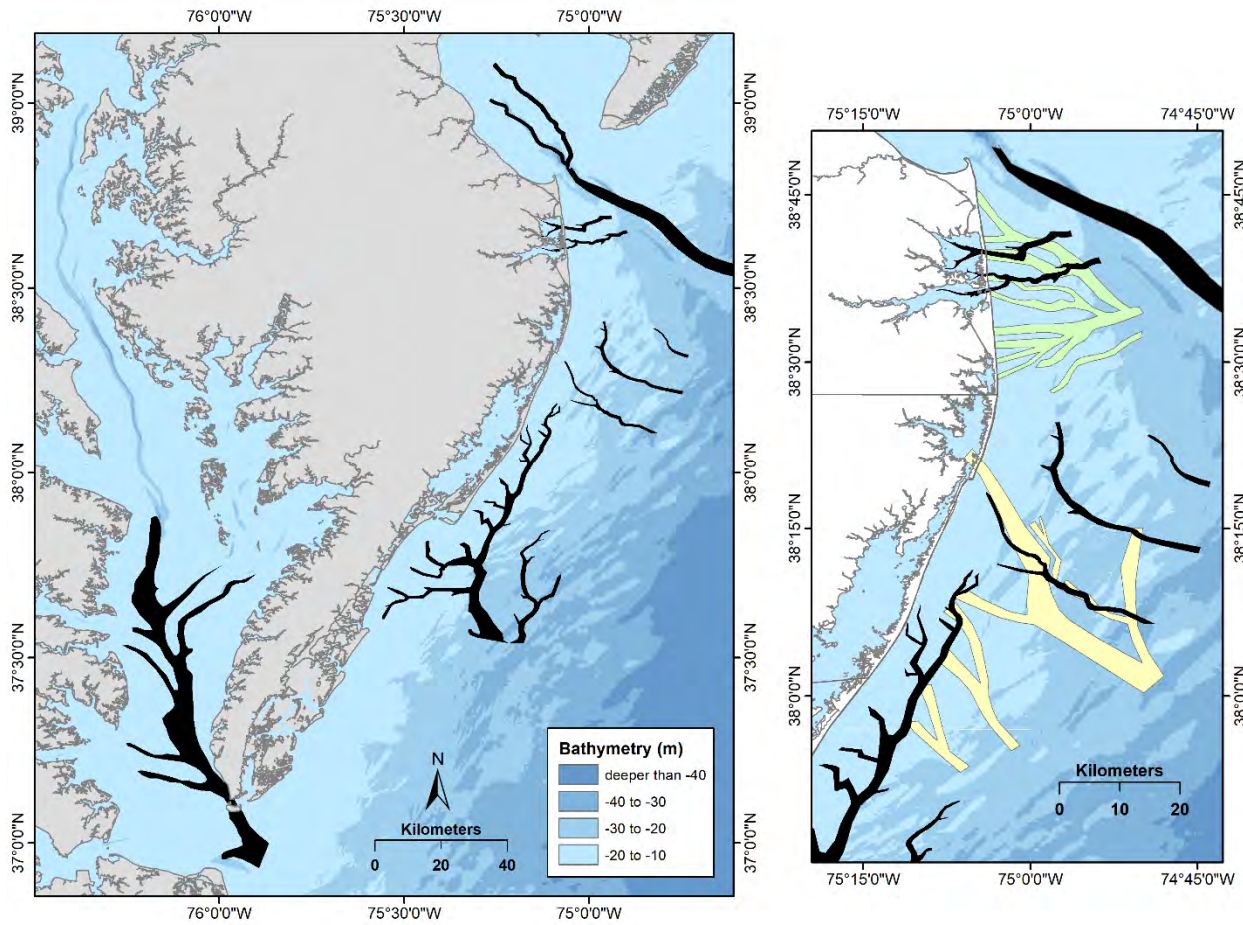


Figure 14) MIS2 drainage map based on results of this study and work by Colman and others (1990), Knebel and Circé (1988), and Twitchell and others (1977), who delineated the St. Charles paleovalley beneath Chesapeake Bay and the Delaware paleovalley in bay and shelf settings, respectively. An inset map compares this study's interpretation of the Maryland and Delaware inner shelf valleys (late Pleistocene) to those by Toscano and others (1989) in yellow and Williams (1999) in green.

REFERENCES

- Barnhardt, W.A., Belknap, D.F. and Kelley, J.T., 1997. Stratigraphic evolution of the inner continental shelf in response to late Quaternary relative sea-level change, northwestern Gulf of Maine. *Geological Society of America Bulletin*, 109(5), pp.612-630.
- Belknap, D.F., and Kraft, J.C., 1981, Preservation Potential of Transgressive Coastal Lithosomes on the U.S. Atlantic Shelf: *Marine Geology*, v. 42, p. 429-442.
- Belknap, D.F., and Kraft, J.C., 1985, Influence of Antecedent Geology on Stratigraphic Preservation Potential and Evolution of Delaware's Barrier Systems: *Marine Geology*, v. 63, p. 235-262.
- Belknap, D.F., Kraft, J.C., and Dunn, R.K., 1994, Transgressive Valley-fill Lithosomes: Delaware and Maine, in Dalrymple, R.W., Boyd, R., and Zaitlin, B.A., eds., *Incised-valley Systems: Origin and Sedimentary Sequences*: SEPM Special Publication 51, p. 303-320.
- Bender, M.A., Knutson, T.R., Tuleya, R.E., Sirutis, J.J., Vecchi, G.A., Garner, S.T., and Held, I.M., 2010, Modeled Impact of Anthropogenic Warming on the Frequency of Intense Atlantic HurricanesL: *Science*, v. 327, p. 454-458.
- Bratton, J.F., Colman, S.M., Thieler, E.R., and Seal, R.R.I., 2003, Birth of the modern Chesapeake Bay estuary between 7.4 and 8.2 ka and implications for global sea-level rise: *Geo-Marine Letters*, v. 22, p. 188-197.
- Chen, Z.-Q., Hobbs, C.H III, Wehmiller, J.F., and Kimball, S.M., 1995, Late Quaternary Paleochannel Systems on the Continental Shelf, South of the Chesapeake Bay Entrance: *Journal of Coastal Research*, v. 11, p. 605-614.
- Childers, D.P., 2014, Paleochannels in Lower Delaware Bay and the Delaware Inner Continental Shelf [Dissertation]: University of Delaware, Newark, Delaware, 121 p.
- Childers, D.P., Madsen, J.A., Krantz, D.E. and Deliberty, T.L., 2019. Constraining the Geometry of Subsurface Paleochannels beneath Delaware Bay and the Mid-Atlantic Inner Continental Shelf. *Journal of Coastal Research*.
- Chrzałkowski, M.J., 1986, Stratigraphic and Geologic History of a Holocene Lagoon: Rehoboth Bay and Indian River Bay, Delaware [Dissertation]: University of Delaware, Newark, Delaware, 337 p.
- Colman, S.M. and Mixon, R.B., 1988. The record of major Quaternary sea-level changes in a large coastal plain estuary, Chesapeake Bay, eastern United States. *Palaeogeography, Palaeoclimatology, Palaeoecology*, 68(2-4), pp.99-116.
- Colman, S.M., Halka, J.P., Hobbs III, C.H., Mixon, R.B., and Foster, D.S., 1990, Ancient channels of the Susquehanna River beneath Chesapeake Bay and the Delmarva Peninsula: *GSA Bulletin*, v. 102, p. 1268-1279.
- Conkwright, R.D. and Williams, C.P., 1996. Offshore sand resources in central Maryland shoal fields. Baltimore: Maryland Geological Survey.

- Conkwright, R.D., Williams, C.P. and Christiansen, L.B., 2000. Offshore sand resources in northern Maryland shoal fields. Contract, (14-35), pp.0001-30769.
- DeConto, R.M., and Pollard, D., 2016, Contribution of Antarctica to past and future sea-level rise: Nature, v. 531, p. 591-597.
- Demarest, J.M. and Leatherman, S.P., 1985. Mainland influence on coastal transgression: Delmarva Peninsula. Marine Geology, 63(1-4), pp.19-33.
- Dix, J., Hamilton, R., Faggetter, M.J., Fry, C.R., Malgorn, J., Pinson, L.J.W., Vardy, M.E. and Dewing-Andrews, E., 2016, September. True 3D High Resolution Imaging for Pre-and Post-Installation of Offshore Infrastructures. In Near Surface Geoscience 2016-Second Applied Shallow Marine Geophysics Conference.
- Domingues, C.M.; Church, J.A.; White, N.J.; Gleckler, P.J.; Wijffels, S.E.; Barker, P.M., and Dunn, J.R., 2008, Improved estimates of upper-ocean warming and multi-decadal sea-level rise: Nature, v. 453, p. 1090-1093.
- Edwards, J.H., Harrison, S.E., Locker, S.D., Hine, A.C., and Twitchell, D.C., 2003, Stratigraphic framework of sediment-starved sand ridges on a mixed siliciclastic/carbonate inner shelf; west central Florida: Marine Geology, v. 200, p. 195-217.
- Field, M.E., 1979. Sediments, shallow subbottom structure, and sand resources of the inner continental shelf, central Delmarva Peninsula (No. CERC-TP-79-2). COASTAL ENGINEERING RESEARCH CENTER FORT BELVOIR VA.
- Finkl, C.W., Andrews, J.L., and Benedet, L., 2006, Assessment of offshore sand resources for beach nourishment along the southwest coast of Florida: 19th Annual National FSBP Association Conference on Beach Preservation Technology, Proceedings, p. 14.
- Foyle, A.M., and Oertel, G.F., 1992, Seismic Stratigraphy and coastal drainage patterns in the Quaternary section of the Delmarva Peninsula, Virginia, USA: Sedimentary Geology, v. 80, p. 261-277.
- Genau, R.B., Madsen, J.A., McGeary, S., and Wehmiller, J.F., 1994, Seismic-Reflection Identification of Susquehanna River Paleochannels on the Mid-Atlantic Coastal Plain: Quaternary Research, v. 42, p. 166-175.
- Heap, A.D., and Nichol, S.L., 1997, The influence of limited accommodation space on the stratigraphy of an incised-valley succession: Weiti River estuary, New Zealand: Marine Geology, v. 144, p. 229-252.
- Knebel, H.J., and Circé, R.C., 1988, Late Pleistocene drainage systems beneath Delaware Bay: Marine Geology, v. 78, p. 285-302.
- Kraft, J.C., 1971, Sedimentary Facies Patterns and Geologic History of a Holocene Marine Transgression: GSA Bulletin, v. 82, p. 2131-2158.

Kraft, J.C., and Belknap, D.F., 1986, Holocene Epoch Coastal Geomorphologies Based on Local Relative Sea-level Data and Stratigraphic Interpretations of Paralic Sediments: Journal of Coastal Research Special Issue 1, p. 53-59.

Krantz, D.E., Manheim, F.T., Bratton, J.F., and Phelan, D.J., 2004, Hydrogeologic Setting and Ground Water Flow Beneath a Section of Indian River Bay, Delaware: Groundwater, v. 42, p. 1035-1051.

Le Bot, S., Van Lancker, V., Deleu, S., De Batist, M., Henriet, J.P. and Haegeman, W., 2005. Geological characteristics and geotechnical properties of Eocene and Quaternary deposits on the Belgian continental shelf: synthesis in the context of offshore wind farming. Netherlands Journal of Geosciences, 84(2), pp.147-160.

Locker, S.D., Hine, A.C. and Brooks, G.R., 2003. Regional stratigraphic framework linking continental shelf and coastal sedimentary deposits of west-central Florida. Marine Geology, 200(1-4), pp.351-378.

Manheim, F.T., Krantz, D.E. and Bratton, J.F., 2004. Studying ground water under Delmarva coastal bays using electrical resistivity. Groundwater, 42(7), pp.1052-1068.

Mattheus, C.R., Rodriguez, A.B., Greene, D.L. Jr., Simms, A.R., and Anderson, J.B., 2007, Control of upstream variables on incised-valley dimension: Journal of Sedimentary Research, v. 77, p. 213-224.

Mattheus, C.R., and Rodriguez, A.B., 2011, Controls on late Quaternary incised-valley dimension along passive margins evaluated using empirical data: Sedimentology, v. 58, p. 1113-1137.

Mattheus, C.R., and Rodriguez, A.B., 2014. Controls on lower-coastal-plain valley morphology and fill architecture: Journal of Sedimentary Research, v. 84, p. 314-325.

Mattheus, C.R., Ramsey, K.W., Tomlinson, J.L., 2020. Geologic Map of Offshore Delaware. Delaware Geological Survey Map Series No. 25, Scale 1:40,000.

Metz, T.L., 2015. Shallow stratigraphy of the Mid-Atlantic Bight: constraints on siting of offshore wind projects (Doctoral dissertation, University of Delaware), 131 pp.

Murphy, S., 1996. A seismic study of the youngest paleo-incised valley of the Delaware River. Newark, Delaware: University of Delaware (Doctoral dissertation, Master's Thesis).

Oertel, G.F., and Foyle, A.M., 1995, Drainage Displacement by Sea-Level Fluctuation at the Outer Margin of the Chesapeake Seaway: Journal of Coastal Research, v. 11, p. 583-604.

Ponte, A., 2016. Utilizing geological and geotechnical parameters to constrain optimal siting of Mid-Atlantic Bight offshore wind projects (Doctoral dissertation, University of Delaware), 94 pp.

Ramsey, K.W., 1992, Coastal response to late Pliocene climate change: middle Atlantic Coastal Plain, Virginia and Delaware, *in* Fletcher, C.H., and Wehmiller, J.F., eds., Quaternary coasts of the United States: marine and lacustrine systems: SEPM, Special Publication 48, p. 121-127.

- Ramsey, K.W., 1999, Cross Section of Pliocene and Quaternary Deposits along the Atlantic Coast of Delaware: Delaware Geological Survey, Miscellaneous Map, no. 6.
- Ramsey, K.W., 2010, Stratigraphy, Correlation, and Depositional Environments of the Middle to Late Pleistocene Interglacial Deposits of Southern Delaware: Delaware Geological Survey, Report of Investigations, no. 76, 43 p.
- Ramsey, K.W., 2011, Geologic Map of the Fairmount and Rehoboth Beach Quadrangle, Delaware: Delaware Geological Survey, Map Series, no. 16, 1:24,000.
- Ramsey, K.W., and Tomlinson, J.L., 2011, Geologic Map of the Harbeston Quadrangle, Delaware: Delaware Geological Survey, Map Series, no. 17, 1:24,000.
- Ramsey, K.W., and Tomlinson, J.L., 2012, Geologic Map of the Bethany Beach and Assawoman Bay Quadrangles, Delaware: Delaware Geological Survey, Map Series, no. 18, 1:24,000.
- Rodriguez, A.B., Anderson, J.B., Siringan, F.P. and Taviani, M., 2004. Holocene evolution of the east Texas coast and inner continental shelf: along-strike variability in coastal retreat rates. *Journal of Sedimentary Research*, 74(3), pp.405-421.
- Rodriguez, A.B., Anderson, J.B. and Simms, A.R., 2005. Terrace inundation as an autocyclic mechanism for parasequence formation: Galveston Estuary, Texas, USA. *Journal of Sedimentary Research*, 75(4), pp.608-620.
- Rodriguez, A.B., Duran, D.M., Mattheus, C.R., and Anderson, J.B., 2008, Sediment accommodation control on estuarine evolution: An example from Weeks Bay, Alabama, USA: GSA, Special Paper, no. 443, 31-42.
- Rodriguez, A.B., Greene, D.L., Anderson, J.B. and Simms, A.R., 2008. Response of Mobile Bay and eastern Mississippi Sound, Alabama, to changes in sediment accommodation and accumulation. Response of upper Gulf Coast estuaries to Holocene climate change and sea-level rise: Geological Society of America Special Paper, 443, pp.13-30.
- Russoniello, C.J., Fernandez, C., Bratton, J.F., Banaszak, J.F., Krantz, D.E., Andres, A.S., Konikow, L.F. and Michael, H.A., 2013. Geologic effects on groundwater salinity and discharge into an estuary. *Journal of hydrology*, 498, pp.1-12.
- Sheridan, R.E., Dill, C.E., Jr., and Kraft, J.C., 1974, Holocene sedimentary environment of the Atlantic inner shelf off Delaware: GSA Bulletin, v. 85, p. 1319-1328.
- Schimanski, A. and Stattegger, K., 2005. Deglacial and Holocene evolution of the Vietnam shelf: stratigraphy, sediments and sea-level change. *Marine Geology*, 214(4), pp.365-387.
- Shideler, G.L., Ludwick, J.C., Oertel, G.F., and Finkelstein, K., 1984, Quaternary stratigraphic evolution of the southern Delmarva Peninsula coastal zone, Cape Charles, Virginia: GSA Bulletin, v. 95, p. 489-502.
- Timmons, E.A., Rodriguez, A.B., Mattheus, C.R., and DeWitt, R., 2010, Transition of a regressive to a transgressive barrier island due to back-barrier erosion, increased storminess, and low sediment supply: Bogue Banks, North Carolina, USA: *Marine Geology*, v. 278, p. 100-114.

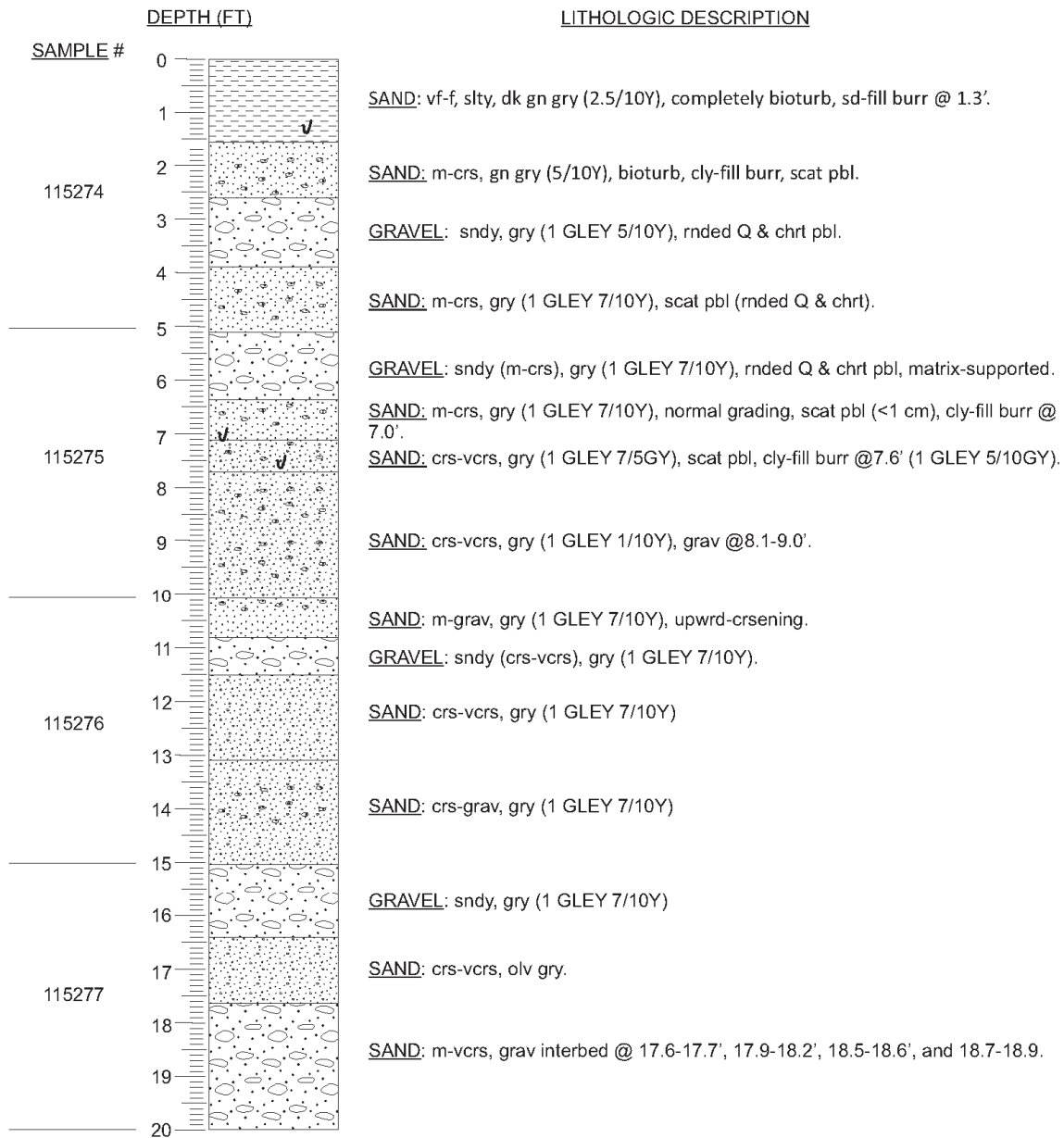
- Toscano, M.A., 1989. Quaternary stratigraphy of the inner continental shelf of Maryland (No. 50). Maryland Geological Survey.
- Twitchell, D.C., Knebel, H.J., and Folger, D.W., 1977, Delaware River: Evidence for Its Former Extension to Wilmington Submarine Canyon: *Science*, v. 195, p. 483-485.
- Twichell, D., 2011. The shallow stratigraphy and sand resources offshore of the Mississippi Barrier Islands. US Department of the Interior, US Geological Survey.
- Webster, P.J., Holland, G.J., Curry, J.A., and Chang, H.R., 2005, Changes in Tropical Cyclone Number, Duration, and Intensity in a Warming Environment: *Science*, v. 309, p. 1844-1846.
- Wehmiller, J.F., and Pellerito, V., 2015, Database of Quaternary Coastal Geochronologic Information for the Atlantic and Pacific Coasts of North America: Delaware Geological Survey, Open File Report, no. 50, 3 p.
- Wells, D.V., Conkwright, R.D., and Park, J., 1994, Geochemistry and geophysical framework of the shallow sediments of Assawoman Bay and Isle of Wight Bay in Maryland: Maryland Geological Survey, Coastal and Estuarine Geology Open File Report, no. 15, 125 p.
- Williams, C.P., 1999, Late Pleistocene and Holocene Stratigraphy of the Delaware Inner Continental Shelf [MS Thesis]: University of Delaware, Newark, Delaware, 175 p.
- Williams, S.J., Flocks, J., Jenkins, C., Khalil, S. and Moya, J., 2012. Offshore sediment character and sand resource assessment of the northern Gulf of Mexico, Florida to Texas. *Journal of Coastal Research*, 60, 30-44.

APPENDIX A – BOEM Vibracore Logs

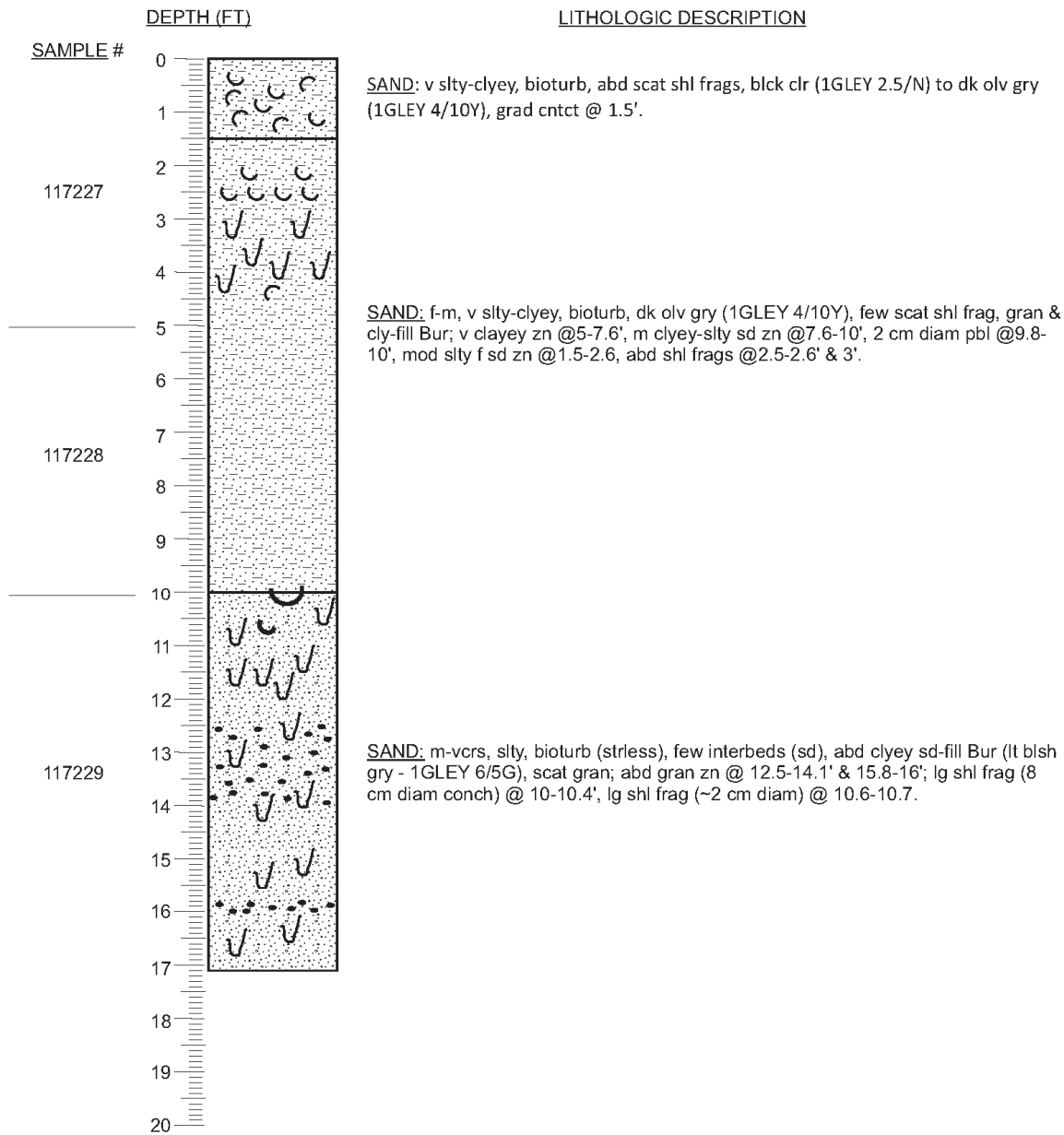
This appendix contains lithologic logs constructed for BOEM cores collected from the Delaware, Maryland, and Virginia shelves from 2015 to 2017 as part of the Atlantic Sand Assessment Project. The legend below details the symbols used to represent different lithotypes and features of interest contained within. Color designations are based on the Munsell soil color chart.

	Mud pebble/marsh rip-up
	Wood
	Shells
	Pebbles
	Burrow
	Laminae
	Crossbeds/laminae
	Clay
	Silty clay/clayey silt
	Sandy silt
	Silty sand
	Very fine-medium sand
	Medium -very coarse sand
	Gravely sand to sandy gravel

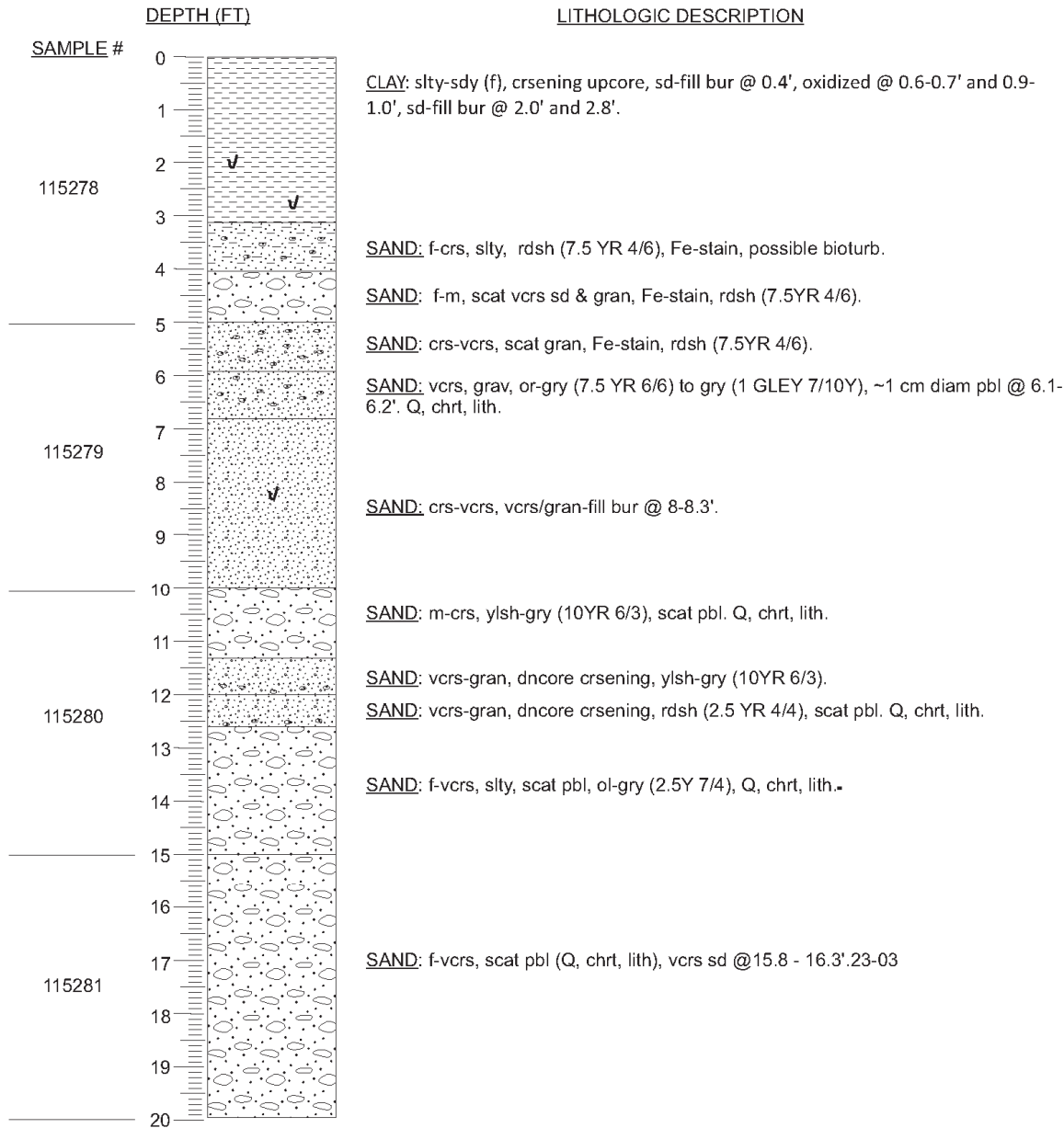
DGSID Pk13-01 DATE DESCRI. 11/14/17 WATER DEPTH (FT) 57.4
LOCAL ID. BOEM-16-01 DESCR. BY CRM



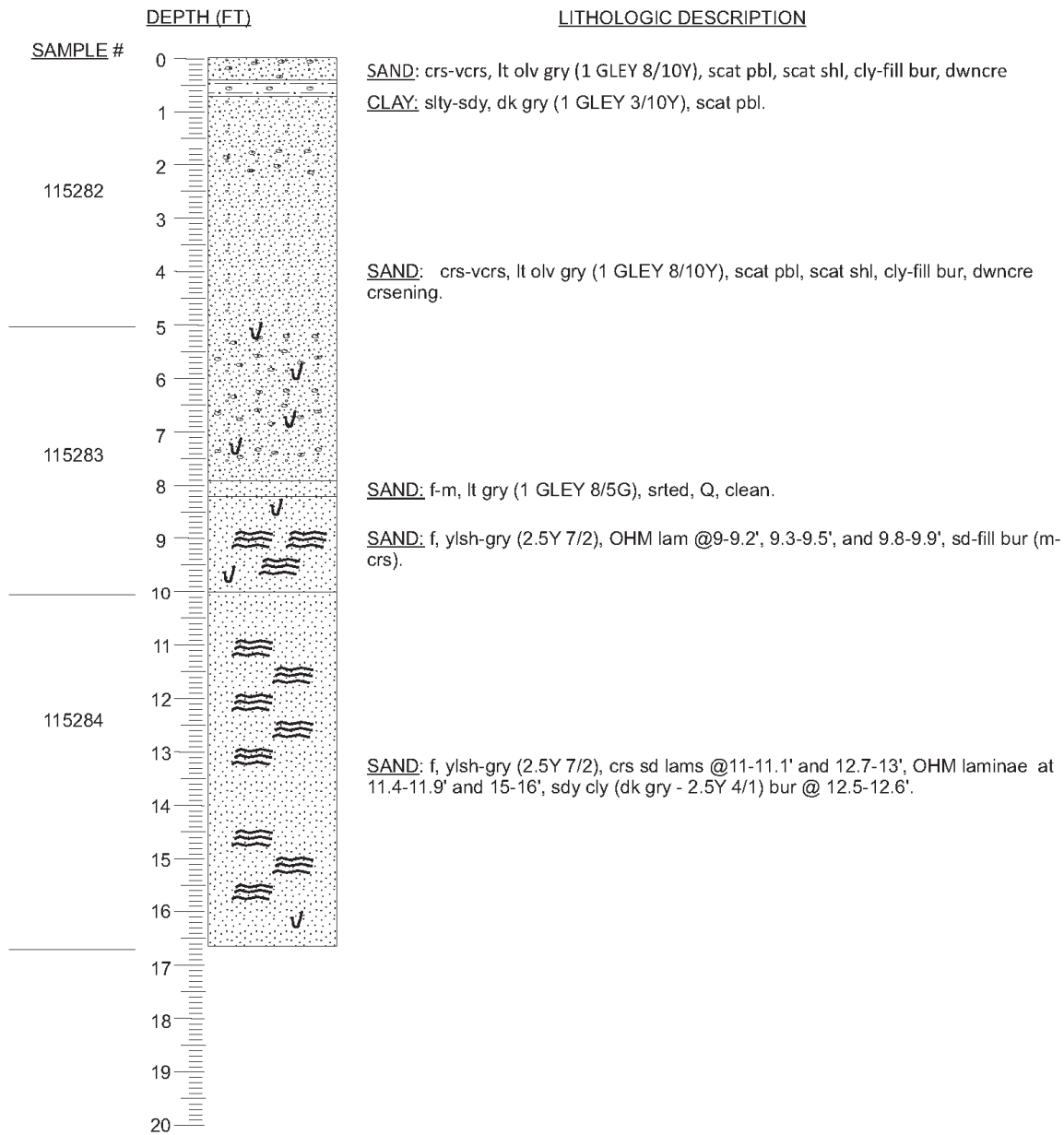
DGSID Pk13-02 DATE DESCRI. 02/01/18 WATER DEPTH (FT) 54.07
LOCAL ID. DE-2017-01 DESCR. BY CRM



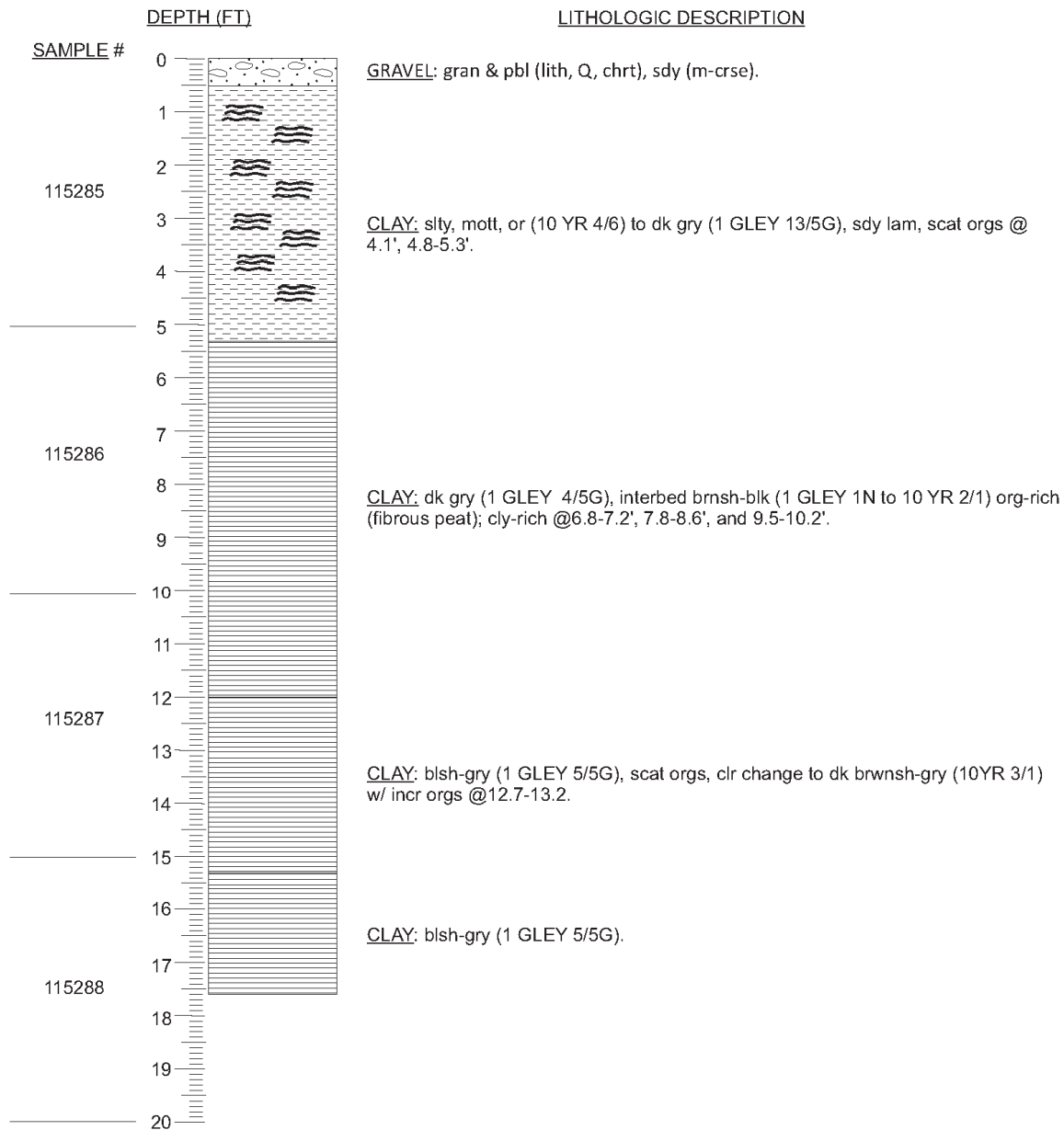
DGSID Pk23-02 DATE DESCRI. 11/15/17 WATER DEPTH (FT) 60.0
LOCAL ID. BOEM-16-02 DESCR. BY CRM



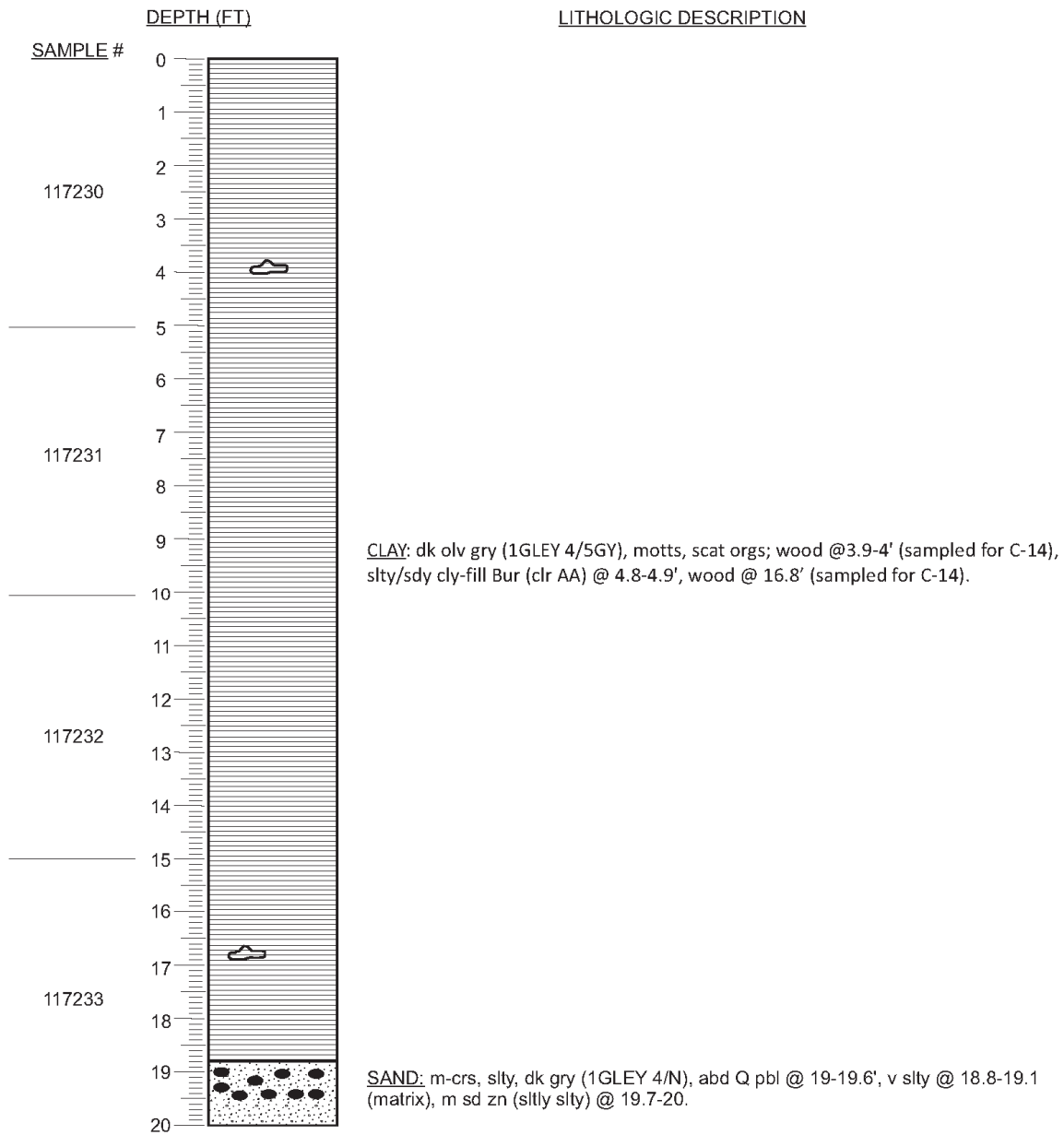
DGSID Pk23-03 DATE DESCRI. 11/15/17 WATER DEPTH (FT) 59.4
LOCAL ID. BOEM-16-03 DESCR. BY CRM



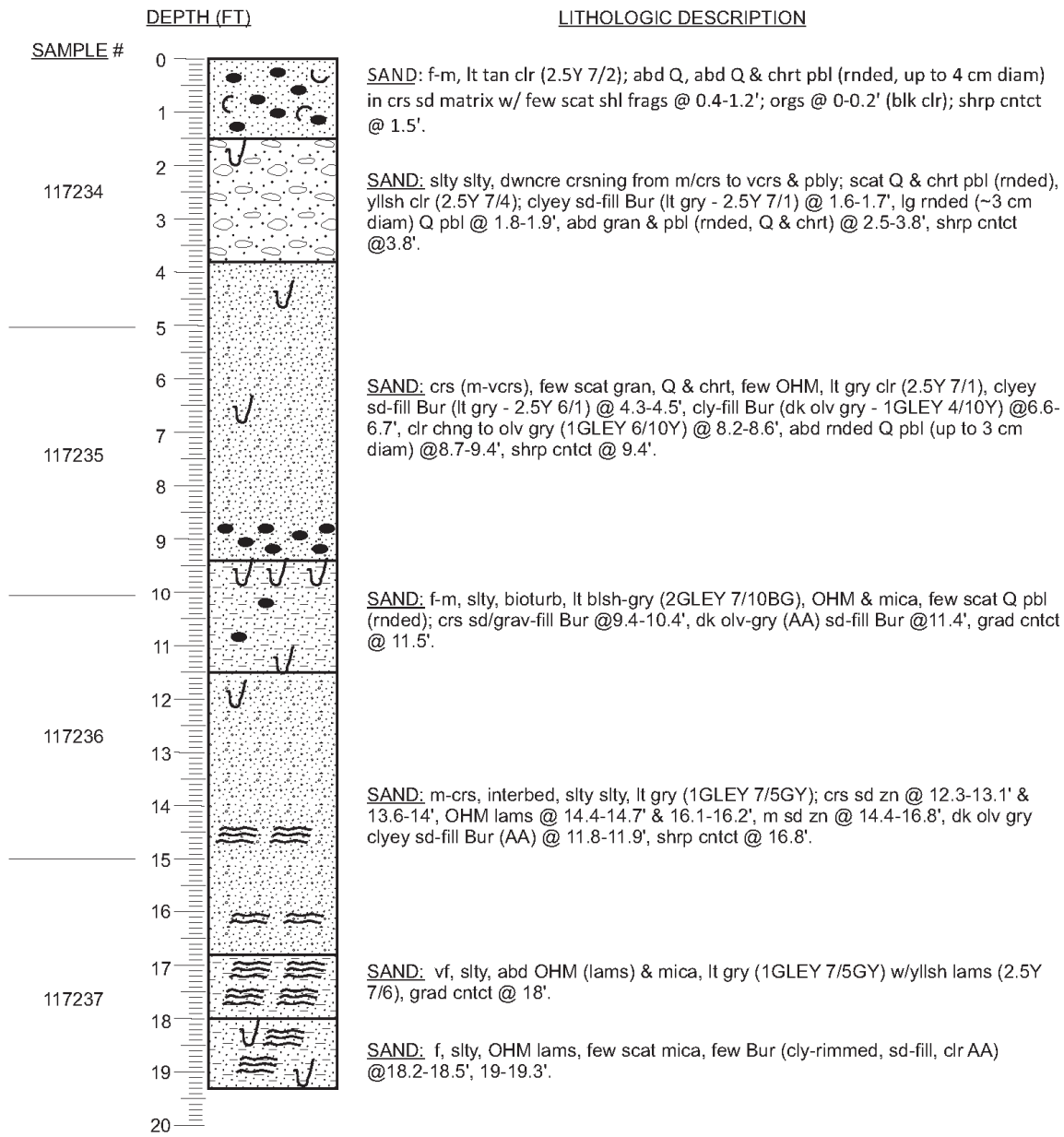
DGSID Pk33-01 DATE DESCRI. 11/15/17 WATER DEPTH (FT) 58.2
LOCAL ID. BOEM-16-04 DESCR. BY CRM



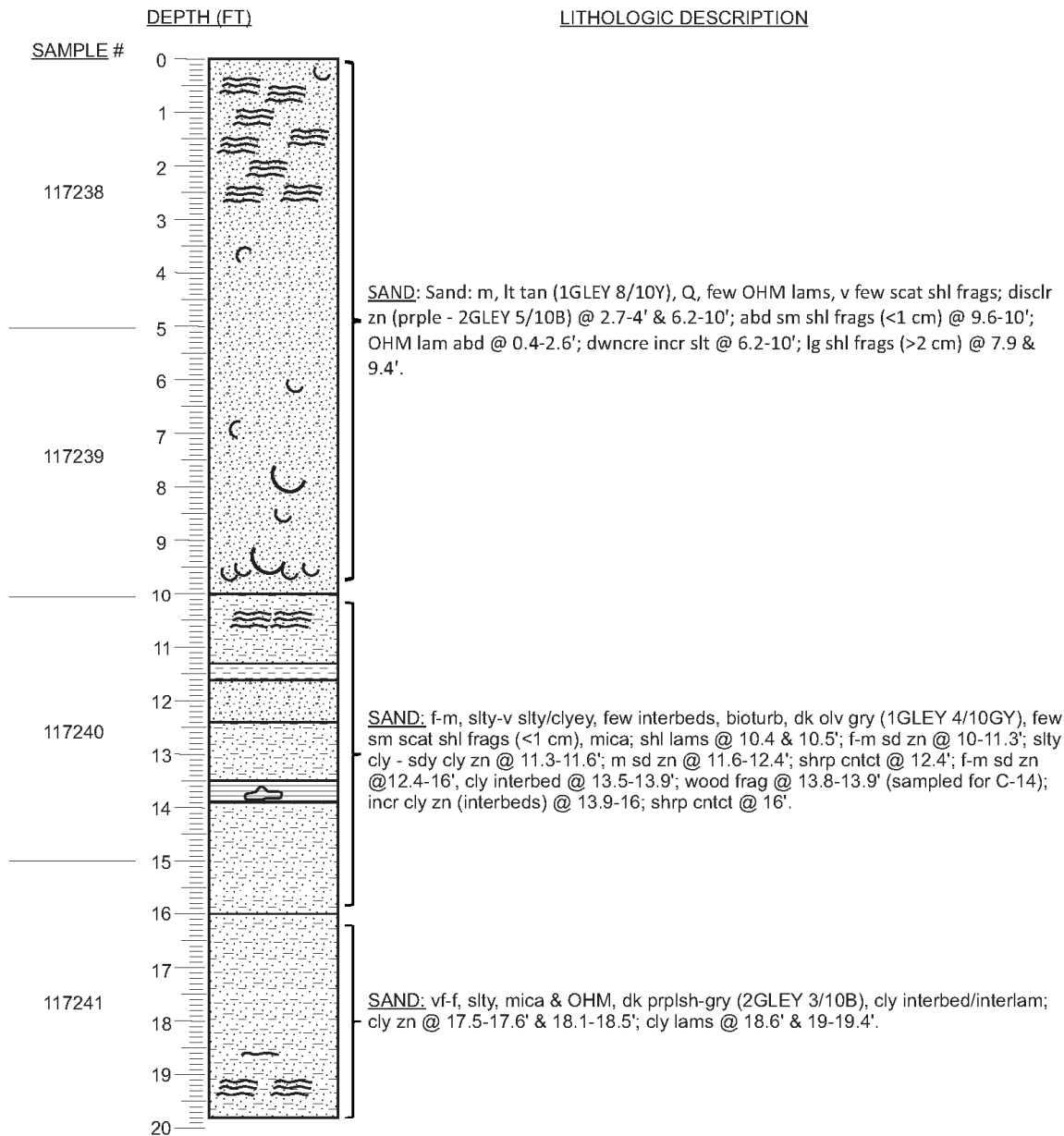
DGSID Pk33-02 DATE DESCRI. 01/31/18 WATER DEPTH (FT) 63.69
LOCAL ID. DE-2017-02 DESCR. BY CRM



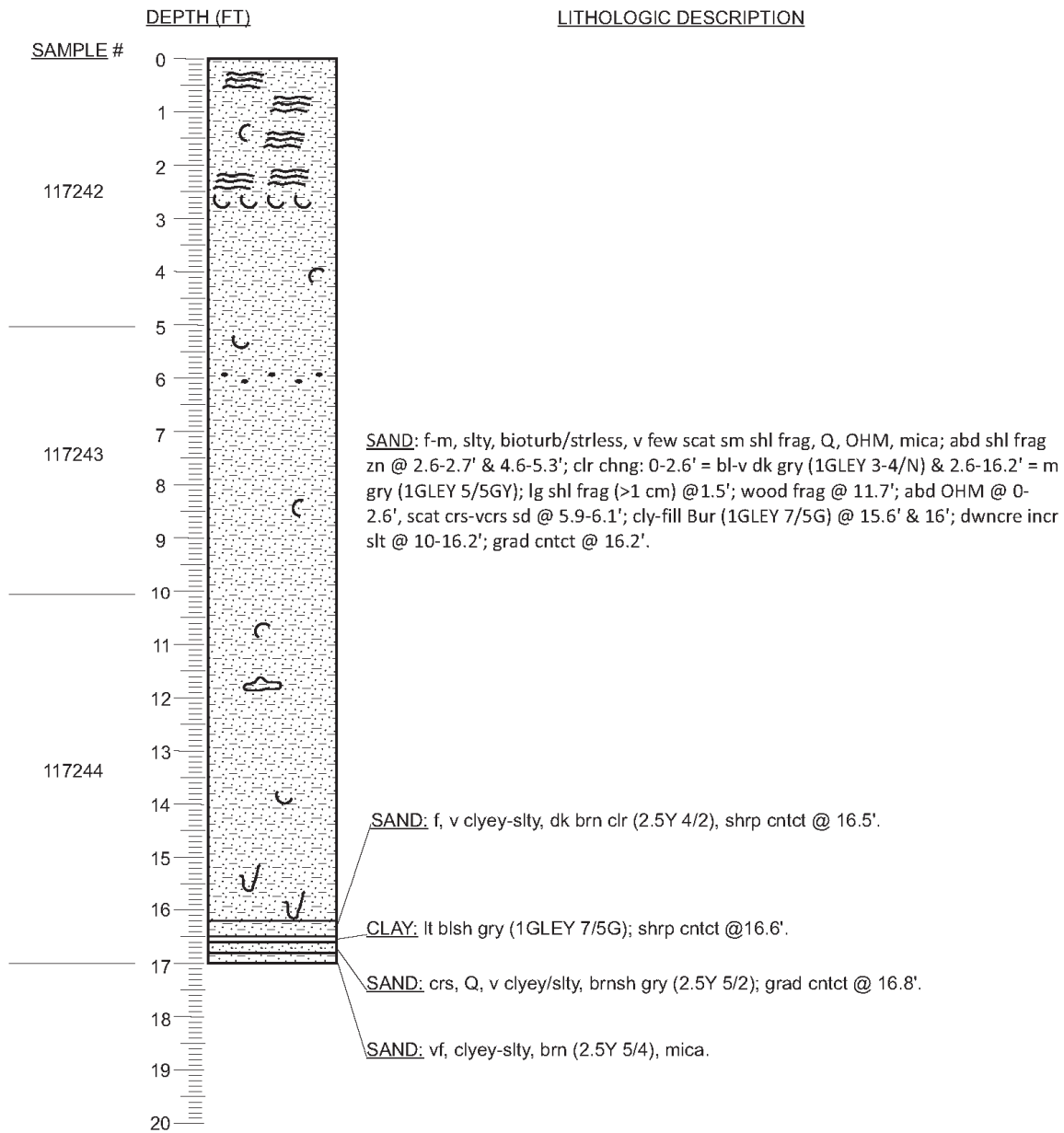
DGSID Pk43-01 DATE DESCRI. 02/01/18 WATER DEPTH (FT) 58.83
LOCAL ID. DE-2017-03 DESCR. BY CRM



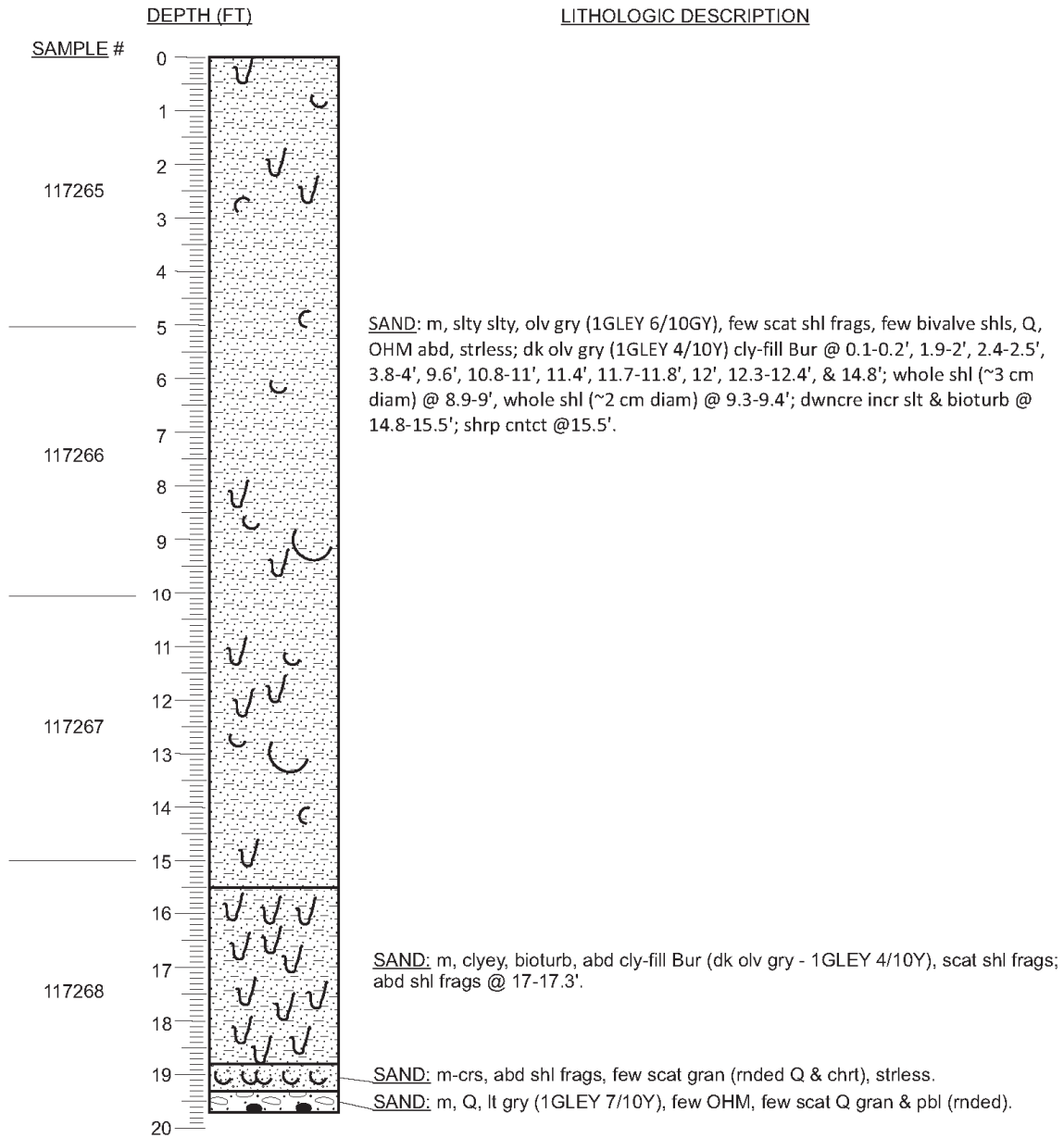
DGSID Sk44-01 DATE DESCRI. 02/01/18 WATER DEPTH (FT) 45.68
LOCAL ID. MD-2017-01 DESCR. BY CRM



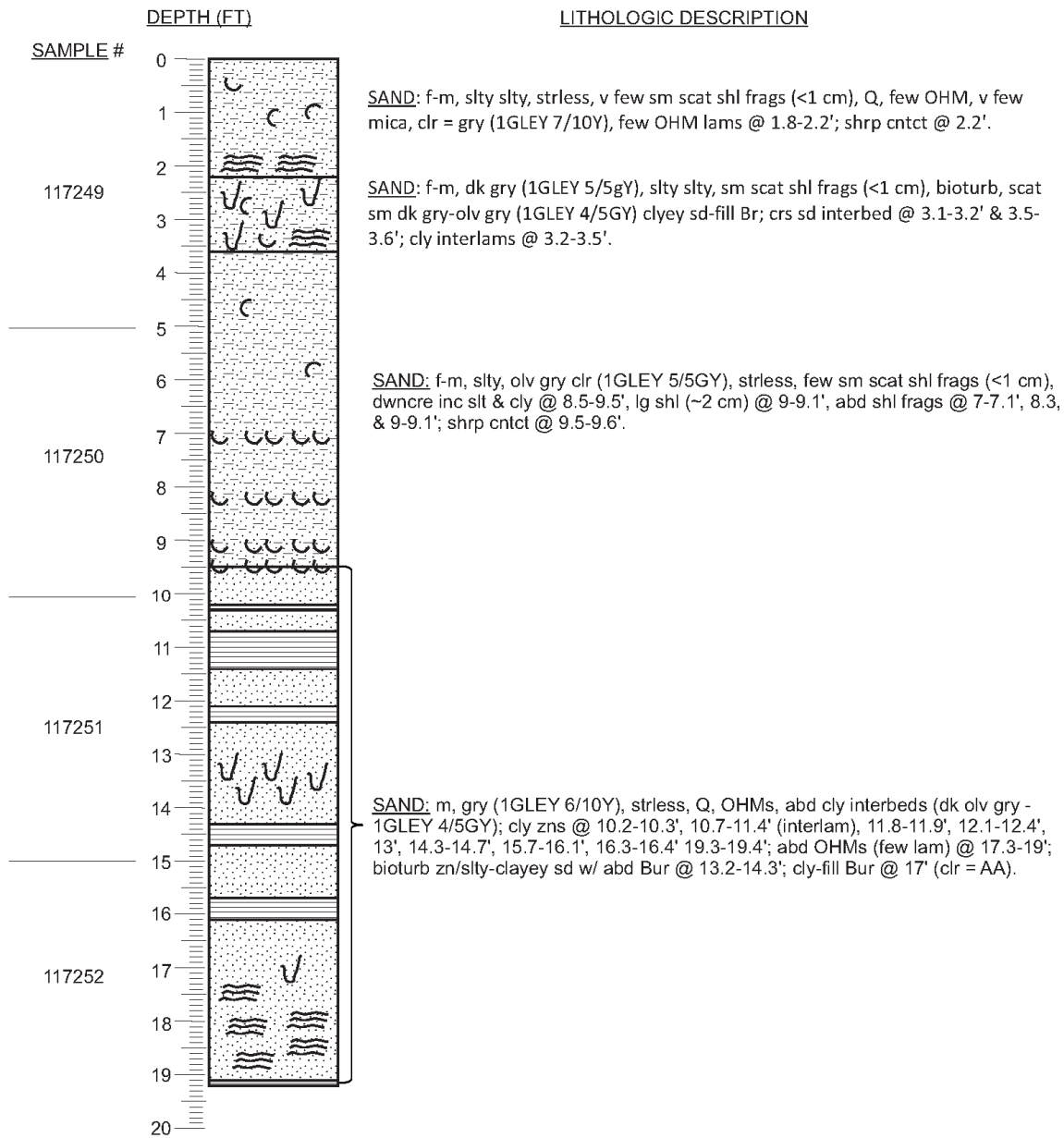
DGSID Sk53-01 DATE DESCRI. 02/01/18 WATER DEPTH (FT) 42.69
LOCAL ID. MD-2017-02 DESCR. BY CRM



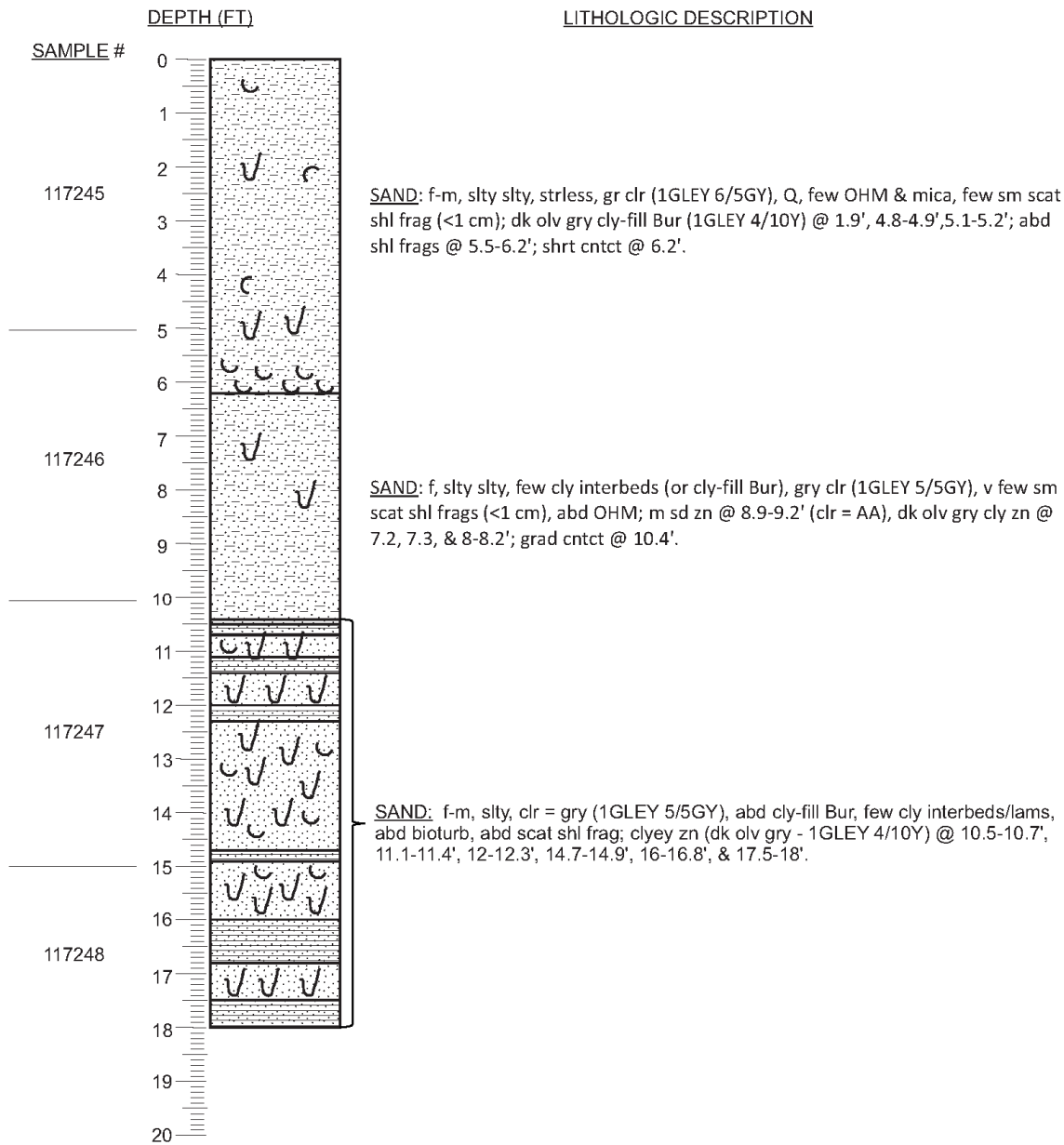
DGSID Tj15-01 DATE DESCRI. 02/07/18 WATER DEPTH (FT) 39.4
LOCAL ID. MD-2017-08 DESCR. BY CRM



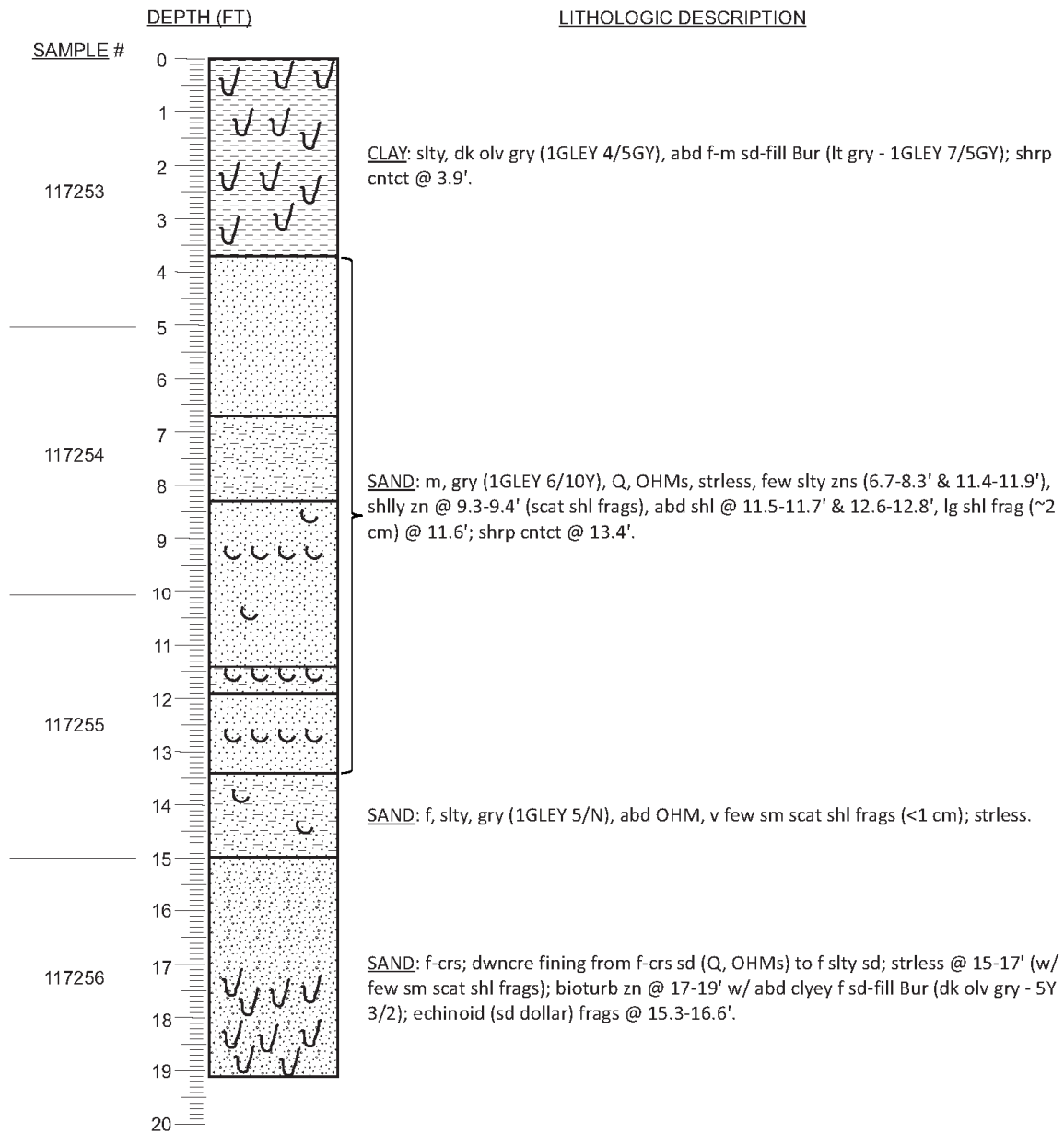
DGSID Tj35-01 DATE DESCRI. 02/02/18 WATER DEPTH (FT) 42.97
LOCAL ID. MD-2017-04 DESCR. BY CRM



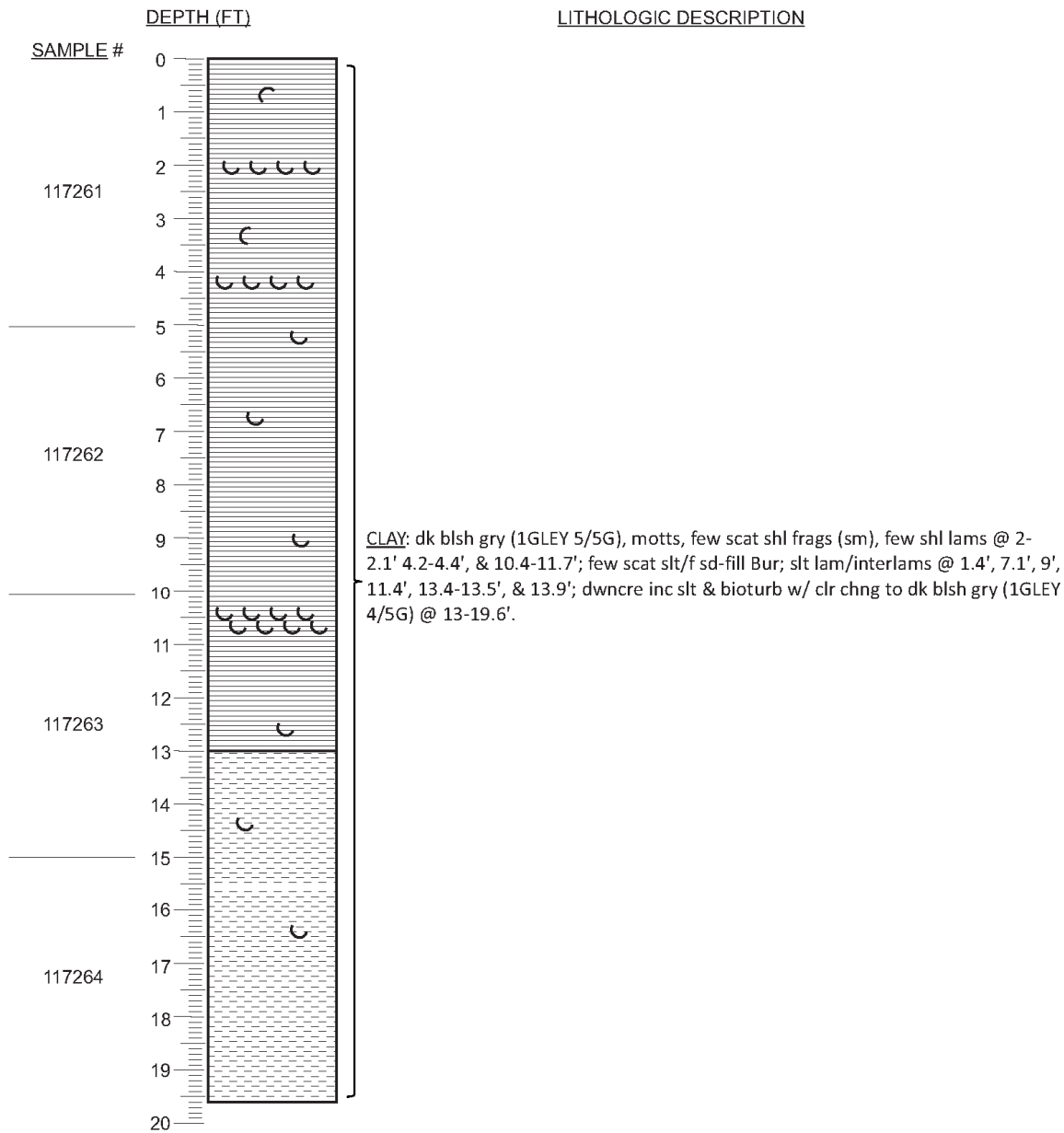
DGSID Tj54-01 DATE DESCRI. 02/02/18 WATER DEPTH (FT) 41.79
LOCAL ID. MD-2017-03 DESCR. BY CRM



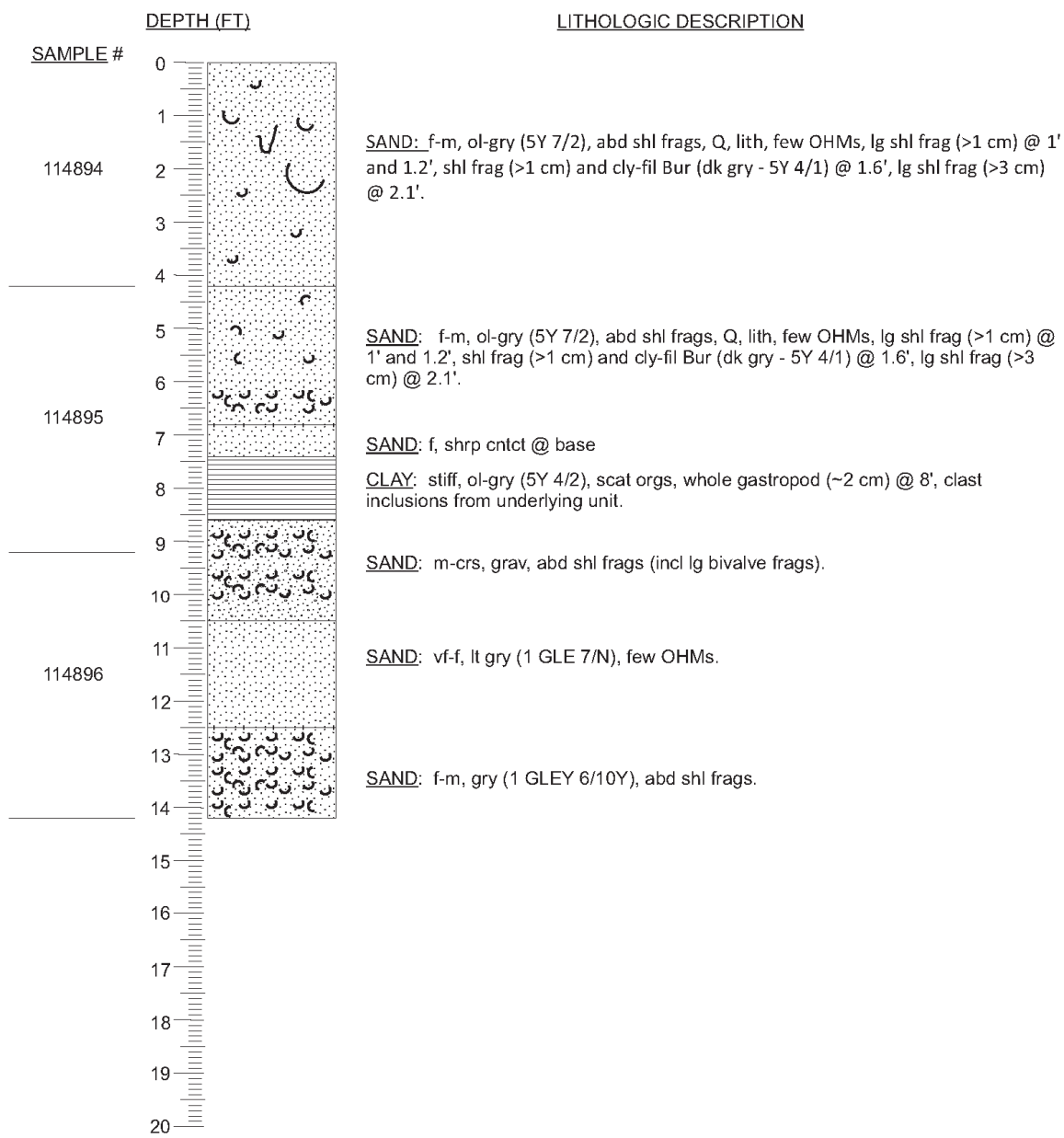
DGSID Tk21-01 DATE DESCRI. 02/06/18 WATER DEPTH (FT) 53.47
LOCAL ID. MD-2017-05 DESCR. BY CRM



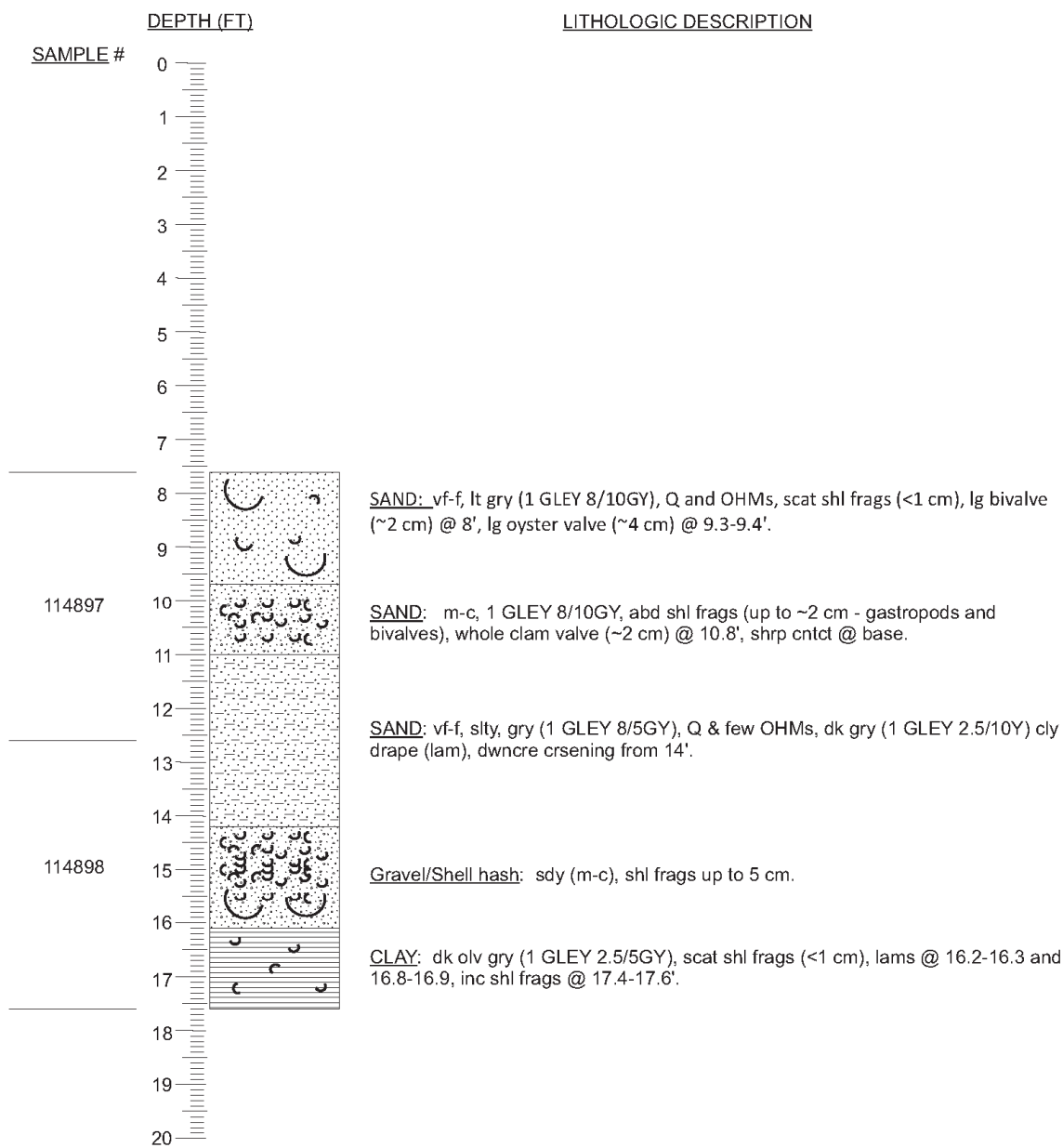
DGSID Ui54-01 DATE DESCRI. 02/06/18 WATER DEPTH (FT) 53.47
LOCAL ID. MD-2017-07 DESCR. BY CRM



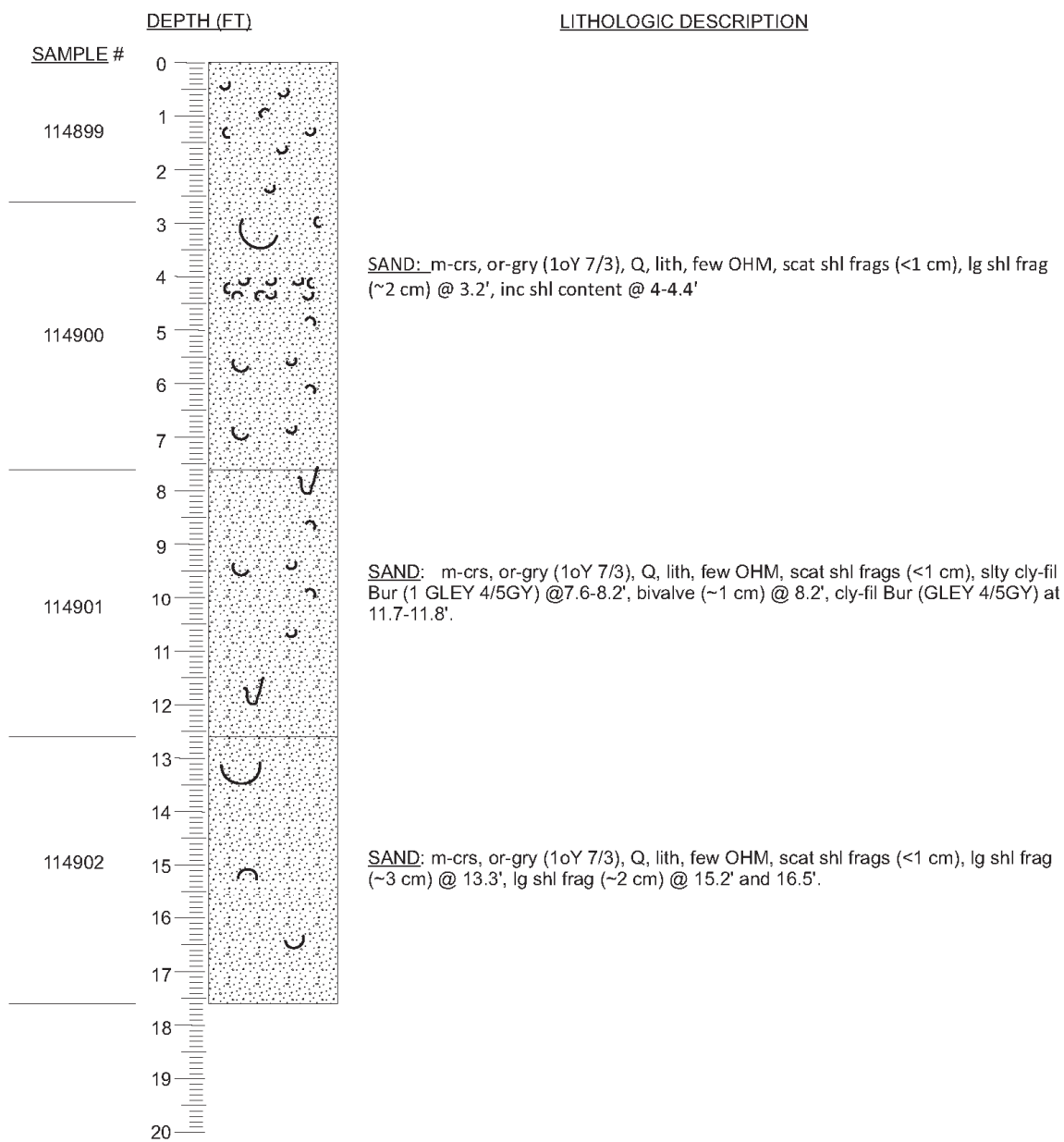
DGSID Uj35-02 DATE DESCRI. 10/30/17 WATER DEPTH (FT) 62.66
LOCAL ID. MD BOEM-15- DESCR. BY CRM
03



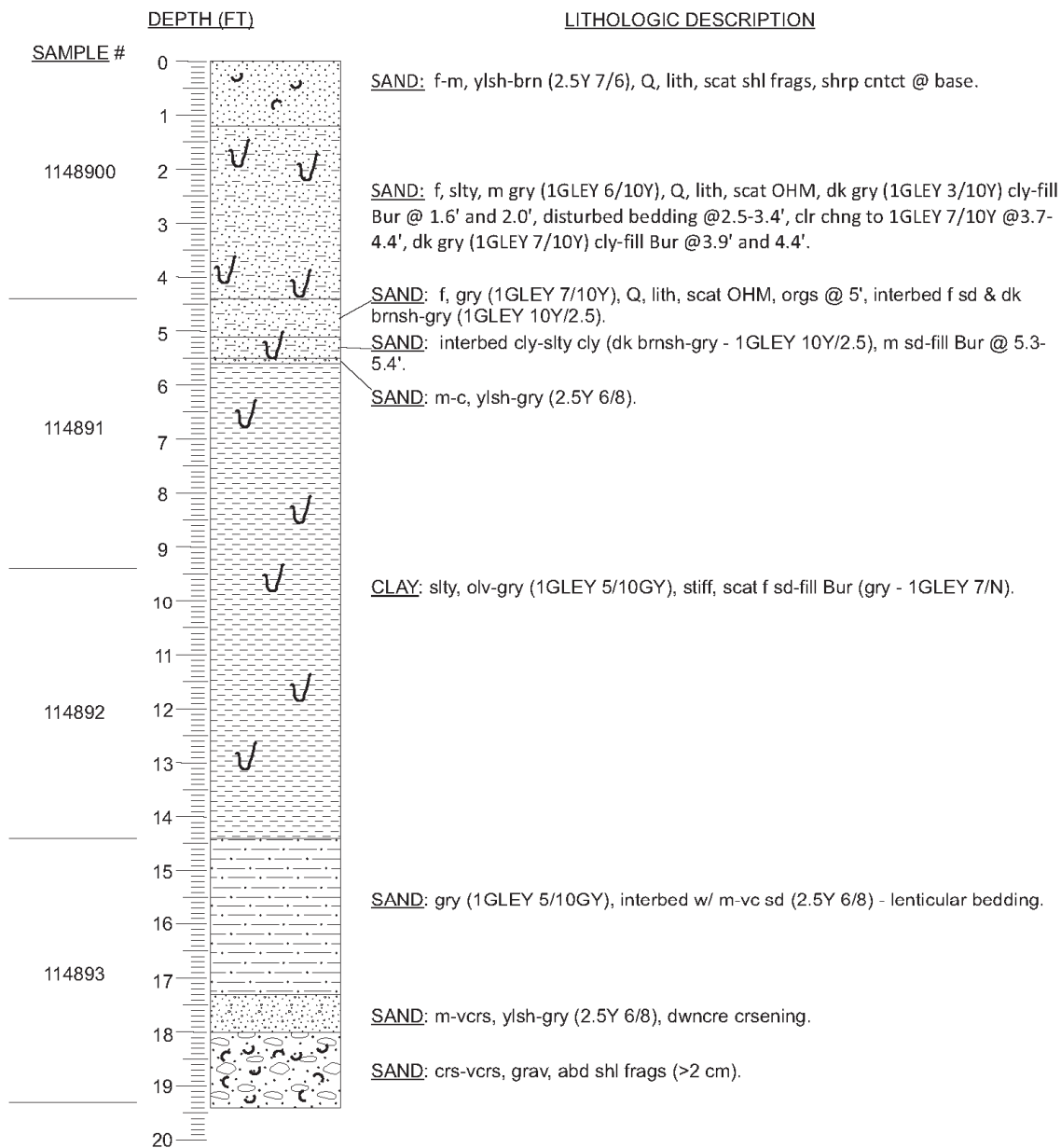
DGSID Uj35-03 DATE DESCRI. 11/01/17 WATER DEPTH (FT) 62.66
LOCAL ID. MD BOEM-15- DESCR. BY CRM
 03a



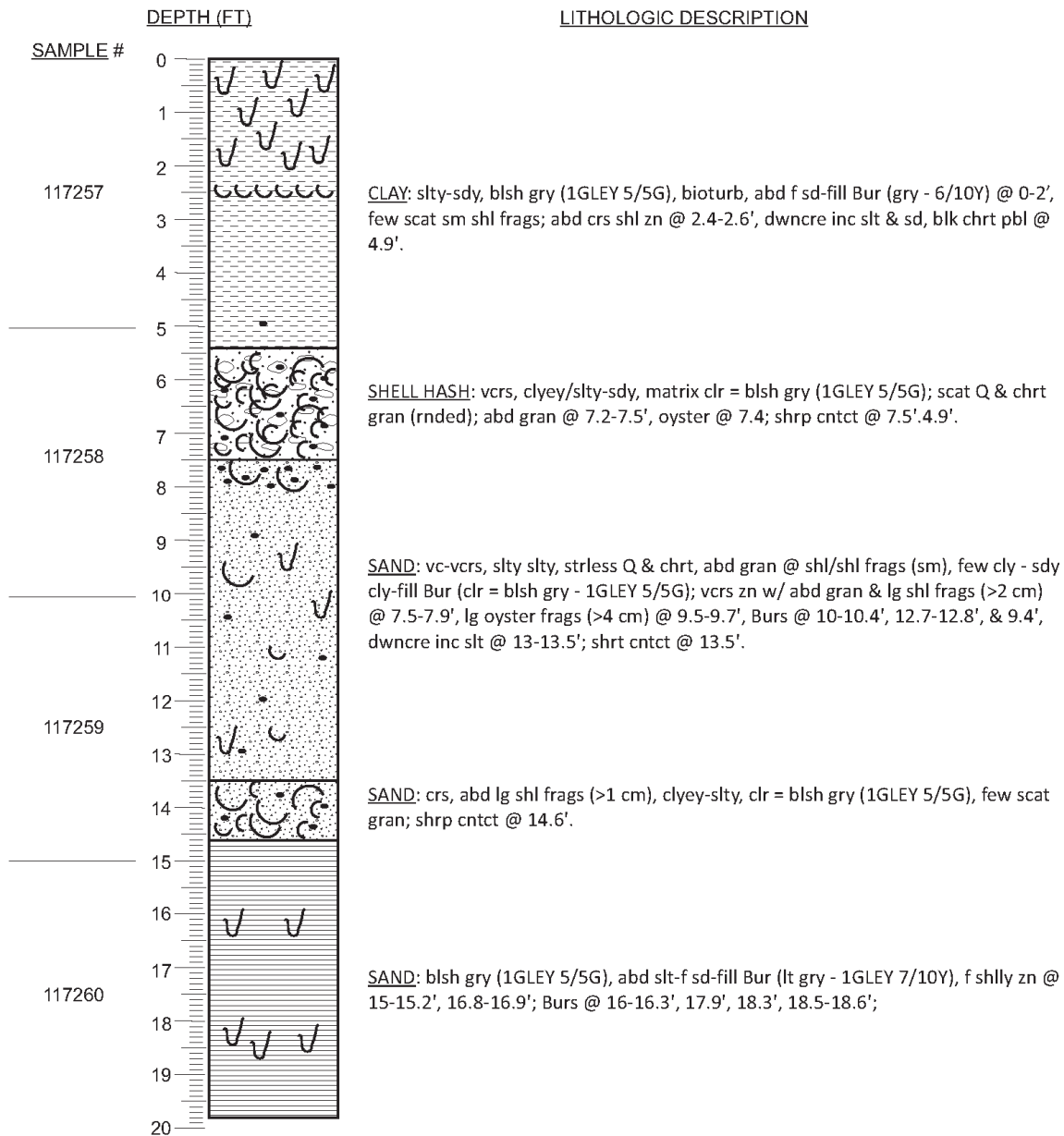
DGSID Uj43-01 DATE DESCRI. 10/24/17 WATER DEPTH (FT) 46.92
LOCAL ID. MD BOEM-15- DESCR. BY CRM
 04



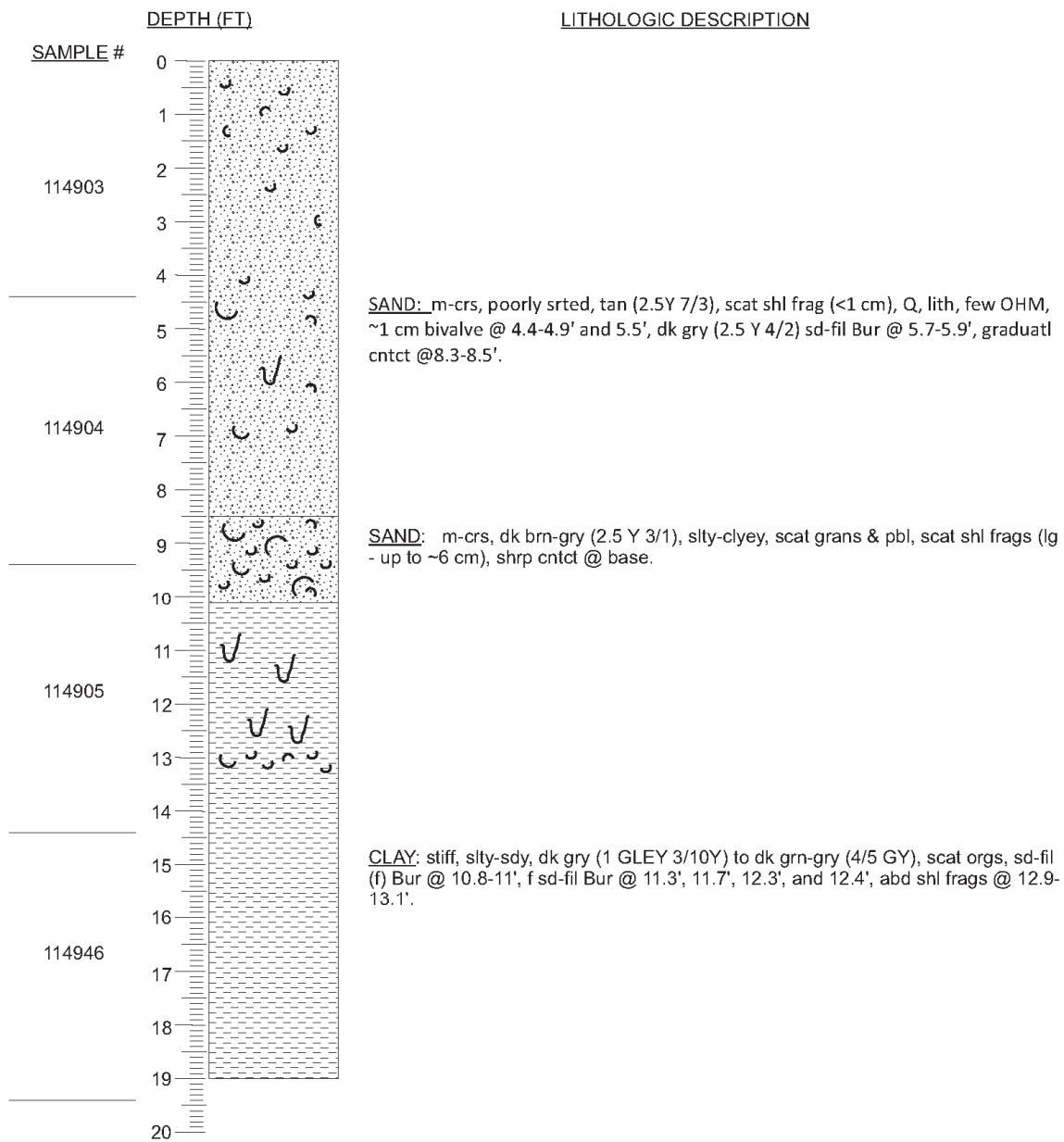
DGSID Uk12-01 DATE DESCRI. 10/31/17 WATER DEPTH (FT) 58.4
LOCAL ID. MD BOEM-15- DESCR. BY CRM
 01



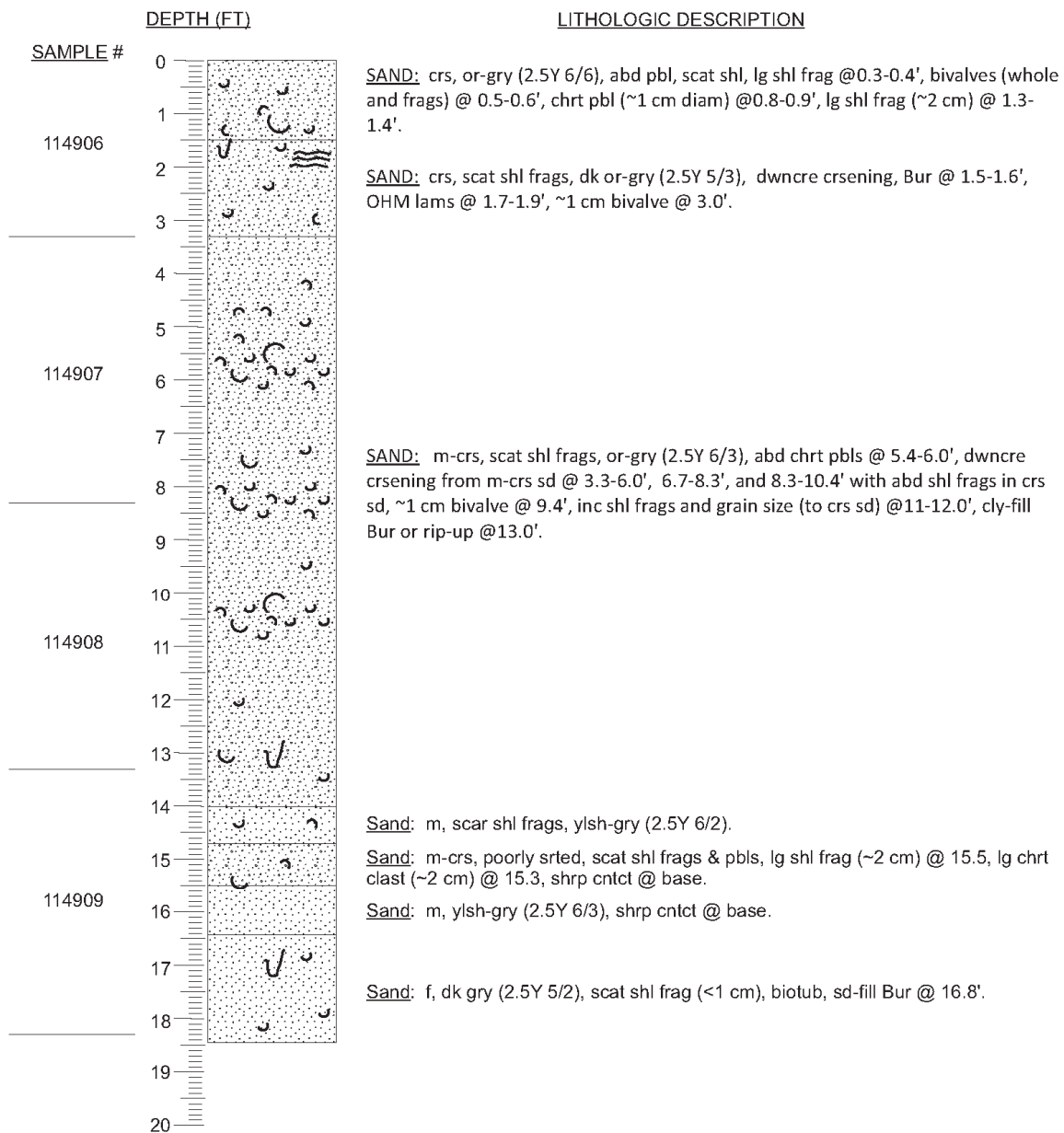
DGSID Vi14-01 DATE DESCRI. 02/06/18 WATER DEPTH (FT) 43.21
LOCAL ID. MD-2017-06 DESCR. BY CRM



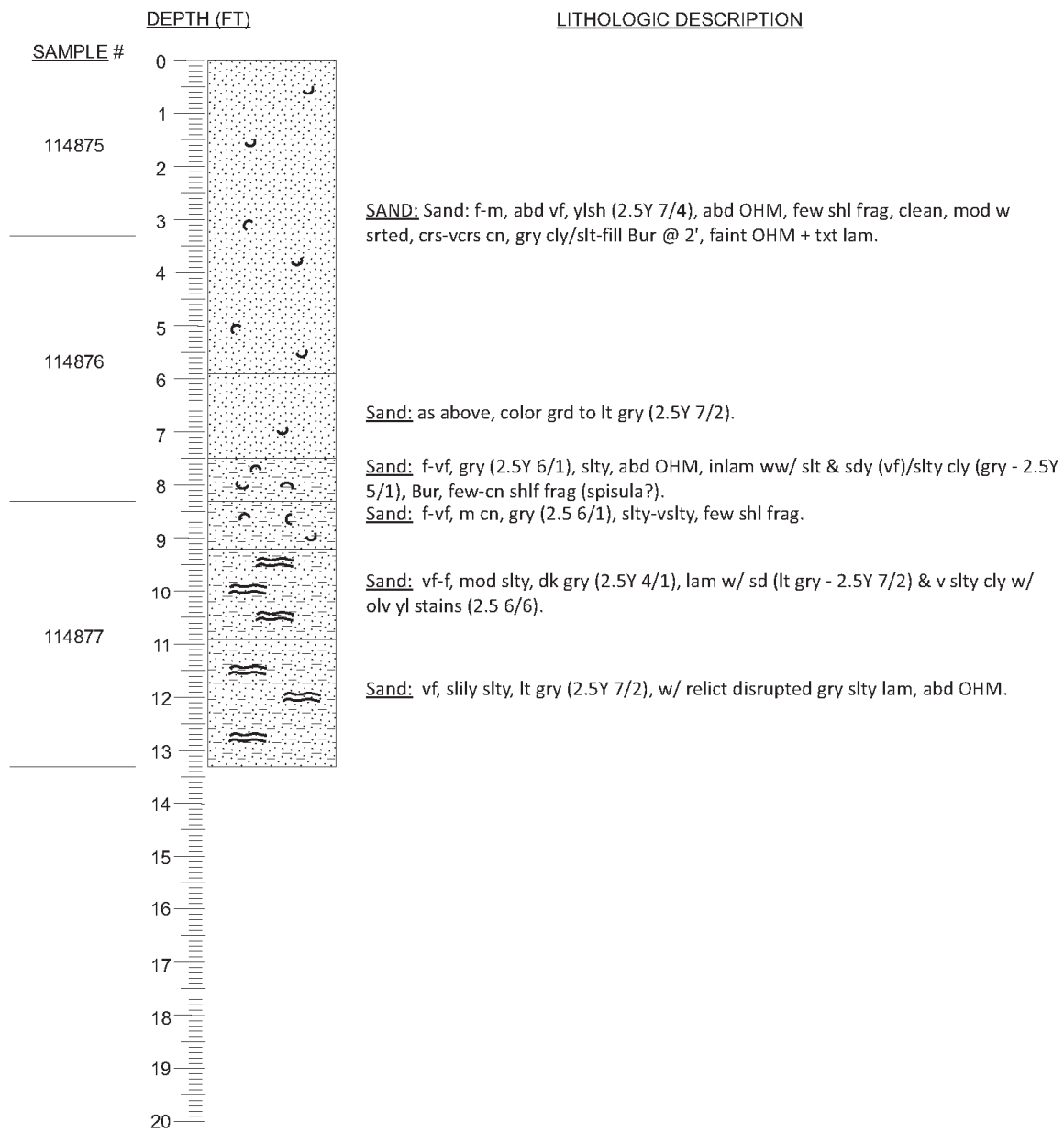
DGSID Vj34-01 DATE DESCRI. 10/18/17 WATER DEPTH (FT) 50.85
LOCAL ID. MD BOEM-15- DESCR. BY CRM
05



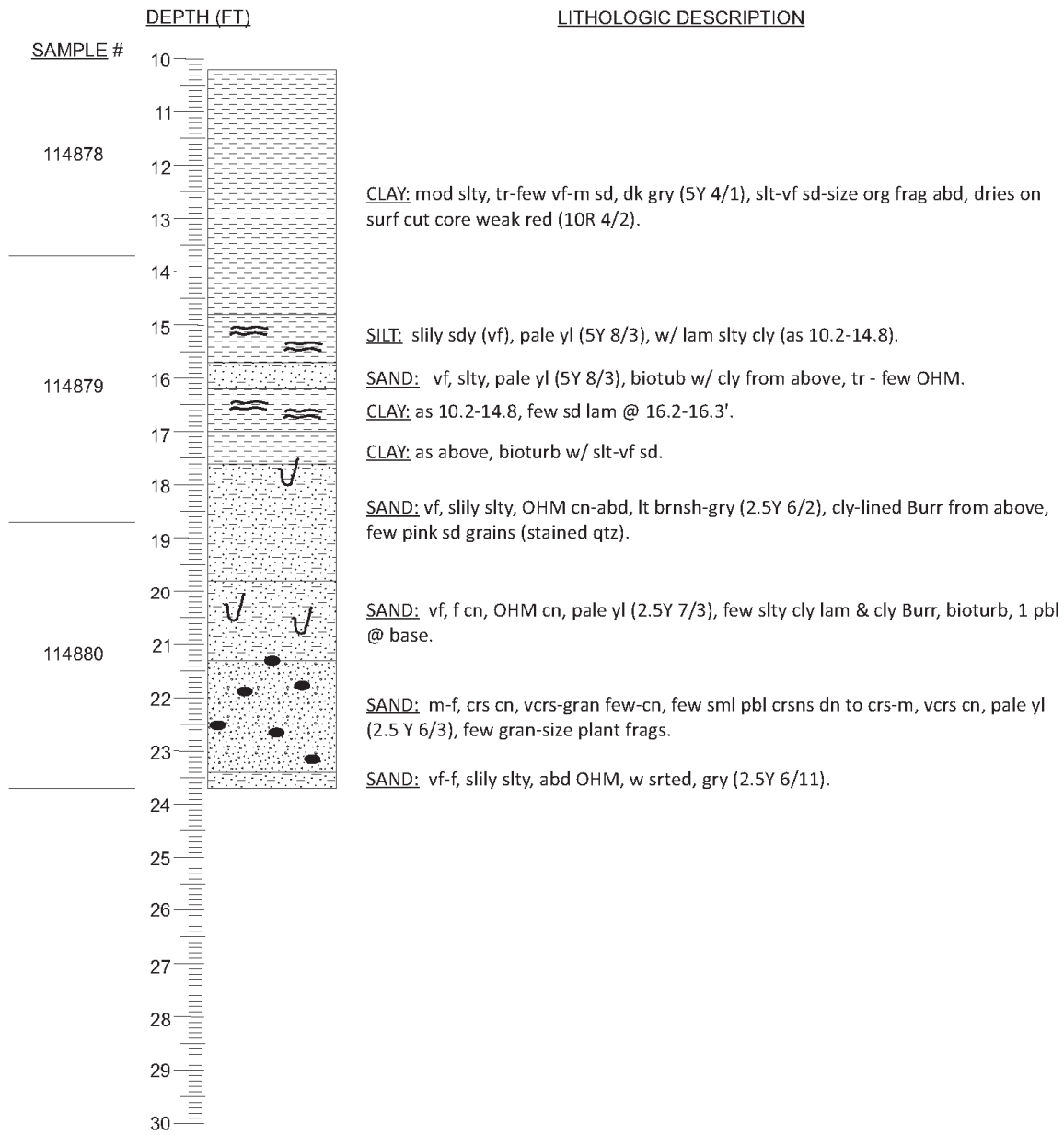
DGSID Wj22-01 DATE DESCRI. 10/16/17 WATER DEPTH (FT) 40.68
LOCAL ID. MD BOEM-15- DESCR. BY CRM
07



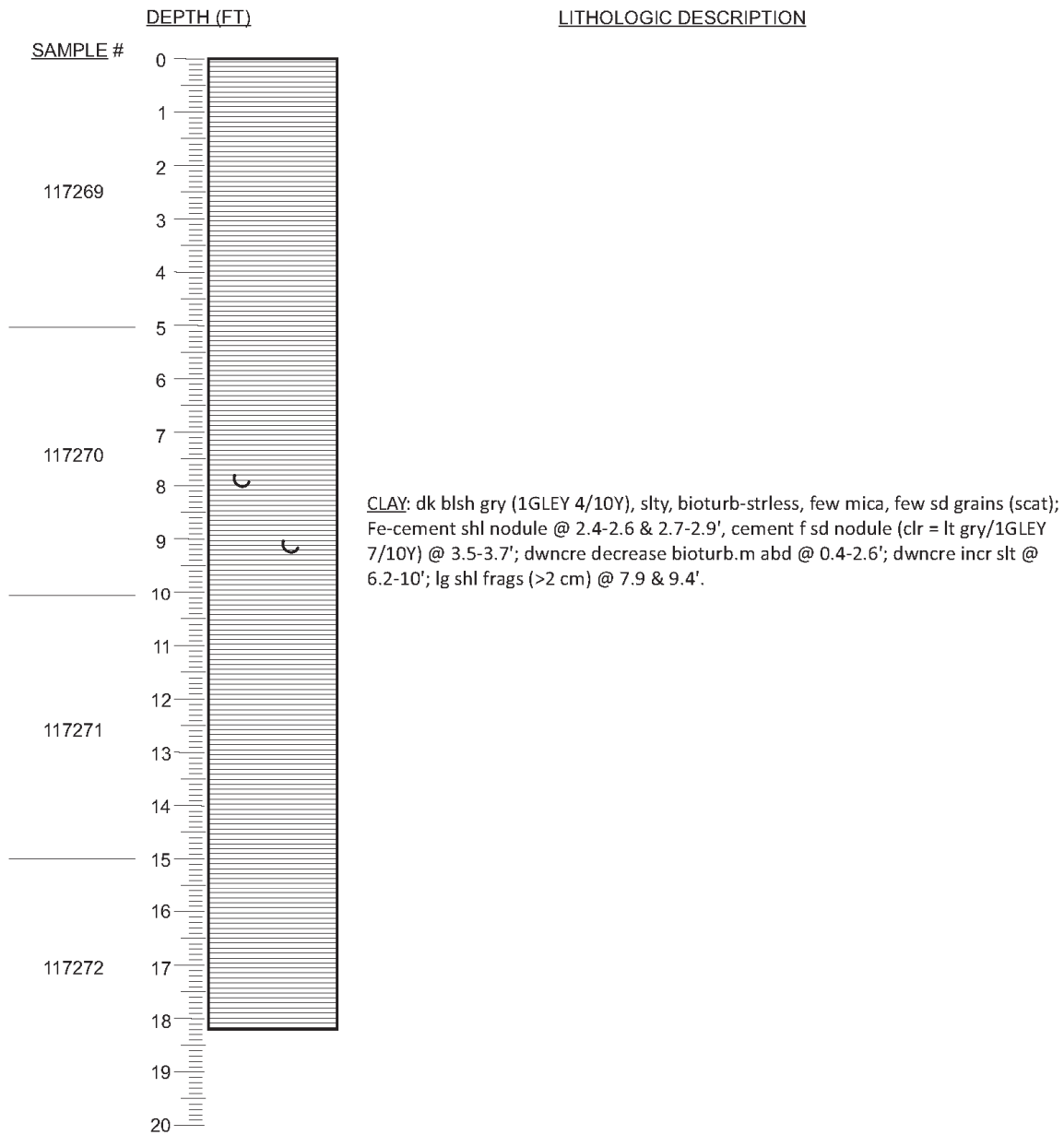
DGSID Xh54-01 DATE DESCRI. 01/30/17 WATER DEPTH (FT) 54.72
LOCAL ID. VA BOEM-15- DESCR. BY KWR
 06



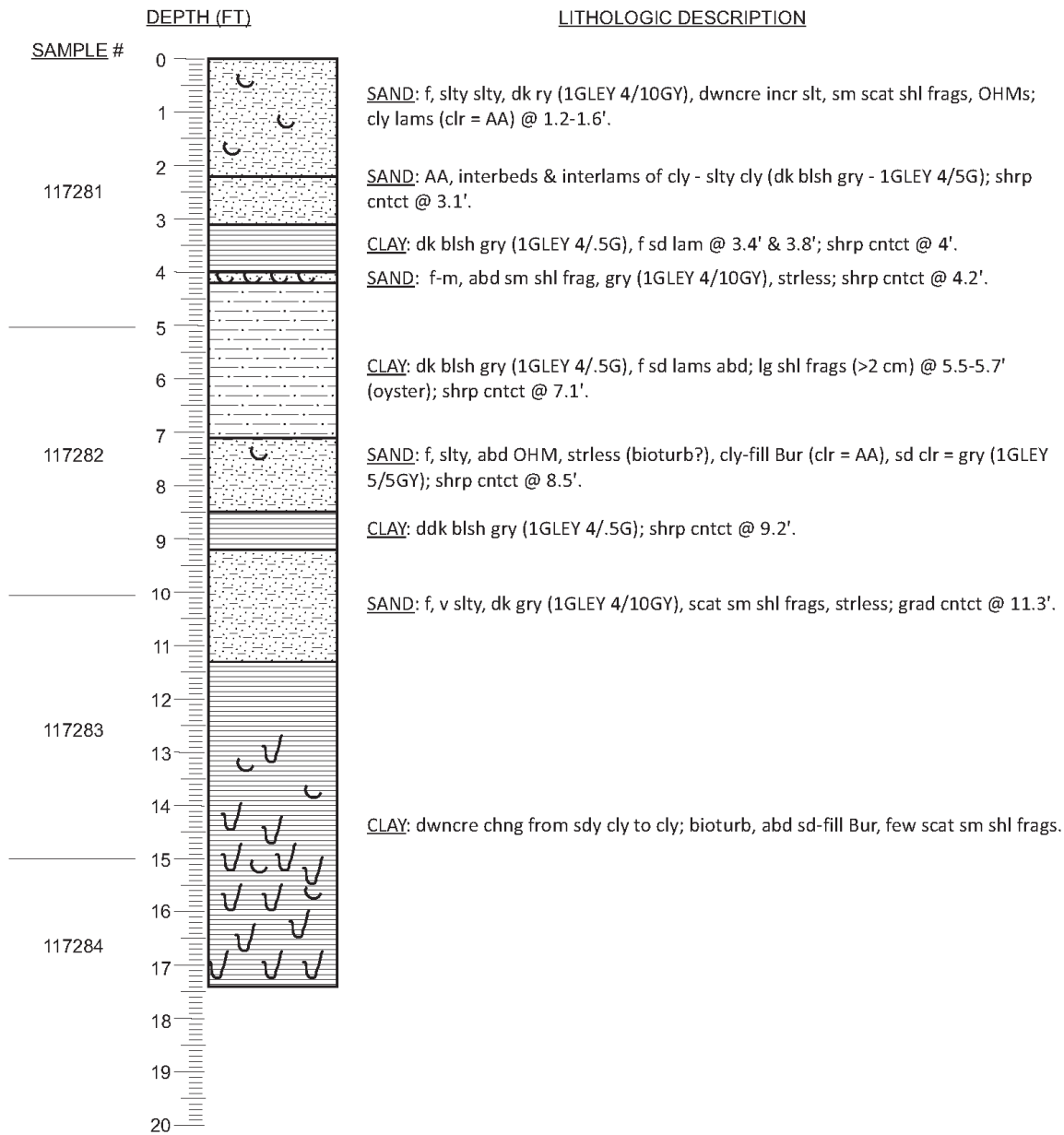
DGSID Xh54-02 DATE DESCRI. 01/30/17 WATER DEPTH (FT) 54.72
LOCAL ID. VA BOEM-15- DESCR. BY KWR
 06a



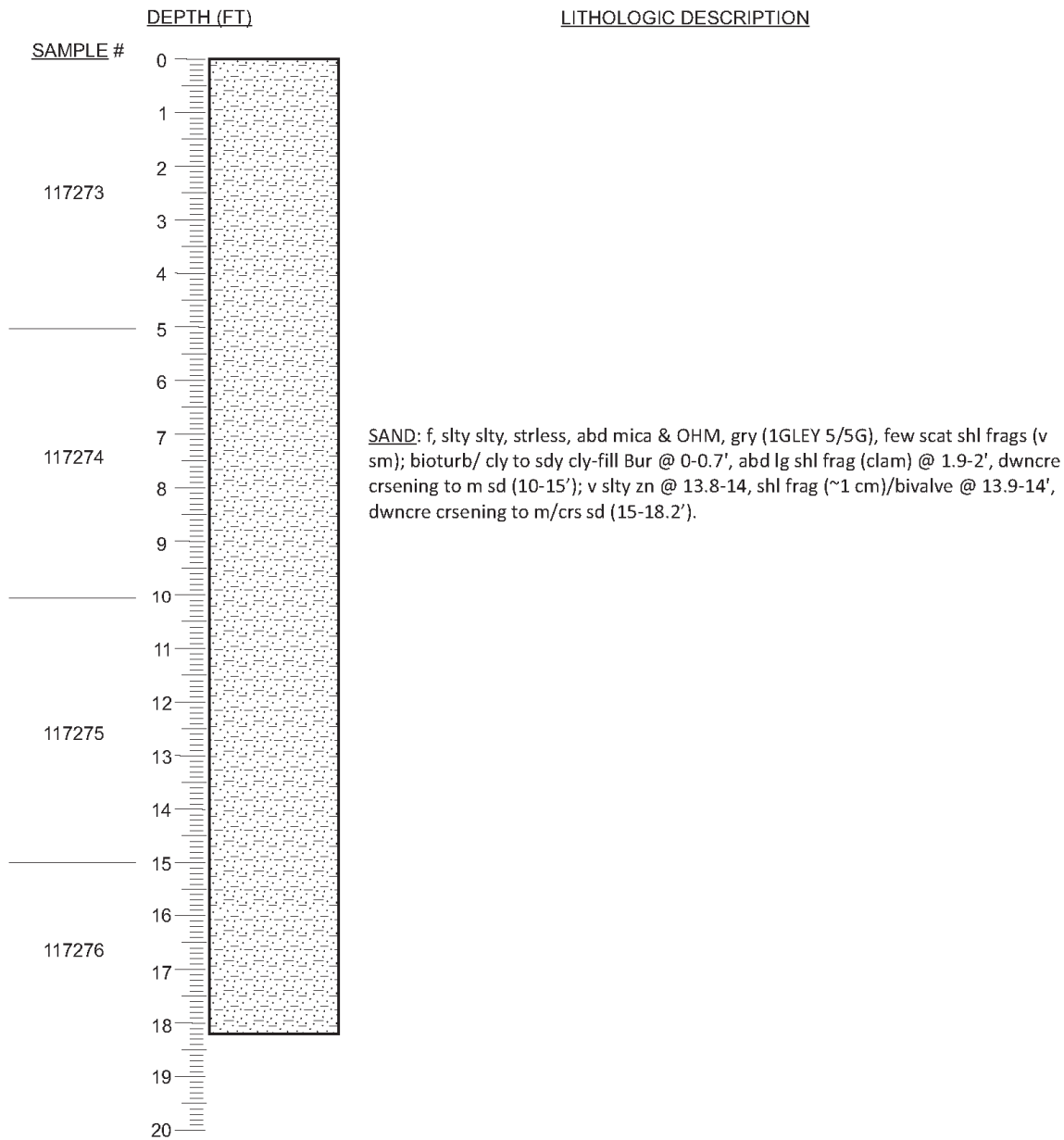
DGSID Yh21-01 DATE DESCRI. 02/13/18 WATER DEPTH (FT) 57.18
LOCAL ID. VA-2017-01 DESCR. BY CRM



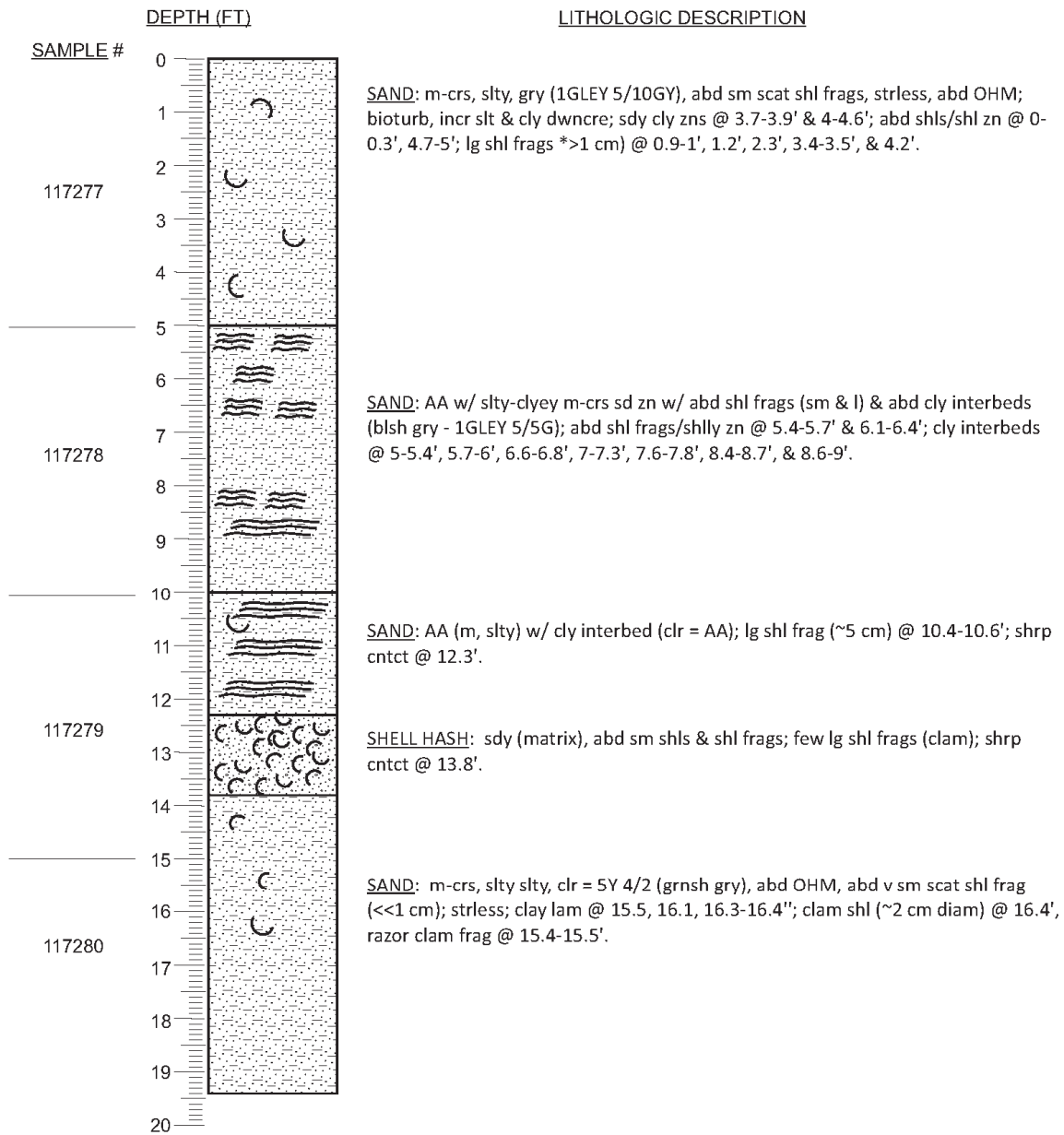
DGSID Yh22-01 DATE DESCRI. 02/15/18 WATER DEPTH (FT) 49.77
LOCAL ID. VA-2017-04 DESCR. BY CRM



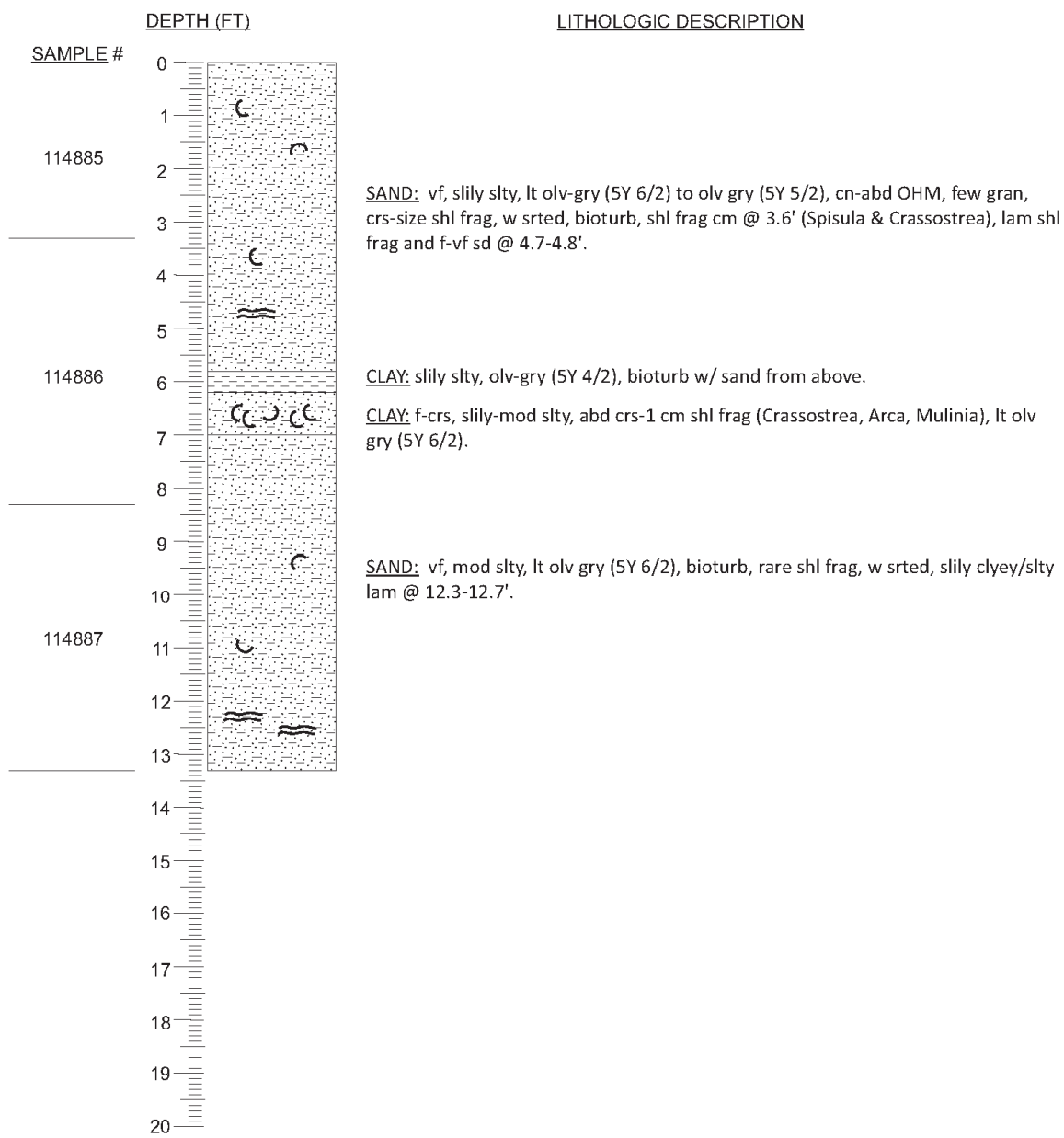
DGSID Yh41-01 DATE DESCRI. 02/13/18 WATER DEPTH (FT) 57.48
LOCAL ID. VA-2017-02 DESCR. BY CRM



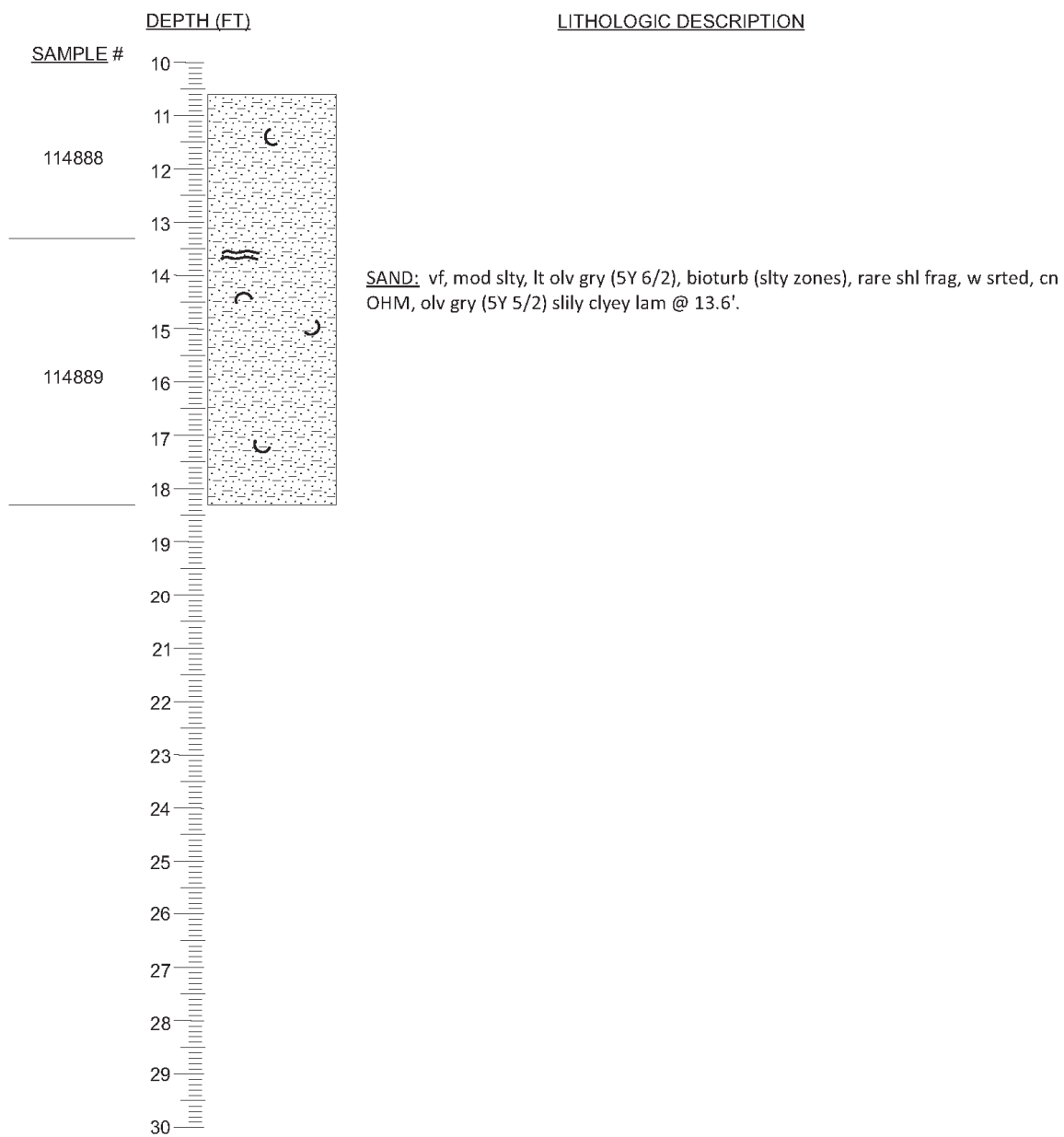
DGSID Yh54-01 DATE DESCRI. 02/14/18 WATER DEPTH (FT) 68.37
LOCAL ID. VA-2017-03 DESCR. BY CRM



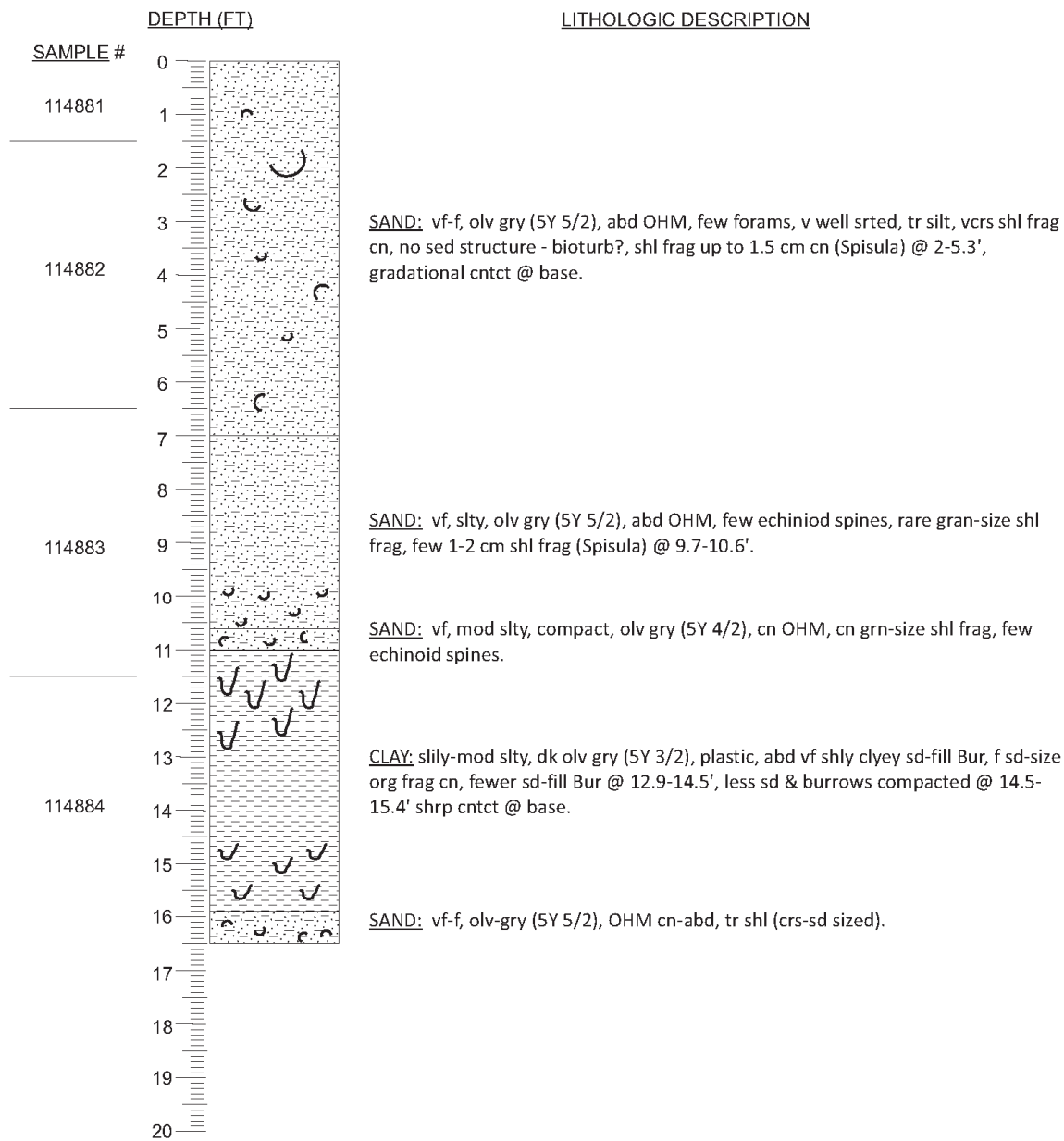
DGSID Zg23-01 DATE DESCRI. 02/01/17 WATER DEPTH (FT) 50.85
LOCAL ID. VA BOEM-15- DESCR. BY KWR
09



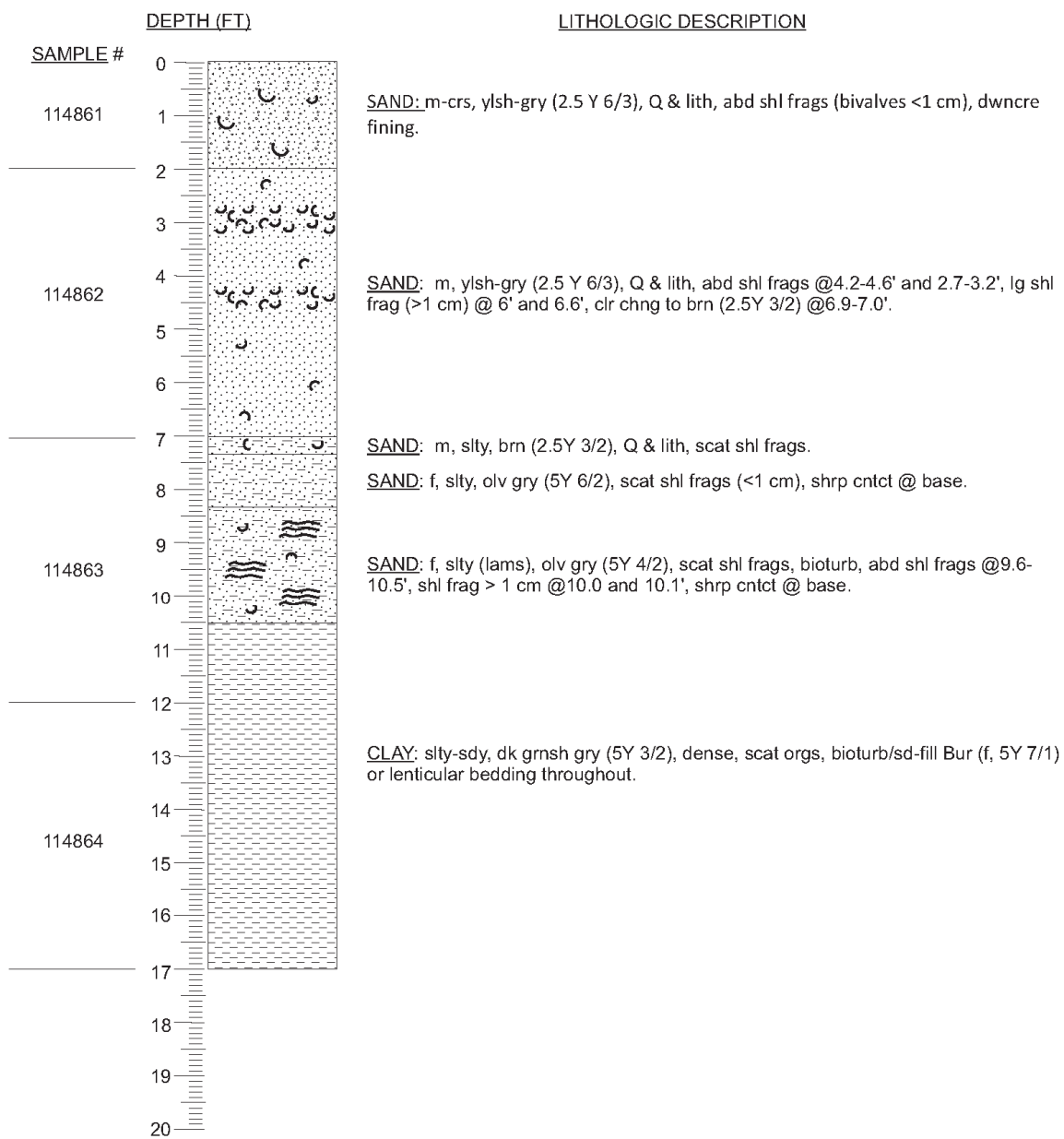
DGSID Zg23-02 DATE DESCRI. 02/01/17 WATER DEPTH (FT) 50.85
LOCAL ID. VA BOEM-15- DESCR. BY KWR
09a



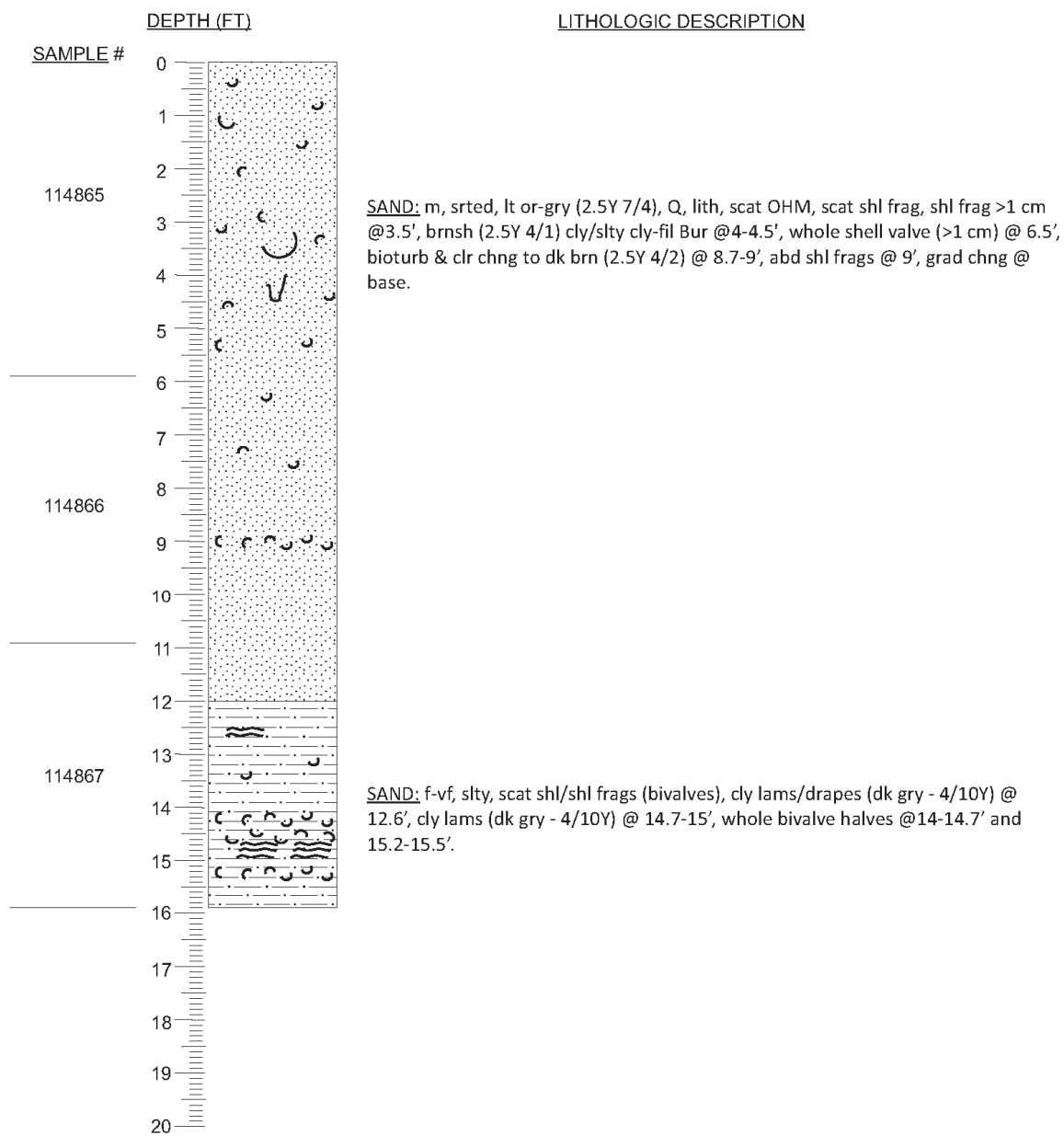
DGSID Zh31-01 DATE DESCR. 02/01/17 WATER DEPTH (FT) 60.37
LOCAL ID. VA BOEM-15- DESCR. BY KWR
 08



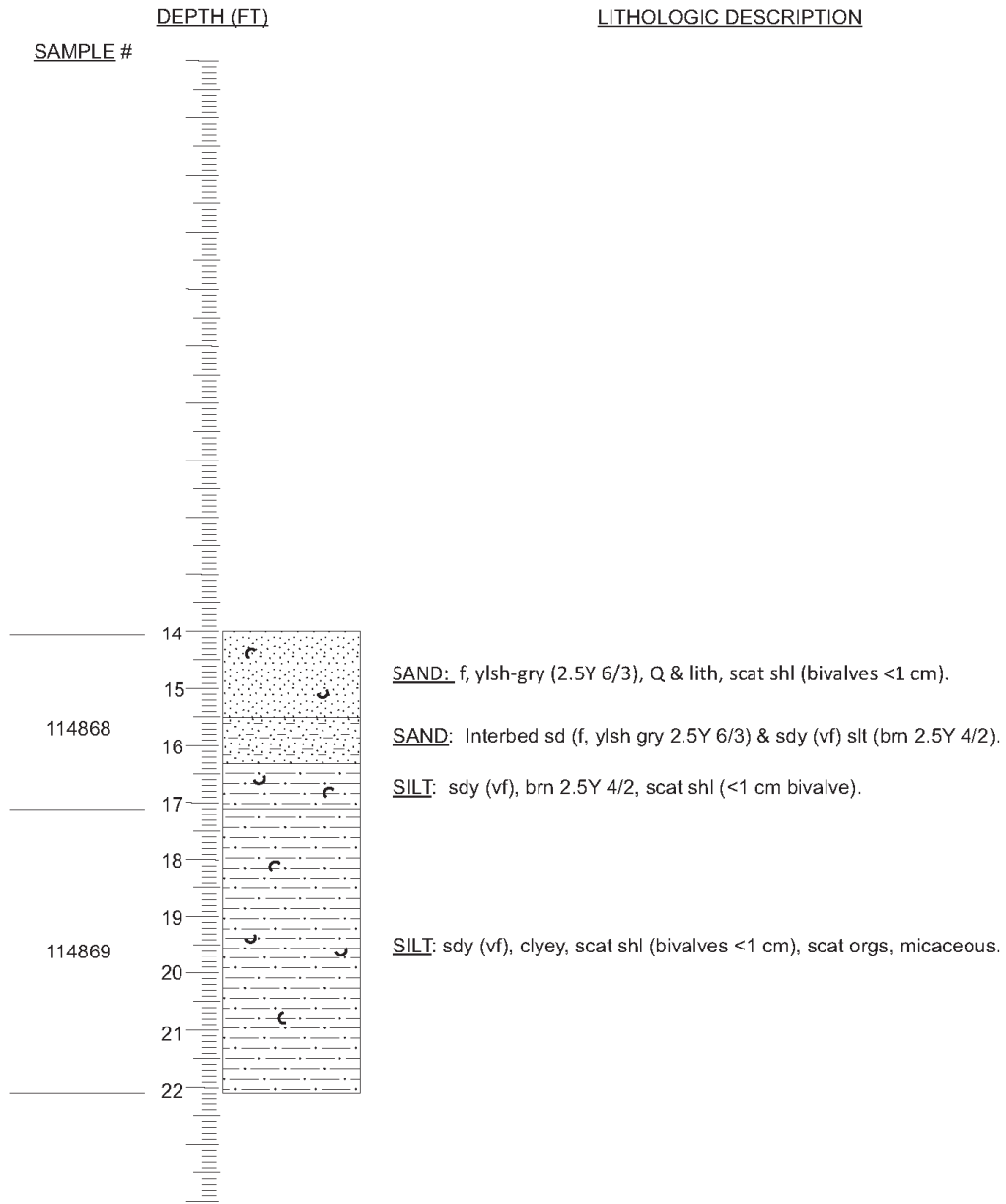
DGSID Zz82-63 DATE DESCRI. 08/17/17 WATER DEPTH (FT) 45.93
LOCAL ID. VA BOEM-15- DESCR. BY CRM
01



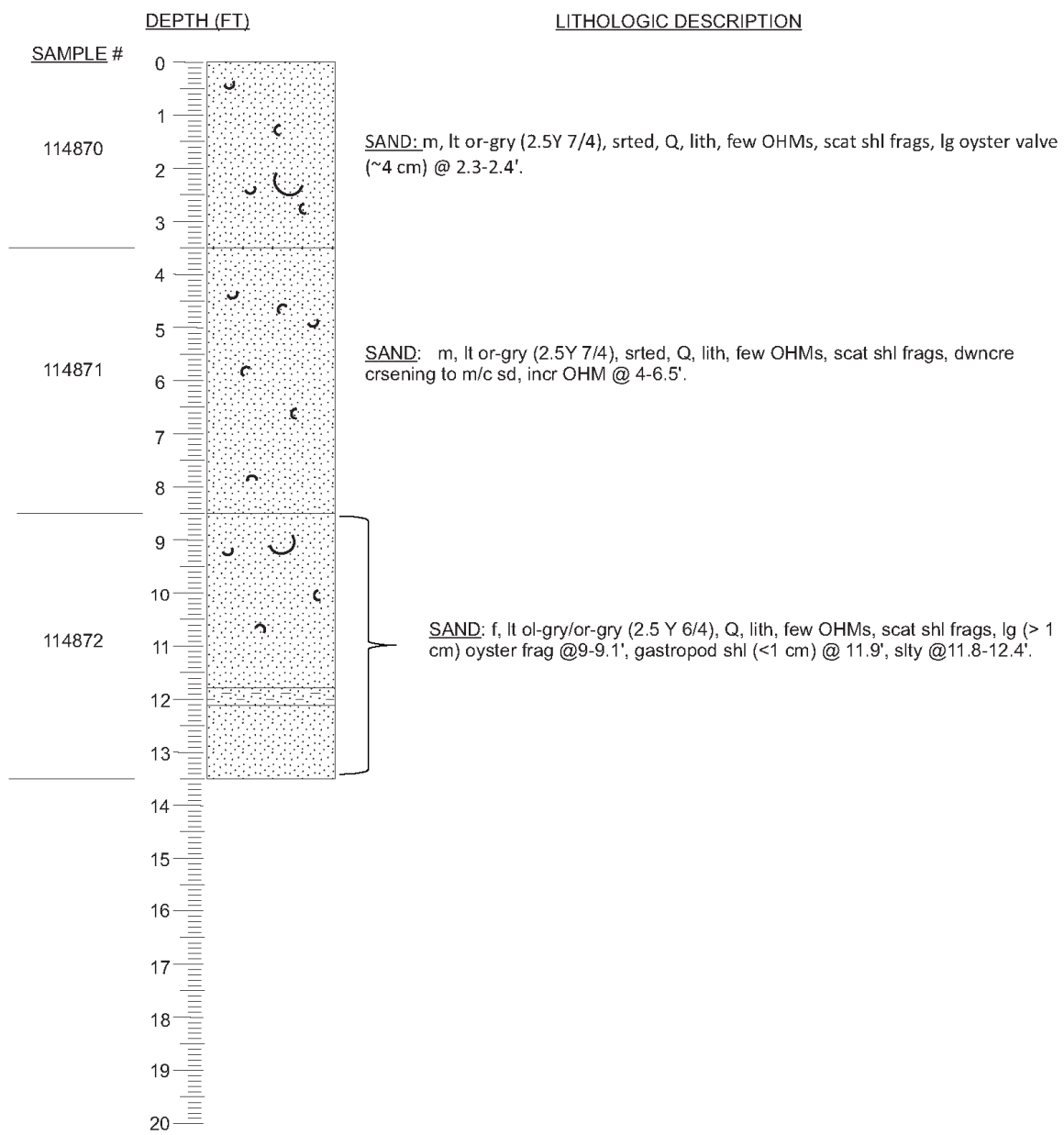
DGSID Zz82-64 DATE DESCRI. 08/15/17 WATER DEPTH (FT) 52.49
LOCAL ID. VA BOEM-15- DESCR. BY CRM
 04



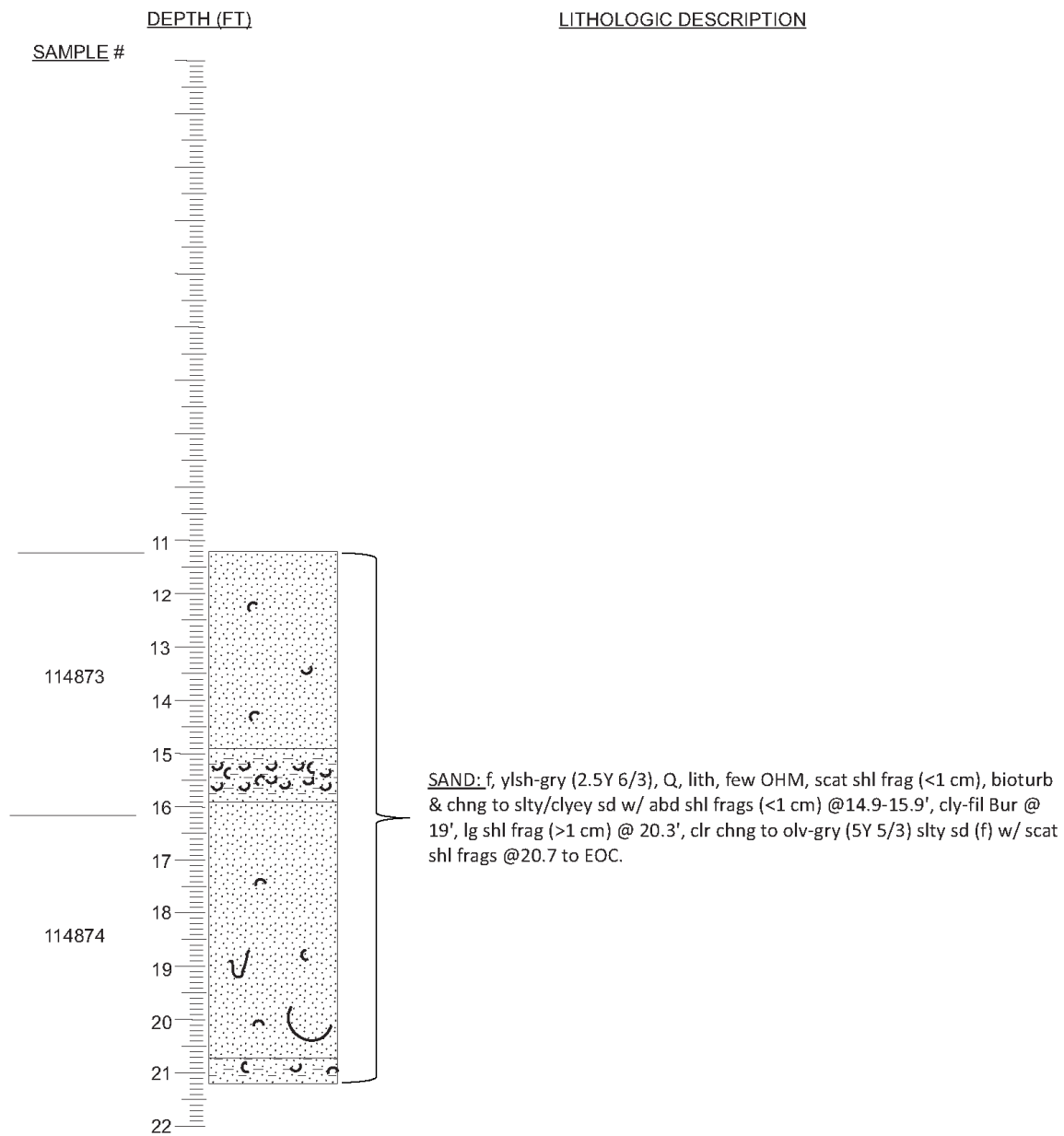
DGSID Zz82-65 DATE DESCRI. 08/16/17 WATER DEPTH (FT) 52.49
LOCAL ID. VA BOEM-15- DESCR. BY CRM
 04a



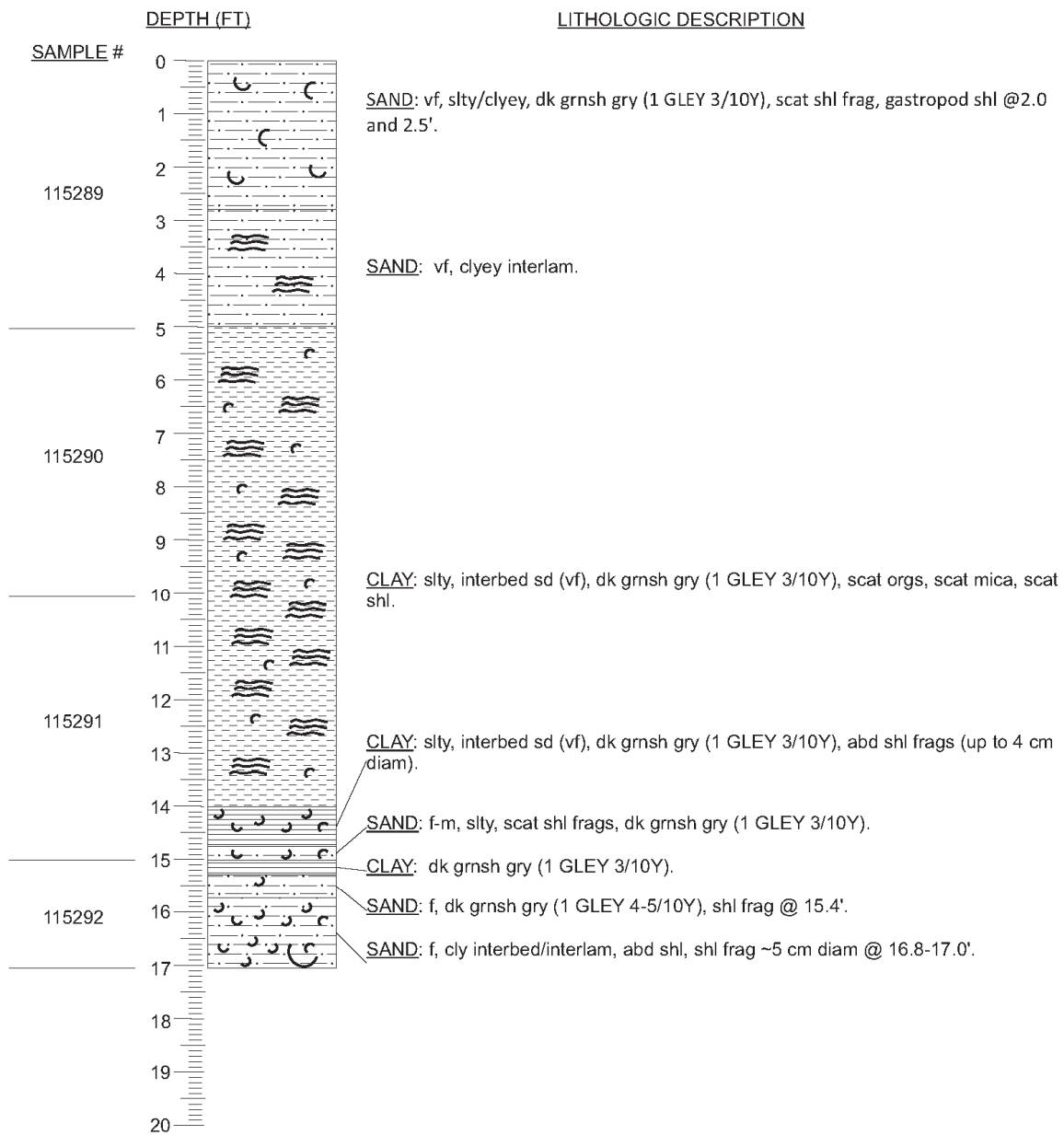
DGSID Zz82-66 DATE DESCRI. 08/15/17 WATER DEPTH (FT) 45.93
LOCAL ID. VA BOEM-15- DESCR. BY CRM
05



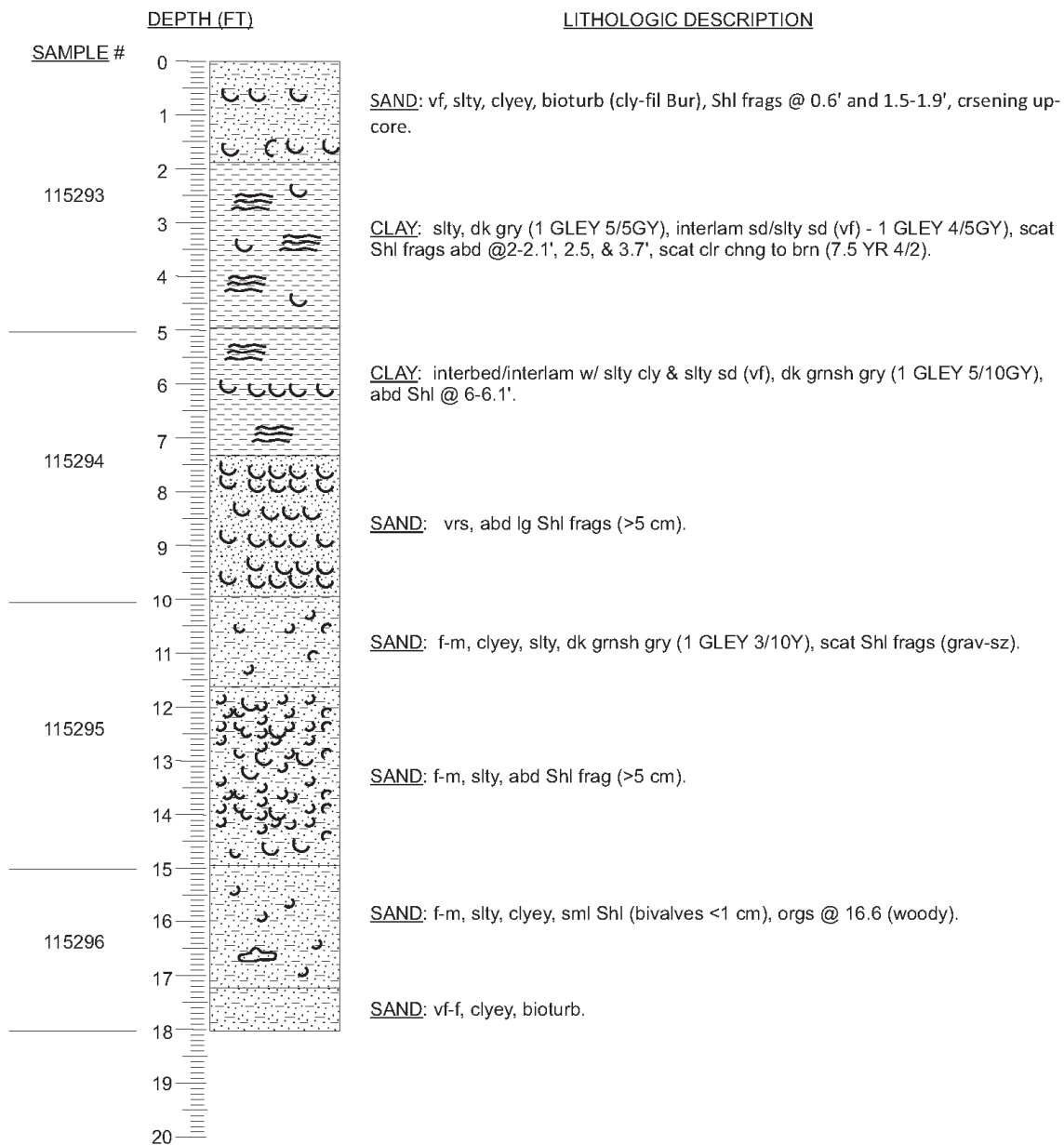
DGSID Zz82-67 DATE DESCRI. 08/17/17 WATER DEPTH (FT) 45.93
LOCAL ID. VA BOEM-15- DESCR. BY CRM
05a



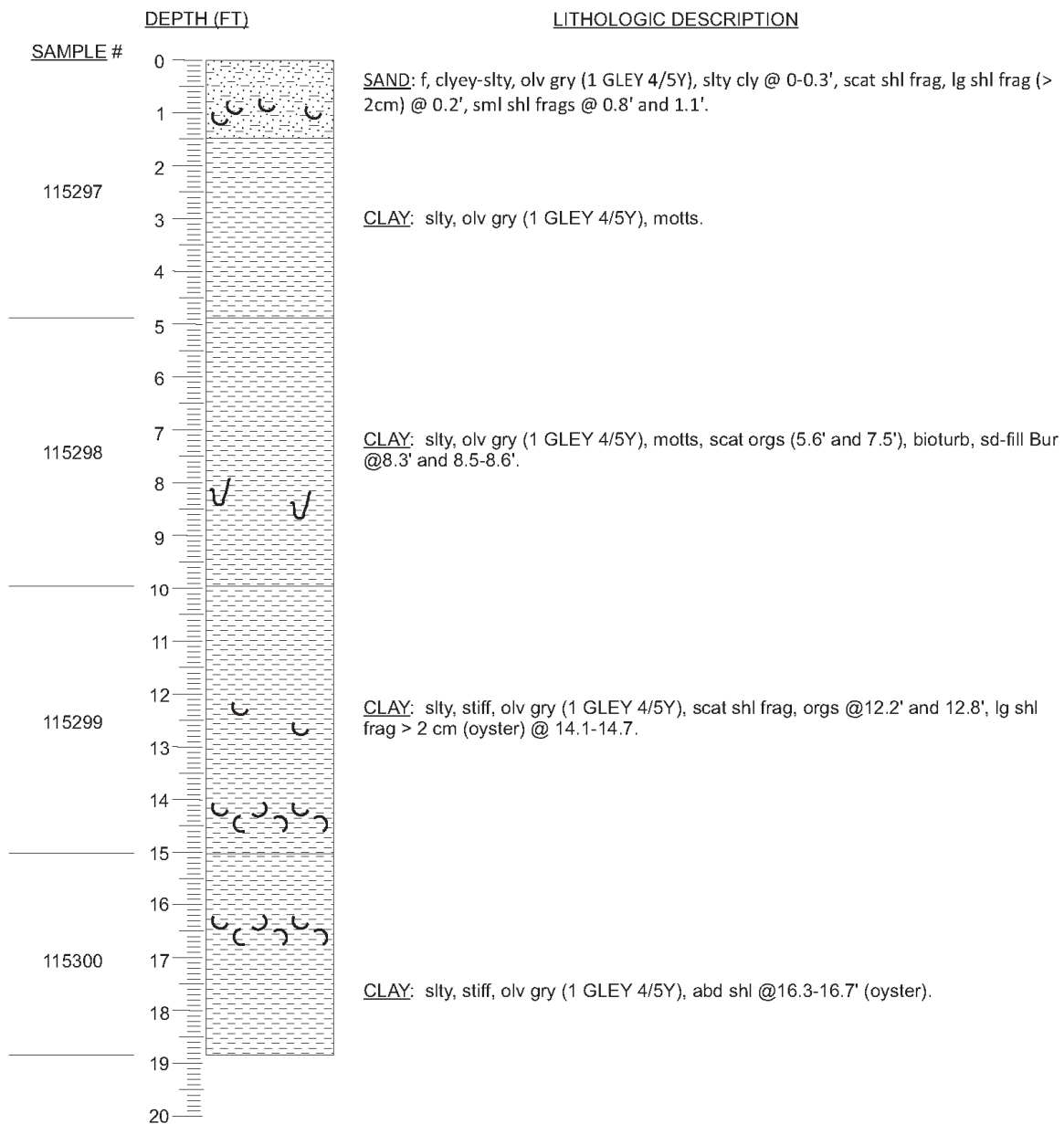
DGSID Zz82-68 DATE DESCRI. 11/16/17 WATER DEPTH (FT) 47.6
LOCAL ID. VA BOEM-16- DESCR. BY CRM
01



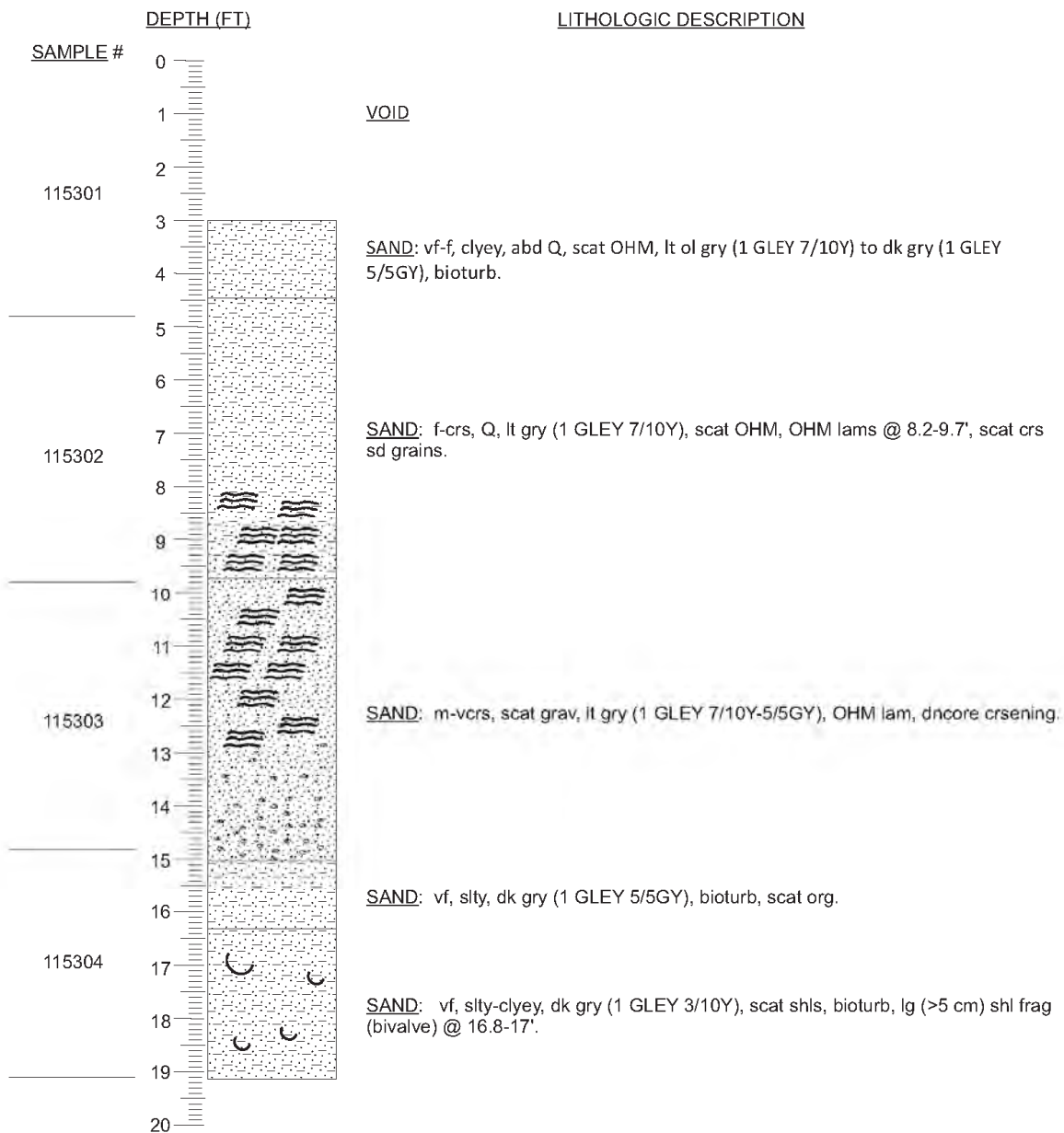
DGSID Zz82-69 DATE DESCRI. 11/16/17 WATER DEPTH (FT) 49.2
LOCAL ID. VA BOEM-16- DESCR. BY CRM
02



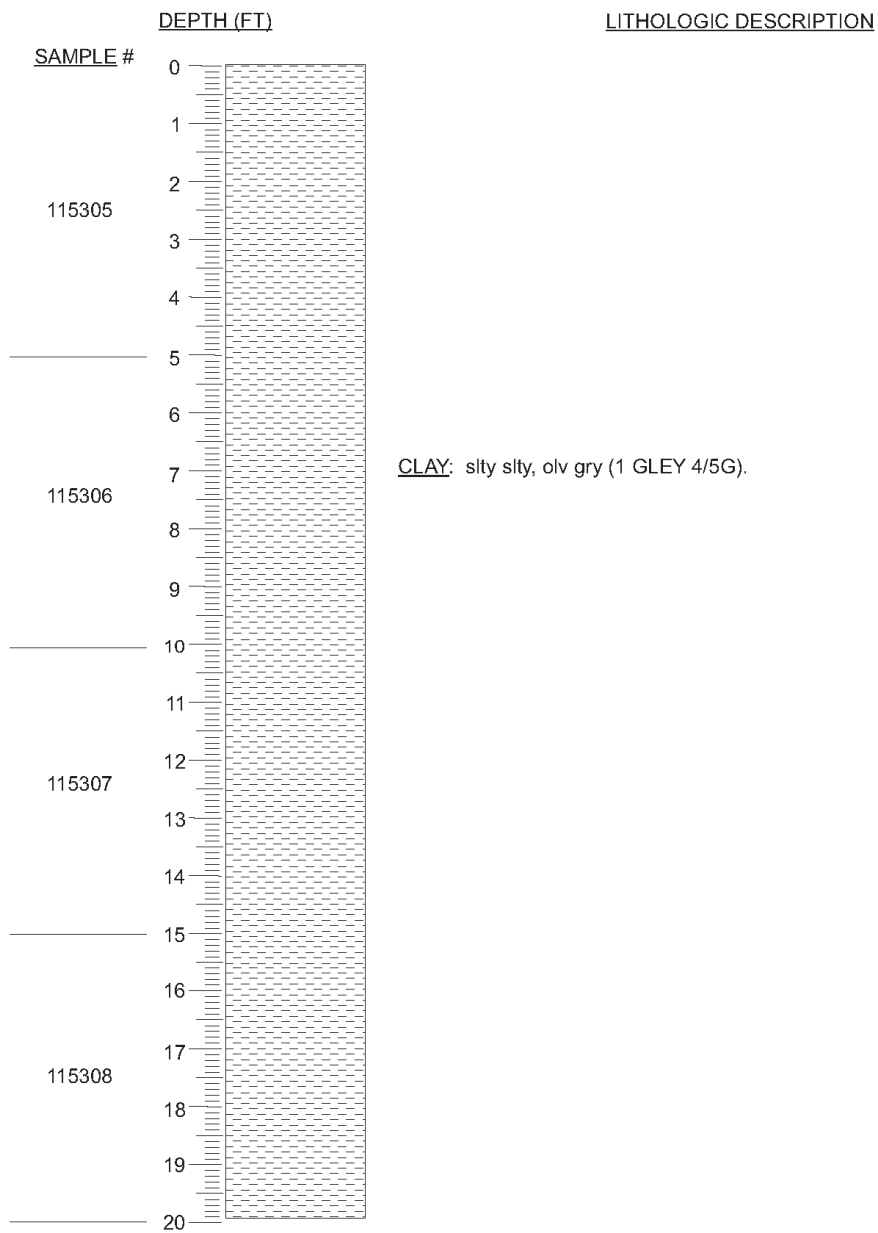
DGSID Zz82-70 DATE DESCRI. 06/27/17 WATER DEPTH (FT) 51.5
LOCAL ID. VA BOEM-16- DESCR. BY CRM
 03



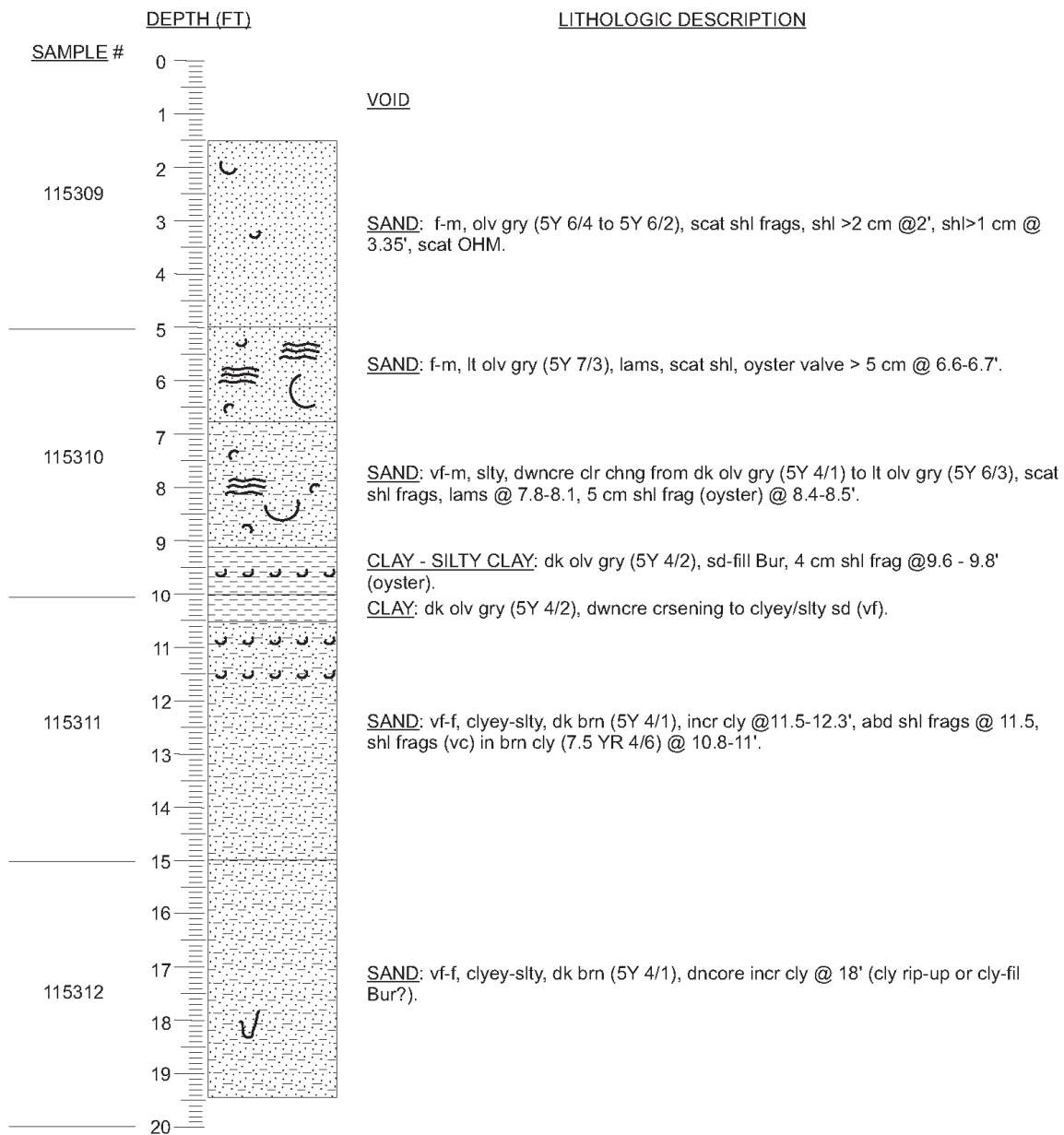
DGSID Zz82-71 DATE DESCRI. 07/05/17 WATER DEPTH (FT) 51.5
LOCAL ID. VA BOEM-16- DESCR. BY CRM
 04



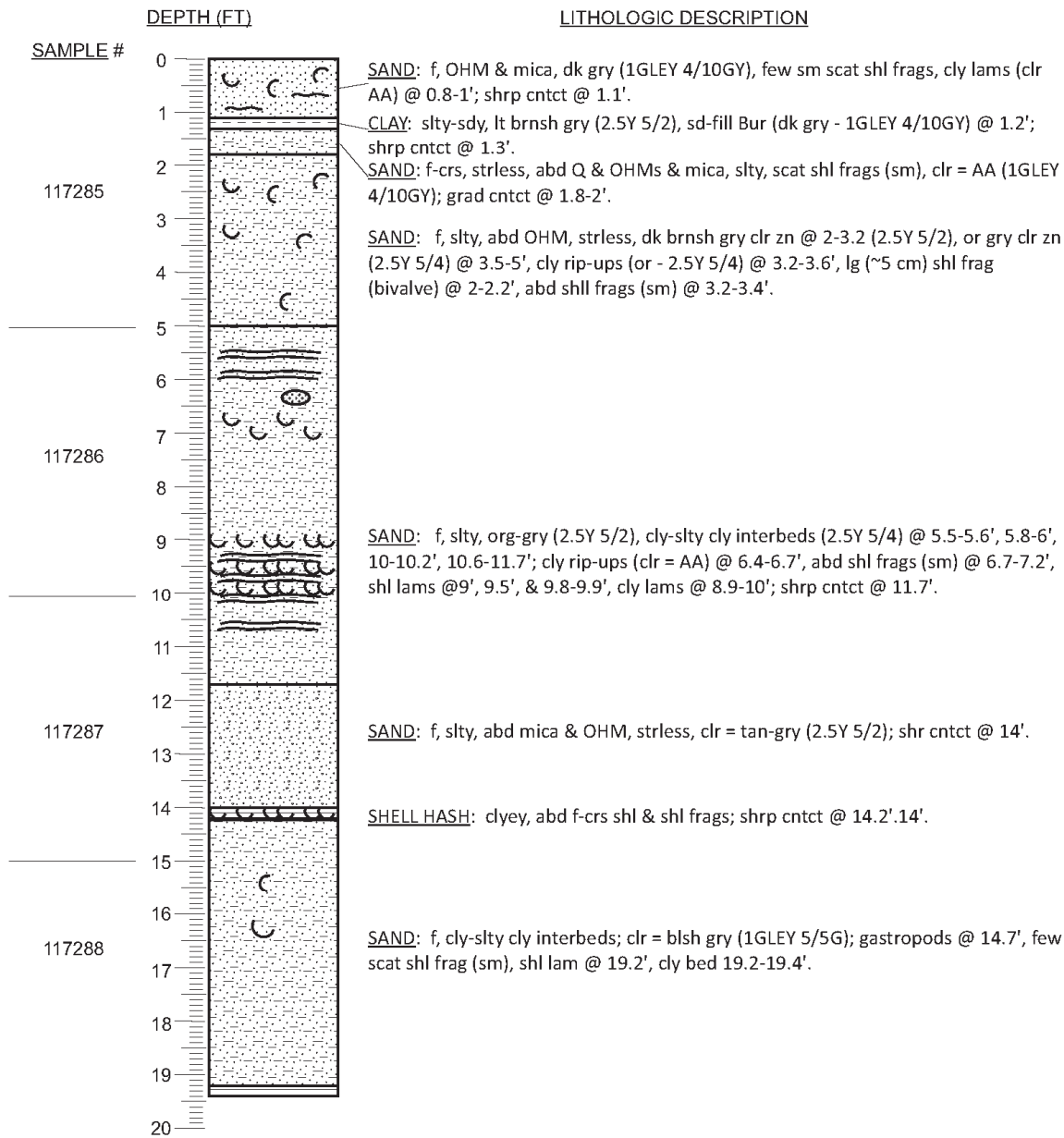
DGSID Zz82-72 DATE DESCRI. 06/26/17 WATER DEPTH (FT) 45.2
LOCAL ID. VA BOEM-16- DESCR. BY CRM
 05



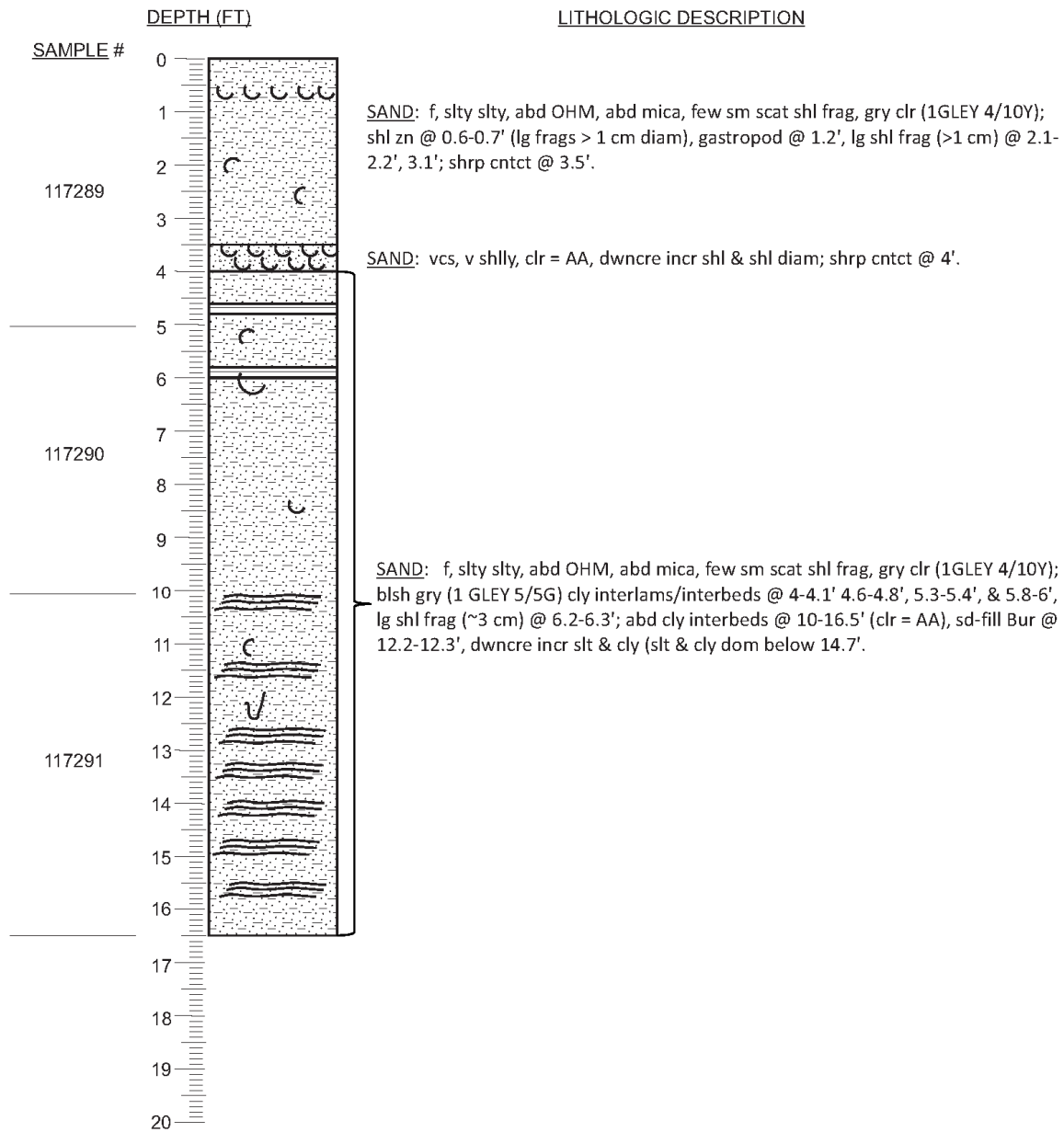
DGSID Zz82-73 DATE DESCRI. 08/20/17 WATER DEPTH (FT) 40.2
LOCAL ID. VA BOEM-16- DESCR. BY CRM
06



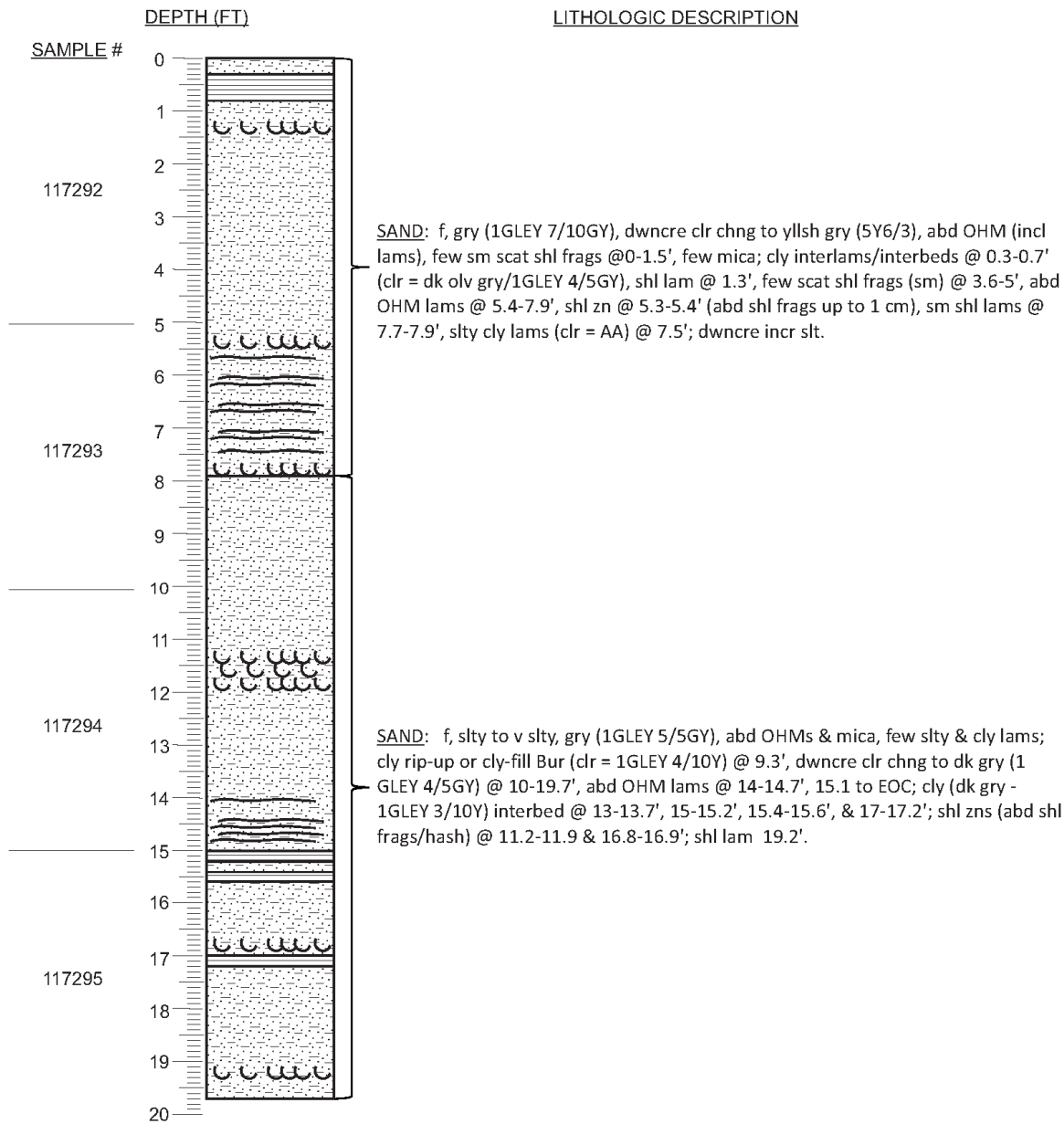
DGSID Zz82-83 DATE DESCRI. 02/05/18 WATER DEPTH (FT) 49.1
LOCAL ID. VA-2017-05 DESCR. BY CRM



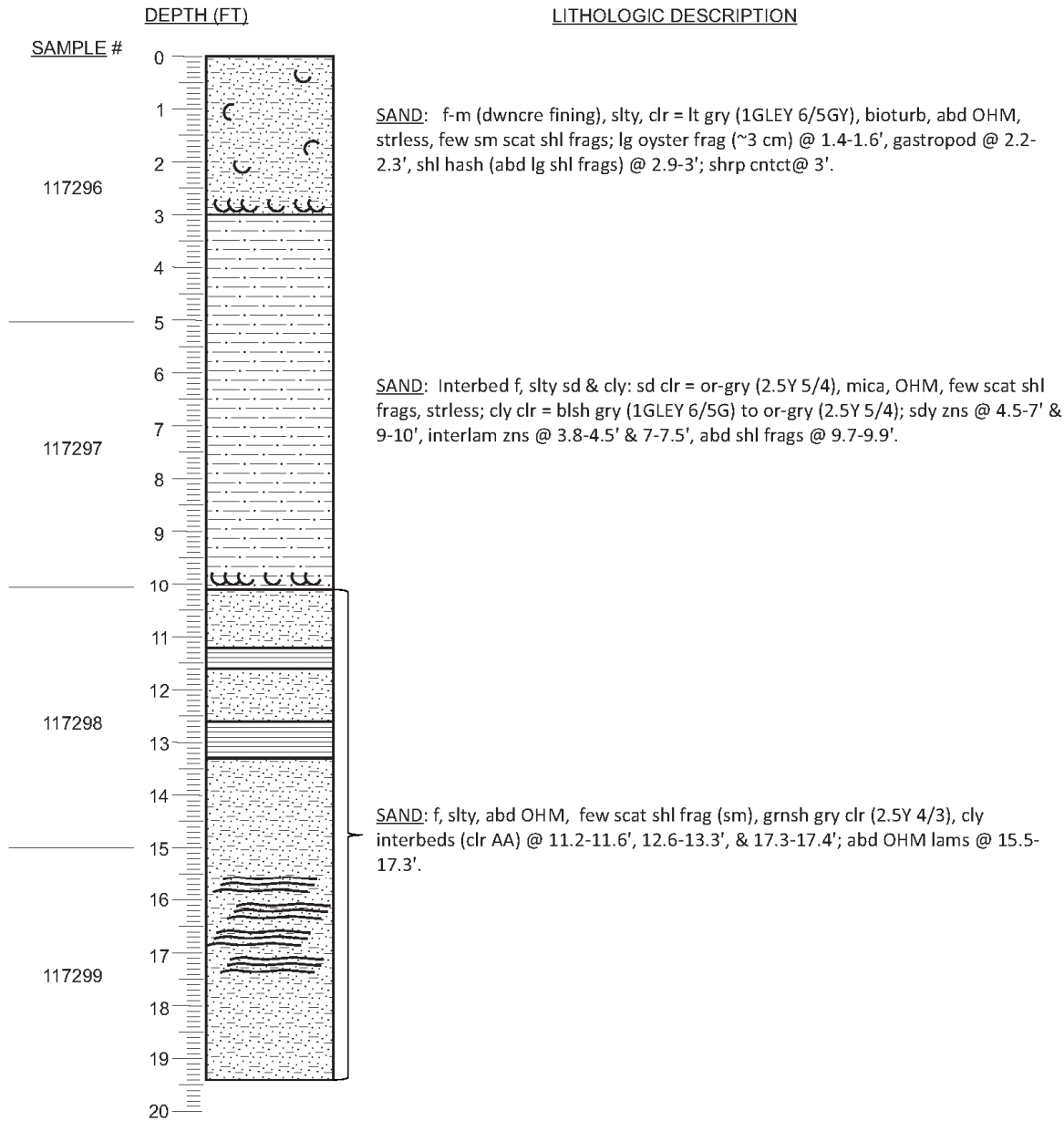
DGSID Zz82-84 DATE DESCRI. 02/13/18 WATER DEPTH (FT) 40.37
LOCAL ID. VA-2017-06 DESCR. BY CRM



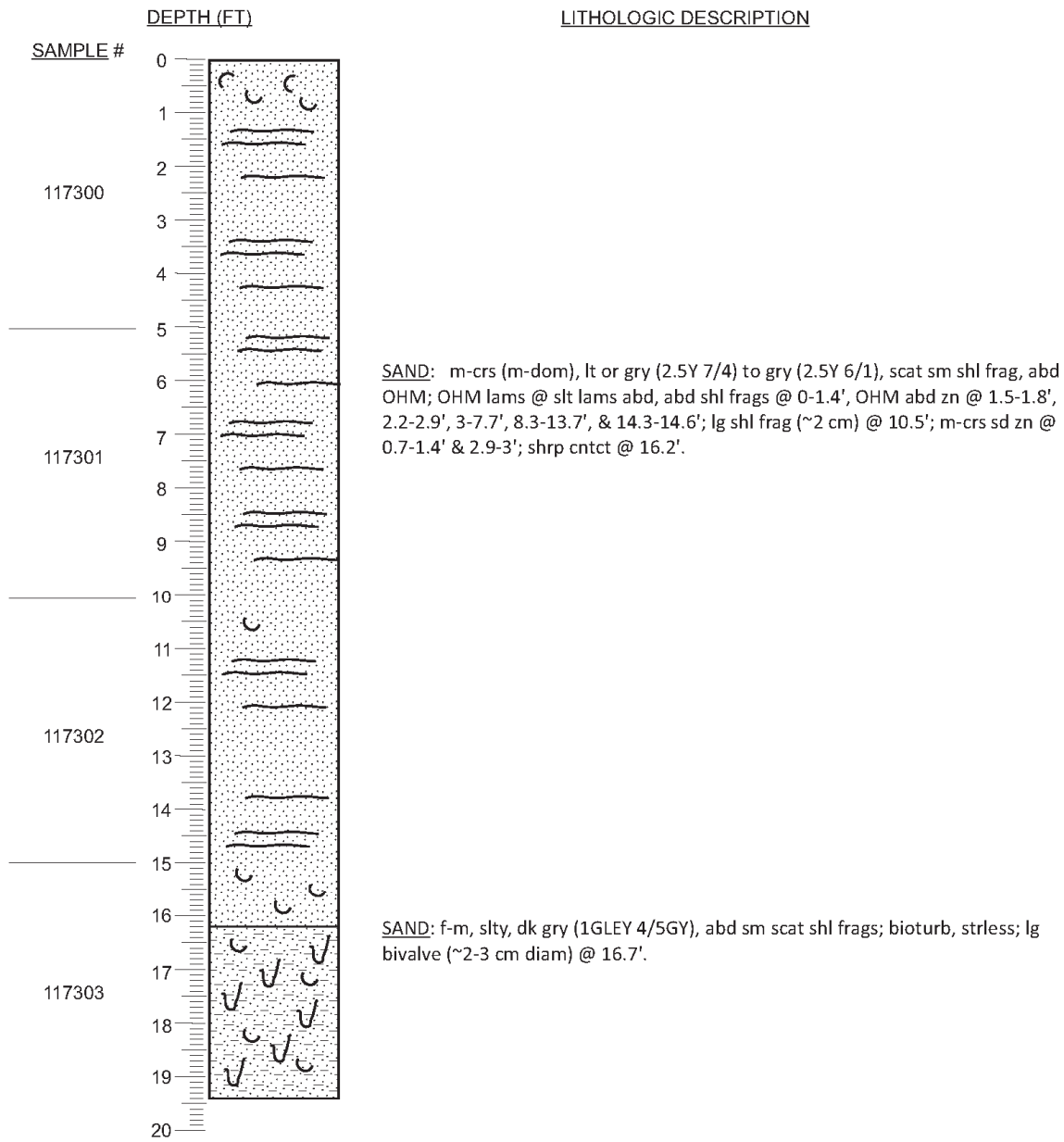
DGSID Zz82-85 DATE DESCRI. 02/14/18 WATER DEPTH (FT) 37.18
LOCAL ID. VA-2017-07 DESCR. BY CRM



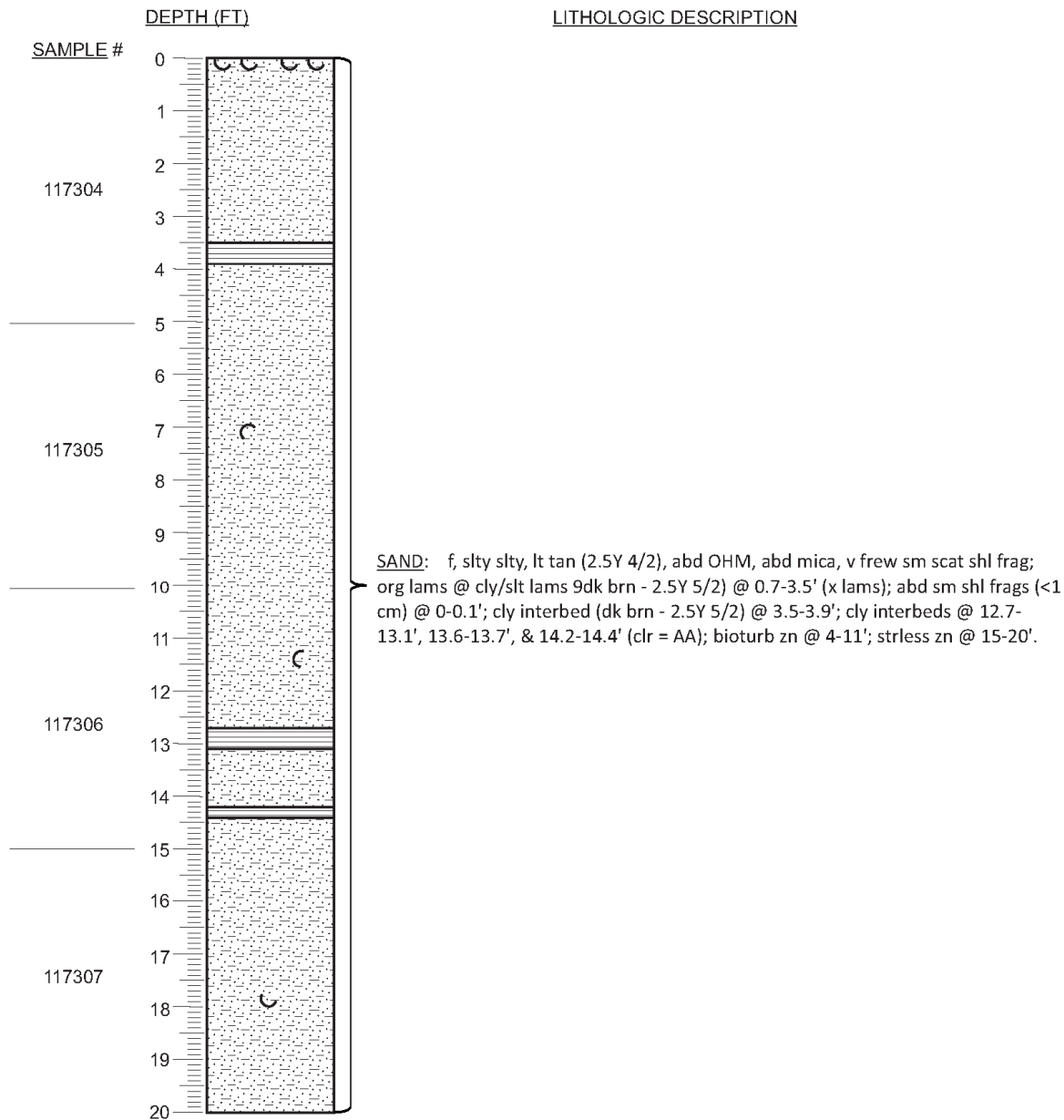
DGSID Zz82-86 DATE DESCRI. 02/14/18 WATER DEPTH (FT) 42.9
LOCAL ID. VA-2017-08 DESCR. BY CRM



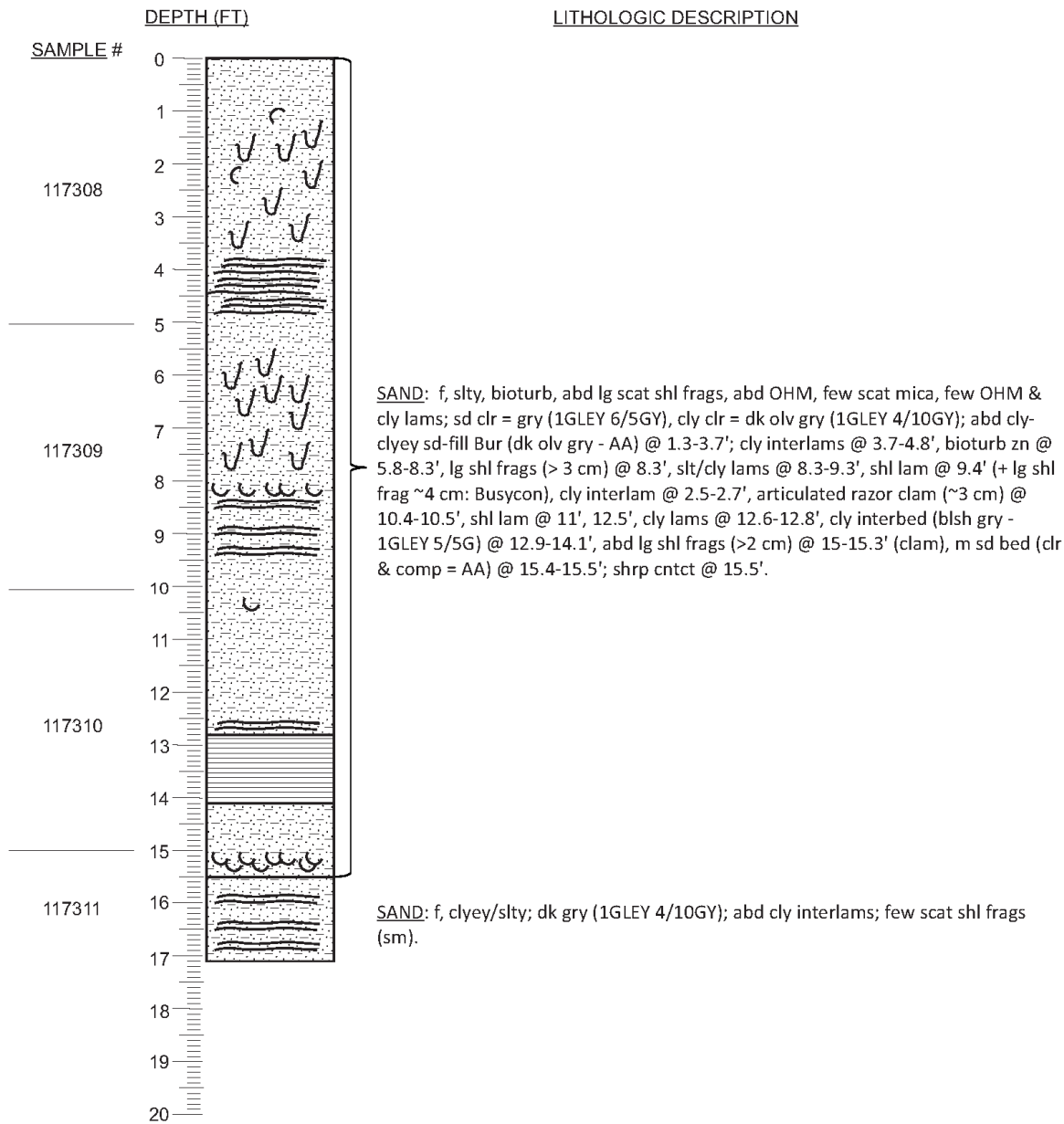
DGSID Zz82-87 DATE DESCRI. 02/15/18 WATER DEPTH (FT) 29.88
LOCAL ID. VA-2017-09 DESCR. BY CRM



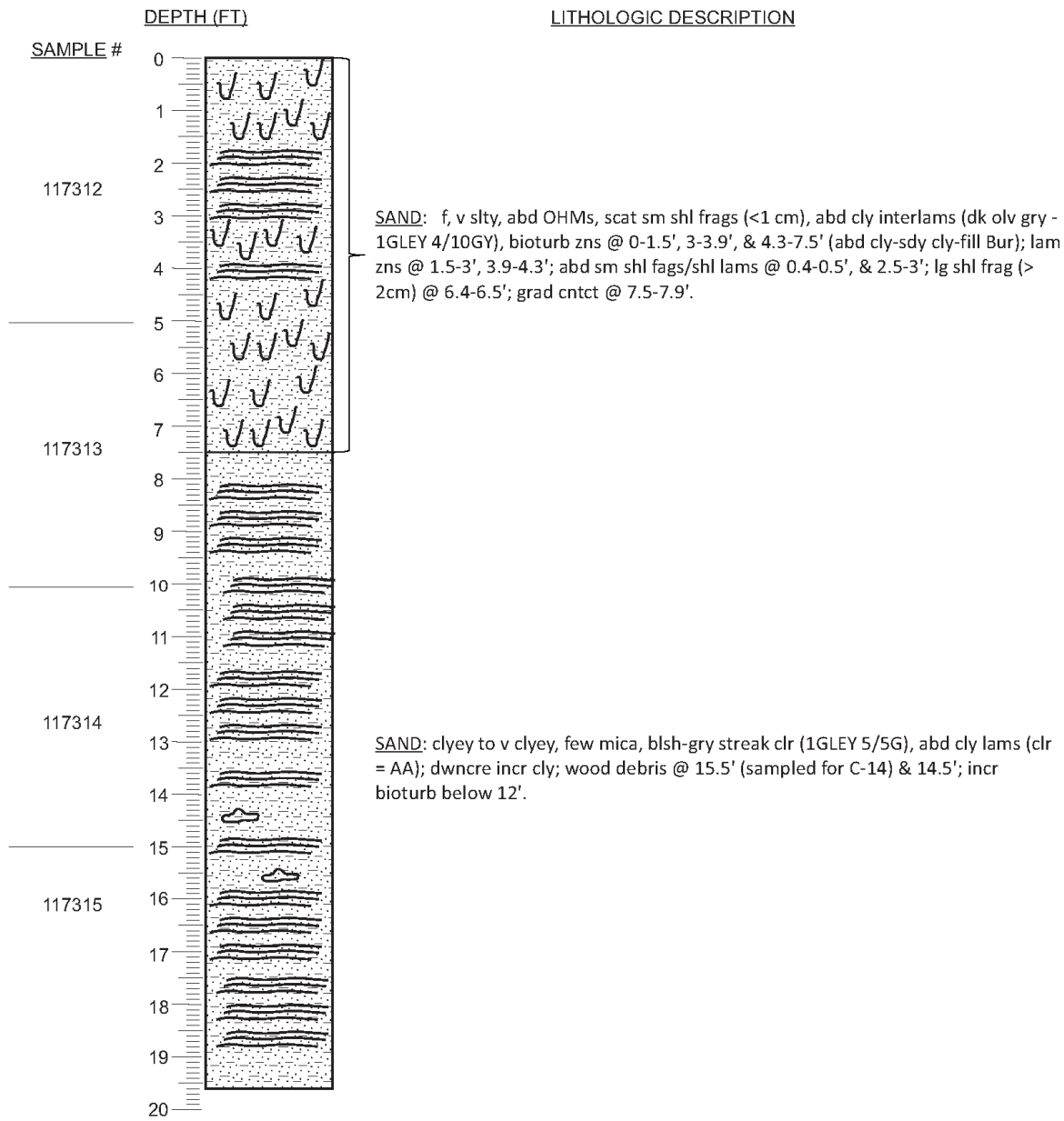
DGSID Zz82-88 DATE DESCRI. 02/20/18 WATER DEPTH (FT) 36.4
LOCAL ID. VA-2017-10 DESCR. BY CRM



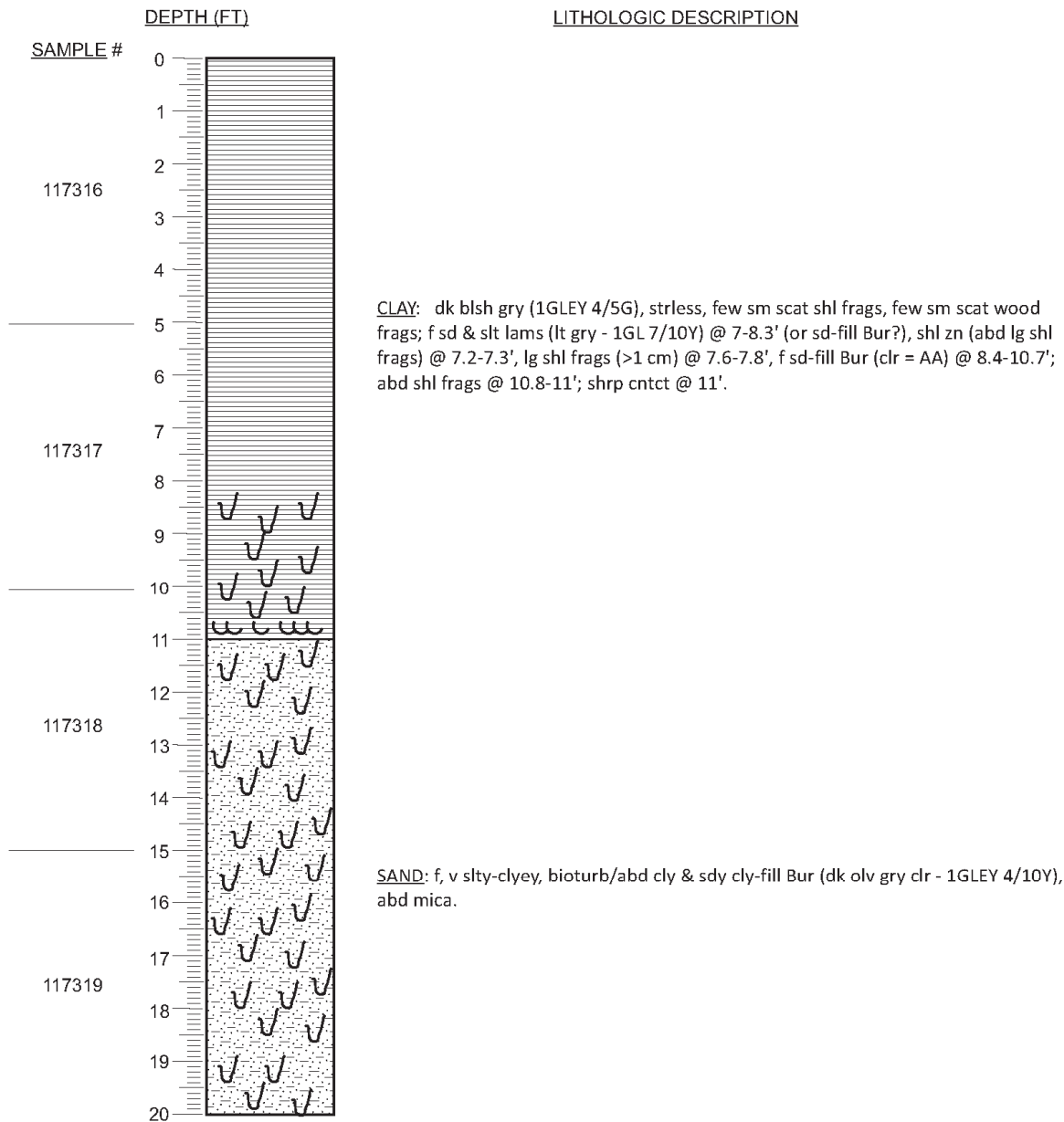
DGSID Zz82-89 DATE DESCRI. 02/22/18 WATER DEPTH (FT) 32.99
LOCAL ID. VA-2017-11 DESCR. BY CRM



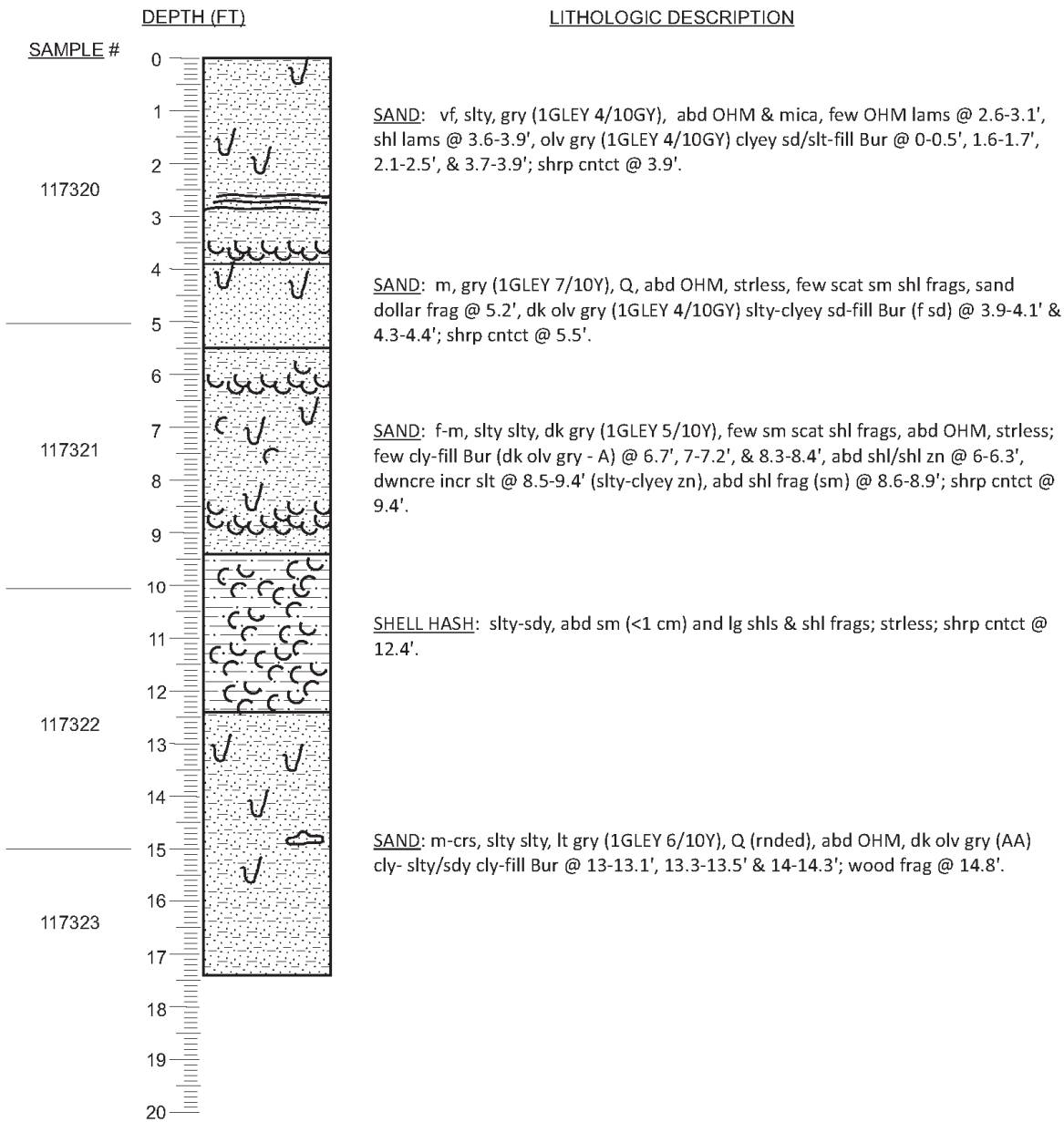
DGSID Zz82-90 DATE DESCRI. 02/22/18 WATER DEPTH (FT) 28.98
LOCAL ID. VA-2017-12 DESCR. BY CRM



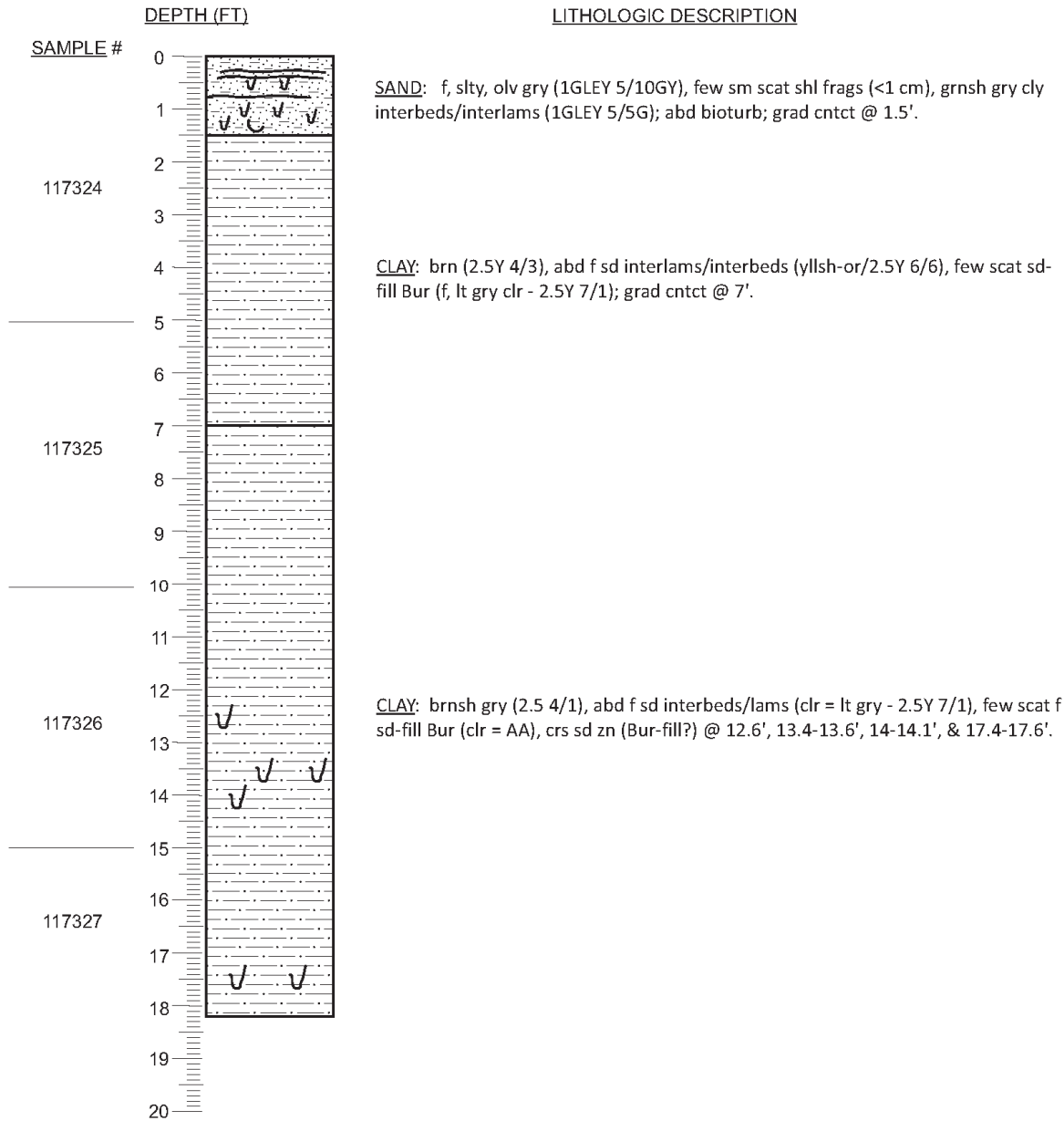
DGSID Zz82-91 DATE DESCRI. 02/26/18 WATER DEPTH (FT) 44.09
LOCAL ID. VA-2017-13 DESCR. BY CRM



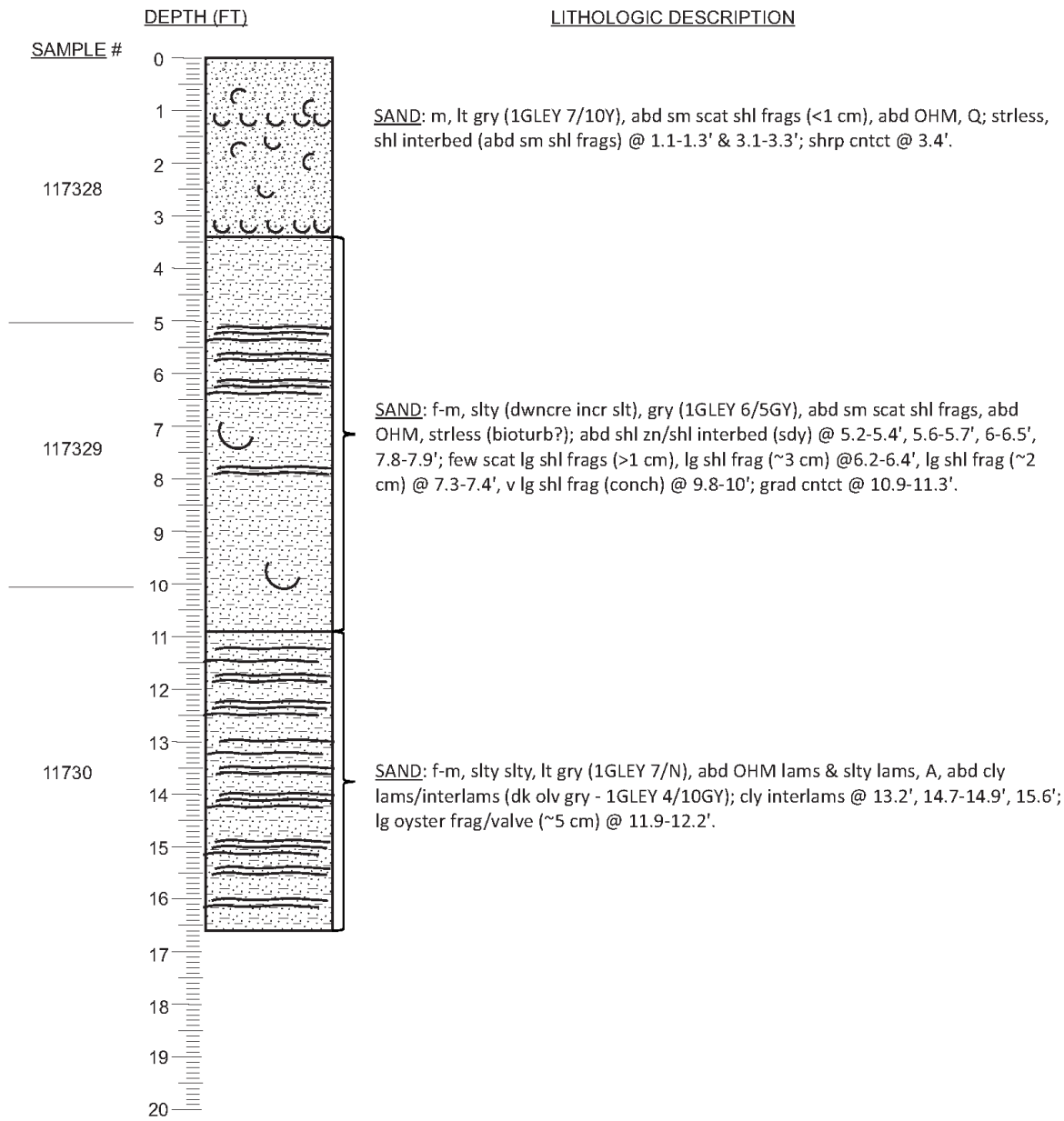
DGSID Zz82-92 DATE DESCRI. 02/26/18 WATER DEPTH (FT) 43.09
LOCAL ID. VA-2017-14 DESCR. BY CRM



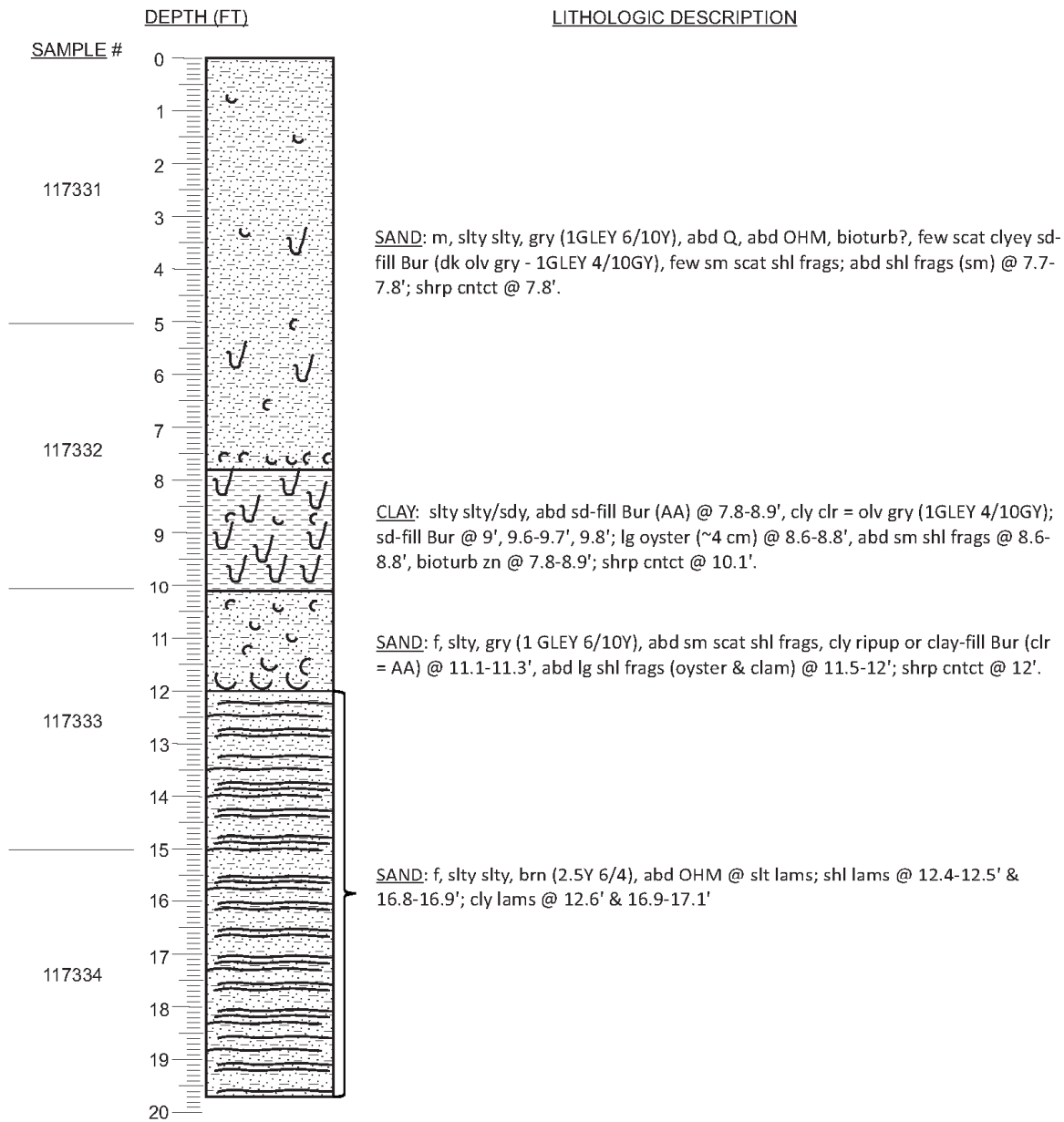
DGSID Zz82-93 DATE DESCRI. 02/26/18 WATER DEPTH (FT) 35.82
LOCAL ID. VA-2017-15 DESCR. BY CRM



DGSID Zz82-94 DATE DESCRI. 02/20/18 WATER DEPTH (FT) 31.48
LOCAL ID. VA-2017-16 DESCR. BY CRM

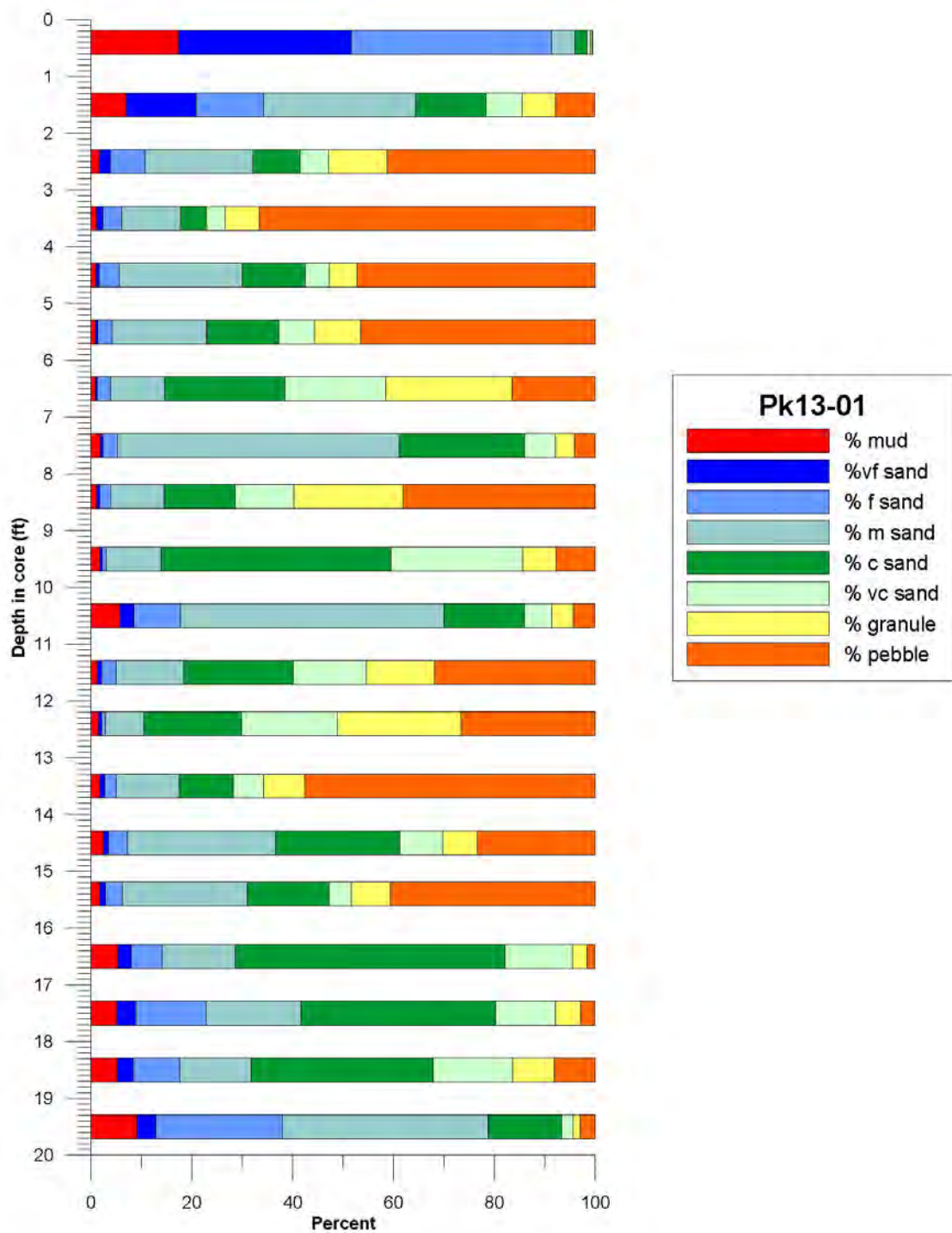


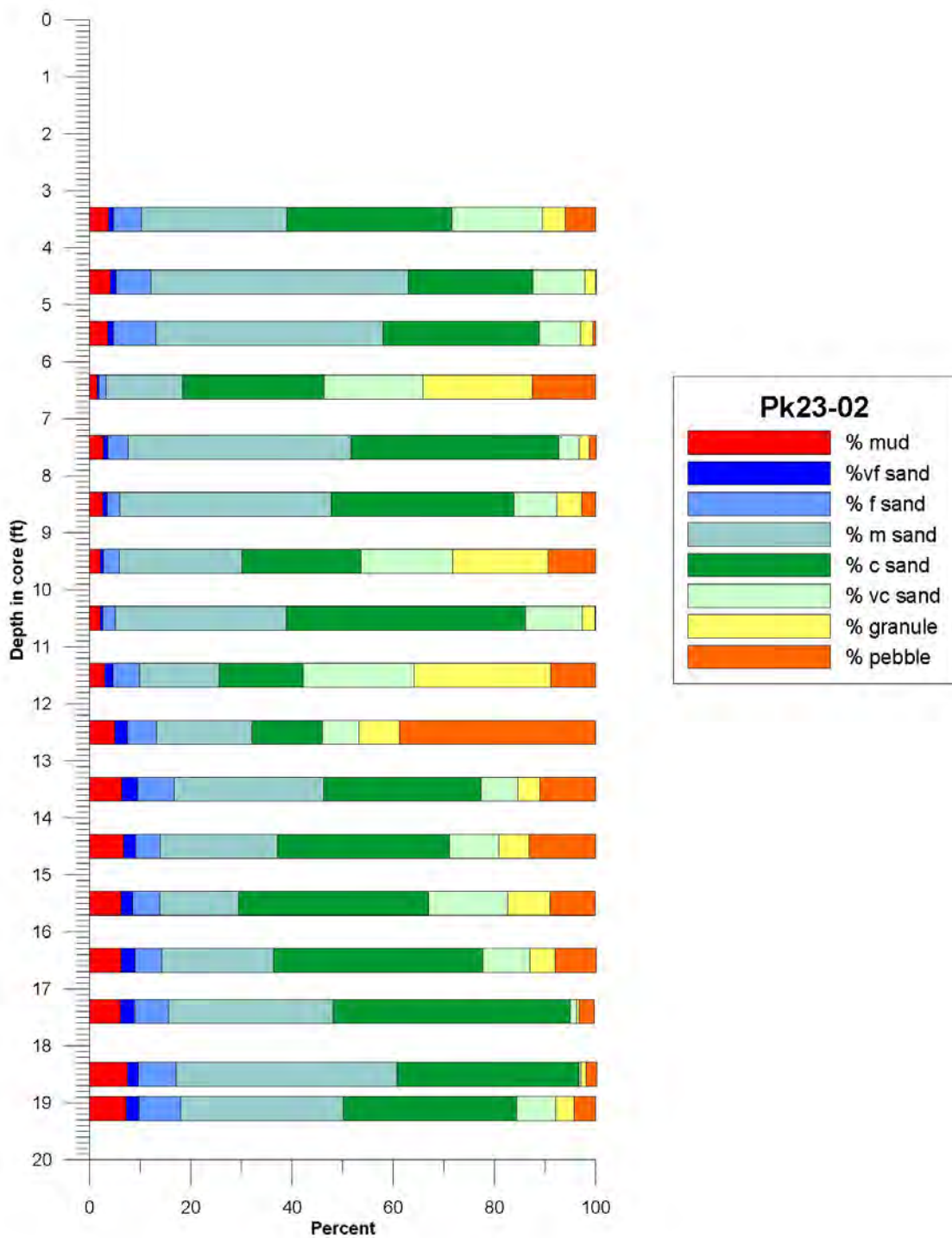
DGSID Zz82-95 DATE DESCRI. 02/20/18 WATER DEPTH (FT) 31.48
LOCAL ID. VA-2017-17 DESCR. BY CRM

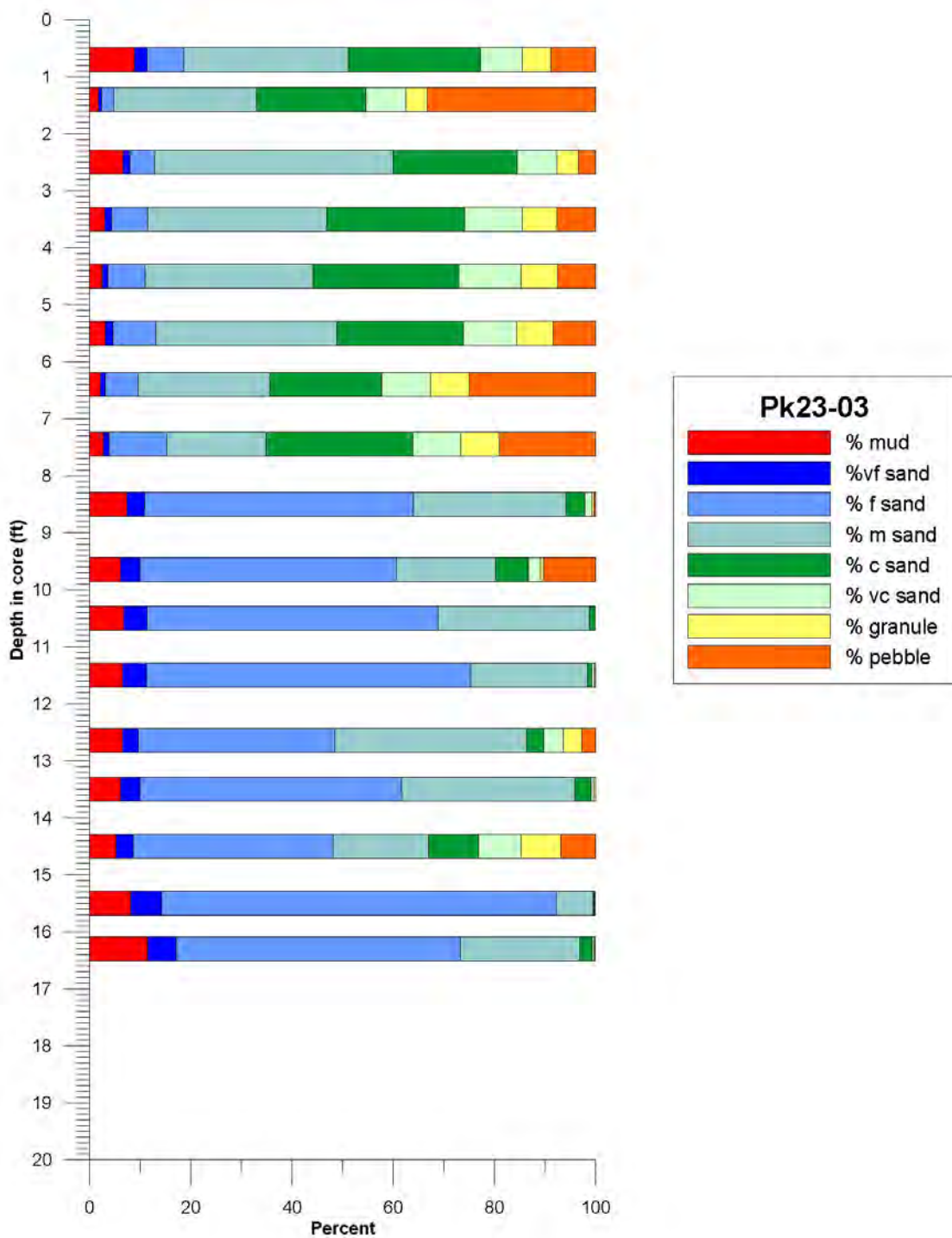


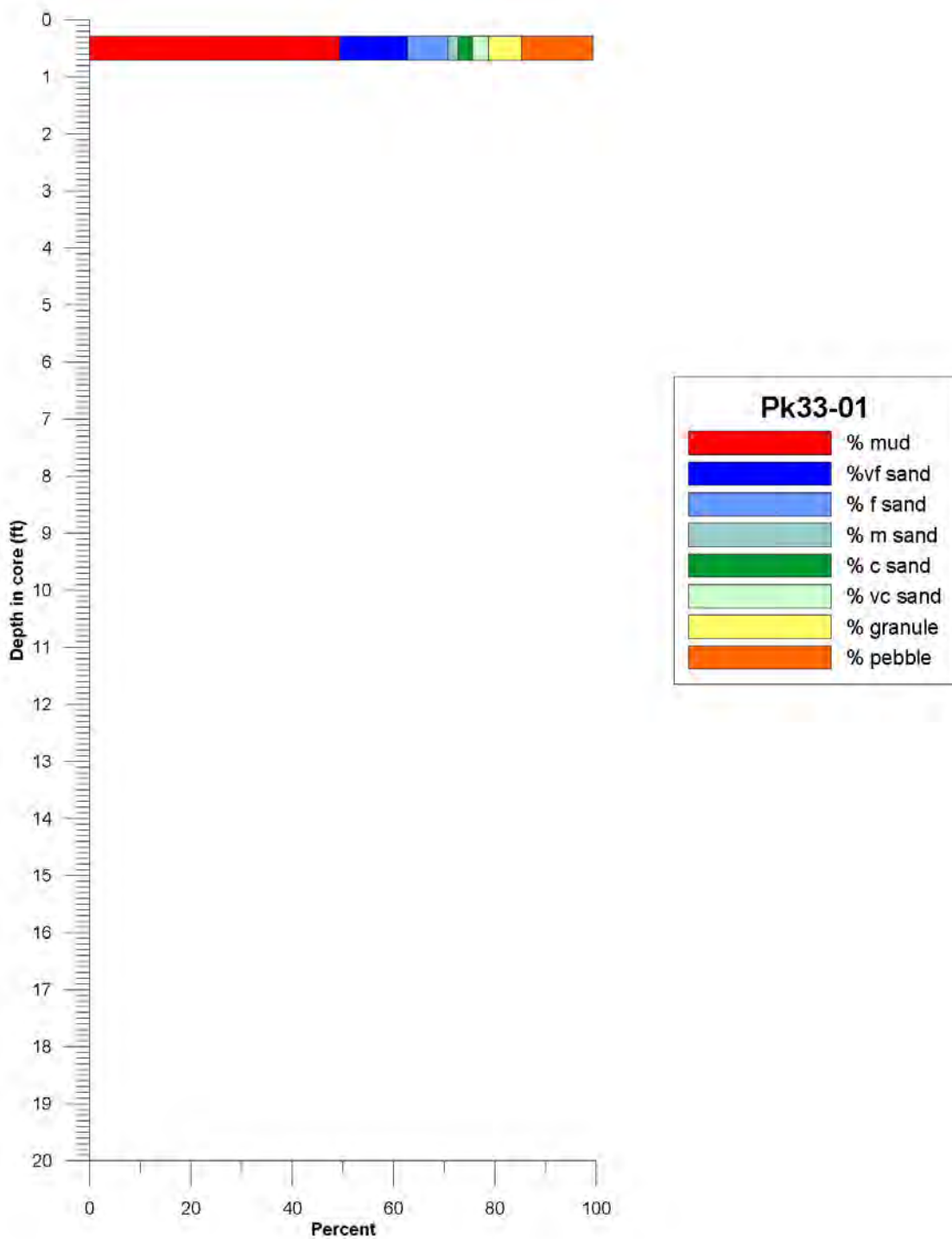
APPENDIX B – DGS Texture Data

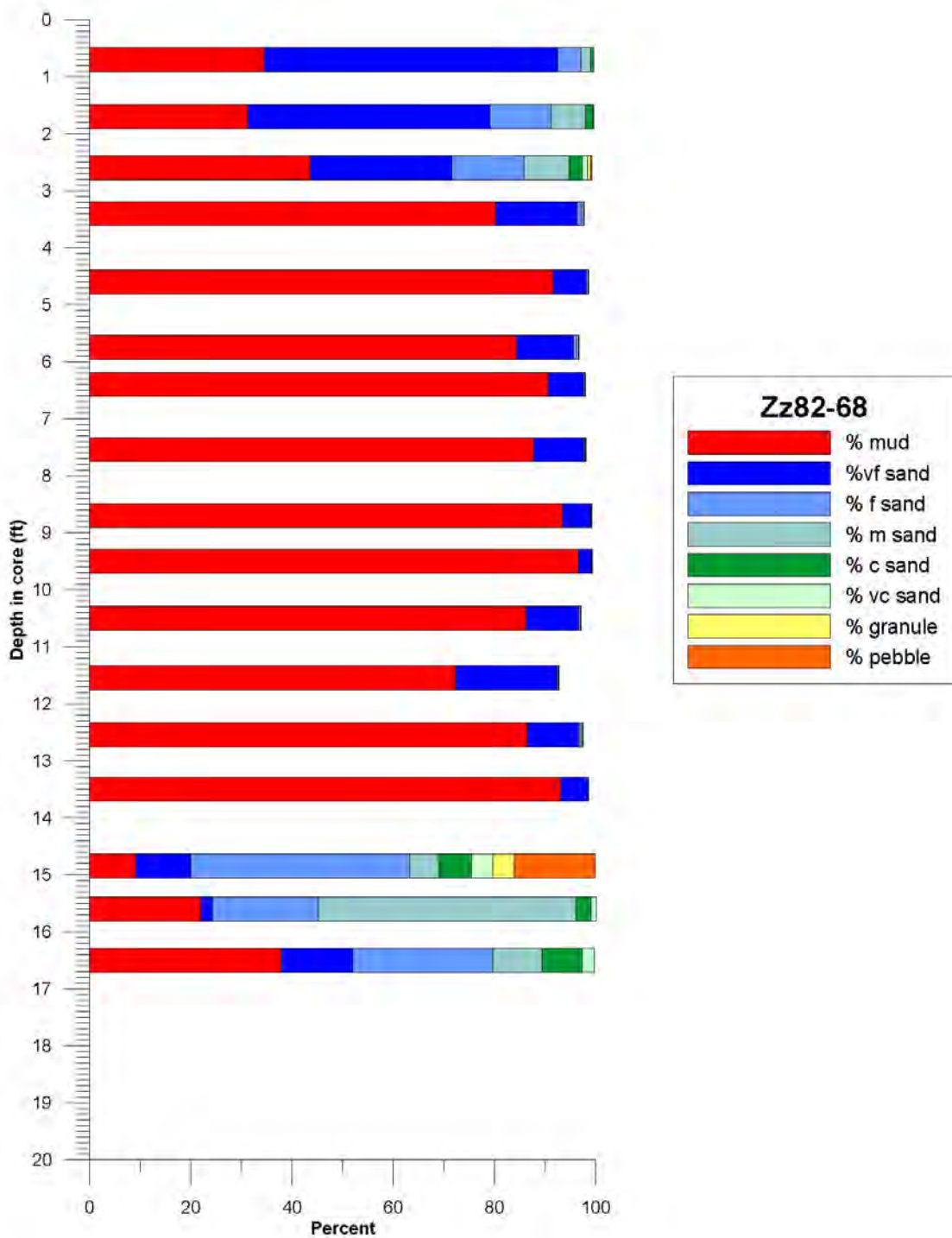
This appendix contains texture information on 2016 BOEM cores, processed and analyzed at the DGS using the Standard Sieve Method. The information has been condensed into a series of core-specific bar-plot diagrams that plot particle-size distributions at appropriate core depths. The raw texture data are housed with the DGS.

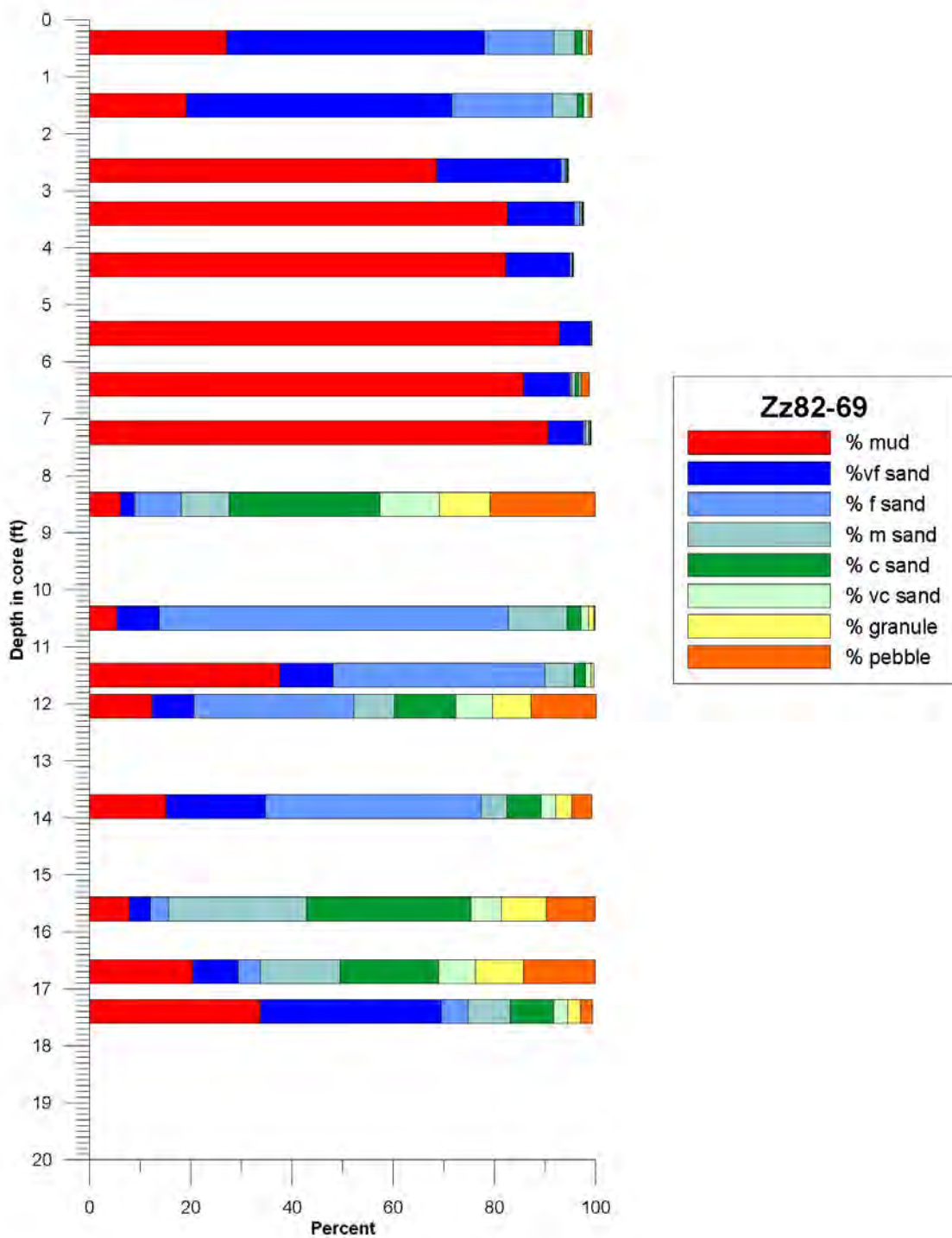


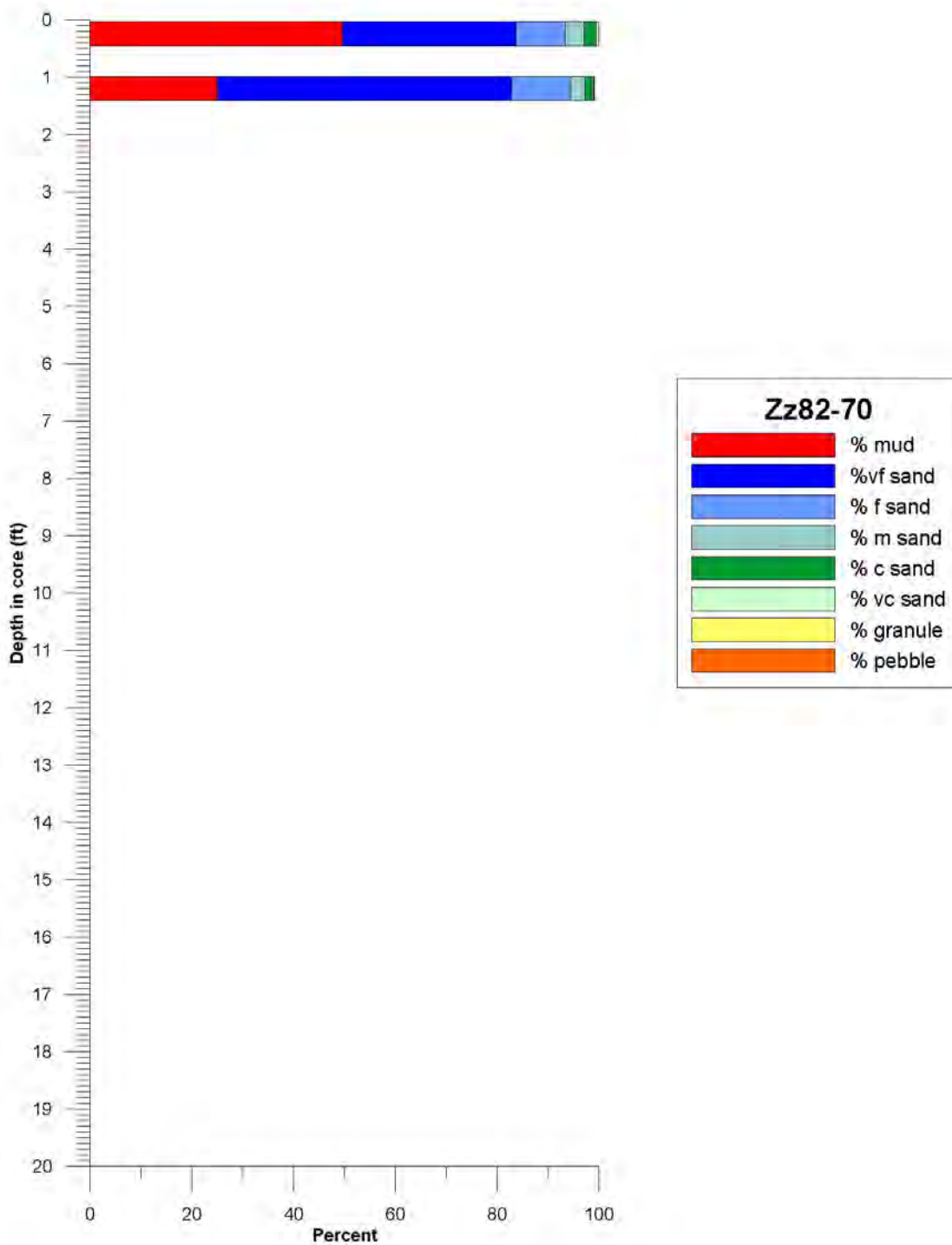


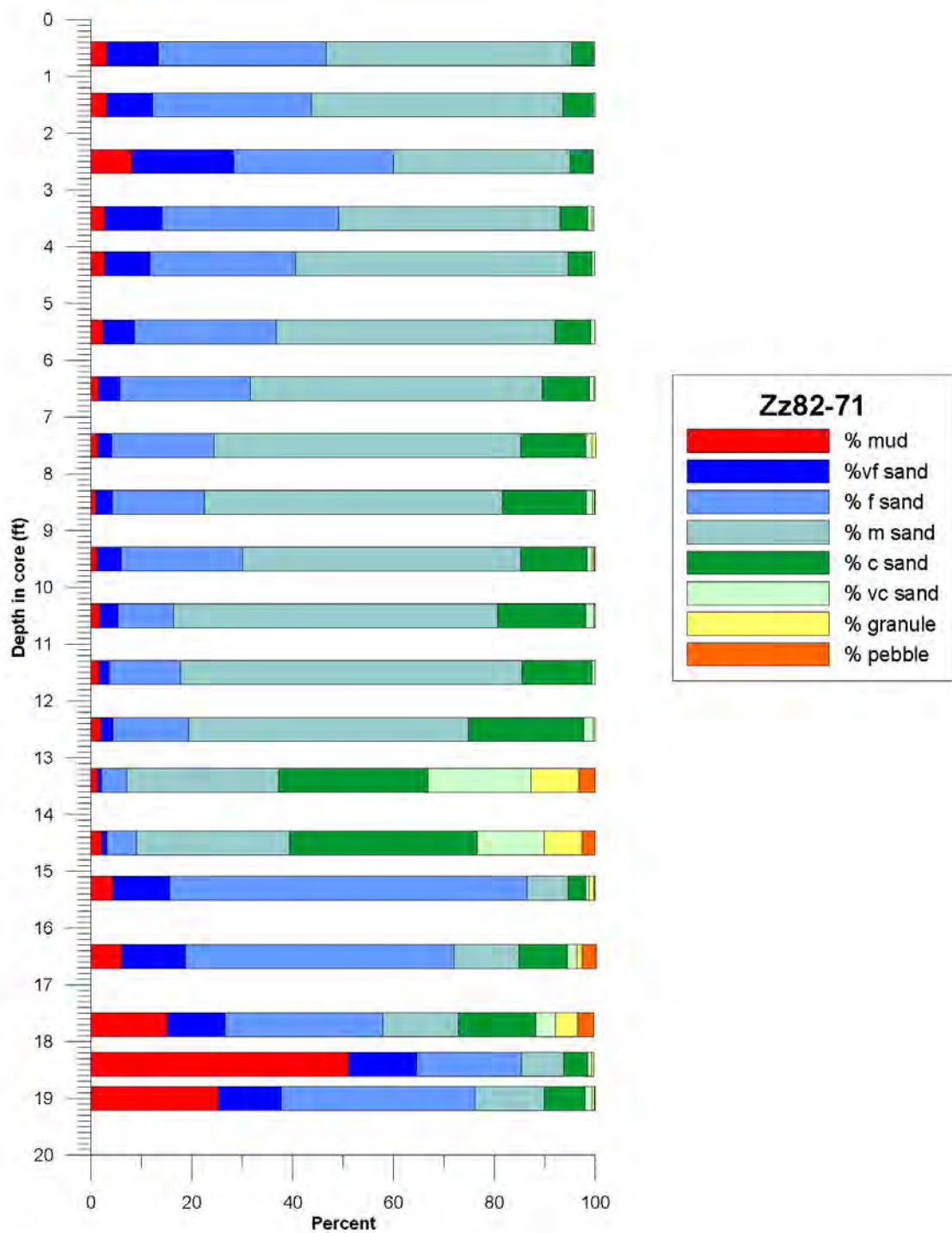


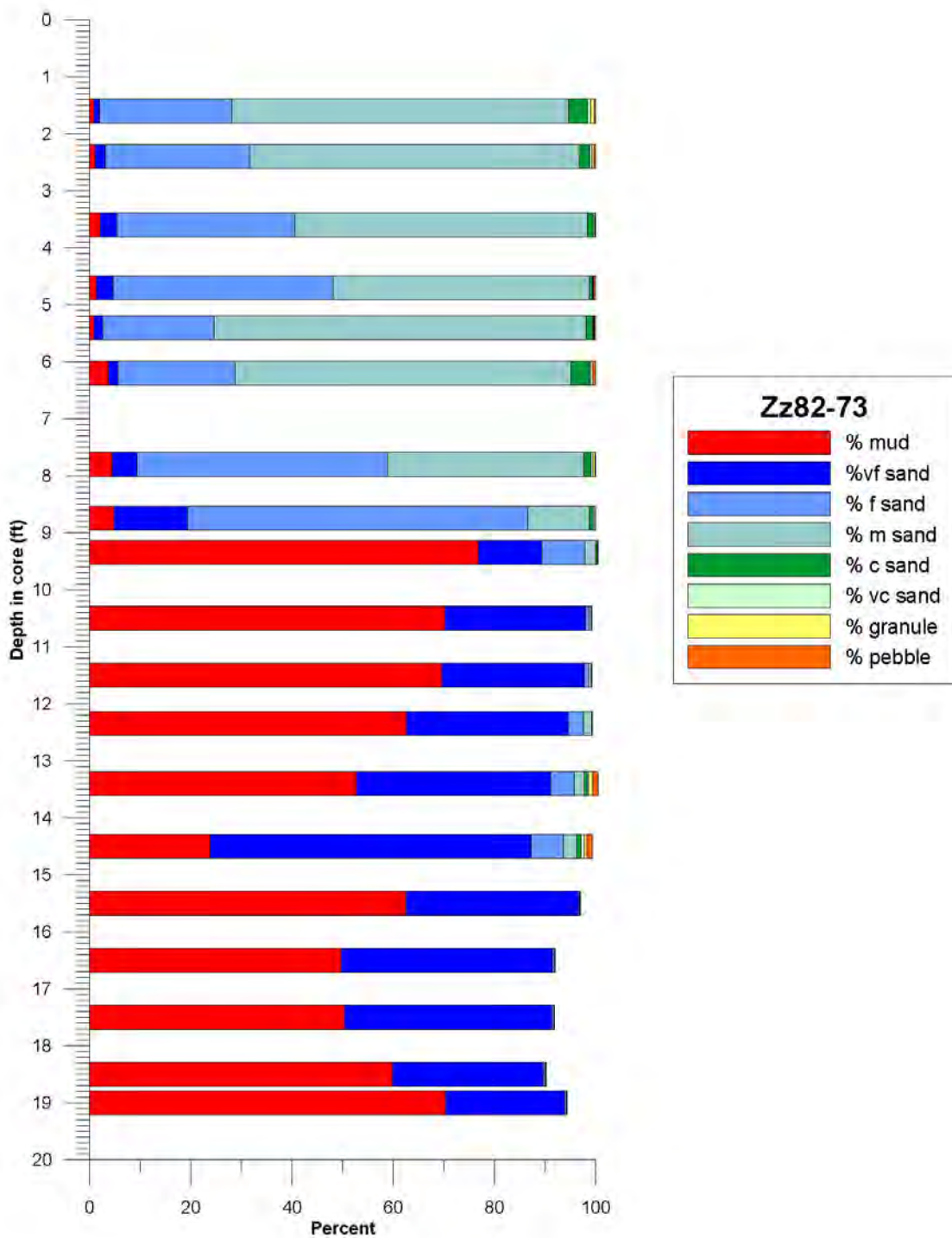












APPENDIX C – AECOM Texture Data

This appendix contains texture information on 2017 BOEM cores, processed and analyzed by AECOM using the Standard Sieve Method. Provided here are the Folk (1974) statistical metrics generated from raw grain weights by class. The raw texture data are housed with the DGS.

DGS ID	Sample ID	Depth Range (ft)	Median	Mean (M_z)	Sorting (σ_i)	Skewness (S_k_i)	Kurtosis (K_o)
Oj12-02	104496.1	2.0-2.2	2.17	2.10	0.63	-0.16	0.77
Oj12-02	104496.2	4.0-4.2	2.32	2.23	0.60	-0.25	0.93
Oj12-02	104497.1	6.0-6.2	2.24	2.15	0.61	-0.21	0.81
Oj12-02	104497.2	8.0-8.2	2.41	2.38	0.50	-0.21	1.09
Oj12-02	104498.1	10.0-10.2	2.41	2.40	0.48	-0.19	1.10
Oj12-02	104498.2	12.0-12.2	2.41	2.40	0.48	-0.19	1.10
Oj33-02	104475.1	2.0-2.2	1.84	1.92	0.75	0.21	0.90
Oj33-02	104475.2	4.0-4.2	2.07	1.95	1.40	-0.17	1.59
Oj33-02	104476.3	6.0-6.2	2.05	2.05	0.81	0.09	0.94
Oj34-04	104479.1	0.0-0.2	2.12	2.08	0.64	-0.10	0.75
Oj34-04	104479.2	2.0-2.2	2.34	2.26	0.58	-0.24	0.99
Oj34-04	104479.3	4.0-4.2	2.50	2.50	0.72	0.10	2.00
Oj34-04	104480.4	6.0-6.2	2.51	2.51	0.86	0.24	2.74
Oj34-04	104480.2	8.0-8.2	2.49	2.49	0.63	0.05	1.71
Oj34-04	104480.3	10.0-10.2	1.40	1.31	1.55	-0.05	1.01
Oj34-06	104501.4	0.0-0.2	2.28	2.01	1.14	-0.31	1.28
Oj34-06	104501.5	2.0-2.2	1.46	0.66	2.74	-0.27	0.94
Oj34-06	104501.6	4.0-4.2	3.01	3.10	1.34	0.04	1.04
Oj34-06	104502.1	6.0-6.2	1.07	0.99	1.24	0.03	1.42
Oj34-06	104502.2	8.0-8.2	0.81	0.86	1.13	0.16	1.44
Oj34-06	104502.3	10.0-10.2	0.56	0.50	1.31	-0.06	1.02
Oj34-06	104503.1	12.0-12.2	0.92	0.73	1.29	-0.17	1.09
Oj34-06	104503.2	14.0-14.2	1.05	0.12	2.31	-0.42	1.36
Oj34-06	104504.1	16.0-16.2	0.42	0.20	1.92	-0.19	1.04
Oj44-01	104509.3	0.0-0.2	1.83	1.88	0.94	0.09	1.06
Oj44-01	104509.4	2.0-2.2	2.12	2.03	0.97	-0.11	1.09
Oj44-02	104510.1	4.0-4.2	2.88	3.09	1.13	0.29	1.09
Oj44-02	104510.2	6.0-6.1	3.10	3.34	1.16	0.18	0.98
Oj44-02	104510.3	8.0-8.2	2.65	2.85	1.16	0.28	1.33
Oj44-02	104511.1	10.0-10.2	2.50	2.60	1.48	0.22	1.47
Oj44-02	104511.2	12.0-12.2	2.00	2.38	1.70	0.35	1.24
Pk13-02	117227.2	1.0-1.2	2.74	2.86	1.11	-0.02	1.66
Pk13-02	117277.3	2.0-2.2	3.00	3.04	0.72	0.07	0.75
Pk13-02	117227.4	3.0-3.2	3.49	3.46	1.07	0.05	1.83
Pk13-02	117227.5	4.0-4.2	3.54	3.59	1.04	0.05	2.10
Pk13-02	117228.1	8.0-8.2	1.49	1.94	1.99	0.40	1.44
Pk13-02	117228.2	9.0-9.2	1.65	2.24	1.82	0.33	1.01

Pk13-02	117229.1	10.0-10.2	3.24	2.83	1.39	-0.42	1.04
Pk13-02	117229.2	11.0-11.2	1.50	1.64	1.58	0.12	1.16
Pk13-02	117229.3	12.0-12.2	1.27	1.18	1.57	0.06	1.78
Pk13-02	117229.4	13.0-13.2	0.43	0.68	2.12	0.37	1.75
Pk13-02	117229.5	14.0-14.2	0.08	0.21	2.09	0.28	1.55
Pk13-02	117229.6	15.2-15.4	1.66	1.72	1.14	0.04	1.63
Pk13-02	117229.7	16.0-16.2	0.84	0.64	1.67	-0.01	1.18
Pk43-01	117234.1	0.0-0.2	0.78	0.74	1.21	-0.04	1.17
Pk43-01	117234.2	1.0-1.2	-0.08	-0.83	2.52	-0.33	0.62
Pk43-01	117234.3	2.0-2.2	0.49	0.46	1.08	-0.14	1.57
Pk43-01	117234.4	3.0-3.2	-0.97	-1.14	1.81	-0.06	0.83
Pk43-01	117234.5	4.0-4.2	-0.40	-1.22	2.42	-0.37	0.57
Pk43-01	117235.1	5.0-5.2	0.43	0.36	1.09	-0.14	1.20
Pk43-01	117225.2	6.0-6.2	0.50	0.48	0.90	-0.04	1.26
Pk43-01	117235.3	7.0-7.2	0.36	0.28	0.84	-0.04	1.08
Pk43-01	117235.4	8.0-8.2	0.31	0.21	0.82	-0.08	1.11
Pk43-01	117235.5	9.0-9.2	-0.41	-1.32	2.30	-0.42	0.78
Pk43-01	117236.1	10.0-10.2	1.77	1.69	2.30	-0.03	1.41
Pk43-01	117236.2	11.0-11.2	1.16	0.79	2.94	-0.07	1.13
Pk43-01	117236.3	12.0-12.2	1.05	1.27	2.26	0.18	1.57
Pk43-01	117236.4	13.0-13.2	0.46	0.21	1.76	-0.19	0.96
Pk43-01	117236.5	14.0-14.2	0.60	0.57	1.29	0.00	1.19
Pk43-01	117237.1	15.0-15.2	1.47	1.49	1.01	0.18	1.76
Pk43-01	117237.2	16.0-16.2	1.58	1.72	1.03	0.31	1.79
Pk43-01	117237.3	17.0-17.2	3.49	3.34	0.89	-0.10	1.43
Pk43-01	117237.4	18.0-18.2	2.98	2.97	0.98	-0.06	1.01
Pk43-01	117237.5	19.0-19.2	2.78	2.94	0.82	0.36	0.99
Sk44-01	117238.1	0.0-0.2	1.78	1.84	0.76	0.02	0.95
Sk44-01	117238.2	1.0-1.2	2.28	2.18	0.62	-0.22	0.84
Sk44-01	117238.3	2.0-2.2	2.20	2.12	0.65	-0.16	0.77
Sk44-01	117238.4	3.0-3.2	2.29	2.20	0.61	-0.22	0.85
Sk44-01	117238.5	4.0-4.2	2.08	2.06	0.75	0.07	0.95
Sk44-01	117239.1	5.0-5.2	2.32	2.23	0.66	-0.16	1.02
Sk44-01	117239.2	6.0-6.2	2.35	2.26	0.62	-0.20	1.08
Sk44-01	117239.3	7.0-7.2	2.43	2.39	0.61	-0.04	1.43
Sk44-01	117239.4	8.0-8.2	2.37	2.28	0.63	-0.19	1.22
Sk44-01	117239.5	9.0-9.2	2.39	2.32	0.64	-0.13	1.31
Sk44-01	117240.1	10.0-10.2	2.47	2.44	0.80	0.07	1.85
Sk44-01	117240.8	11.0-11.2	2.44	2.42	0.61	-0.08	1.50
Sk44-01	117240.3	12.0-12.2	2.21	2.08	0.94	-0.23	1.21
Sk44-01	117240.4	13.0-13.2	2.67	2.86	1.08	0.36	1.62
Sk44-01	117240.5	14.0-14.2	2.73	2.89	1.03	0.21	1.25
Sk44-01	117241.1	15.0-15.2	2.89	3.05	1.61	0.10	1.16
Sk44-01	117241.2	16.0-16.2	4.00	4.15	1.23	0.15	1.53
Sk44-01	117241.3	17.0-17.2	3.65	3.70	0.60	0.21	1.19
Sk44-01	117241.4	18.0-18.2	3.57	3.61	0.61	0.06	1.34
Sk44-01	117241.5	19.0-19.2	4.15	4.35	1.06	0.31	0.92

Sk53-01	117242.2	0.0-0.2	2.41	2.37	0.62	-0.07	1.38
Sk53-01	117242.3	1.0-1.2	2.23	2.15	0.62	-0.19	0.79
Sk53-01	111242.4	2.0-2.2	2.24	2.16	0.62	-0.19	0.80
Sk53-01	117242.5	3.0-3.2	2.28	2.20	0.61	-0.21	0.84
Sk53-01	117242.6	4.0-4.2	2.43	2.40	0.55	-0.10	1.27
Sk53-01	117243.1	5.0-5.3	2.22	2.15	0.74	-0.03	1.00
Sk53-01	117243.2	6.0-6.2	1.72	1.63	1.07	-0.22	1.14
Sk53-01	117243.3	7.0-7.2	2.16	2.12	0.65	-0.08	0.79
Sk53-01	117243.4	8.0-8.2	2.00	2.02	0.64	0.03	0.74
Sk53-01	117243.5	9.0-9.2	2.18	2.12	0.63	-0.13	0.76
Sk53-01	117244.1	10.0-10.2	2.26	2.19	0.70	-0.06	1.00
Sk53-01	117244.2	11.0-11.2	2.38	2.31	0.63	-0.12	1.26
Sk53-01	117244.3	12.0-12.2	2.34	2.26	0.65	-0.12	1.10
Sk53-01	117244.4	13.0-13.2	2.39	2.32	0.69	-0.05	1.40
Sk53-01	117244.5	14.0-14.2	2.43	2.37	0.68	-0.06	1.48
Sk53-01	117244.6	15.0-15.2	2.55	2.74	1.16	0.40	2.47
Sk53-01	117244.7	16.0-16.2	2.88	3.32	1.81	0.41	1.30
Tj15-01	117265.1	0.0-0.2	2.49	2.55	1.56	0.24	3.95
Tj15-01	117265.2	1.0-1.2	2.49	2.49	0.44	-0.03	1.16
Tj15-01	117265.3	2.0-2.2	2.54	2.54	0.50	0.23	1.35
Tj15-01	117265.4	3.0-3.2	2.48	2.48	0.51	-0.05	1.40
Tj15-01	117265.5	4.0-4.2	2.51	2.51	0.61	0.08	1.64
Tj15-01	117266.1	5.0-5.2	2.21	2.11	0.76	-0.24	0.96
Tj15-01	117266.2	6.0-6.2	2.44	2.42	0.58	-0.05	1.40
Tj15-01	117266.3	7.0-7.2	2.39	2.33	0.60	-0.18	1.23
Tj15-01	117266.4	8.0-8.2	1.97	1.93	0.83	-0.17	0.94
Tj15-01	117266.5	9.0-9.2	2.04	1.79	1.15	-0.41	1.12
Tj15-01	117267.1	10.0-10.2	2.28	2.14	0.91	-0.25	1.32
Tj15-01	117267.2	11.0-11.2	2.48	2.48	0.69	0.01	1.74
Tj15-01	117267.3	12.0-12.2	2.51	2.51	0.49	0.08	1.32
Tj15-01	117267.4	13.0-13.2	1.54	1.50	1.07	-0.08	0.77
Tj15-01	117267.5	14.0-14.2	2.56	2.56	0.56	0.12	1.45
Tj35-01	117249.2	0.0-0.2	2.44	2.40	0.69	0.00	1.67
Tj35-01	117249.3	1.0-1.2	2.47	2.47	0.56	0.05	1.54
Tj35-01	117249.4	2.0-2.2	1.92	1.96	0.92	0.12	1.15
Tj35-01	117249.5	3.0-3.2	2.25	1.98	1.21	-0.31	1.37
Tj35-01	117249.6	4.0-4.2	2.54	2.60	0.76	0.19	1.75
Tj35-01	117250.2	5.0-5.2	2.49	2.57	1.23	0.24	1.95
Tj35-01	117250.3	6.0-6.2	2.62	2.74	0.88	0.22	1.76
Tj35-01	117250.4	7.0-7.2	2.70	2.88	1.04	0.26	1.35
Tj35-01	117250.5	8.0-8.2	2.61	2.66	0.98	0.05	1.12
Tj35-01	117250.6	9.0-9.2	2.42	2.44	1.28	-0.01	0.97
Tj35-01	117251.1	10.0-10.2	2.00	2.53	1.37	0.52	1.09
Tj35-01	117251.2	11.0-11.2	4.88	4.27	1.76	-0.43	0.80
Tj35-01	117251.3	12.0-12.2	4.00	3.71	1.62	-0.20	0.71
Tj35-01	117251.4	13.0-13.2	2.45	2.87	1.41	0.38	0.81
Tj35-01	117251.5	14.0-14.2	2.54	2.91	1.42	0.31	0.87

Tj35-01	117252.1	15.0-15.2	2.46	2.94	1.56	0.41	0.73
Tj35-01	117252.2	16.0-16.2	1.65	1.78	1.25	0.26	1.30
Tj35-01	117252.3	17.0-17.2	1.30	1.22	0.83	-0.02	1.06
Tj35-01	117252.4	18.0-18.2	2.05	2.04	0.65	-0.03	0.74
Tj35-01	117252.5	19.0-19.2	2.60	2.85	1.04	0.34	1.46
Tj54-01	117245.2	0.0-0.2	2.41	2.29	0.89	-0.26	2.13
Tj54-01	117245.3	1.0-1.2	2.42	2.36	0.65	-0.19	1.50
Tj54-01	117245.4	2.0-2.2	2.54	2.54	0.50	0.20	1.33
Tj54-01	117245.5	3.0-3.2	2.37	2.22	0.84	-0.30	1.67
Tj54-01	117245.6	4.0-4.2	2.45	2.44	0.61	-0.06	1.53
Tj54-01	117246.2	5.0-5.2	2.45	2.38	0.83	-0.15	1.98
Tj54-01	117246.3	6.0-6.2	2.21	1.69	1.94	-0.61	2.04
Tj54-01	117246.4	7.0-7.2	2.55	2.56	0.61	0.09	1.55
Tj54-01	117246.5	8.0-8.2	2.62	2.90	1.21	0.42	2.38
Tj54-01	117246.6	9.0-9.2	2.07	1.81	1.03	-0.39	0.88
Tj54-01	117247.2	10.0-10.2	2.55	2.55	0.59	0.09	1.57
Tj54-01	117247.3	11.0-11.2	2.62	2.81	0.92	0.27	1.88
Tj54-01	117247.4	12.0-12.2	2.67	3.36	1.91	0.42	1.87
Tj54-01	117247.5	13.0-13.2	2.80	4.01	2.49	0.51	0.90
Tj54-01	117247.6	14.0-14.6	2.64	2.83	1.17	0.16	1.71
Tj54-01	117248.1	15.0-15.2	2.53	2.49	1.36	-0.03	1.95
Tj54-01	117248.2	16.0-16.2	1.77	2.10	2.21	0.18	0.95
Tj54-01	117248.3	17.0-17.2	1.66	2.34	1.74	0.47	1.19
Tk21-01	117253.1	4.0-4.2	1.84	1.87	0.79	-0.04	0.92
Tk21-01	117254.1	5.0-5.2	1.66	1.74	0.79	0.04	1.01
Tk21-01	117254.2	6.0-6.2	2.02	2.00	0.71	-0.08	0.80
Tk21-01	117254.3	7.0-7.2	2.06	2.00	0.76	-0.20	0.89
Tk21-01	117254.4	8.0-8.2	1.72	1.80	0.78	0.06	0.96
Tk21-01	117254.5	9.0-9.2	1.75	1.82	0.76	0.05	0.94
Tk21-01	117255.1	10.0-10.2	1.52	1.55	0.70	0.05	1.33
Tk21-01	117255.2	11.0-11.2	1.41	1.37	0.82	-0.03	1.11
Tk21-01	117255.3	12.0-12.2	1.65	1.69	0.83	0.01	0.98
Tk21-01	117255.4	13.0-13.2	2.25	2.11	0.86	-0.24	1.13
Tk21-01	117255.5	14.0-14.2	2.45	2.45	0.54	-0.04	1.38
Tk21-01	117256.1	15.0-15.2	2.12	2.04	0.75	-0.21	0.86
Tk21-01	117256.2	16.0-16.2	2.32	2.21	0.65	-0.29	0.98
Tk21-01	117256.3	17.0-17.2	2.40	2.33	0.57	-0.24	1.19
Tk21-01	117256.4	18.0-18.2	2.51	2.51	0.57	0.08	1.58
Vi14-01	117258.1	8.0-8.2	-0.01	-0.10	2.21	0.12	1.65
Vi14-01	117258.2	9.0-9.2	0.40	0.36	1.28	-0.04	1.20
Vi14-01	117259.1	10.0-10.2	0.63	0.67	1.06	0.08	1.35
Vi14-01	117259.2	11.0-11.2	0.72	0.72	1.15	0.00	1.30
Vi14-01	117259.3	12.0-12.2	0.47	0.47	0.95	0.02	1.20
Vi14-01	117259.4	13.0-13.2	0.29	0.23	0.99	-0.06	1.11
Yh22-01	117281.1	0.0-0.2	2.55	2.61	0.69	0.07	1.50
Yh22-01	117281.2	1.0-1.2	2.73	2.86	0.64	0.28	0.87
Yh22-01	117281.3	2.0-2.2	2.71	2.84	0.66	0.35	1.05

Yh22-01	117282.1	8.0-8.2	3.15	3.27	0.99	0.26	1.02
Yh22-01	117282.2	9.5-9.7	2.98	3.00	0.89	0.01	1.06
Yh22-01	117283.1	10.0-10.2	2.95	3.00	1.08	-0.02	1.22
Yh22-01	117283.2	11.0-11.2	2.81	2.77	1.13	-0.16	1.20
Yh22-01	117283.3	12.0-12.2	2.92	2.67	1.71	-0.15	0.88
Yh41-01	117273.1	0.0-0.2	2.71	2.84	0.69	0.33	1.01
Yh41-01	117273.2	1.0-1.2	2.63	2.72	0.59	0.28	1.12
Yh41-01	117273.3	2.0-2.2	2.73	2.85	0.65	0.27	0.86
Yh41-01	117273.4	3.0-3.2	2.63	2.72	0.59	0.28	1.12
Yh41-01	117273.5	4.0-4.2	2.68	2.78	0.60	0.28	1.00
Yh41-01	117274.1	5.0-5.2	2.69	2.80	0.64	0.25	0.92
Yh41-01	117274.2	6.0-6.2	2.71	2.82	0.64	0.26	0.88
Yh41-01	117274.3	7.0-7.2	2.59	2.62	0.51	0.23	1.18
Yh41-01	117274.4	8.0-8.2	2.59	2.64	0.55	0.26	1.21
Yh41-01	117274.5	9.0-9.2	2.71	2.82	0.63	0.26	0.89
Yh41-01	117275.1	10.0-10.2	2.62	2.71	0.68	0.15	1.27
Yh41-01	117275.2	11.0-11.2	2.74	2.84	0.63	0.25	0.84
Yh41-01	117275.3	12.0-12.2	2.69	2.79	0.60	0.29	0.99
Yh41-01	117275.4	13.0-13.2	2.63	2.70	0.55	0.28	1.14
Yh41-01	117275.5	14.0-14.2	2.57	2.57	0.47	0.19	1.19
Yh41-01	117276.1	15.0-15.2	2.56	2.56	0.51	0.21	1.28
Yh41-01	117276.2	16.0-16.2	2.55	2.55	0.46	0.19	1.18
Yh41-01	117276.3	17.0-17.2	2.54	2.54	0.47	0.21	1.26
Yh54-01	117277.1	0.0-0.2	2.15	1.70	1.75	-0.47	1.55
Yh54-01	117277.2	1.0-1.2	2.81	2.93	0.69	0.26	0.82
Yh54-01	117277.3	2.0-2.2	2.80	2.91	0.65	0.23	0.78
Yh54-01	117277.4	3.0-3.2	2.74	2.83	0.64	0.24	0.84
Yh54-01	117277.5	4.0-4.2	2.97	3.44	1.49	0.40	0.83
Yh54-01	117278.1	5.0-5.1	2.22	2.14	1.12	0.00	1.43
Yh54-01	117278.2	6.0-6.2	2.32	2.87	1.85	0.42	0.79
Yh54-01	117278.3	7.0-7.2	2.40	2.78	1.65	0.33	0.86
Yh54-01	117278.4	8.0-8.2	1.84	2.43	1.57	0.45	1.24
Yh54-01	117278.5	9.0-9.2	1.75	2.37	1.76	0.28	0.92
Yh54-01	117279.1	10.0-10.2	2.65	3.04	1.35	0.35	0.80
Yh54-01	117279.2	11.0-11.2	2.84	3.17	1.72	0.20	0.78
Yh54-01	117279.3	12.0-12.2	1.73	2.43	1.62	0.50	1.38
Yh54-01	117279.5	14.0-14.2	2.51	2.51	0.43	0.16	1.12
Yh54-01	117280.1	15.0-15.2	2.52	2.52	0.48	0.22	1.32
Yh54-01	117280.2	16.0-16.2	2.51	2.51	0.48	0.13	1.32
Yh54-01	117280.3	17.0-17.2	2.53	2.53	0.44	0.19	1.21
Yh54-01	117280.4	18.0-18.2	2.53	2.53	0.47	0.21	1.29
Yh54-01	117280.5	19.0-19.2	2.52	2.52	0.47	0.21	1.27
Zz82-83	117285.2	0.0-0.2	3.53	3.53	0.49	0.06	1.23
Zz82-83	117285.3	1.0-1.2	3.71	3.81	0.69	0.32	1.18
Zz82-83	117285.4	2.0-2.2	3.59	3.59	0.38	0.06	0.83
Zz82-83	117285.5	3.0-3.2	3.61	3.60	0.41	0.06	0.89
Zz82-83	117285.6	4.0-4.2	3.63	3.61	0.40	0.05	0.88

Zz82-83	117286.1	5.0-5.2	3.56	3.56	0.39	0.09	0.91
Zz82-83	117286.2	6.0-6.2	3.63	3.61	0.45	0.08	1.00
Zz82-83	117286.3	7.0-7.2	3.55	3.77	1.26	0.00	3.46
Zz82-83	117286.4	8.0-8.2	3.79	3.97	0.82	0.39	1.18
Zz82-83	117286.5	9.0-9.2	3.79	3.89	0.73	0.29	1.06
Zz82-83	117287.1	12.0-12.2	3.78	3.88	0.73	0.31	1.06
Zz82-83	117287.2	13.0-13.2	3.65	3.72	0.60	0.32	1.33
Zz82-83	117288.1	15.0-15.2	3.93	4.05	0.91	0.31	1.13
Zz82-83	117288.2	16.0-16.2	3.83	3.93	0.78	0.31	1.17
Zz82-83	117288.3	17.0-17.2	4.20	4.36	1.07	0.29	1.37
Zz82-83	117288.4	18.0-18.2	3.67	3.74	0.60	0.27	1.21
Zz82-84	117289.3	0.0-0.2	3.22	3.15	0.69	-0.12	0.85
Zz82-84	117289.4	1.0-1.2	3.36	3.28	0.58	-0.24	1.02
Zz82-84	117289.5	2.0-2.2	3.43	3.42	0.52	-0.14	1.16
Zz82-84	117289.6	3.0-3.2	3.36	3.25	0.75	-0.39	1.54
Zz82-84	117289.7	4.0-4.2	3.40	3.15	1.20	-0.51	2.54
Zz82-84	117290.2	5.0-5.2	3.75	3.94	1.41	0.06	1.22
Zz82-84	117290.3	6.0-6.2	3.42	3.25	1.08	-0.43	2.45
Zz82-84	117290.4	7.0-7.2	3.59	3.56	0.51	-0.13	1.08
Zz82-84	117290.5	8.0-8.2	3.71	3.80	0.61	0.21	0.84
Zz82-84	117290.6	9.0-9.2	3.69	3.80	0.72	0.15	0.94
Zz82-84	117291.1	10.0-10.2	3.55	3.59	0.66	-0.05	1.25
Zz82-84	117291.2	11.0-11.2	3.69	3.74	0.57	0.10	0.86
Zz82-84	117291.3	12.0-12.2	3.70	3.75	0.54	0.13	0.80
Zz82-84	117291.5	13.0-13.2	3.72	3.71	0.58	0.16	1.16
Zz82-84	117291.4	14.0-14.2	3.78	3.87	0.70	0.25	0.97
Zz82-85	117292.1	0.0-0.2	3.58	3.58	0.43	0.13	1.00
Zz82-85	117292.2	1.0-1.2	3.55	3.55	0.37	0.03	0.79
Zz82-85	117292.3	2.0-2.2	3.56	3.56	0.37	0.03	0.79
Zz82-85	117292.4	3.0-3.2	3.54	3.54	0.36	0.04	0.81
Zz82-85	117292.5	4.0-4.2	3.55	3.55	0.37	0.06	0.83
Zz82-85	117293.1	5.0-5.2	3.58	3.58	0.37	0.04	0.81
Zz82-85	117293.2	6.0-6.2	3.55	3.55	0.37	0.06	0.84
Zz82-85	117293.3	7.0-7.2	3.54	3.54	0.37	0.04	0.80
Zz82-85	117293.4	8.0-8.2	3.66	3.69	0.44	0.06	0.77
Zz82-85	117293.5	9.0-9.2	3.85	3.86	0.55	0.05	0.55
Zz82-85	117294.1	10.0-10.2	3.59	3.59	0.41	0.10	0.92
Zz82-85	117294.2	11.0-11.2	3.65	3.67	0.48	0.15	0.98
Zz82-85	117294.3	12.0-12.5	3.85	3.92	0.64	0.19	0.91
Zz82-85	117294.4	13.0-13.2	4.62	4.84	1.43	0.28	0.90
Zz82-85	117294.5	14.0-14.2	3.94	4.20	1.04	0.42	0.95
Zz82-85	117295.1	16.0-16.2	4.32	4.61	1.31	0.37	0.91
Zz82-85	117295.2	18.0-18.2	4.88	5.19	1.79	0.33	0.93
Zz82-85	117295.3	19.0-19.2	4.57	4.91	1.78	0.41	1.05
Zz82-86	117296.2	0.0-0.2	3.14	3.06	0.78	-0.25	0.96
Zz82-86	117296.3	1.0-1.2	3.29	3.21	0.63	-0.19	0.83
Zz82-86	117296.4	2.0-2.2	3.36	3.28	0.60	-0.22	0.98

Zz82-86	117296.5	4.0-4.2	3.79	3.89	0.67	0.26	0.92
Zz82-86	117297.1	5.0-5.2	3.90	5.20	2.33	0.76	0.63
Zz82-86	117297.2	6.0-6.2	3.86	5.17	2.33	0.77	0.62
Zz82-86	117297.3	9.0-9.2	3.89	5.19	2.33	0.76	0.63
Zz82-86	117298.1	10.0-10.2	3.87	4.13	0.94	0.43	0.90
Zz82-86	117298.2	11.0-11.2	3.99	4.29	1.07	0.43	0.89
Zz82-86	117298.3	12.0-12.2	3.98	4.28	1.07	0.44	0.89
Zz82-86	117298.4	13.0-13.2	4.41	4.71	1.42	0.37	0.88
Zz82-86	117298.5	14.0-14.2	4.00	4.37	1.17	0.48	0.91
Zz82-86	117299.1	15.0-15.2	4.41	4.72	1.42	0.37	0.89
Zz82-86	117299.2	16.0-16.2	3.95	4.22	0.99	0.42	0.90
Zz82-86	117299.3	17.0-17.2	3.82	4.02	0.82	0.38	0.91
Zz82-86	117299.4	18.0-18.2	5.29	5.64	2.12	0.31	0.89
Zz82-86	117299.5	19.0-19.2	4.64	4.97	1.55	0.33	0.80
Zz82-87	117300.1	0.0-0.2	2.27	2.17	0.65	-0.21	0.85
Zz82-87	117300.2	1.0-1.2	1.79	1.59	1.38	-0.41	1.46
Zz82-87	117300.3	2.0-2.2	1.69	1.72	0.84	-0.02	0.96
Zz82-87	117300.4	3.0-3.2	2.43	2.42	0.53	-0.12	1.28
Zz82-87	117300.5	4.0-4.2	2.50	2.50	0.49	0.00	1.29
Zz82-87	117301.1	5.0-5.2	2.29	2.19	0.64	-0.22	0.88
Zz82-87	117301.2	6.0-6.2	2.23	2.13	0.66	-0.20	0.79
Zz82-87	117301.3	7.0-7.2	0.76	0.87	0.64	0.25	0.83
Zz82-87	117301.4	8.0-8.2	2.20	2.13	0.71	-0.08	0.89
Zz82-87	117301.5	9.0-9.2	2.46	2.46	0.57	0.00	1.43
Zz82-87	117302.1	10.0-10.2	2.31	2.22	0.63	-0.19	0.94
Zz82-87	117302.2	11.0-11.2	2.32	2.22	0.67	-0.19	1.03
Zz82-87	117302.3	12.0-12.2	2.39	2.31	0.71	-0.07	1.33
Zz82-87	117302.4	13.0-13.2	2.25	2.16	0.74	-0.08	0.97
Zz82-87	117302.5	14.0-14.2	2.08	2.03	0.74	-0.14	0.84
Zz82-87	117303.2	15.0-15.2	2.42	2.34	0.74	-0.09	1.51
Zz82-87	117303.3	16.0-16.2	2.09	2.03	0.89	-0.12	1.05
Zz82-87	117303.4	17.0-17.2	2.80	2.89	0.77	0.18	0.96
Zz82-87	117303.5	18.0-18.2	2.85	2.93	0.77	0.12	0.91
Zz82-88	117304.1	0.0-0.2	3.49	3.49	0.99	-0.25	2.87
Zz82-88	117304.2	1.0-1.2	3.81	4.08	0.94	0.45	1.13
Zz82-88	117304.3	2.0-2.2	3.65	3.75	0.63	0.35	1.32
Zz82-88	117304.4	3.0-3.2	3.70	3.83	0.70	0.38	1.21
Zz82-88	117304.5	4.0-4.2	4.31	4.56	1.26	0.35	0.93
Zz82-88	117305.1	5.0-5.2	3.84	4.10	0.96	0.46	1.09
Zz82-88	117305.2	6.0-6.2	3.84	4.10	0.97	0.46	1.09
Zz82-88	117305.3	7.0-7.2	3.93	3.93	0.57	0.01	0.82
Zz82-88	117305.4	8.0-8.2	4.20	4.20	0.75	-0.01	0.73
Zz82-88	117305.5	9.0-9.2	3.97	4.00	0.64	0.07	0.75
Zz82-88	117306.1	10.0-10.2	3.83	4.07	0.94	0.45	1.05
Zz82-88	117306.2	11.0-11.2	3.98	4.31	1.18	0.48	1.01
Zz82-88	117306.3	12.0-12.2	3.67	3.78	0.57	0.28	1.05
Zz82-88	117306.4	13.0-13.2	4.78	5.09	1.65	0.33	0.89

Zz82-88	117306.5	14.0-14.2	4.00	4.38	1.24	0.50	1.02
Zz82-88	117307.1	15.0-15.2	4.20	4.52	1.36	0.43	1.03
Zz82-88	117307.2	16.0-16.2	4.88	5.11	1.70	0.28	0.90
Zz82-88	117307.3	17.0-17.2	4.00	4.38	1.24	0.51	1.04
Zz82-88	117307.4	18.0-18.2	3.86	4.06	0.92	0.42	1.11
Zz82-88	117307.5	19.0-19.2	3.96	4.25	1.09	0.45	1.00
Zz82-89	117308.1	0.0-0.2	3.18	3.13	0.63	-0.12	0.76
Zz82-89	117308.2	1.0-1.2	3.23	3.18	0.72	-0.02	0.94
Zz82-89	117308.3	2.0-2.2	3.23	3.16	0.63	-0.16	0.78
Zz82-89	117308.4	3.0-3.2	3.18	3.13	0.69	-0.05	0.84
Zz82-89	117308.5	4.0-4.2	3.21	3.14	0.65	-0.16	0.76
Zz82-89	117309.1	5.0-5.2	3.43	3.35	0.69	-0.12	1.18
Zz82-89	117309.2	6.0-6.2	3.32	3.24	0.69	-0.13	0.92
Zz82-89	117309.3	7.0-7.2	3.27	3.19	0.72	-0.11	0.87
Zz82-89	117309.4	8.0-8.2	3.05	3.04	0.76	-0.09	0.85
Zz82-89	117309.5	9.0-9.2	3.25	3.17	0.69	-0.14	0.81
Zz82-89	117310.1	10.0-10.2	3.32	3.23	0.71	-0.15	0.91
Zz82-89	117310.2	11.0-11.2	3.18	3.12	0.79	-0.05	0.94
Zz82-89	117310.3	12.0-12.2	3.18	3.14	0.98	-0.01	1.09
Zz82-89	117311.1	15.3-15.5	3.28	3.12	1.30	-0.34	1.67
Zz82-89	117311.2	16.0-16.2	4.00	4.32	1.15	0.46	1.32
Zz82-90	117312.1	0.0-0.2	3.79	3.99	0.88	0.41	1.03
Zz82-90	117312.2	1.0-1.2	3.72	3.84	0.84	0.20	1.32
Zz82-90	117312.3	2.0-2.2	3.78	4.00	0.89	0.43	1.12
Zz82-90	117312.4	3.0-3.2	3.52	3.51	1.06	-0.03	1.65
Zz82-90	117312.5	4.0-4.2	3.41	3.32	0.69	-0.18	1.27
Zz82-90	117313.1	5.0-5.2	3.61	3.72	0.94	0.15	1.37
Zz82-90	117313.2	6.0-6.2	3.58	3.61	0.61	0.03	1.35
Zz82-90	117313.3	7.0-7.2	3.62	3.67	1.17	0.06	1.37
Zz82-90	117313.4	8.0-8.2	4.62	4.75	1.45	0.14	1.12
Zz82-90	117313.5	9.0-9.2	5.50	5.80	1.98	0.29	1.05
Zz82-91	117318.2	12.0-12.2	2.98	3.04	0.96	0.01	1.11
Zz82-91	117318.3	13.0-13.2	3.02	3.09	0.81	0.16	0.79
Zz82-91	117318.4	14.0-14.2	3.26	3.26	0.83	0.05	0.80
Zz82-91	117319.1	15.0-15.2	3.17	3.22	1.31	-0.16	1.60
Zz82-91	117319.2	16.0-16.2	2.88	3.14	0.98	0.41	0.91
Zz82-91	117319.3	17.0-17.2	3.14	3.15	0.82	0.08	0.84
Zz82-91	117319.4	18.0-18.2	3.20	3.29	1.03	0.26	1.10
Zz82-91	117319.5	19.0-19.2	3.31	3.35	0.99	0.16	1.06
Zz82-92	117320.1	0.0-0.2	4.26	4.54	1.32	0.36	0.90
Zz82-92	117320.2	1.0-1.2	3.75	3.93	0.83	0.42	1.20
Zz82-92	117320.3	2.0-2.2	3.89	4.15	0.98	0.41	0.97
Zz82-92	117320.4	3.0-3.2	3.94	4.24	1.02	0.42	0.82
Zz82-92	117320.5	4.0-4.2	2.00	2.49	1.84	0.40	1.42
Zz82-92	117321.1	5.0-5.2	2.20	2.16	0.81	0.05	1.03
Zz82-92	117321.2	6.0-6.2	2.48	2.48	0.65	0.01	1.64
Zz82-92	117321.3	7.0-7.2	2.71	2.88	0.83	0.37	1.14

Zz82-92	117313.4	8.0-8.2	2.57	2.64	0.70	0.13	1.52
Zz82-92	117321.5	9.0-9.2	2.53	2.59	0.77	0.14	1.78
Zz82-92	117322.5	13.0-13.2	2.53	2.69	1.26	0.37	2.33
Zz82-92	117322.6	14.0-14.2	2.52	2.57	0.70	0.10	1.41
Zz82-92	117323.1	15.0-15.2	1.41	1.33	0.88	-0.09	1.22
Zz82-92	117303.3	16.0-16.2	0.63	0.60	1.02	-0.03	0.88
Zz82-92	117323.3	17.0-17.2	0.70	0.62	1.19	-0.16	1.18
Zz82-94	117328.1	0.0-0.2	2.54	2.54	0.52	0.09	1.33
Zz82-94	117328.2	1.0-1.2	2.02	1.63	1.41	-0.47	1.04
Zz82-94	117328.3	2.0-2.2	2.42	2.37	0.70	-0.27	1.77
Zz82-94	117328.4	3.0-3.2	2.29	1.79	1.40	-0.60	1.50
Zz82-94	117328.5	4.0-4.2	2.51	2.51	0.61	-0.03	1.61
Zz82-94	117329.2	5.0-5.2	2.55	2.59	0.68	0.05	1.61
Zz82-94	117329.3	6.0-6.2	2.45	1.91	1.60	-0.53	2.78
Zz82-94	117329.4	7.0-7.2	2.65	2.75	0.79	0.04	1.55
Zz82-94	117329.5	8.0-8.2	2.62	2.73	1.11	-0.11	2.27
Zz82-94	117329.6	9.0-9.2	2.74	2.86	0.96	0.04	1.44
Zz82-94	117330.1	10.0-10.2	2.72	2.84	0.65	0.27	0.87
Zz82-94	117330.2	11.0-11.2	2.86	2.92	1.17	-0.10	1.56
Zz82-94	117330.2	12.0-12.2	2.75	2.88	0.70	0.34	0.98
Zz82-94	117330.4	13.0-13.2	3.03	3.20	1.07	0.27	1.07
Zz82-94	117330.5	14.0-14.2	2.74	2.89	0.80	0.35	1.05
Zz82-94	117330.6	15.0-15.2	2.77	2.89	0.67	0.30	0.88
Zz82-95	117331.1	0.0-0.2	2.48	2.47	0.63	-0.01	1.48
Zz82-95	117331.2	1.0-1.2	2.53	2.53	0.56	0.04	1.41
Zz82-95	117331.3	2.0-2.2	2.51	2.51	0.57	0.03	1.45
Zz82-95	117331.4	3.0-3.2	2.56	2.57	0.54	0.12	1.32
Zz82-95	117331.5	4.0-4.2	2.56	2.56	0.52	0.14	1.28
Zz82-95	117332.1	5.0-5.2	2.58	2.61	0.55	0.20	1.29
Zz82-95	117332.2	6.0-6.2	2.58	2.63	0.60	0.20	1.36
Zz82-95	117332.3	7.0-7.2	2.59	2.63	0.55	0.26	1.22
Zz82-95	117332.4	8.0-8.2	2.60	2.71	0.75	0.24	1.59
Zz82-95	117333.1	10.1-10.3	2.87	3.37	1.36	0.47	0.76
Zz82-95	117333.2	11.0-11.2	2.66	2.86	0.82	0.47	1.49
Zz82-95	117333.3	12.0-12.2	4.26	4.58	1.38	0.42	1.00
Zz82-95	117333.4	13.0-13.2	4.57	4.88	1.61	0.37	0.99
Zz82-95	117333.5	14.0-14.2	3.80	3.97	0.82	0.39	1.03
Zz82-95	117334.1	15.0-15.2	3.79	4.01	0.97	0.45	1.25
Zz82-95	117334.2	16.0-16.2	4.00	4.32	1.17	0.48	1.02
Zz82-95	117334.3	17.0-17.2	5.64	5.88	1.89	0.19	0.84
Zz82-95	117334.4	18.0-18.2	3.87	4.14	0.95	0.42	0.85
Zz82-95	117334.5	19.0-19.2	4.26	4.54	1.23	0.35	0.82

APPENDIX D Amino Acid Racemization results

AMINO ACID RACEMIZATION (AAR) STUDIES, MID-ATLANTIC VIBRACORES, BOEM ASAP PROGRAM, 2015-2019

J. F. WEHMILLER, DEPARTMENT OF GEOLOGICAL SCIENCES (now Earth Sciences) and DELAWARE GEOLOGICAL SURVEY, UNIVERSITY OF DELAWARE, NEWARK DE 19716

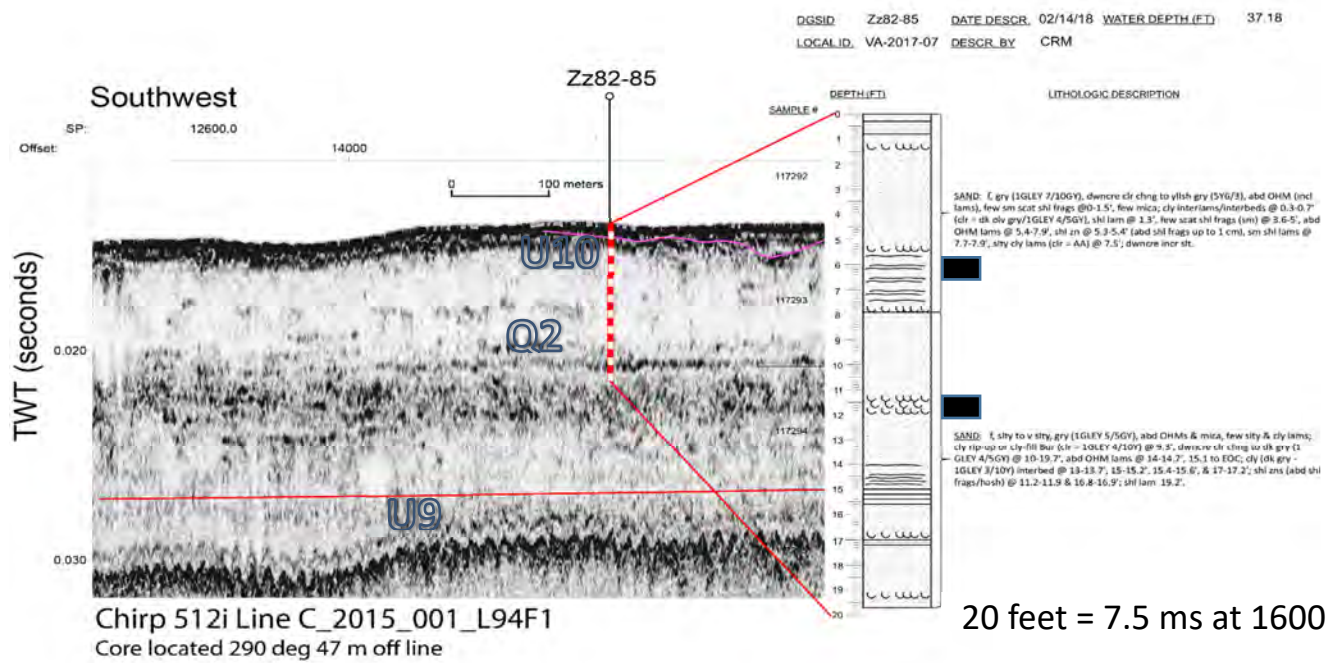
Amino acid racemization (AAR) data have been obtained on mollusk specimens from offshore and onshore sites on the US Atlantic Coastal Plain as part of the BOEM project (2015-2019). The analyses have been conducted within the framework of both the mid- and southeast Atlantic projects, with a summary report for both regions in the form of a poster presented at the 2019 SE GSA meeting in Charleston, SC. (Wehmiller et al., 2019).

Samples for AAR analysis were obtained from 79 BOEM vibracores from the NJ, DE, MD, VA, NC, SC and GA shelves. Analyses have been conducted in the AAR laboratory at Northern Arizona University (<https://www2.nau.edu/geochron-lab/wordpress/>). In order to compare the offshore results with onshore sites, samples from selected onshore sites ($n > 20$) were also analyzed as part of the current study. Data for these sites had been available prior to 2015 as a result of numerous stratigraphic studies at the University of Delaware (summarized in Wehmiller et al., 2015: GSA Baltimore).

AAR analyses provide insights into the ages of analyzed shell samples. Although a variety of factors affect age estimation, with enough data it is possible to assign age estimates (Holocene, late Pleistocene, middle Pleistocene, etc.) to samples from onshore or offshore sites. Evidence of age mixing with the core samples is also seen. Age estimates are useful for discerning whether offshore units (particularly sand bodies that might be exploited) are relict or “modern” (active) features. In selected cases AAR results have been calibrated with paired ^{14}C analyses (same shell for both analyses) – this approach allows the AAR results to be clearly categorized as Holocene or pre-Holocene. An example of how the AAR results contribute to our understanding of the ages of shell material in the coastal zone is seen in Figure 1, where results for one core offshore of southern Delmarva can be relate to results from an onshore core (Kiptopeake, VA) and beach shells from Smith Island, VA).

A complete table of the AAR data can be found in the supplemental data files. A table of the all the analyses with their corresponding sites is found at the end of this appendix. (Table 1).

Figure 1. Example of racemization results for BOEM core VA-2017-07, offshore Smith Island, southern Delmarva Peninsula. Results for *Spisula* at two depths (black rectangles) indicate that the two layers are both late Pleistocene (~80-100 ka) based on comparison with onshore calibration sites. *Mulinia* data from the deeper layer are also the same age. *Mulinia* and *Mercenaria* results from ~3.5' depth indicate a mixture of Holocene and Pleistocene ages. The *Spisula* D/L values are equivalent to those seen in *Spisula* from a beach collection site on nearby Smith Island, suggesting that the offshore unit sampled in core VA-2017-07 is a potential source for the Smith Island beach sediments. Additionally, similar D/L values are observed for *Spisula* samples from a core taken at Kiptopeake, on the Delmarva mainland west of Smith Island. Seismic stratigraphic interpretation courtesy of Laura Brothers, USGS Woods Hole.



Methods of data management are summarized as follows: 1) a 2015 [summary](#) by Wehmiller and Pellerito; 2) an on-line [database](#) managed by the Delaware Geological Survey; 3) ArcGIS online [maps](#) that provide data summaries, explanatory text, and [preliminary](#) interpretations of results. The latter site also contains embedded spreadsheets with summaries of all the amino acid data for the region. These maps are constantly being updated with either interpretations or descriptive information about the samples and/or sites.

In addition to the results summarized in the databases listed above, presentations of this research have been made at two recent Southeastern Section Geological Society of America meetings. A manuscript presenting the southern Delmarva barrier island data (Wehmiller et al, 2019a) in the context of offshore regional stratigraphy is now in draft form

Wehmiller et al., 2015: GSA Baltimore 2015 (poster available online): RACEMIZATION-INFERRED AGE DISTRIBUTION OF MOLLUSKS IN THE US ATLANTIC MARGIN COASTAL SYSTEM

<https://gsa.confex.com/gsa/2015AM/webprogram/Paper263915.html>

Wehmiller et al., 2017: SE GSA Richmond 2017

PAIRED RACEMIZATION AND RADIOCARBON ANALYSIS OF PLEISTOCENE AND HOLOCENE SHELLS, US ATLANTIC COASTAL PLAIN: IMPLICATIONS FOR SHELL GEOCHRONOLOGY, PLEISTOCENE SEA LEVEL HISTORY, AND PALEOCLIMATE

<https://gsa.confex.com/gsa/2017SE/webprogram/Paper290532.html>

Wehmiller et al., 2019a: SE GSA Charleston 2019

SOUTHERN DELMARVA BARRIER ISLAND BEACHES: LINKING OFFSHORE AND ONSHORE UNITS USING RACEMIZATION GEOCHRONOLOGY TO INFER SEDIMENT SOURCES DURING SHORELINE MIGRATION

<https://gsa.confex.com/gsa/2019SE/webprogram/Paper326646.html>

Wehmiller et al, 2019b: SE GSA Charleston 2019 (poster available online):

NEW PERSPECTIVES ON US ATLANTIC COASTAL PLAIN AMINOSTRATIGRAPHY GLEANED FROM EXTENSIVE ANALYSES OF SHELL SPECIMENS FROM INNER CONTINENTAL SHELF VIBRACORES

<https://gsa.confex.com/gsa/2019SE/webprogram/Paper326300.html>

Database management links:

Wehmiller and POellerito, 2015: Paper describing the structure of the UD AAR database:

<https://www.sciencedirect.com/science/article/pii/S2214242815000170?via%3Dihub>

Link to the actual UD AAR database hosted at the Delaware Geological Survey:

<https://www.dgs.udel.edu/publications/ofr50-database-quaternary-coastal-geochronologic-information-atlantic-and-pacific-coast>

Online maps with interpretations:

<https://www.arcgis.com/home/item.html?id=49c4b9d1312c433b9ca461fab7fce8b5>

The online files contain summaries of the AAR and ^{14}C analytical data, and brief comments about the age interpretations derived from these results. In cases where multiple core depths have been sampled, interpretations are provided for each core depth. Comments about age mixing, sample quality, and overall confidence in the results are also provided. The interpretations depend on a number of criteria, including sample preservation, number of samples analyzed, and the possibility of mixed ages. At this point in the overall analysis of the cores, we use AAR to assign ages of either “Holocene” or “Pleistocene.” In some cases, the AAR results indicate “mid-” or “early-Pleistocene” age based on comparison with units of these ages found in onshore studies (Wehmiller et al., 2010; Wehmiller, 2013).

Many of the Pleistocene samples have ^{14}C ages that fall in the range of 30-45 ka; this range is uncertain and debatable because of the potential for contamination with modern carbon (Wehmiller et al., 2017: SEGSA Richmond). The question of carbon contamination of the radiocarbon results is under further investigation.

Data table 1 contains all the AAR results for the mid- and southeast Atlantic BOEM projects provided by the Northern Arizona laboratory. The table is an output from the University of Delaware AAR database (UDAARDDB) and lists localities, sample numbers, and D/L values. An explanation of UDAARDDB is found in [Wehmiller and Pellerito \(2015\)](#).

Table 1. Listing of all analyses with corresponding sites. Complete table with analyses is in the supplemental data.

UDAMS	General location	LocalityID	Latitude	Longitude
05166	NJ Shelf	New Jersey shelf Core 12	39.65241	-74.08417
05166	NJ Shelf	New Jersey shelf Core 12	39.65241	-74.08417
05166	NJ Shelf	New Jersey shelf Core 12	39.65241	-74.08417
05166	NJ Shelf	New Jersey shelf Core 12	39.65241	-74.08417
05166	NJ Shelf	New Jersey shelf Core 12	39.65241	-74.08417
05168	NJ Shelf	New Jersey shelf Core 17a/R2	39.64486	-74.05144
05168	NJ Shelf	New Jersey shelf Core 17a/R2	39.64486	-74.05144
05169	NJ Shelf	New Jersey shelf Core 13	39.65229	-74.07269
05170	NJ Shelf	New Jersey shelf Core 18	39.59807	-74.03946
05177	DE shelf	Qk22-02	38.68825	-75.09237
05179	DE shelf	Qk41-02	38.5198386	-74.98768574
05179	DE shelf	Qk41-02	38.5198386	-74.98768574
05180	DE shelf	Qk42-02	38.52132419	-74.97369934
05183	DE shelf	Qk53-03	38.51365198	-74.96022733
05183	DE shelf	Qk53-03	38.51365198	-74.96022733
05183	DE shelf	Qk53-03	38.51365198	-74.96022733
05183	DE shelf	Qk53-03	38.51365198	-74.96022733
05183	DE shelf	Qk53-03	38.51365198	-74.96022733
05183	DE shelf	Qk53-03	38.51365198	-74.96022733
05183	DE shelf	Qk53-03	38.51365198	-74.96022733
05183	DE shelf	Qk53-03	38.51365198	-74.96022733
05183	DE shelf	Qk53-03	38.51365198	-74.96022733
05183	DE shelf	Qk53-03	38.51365198	-74.96022733
05183	DE shelf	Qk53-03	38.51365198	-74.96022733
05183	DE shelf	Qk53-03	38.51365198	-74.96022733
05183	DE shelf	Qk53-03	38.51365198	-74.96022733
05183	DE shelf	Qk53-03	38.51365198	-74.96022733
05183	DE shelf	Qk53-03	38.51365198	-74.96022733
05183	DE shelf	Qk53-03	38.51365198	-74.96022733
05183	DE shelf	Qk53-03	38.51365198	-74.96022733
05185	NJ Shelf	NJGSCore53	40.115	-73.9379
05185	NJ Shelf	NJGSCore53	40.115	-73.9379
05185	NJ Shelf	NJGSCore53	40.115	-73.9379
05185	NJ Shelf	NJGSCore53	40.115	-73.9379
05185	NJ Shelf	NJGSCore53	40.115	-73.9379
05185	NJ Shelf	NJGSCore53	40.115	-73.9379
05186	NJ Shelf	NJGScore31	40.145	-73.9541
05186	NJ Shelf	NJGScore31	40.145	-73.9541
05186	NJ Shelf	NJGScore31	40.145	-73.9541
05186	NJ Shelf	NJGScore31	40.145	-73.9541

05186	NJ Shelf	NJGScore31	40.145	-73.9541
05186	NJ Shelf	NJGScore31	40.145	-73.9541
05186	NJ Shelf	NJGScore31	40.145	-73.9541
05186	NJ Shelf	NJGScore31	40.145	-73.9541
05186	NJ Shelf	NJGScore31	40.145	-73.9541
05186	NJ Shelf	NJGScore31	40.145	-73.9541
05186	NJ Shelf	NJGScore31	40.145	-73.9541
05186	NJ Shelf	NJGScore31	40.145	-73.9541
05186	NJ Shelf	NJGScore31	40.145	-73.9541
05186	NJ Shelf	NJGScore31	40.145	-73.9541
05186	NJ Shelf	njgs core 36r1	40.112	-73.9348
05188	NJ Shelf	njgs core 36r1	40.112	-73.9348
05188	NJ Shelf	njgs core 36r1	40.112	-73.9348
05188	NJ Shelf	njgs core 36r1	40.112	-73.9348
05188	NJ Shelf	njgs core 36r1	40.112	-73.9348
05188	NJ Shelf	njgs core 36r1	40.112	-73.9348
05188	NJ Shelf	njgs core 36r1	40.112	-73.9348
05189	NJ Shelf	njgs core 49	40.152	-73.9342
05189	NJ Shelf	njgs core 49	40.152	-73.9342
05189	NJ Shelf	njgs core 49	40.152	-73.9342
05189	NJ Shelf	njgs core 49	40.152	-73.9342
05190	NJ Shelf	njgs core 50	40.144	-73.9109
05190	NJ Shelf	njgs core 50	40.144	-73.9109
05190	NJ Shelf	njgs core 50	40.144	-73.9109
05190	NJ Shelf	njgs core 50	40.144	-73.9109
05190	NJ Shelf	njgs core 50	40.144	-73.9109
05190	NJ Shelf	njgs core 50	40.144	-73.9109
05190	NJ Shelf	njgs core 50	40.144	-73.9109
05191	NJ Shelf	njgs core 52	40.152	-73.8725
05191	NJ Shelf	njgs core 52	40.152	-73.8725
05191	NJ Shelf	njgs core 52	40.152	-73.8725
05191	NJ Shelf	njgs core 52	40.152	-73.8725
05191	NJ Shelf	njgs core 52	40.152	-73.8725
05192	NJ Shelf	njgs core 55	40.107	-73.9708
05192	NJ Shelf	njgs core 55	40.107	-73.9708
05192	NJ Shelf	njgs core 55	40.107	-73.9708

05192	NJ Shelf	njgs core 55	40.107	-73.9708
05194	NJ Shelf	njgs core 62	40.174	-73.9118
05194	NJ Shelf	njgs core 62	40.174	-73.9118
05196	NJ Shelf	njgs core 65	40.281	-73.9194
05196	NJ Shelf	njgs core 65	40.281	-73.9194
05196	NJ Shelf	njgs core 65	40.281	-73.9194
05196	NJ Shelf	njgs core 65	40.281	-73.9194
05197	NJ Shelf	njgs core 66	40.156	-73.8993
05197	NJ Shelf	njgs core 66	40.156	-73.8993
05197	NJ Shelf	njgs core 66	40.156	-73.8993
05197	NJ Shelf	njgs core 66	40.156	-73.8993
05197	NJ Shelf	njgs core 66	40.156	-73.8993
05197	NJ Shelf	njgs core 66	40.156	-73.8993
05198	NJ Shelf	njgs core 69	40.298	-73.9102
05198	NJ Shelf	njgs core 69	40.298	-73.9102
05198	NJ Shelf	njgs core 69	40.298	-73.9102
05201	MD shelf	Md Geol Survey Core B-1	38.28322	-74.91203
05201	MD shelf	Md Geol Survey Core B-1	38.28322	-74.91203
05201	MD shelf	Md Geol Survey Core B-1	38.28322	-74.91203
05201	MD shelf	Md Geol Survey Core B-1	38.28322	-74.91203
05201	MD shelf	Md Geol Survey Core B-1	38.28322	-74.91203
05201	MD shelf	Md Geol Survey Core B-1	38.28322	-74.91203
05201	MD shelf	Md Geol Survey Core B-1	38.28322	-74.91203
05201	MD shelf	Md Geol Survey Core B-1	38.28322	-74.91203
05201	MD shelf	Md Geol Survey Core B-1	38.28322	-74.91203
05203	DE shelf	Rk23-03	38.48122	-74.95796
05204	DE shelf	Rk13-04	38.49567	-74.95962
05204	DE shelf	Rk13-04	38.49567	-74.95962
05204	DE shelf	Rk13-04	38.49567	-74.95962
05204	DE shelf	Rk13-04	38.49567	-74.95962
05204	DE shelf	Rk13-04	38.49567	-74.95962
05207	DE shelf	Rl21-06	38.47511	-74.90823
05212	Seaford	Oj31-14	38.70789	-75.08102
05212	Seaford	Oj31-14	38.70789	-75.08102
05212	Seaford	Oj31-14	38.70789	-75.08102
05212	Seaford	Oj31-14	38.70789	-75.08102
05220	DE shelf	Qj12-01	38.57511	-75.0549
05220	DE shelf	Qj12-01	38.57511	-75.0549
05220	DE shelf	Qj12-01	38.57511	-75.0549

05224	DE shelf	Rj13-01	38.49678	-75.04629
05225	VA shelf	Smith Island shoal transect	37.00946	-75.17985
05225	VA shelf	Smith Island shoal transect	37.00946	-75.17985
05225	VA shelf	Smith Island shoal transect	37.00946	-75.17985
05225	VA shelf	Smith Island shoal transect	37.00946	-75.17985
05225	VA shelf	Smith Island shoal transect	37.00946	-75.17985
05225	VA shelf	Smith Island shoal transect	37.00946	-75.17985
05225	VA shelf	Smith Island shoal transect	37.00946	-75.17985
05225	VA shelf	Smith Island shoal transect	37.00946	-75.17985
05225	VA shelf	Smith Island shoal transect	37.00946	-75.17985
05225	VA shelf	Smith Island shoal transect	37.00946	-75.17985
05225	VA shelf	Smith Island shoal transect	37.00946	-75.17985
05225	VA shelf	Smith Island shoal transect	37.00946	-75.17985
05225	VA shelf	Smith Island shoal transect	37.00946	-75.17985
05225	VA shelf	Smith Island shoal transect	37.00946	-75.17985
05225	VA shelf	Smith Island shoal transect	37.00946	-75.17985
05225	VA shelf	Smith Island shoal transect	37.00946	-75.17985
05225	VA shelf	Smith Island shoal transect	37.00946	-75.17985
05227	Seaford	Oj11-05	38.73694	-75.0805
05227	Seaford	Oj11-05	38.73694	-75.0805
05227	Seaford	Oj11-05	38.73694	-75.0805
05227	Seaford	Oj11-05	38.73694	-75.0805
05227	Seaford	Oj11-05	38.73694	-75.0805
05228	Seaford	Oi25-39	38.73267	-75.09181
05228	Seaford	Oi25-39	38.73267	-75.09181
05228	Seaford	Oi25-39	38.73267	-75.09181
05228	Seaford	Oi25-39	38.73267	-75.09181
05228	Seaford	Oi25-39	38.73267	-75.09181
05261	DE shelf	Oj23-09	38.72396	-75.0383
05261	DE shelf	Oj23-09	38.72396	-75.0383
05265	DE shelf	Ok51-02	38.67776	-74.99341
05265	DE shelf	Ok51-02	38.67776	-74.99341
05266	DE shelf	Ok51-05	38.68324	-74.98513
05266	DE shelf	Ok51-05	38.68324	-74.98513
05266	DE shelf	Ok51-05	38.68324	-74.98513
05266	DE shelf	Ok51-05	38.68324	-74.98513
05266	DE shelf	Ok51-05	38.68324	-74.98513
05266	DE shelf	Ok51-05	38.68324	-74.98513
05267	DE shelf	Oj44-03	38.69633	-75.01938
05267	DE shelf	Oj44-03	38.69633	-75.01938
05267	DE shelf	Oj44-03	38.69633	-75.01938
05268	DE shelf	Oj53-02	38.6707	-75.03823
05268	DE shelf	Oj53-02	38.6707	-75.03823
05268	DE shelf	Oj53-02	38.6707	-75.03823
05269	DE shelf	Ni35-15	38.79842	-75.08499

05303	Leonardtown	Maint Yard	38.44899	-76.091741
05304	Leonardtown	Golden Hill	38.424934	-76.206327
05304	Leonardtown	Golden Hill	38.424934	-76.206327
05309	Seaford	Qj31-20	38.54318	-75.07416
05309	Seaford	Qj31-20	38.54318	-75.07416
05309	Seaford	Qj31-20	38.54318	-75.07416
05309	Seaford	Qj31-20	38.54318	-75.07416
05309	Seaford	Qj31-20	38.54318	-75.07416
05309	Seaford	Qj31-20	38.54318	-75.07416
05309	Seaford	Qj31-20	38.54318	-75.07416
05309	Seaford	Qj31-20	38.54318	-75.07416
05309	Seaford	Qj31-20	38.54318	-75.07416
05309	Seaford	Qj31-20	38.54318	-75.07416
05309	Seaford	Qj31-20	38.54318	-75.07416
05338	DE shelf	JCK-HCS-1	38.76178	-75.05935
05338	DE shelf	JCK-HCS-1	38.76178	-75.05935
05363	DE shelf	Oj34-04	38.71583	-75.0281
05365	DE shelf	Oj33-03	38.70523	-75.04864
05365	DE shelf	Oj33-03	38.70523	-75.04864
05366	DE shelf	Oj55-02	38.67063	-75.00065
05367	DE shelf	Nk32a	38.78668	-74.97336
05367	DE shelf	Nk32a	38.78668	-74.97336
05368	DE shelf	Nk32b	38.78668	-74.97336
05369	DE shelf	Pj15-06	38.65222	-75.01301
05370	DE shelf	Oj54-02	38.68299	-75.02002
05371	NJ Shelf	Ln15-01	38.99046	-74.66718
05371	NJ Shelf	Ln15-01	38.99046	-74.66718
05371	NJ Shelf	Ln15-01	38.99046	-74.66718
05371	NJ Shelf	Ln15-01	38.99046	-74.66718
05371	NJ Shelf	Ln15-01	38.99046	-74.66718
05372	NJ Shelf	Lo51-01	38.92843	-74.66211
05372	NJ Shelf	Lo51-01	38.92843	-74.66211
05373	NJ Shelf	Ko51-01	39.00359	-74.65234
05373	NJ Shelf	Ko51-01	39.00359	-74.65234
05373	NJ Shelf	Ko51-01	39.00359	-74.65234
05373	NJ Shelf	Ko51-01	39.00359	-74.65234
05374	DE shelf	Qk24-01	38.55394	-74.93848
05374	DE shelf	Qk24-01	38.55394	-74.93848
05374	DE shelf	Qk24-01	38.55394	-74.93848
05375	DE shelf	Rk25-03	38.47514	-74.92449
05375	DE shelf	Rk25-03	38.47514	-74.92449

05375	DE shelf	Rk25-03	38.47514	-74.92449
05376	DE shelf	Ok52-06	38.66975	-74.96978
05376	DE shelf	Ok52-06	38.66975	-74.96978
05376	DE shelf	Ok52-06	38.66975	-74.96978
05376	DE shelf	Ok52-06	38.66975	-74.96978
05376	DE shelf	Ok52-06	38.66975	-74.96978
05376	DE shelf	Ok52-06	38.66975	-74.96978
05376	DE shelf	Ok52-06	38.66975	-74.96978
05377	DE shelf	Ok52-05	38.66978	-74.96977
05377	DE shelf	Ok52-05	38.66978	-74.96977
05377	DE shelf	Ok52-05	38.66978	-74.96977
05377	DE shelf	Ok52-05	38.66978	-74.96977
05378	MD shelf	Uk12-01	38.23973	-74.97477
05378	MD shelf	Uk12-01	38.23973	-74.97477
05379	MD shelf	Uj35-02	38.20661	-75.01119
05379	MD shelf	Uj35-02	38.20661	-75.01119
05379	MD shelf	Uj35-02	38.20661	-75.01119
05379	MD shelf	Uj35-02	38.20661	-75.01119
05379	MD shelf	Uj35-02	38.20661	-75.01119
05379	MD shelf	Uj35-02	38.20661	-75.01119
05380	MD shelf	Uj35-03	38.2066	-75.01122
05380	MD shelf	Uj35-03	38.2066	-75.01122
05380	MD shelf	Uj35-03	38.2066	-75.01122
05380	MD shelf	Uj35-03	38.2066	-75.01122
05380	MD shelf	Uj35-03	38.2066	-75.01122
05380	MD shelf	Uj35-03	38.2066	-75.01122
05380	MD shelf	Uj35-03	38.2066	-75.01122
05380	MD shelf	Uj35-03	38.2066	-75.01122
05380	MD shelf	Uj35-03	38.2066	-75.01122
05380	MD shelf	Uj35-03	38.2066	-75.01122
05380	MD shelf	Uj35-03	38.2066	-75.01122
05380	MD shelf	Uj35-03	38.2066	-75.01122
05380	MD shelf	Uj35-03	38.2066	-75.01122
05380	MD shelf	Uj35-03	38.2066	-75.01122
05380	MD shelf	Uj35-03	38.2066	-75.01122
05380	MD shelf	Uj35-03	38.2066	-75.01122
05381	MD shelf	Vj34-01	38.12247	-75.02035
05381	MD shelf	Vj34-01	38.12247	-75.02035
05381	MD shelf	Vj34-01	38.12247	-75.02035

05381	MD shelf	Vj34-01	38.12247	-75.02035
05381	MD shelf	Vj34-01	38.12247	-75.02035
05381	MD shelf	Vj34-01	38.12247	-75.02035
05381	MD shelf	Vj34-01	38.12247	-75.02035
05381	MD shelf	Vj34-01	38.12247	-75.02035
05381	MD shelf	Vj34-01	38.12247	-75.02035
05381	MD shelf	Vj34-01	38.12247	-75.02035
05381	MD shelf	Vj34-01	38.12247	-75.02035
05381	MD shelf	Vj34-01	38.12247	-75.02035
05381	MD shelf	Vj34-01	38.12247	-75.02035
05381	MD shelf	Vj34-01	38.12247	-75.02035
05381	MD shelf	Vj34-01	38.12247	-75.02035
05381	MD shelf	Vj34-01	38.12247	-75.02035
05381	MD shelf	Vj34-01	38.12247	-75.02035
05381	MD shelf	Vj34-01	38.12247	-75.02035
05381	MD shelf	Vj34-01	38.12247	-75.02035
05381	MD shelf	Vj34-01	38.12247	-75.02035
05381	MD shelf	Vj34-01	38.12247	-75.02035
05381	MD shelf	Vj34-01	38.12247	-75.02035
05381	MD shelf	Vj34-01	38.12247	-75.02035
05381	MD shelf	Vj34-01	38.12247	-75.02035
05381	MD shelf	Vj34-01	38.12247	-75.02035
05382	MD shelf	Uj43-01	38.19127	-75.03538
05382	MD shelf	Uj43-01	38.19127	-75.03538
05382	MD shelf	Uj43-01	38.19127	-75.03538
05382	MD shelf	Uj43-01	38.19127	-75.03538
05382	MD shelf	Uj43-01	38.19127	-75.03538
05382	MD shelf	Uj43-01	38.19127	-75.03538
05383	MD shelf	Wj22-01	38.06491	-75.05153
05383	MD shelf	Wj22-01	38.06491	-75.05153
05383	MD shelf	Wj22-01	38.06491	-75.05153
05383	MD shelf	Wj22-01	38.06491	-75.05153
05383	MD shelf	Wj22-01	38.06491	-75.05153
05384	Dover	Gd33-10	39.37015	-75.54473
05384	Dover	Gd33-10	39.37015	-75.54473
05384	Dover	Gd33-10	39.37015	-75.54473
05384	Dover	Gd33-10	39.37015	-75.54473
05384	Dover	Gd33-10	39.37015	-75.54473
05384	Dover	Gd33-10	39.37015	-75.54473
05388	Md Shelf	Sk44-01	38.35337981	-74.94751686
05388	Md Shelf	Sk44-01	38.35337981	-74.94751686
05390	Md Shelf	Tj54-01	38.25520617	-75.02467672
05390	Md Shelf	Tj54-01	38.25520617	-75.02467672
05390	Md Shelf	Tj54-01	38.25520617	-75.02467672
05390	Md Shelf	Tj54-01	38.25520617	-75.02467672
05393	Md Shelf	Vi14-01	38.16102775	-75.10712436
05393	Md Shelf	Vi14-01	38.16102775	-75.10712436
05393	Md Shelf	Vi14-01	38.16102775	-75.10712436
05393	Md Shelf	Vi14-01	38.16102775	-75.10712436

05393	Md Shelf	Vi14-01	38.16102775	-75.10712436
05393	Md Shelf	Vi14-01	38.16102775	-75.10712436
05395	Md Shelf	Tj15-01	38.33013989	-75.002402
05395	Md Shelf	Tj15-01	38.33013989	-75.002402
05395	Md Shelf	Tj15-01	38.33013989	-75.002402
05395	Md Shelf	Tj15-01	38.33013989	-75.002402
05395	Md Shelf	Tj15-01	38.33013989	-75.002402
05395	Md Shelf	Tj15-01	38.33013989	-75.002402
05395	Md Shelf	Tj15-01	38.33013989	-75.002402
05395	Md Shelf	Tj15-01	38.33013989	-75.002402
05395	Md Shelf	Tj15-01	38.33013989	-75.002402
05133H	MD shelf	WS4	38.4272	-74.9361

06000	Tappahanock	Norris Bridge	37.63227	-76.40832
06000	Tappahanock	Norris Bridge	37.63227	-76.40832
06000	Tappahanock	Norris Bridge	37.63227	-76.40832
06000	Tappahanock	Norris Bridge	37.63227	-76.40832
06000	Tappahanock	Norris Bridge	37.63227	-76.40832
06000	Tappahanock	Norris Bridge	37.63227	-76.40832
06000	Tappahanock	Norris Bridge	37.63227	-76.40832
06000	Tappahanock	Norris Bridge	37.63227	-76.40832
06002	Chincoteague	Ts Corner	37.9455	-75.5412
06002	Chincoteague	Ts Corner	37.9455	-75.5412
06002	Chincoteague	Ts Corner	37.9455	-75.5412
06002	Chincoteague	Ts Corner	37.9455	-75.5412
06002	Chincoteague	Ts Corner	37.9455	-75.5412
06002	Chincoteague	Ts Corner	37.9455	-75.5412
06002	Chincoteague	Ts Corner	37.9455	-75.5412
06002	Chincoteague	Ts Corner	37.9455	-75.5412
06004	Chincoteague	MF	37.94938	-75.50013
06004	Chincoteague	MF	37.94938	-75.50013
06004	Chincoteague	MF	37.94938	-75.50013
06004	Chincoteague	MF	37.94938	-75.50013
06005	Chincoteague	MSG-1-76	37.89588	-75.36004
06008	Chincoteague	Parksley P	37.8082	-75.68357
06008	Chincoteague	Parksley P	37.8082	-75.68357
06009	Chincoteague	CW-4	37.95484	-75.49186
06010	Cheriton	F-30	37.41635	-75.89832
06011	Cheriton	Ch-13	37.3003	-75.98353
06011	Cheriton	Ch-13	37.3003	-75.98353
06011	Cheriton	Ch-13	37.3003	-75.98353
06011	Cheriton	Ch-13	37.3003	-75.98353
06012	Chincoteague	SN	37.56595	-75.8997

06013	Chincoteague	BN	37.54412	-75.77101
06014	Cheriton	CC	37.21068	-75.96583
06014	Cheriton	CC	37.21068	-75.96583
06015	Cheriton	EC-1	37.20675	-76.00833
06017	Tappahanock	RRB-East	37.63227	-76.40832
06018	Tappahanock	RRB	37.63805	-76.41423
06026	VA shelf	VB	36.8221	-75.9861
06026	VA shelf	VB	36.8221	-75.9861
06058	Norfolk	GOMEZ PIT A Zz82-I	36.782904	-76.197504
06058	Norfolk	GOMEZ PIT A Zz82-I	36.782904	-76.197504
06058	Norfolk	GOMEZ PIT A Zz82-I	36.782904	-76.197504
06058	Norfolk	GOMEZ PIT A Zz82-I	36.782904	-76.197504
06058	Norfolk	GOMEZ PIT A Zz82-I	36.782904	-76.197504
06058	Norfolk	GOMEZ PIT A Zz82-I	36.782904	-76.197504
06058	Norfolk	GOMEZ PIT A Zz82-I	36.782904	-76.197504
06058	Norfolk	GOMEZ PIT A Zz82-I	36.782904	-76.197504
06080	Shelf	AMCOR 6020	39.42355	-73.59379
06192	Norfolk	PR #1	36.7445	-76.0202
06192	Norfolk	PR #1	36.7445	-76.0202
06192	Norfolk	PR #1	36.7445	-76.0202
06192	Norfolk	PR #1	36.7445	-76.0202
06192	Norfolk	PR #1	36.7445	-76.0202
06192	Norfolk	PR #1	36.7445	-76.0202
06192	Norfolk	PR #1	36.7445	-76.0202
06192	Norfolk	PR #1	36.7445	-76.0202
06192	Norfolk	PR #1	36.7445	-76.0202
06192	Norfolk	PR #1	36.7445	-76.0202
06192	Norfolk	PR #1	36.7445	-76.0202
06196	Chincoteague	Parramore Island Beach	37.57525	-75.60249
06204	Cheriton	Kiptopeake Borehole	37.1381	-75.96497
06204	Cheriton	Kiptopeake Borehole	37.1381	-75.96497
06204	Cheriton	Kiptopeake Borehole	37.1381	-75.96497
06204	Cheriton	Kiptopeake Borehole	37.1381	-75.96497
06204	Cheriton	Kiptopeake Borehole	37.1381	-75.96497
06204	Cheriton	Kiptopeake Borehole	37.1381	-75.96497
06204	Cheriton	Kiptopeake Borehole	37.1381	-75.96497
06207	Norfolk	Gomez GP-6/7	36.781463	-76.196891
06212	Norfolk	Gomez Sept 95 MS#2	36.780599	-76.196522
06212	Norfolk	Gomez Sept 95 MS#2	36.780599	-76.196522
06212	Norfolk	Gomez Sept 95 MS#2	36.780599	-76.196522

06273	Va Shelf	Zz82-84	37.10299897	-75.75600358
06273	Va Shelf	Zz82-84	37.10299897	-75.75600358
06273	Va Shelf	Zz82-84	37.10299897	-75.75600358
06273	Va Shelf	Zz82-84	37.10299897	-75.75600358
06273	Va Shelf	Zz82-84	37.10299897	-75.75600358
06274	Va Shelf	Zz82-85	37.13100147	-75.77499597
06274	Va Shelf	Zz82-85	37.13100147	-75.77499597
06274	Va Shelf	Zz82-85	37.13100147	-75.77499597
06274	Va Shelf	Zz82-85	37.13100147	-75.77499597
06274	Va Shelf	Zz82-85	37.13100147	-75.77499597
06274	Va Shelf	Zz82-85	37.13100147	-75.77499597
06274	Va Shelf	Zz82-85	37.13100147	-75.77499597
06274	Va Shelf	Zz82-85	37.13100147	-75.77499597
06274	Va Shelf	Zz82-85	37.13100147	-75.77499597
06274	Va Shelf	Zz82-85	37.13100147	-75.77499597
06274	Va Shelf	Zz82-85	37.13100147	-75.77499597
06275	Va Shelf	Zz82-86	37.12901136	-75.73101706
06275	Va Shelf	Zz82-86	37.12901136	-75.73101706
06275	Va Shelf	Zz82-86	37.12901136	-75.73101706
06275	Va Shelf	Zz82-86	37.12901136	-75.73101706
06275	Va Shelf	Zz82-86	37.12901136	-75.73101706
06275	Va Shelf	Zz82-86	37.12901136	-75.73101706
06276	Va Shelf	Zz82-87	37.52699703	-75.51399869
06276	Va Shelf	Zz82-87	37.52699703	-75.51399869
06278	Va Shelf	Zz82-89	37.79522014	-75.36950247
06278	Va Shelf	Zz82-89	37.79522014	-75.36950247
06278	Va Shelf	Zz82-89	37.79522014	-75.36950247
06278	Va Shelf	Zz82-89	37.79522014	-75.36950247
06278	Va Shelf	Zz82-89	37.79522014	-75.36950247
06278	Va Shelf	Zz82-89	37.79522014	-75.36950247
06281	Va Shelf	Zz82-92	37.71047756	-75.45907431
06281	Va Shelf	Zz82-92	37.71047756	-75.45907431
06281	Va Shelf	Zz82-92	37.71047756	-75.45907431
06281	Va Shelf	Zz82-92	37.71047756	-75.45907431
06281	Va Shelf	Zz82-92	37.71047756	-75.45907431
06281	Va Shelf	Zz82-92	37.71047756	-75.45907431
06281	Va Shelf	Zz82-92	37.71047756	-75.45907431
06281	Va Shelf	Zz82-92	37.71047756	-75.45907431
06281	Va Shelf	Zz82-92	37.71047756	-75.45907431
06281	Va Shelf	Zz82-92	37.71047756	-75.45907431
06281	Va Shelf	Zz82-92	37.71047756	-75.45907431
06283	Va Shelf	Zz82-94	37.58990683	-75.50192856
06283	Va Shelf	Zz82-94	37.58990683	-75.50192856

06283	Va Shelf	Zz82-94	37.58990683	-75.50192856
06283	Va Shelf	Zz82-94	37.58990683	-75.50192856
06284	Va Shelf	Zz82-95	37.64925331	-75.46677758
06284	Va Shelf	Zz82-95	37.64925331	-75.46677758
06284	Va Shelf	Zz82-95	37.64925331	-75.46677758
06285	Chincoteague	PARGO4	37.55925	-75.62404
06285	Chincoteague	PARGO4	37.55925	-75.62404
06285	Chincoteague	PARGO4	37.55925	-75.62404
06285	Chincoteague	PARGO4	37.55925	-75.62404
06285	Chincoteague	PARGO4	37.55925	-75.62404
06285	Chincoteague	PARGO4	37.55925	-75.62404
06286	Salisbury	ASSGO2	38.204074	-75.153081
06286	Salisbury	ASSGO2	38.204074	-75.153081
06286	Salisbury	ASSGO2	38.204074	-75.153081
06286	Salisbury	ASSGO2	38.204074	-75.153081
06286	Salisbury	ASSGO2	38.204074	-75.153081
06287	Chincoteague	CEDGO1	37.655455	-75.595539
06287	Chincoteague	CEDGO1	37.655455	-75.595539
06287	Chincoteague	CEDGO1	37.655455	-75.595539
06288	Chincoteague	CEDVO3	37.60010051	-75.64117393
06288	Chincoteague	CEDVO3	37.60010051	-75.64117393
06288	Chincoteague	CEDVO3	37.60010051	-75.64117393
06288	Chincoteague	CEDVO3	37.60010051	-75.64117393
06289	Chincoteague	CEDGO4	37.594738	-75.61976
06289	Chincoteague	CEDGO4	37.594738	-75.61976
06289	Chincoteague	CEDGO4	37.594738	-75.61976
06289	Chincoteague	CEDGO4	37.594738	-75.61976
06289	Chincoteague	CEDGO4	37.594738	-75.61976
06289	Chincoteague	CEDGO4	37.594738	-75.61976
06289	Chincoteague	CEDGO4	37.594738	-75.61976
06290	Chincoteague	WC-1	37.6034	-75.6936
06290	Chincoteague	WC-1	37.6034	-75.6936
06290	Chincoteague	WC-1	37.6034	-75.6936
06301	VA shelf	DGS118142	36.85573	-75.30768
06301	VA shelf	DGS118142	36.85573	-75.30768
06301	VA shelf	DGS118142	36.85573	-75.30768
06301	VA shelf	DGS118142	36.85573	-75.30768
06302	VA shelf	DGS118144	36.96169	-75.48295
06302	VA shelf	DGS118144	36.96169	-75.48295

